



University of Pennsylvania
ScholarlyCommons

Publicly Accessible Penn Dissertations

2017

Structural And Computational Insights In Collagen Stability With Applications In Light Harvesting

Roy Mathew Malamakal

University of Pennsylvania, roymalamakal@gmail.com

Follow this and additional works at: <https://repository.upenn.edu/edissertations>



Part of the [Biochemistry Commons](#), and the [Organic Chemistry Commons](#)

Recommended Citation

Malamakal, Roy Mathew, "Structural And Computational Insights In Collagen Stability With Applications In Light Harvesting" (2017). *Publicly Accessible Penn Dissertations*. 2688.

<https://repository.upenn.edu/edissertations/2688>

This paper is posted at ScholarlyCommons. <https://repository.upenn.edu/edissertations/2688>

For more information, please contact repository@pobox.upenn.edu.

Structural And Computational Insights In Collagen Stability With Applications In Light Harvesting

Abstract

Collagen is the most abundant protein in mammals, constituting almost a third of the total protein content in the body. Its unique structure and versatility has attracted the attention of many researchers for the development of new types of materials. Here, the influence of the aza-amino acids α -azaproline, azaglycine, and β -azaproline on the structure and stability of collagen is studied through incorporation into collagen model peptides (CMPs) and analyzed through a variety of computational methods including DFT and molecular dynamics calculations. Inspired by the success of generating multispectral imaging agents by using DNA as a scaffold for multichromophore assembly, the utilization of the distinctive self-assembly of collagen to template the arrangement of chromophores is also explored for the first time. Simple modifications regarding linker length, chromophore loading, chromophore spacing, and chromophore type are investigated and analyzed by computational methods to develop key insights in utilizing this novel scaffold for use in light harvesting applications. Separate projects regarding the development of novel photo-activatable probes based on the structure of xylopyridine, as well as chemical modifications to the pigment carbon black for the improvement of the jetness of coatings are also examined.

Degree Type

Dissertation

Degree Name

Doctor of Philosophy (PhD)

Graduate Group

Chemistry

First Advisor

David M. Chenoweth

Keywords

Aza-peptide, azaproline, Collagen, Multichromophore, Stability, xylopyridine

Subject Categories

Biochemistry | Chemistry | Organic Chemistry

STRUCTURAL AND COMPUTATIONAL INSIGHTS IN COLLAGEN STABILITY WITH
APPLICATIONS IN LIGHT HARVESTING

Roy M. Malamakal

A DISSERTATION

in

Chemistry

Presented to the Faculties of the University of Pennsylvania

in

Partial Fulfillment of the Requirements for the

Degree of Doctor of Philosophy

2017

Supervisor of Dissertation

Prof. David M. Chenoweth

Associate Professor of Chemistry

Graduate Group Chairperson

Prof. Gary A. Molander

Hirschmann-Makineni Professor of Chemistry

Dissertation Committee

Prof. E. James Petersson, Associate Professor of Chemistry

Prof. Eric J. Schelter, Associate Professor of Chemistry

Prof. William P. Dailey, Associate Professor of Chemistry

STRUCTURAL AND COMPUTATIONAL INSIGHTS IN COLLAGEN STABILITY WITH
APPLICATIONS IN LIGHT HARVESTING

2017

Roy Mathew Malamakal

*For everyone who supported and believed in me throughout these long and difficult years,
especially my parents*

ACKNOWLEDGMENTS

I am so grateful for everyone who supported and believed in me throughout my time here at the University of Pennsylvania. Firstly, I would like to thank my advisor, David M. Chenoweth, for the opportunity to work in his lab, and especially for his overwhelming patience to allow me to grow as a scientist over the course of these years. By working in his lab, I was able to be exposed to a variety of different chemistry and greatly expand the knowledge on various chemical techniques. I would also like to especially thank my committee members, E. James Petersson, Eric J. Schelter, and William P. Dailey for their guidance and suggestions every year. Dr. Petersson was always a pleasure to talk with, and I will always appreciate the encouragement and advice he gave me after each meeting. Simon Berritt was also an amazing mentor during my time here, and I will always appreciate the guidance he would give in our short encounters. I would also like to thank my undergraduate and master's advisor Todd A. Davis. He was instrumental in cultivating my interest in chemistry, and to this day continues to be a source of encouragement, support, and friendship. I would also like to thank the NSF Graduate Research Fellowship for funding my time here at UPenn.

I would also like to acknowledge the amazing colleagues I had to opportunity to work with. Having great lab members makes life significantly better, especially when things don't seem to work out with the chemistry. Robert A. Rarig always had a way of uplifting any situation in lab, and I am especially grateful for his mentorship and friendship that has grown over the years. I couldn't have asked for a better benchmate with Mai Tran, who I would always have nice and light-hearted conversations with. Yitao Zhang was an amazing friend and mentor, and instrumental in learning all the techniques I had to use for the collagen project. Sung-Eun Suh was also an especially good friend to me, in particular during the last few months of our time together. He continues to inspire me to become a better chemist. I would also like to acknowledge Chant (Jay) Aonbangkhen, who continually encouraged group activities outside of

the lab. Joomyung (Vicky) Jun and Dan Wu have been amazing friends as well, and it has been a pleasure getting to know them. Vicky has been an especially good friend to me, particularly in these last few months; I always enjoyed our late night conversations in lab. I would also like to thank Stephanie Barros, Adrienne Pesce, Jisun Lee, Ina Yoon, Alexander Kasznel, Samuel Melton, and my newest benchmate Jinxing Li for being awesome friends and making the time spent in lab so much lighter. From the department, I would like to thank Geraint Davies, Jake Nagy, and Kim Mullane, all of which who I had the pleasure of living with during my time in Philadelphia. All of them continued to encourage me during my time here, and I will always remember our friendship.

Lastly, I would like to specially thank friends at St. Agatha St. James. Fr. Carlos Keen was there for me at one of my lowest points and always made time for me, even after having a completely booked schedule; he continues to be a close friend and spiritual mentor to me. Fr. George Strausser always did his best to lift my spirits, and also always made time for me. Teresa Brugarolas, Marisa March, Jessi Rosario, Salvatore Bellante, Shannon Sweeney, Sergio Arrangoiz, Andrew Dierkes, Theresa Dierkes, Michael Gokie, Alan Teran, Adam Urennek, Javier de la Flor, Remi, Patrick Travers, Pepe, Leo, Jennifer Dabovich, Sarah Chavez, Frank and Katherine Wessling, Brian Credo, Jacque Faylo, and Angela Bae were also so encouraging to me, and I will never forget our friendship. There were so many people at the Newman Center who continually prayed for me and encouraged me – I am eternally grateful for their support. Additionally, I would like to especially thank Dr. Alex Punnoose and his family Tina, Cathy, Paul, and Peter. Dr. Punnoose gave me so much support before he passed away, and his family has continued to pray for me over these years. I would like to specially thank my family as well, especially my parents Mathew and Jane, who always told me to keep my head up and were a constant source of support. My siblings Tom and Van, Prabha and Tony, and John and Misty also encouraged me so much during my time here.

I will be forever grateful for all the love and support I received here, and thank God for all the wonderful blessings He has poured on me during this chapter of my life.

ABSTRACT

STRUCTURAL AND COMPUTATIONAL INSIGHTS IN COLLAGEN STABILITY WITH APPLICATIONS IN LIGHT HARVESTING

Roy M. Malamakal

Dr. David M. Chenoweth

Collagen is the most abundant protein in mammals, constituting almost a third of the total protein content in the body. Its unique structure and versatility has attracted the attention of many researchers for the development of new types of materials. Here, the influence of the aza-amino acids α -azaproline, azaglycine, and δ -azaproline on the structure and stability of collagen is studied through incorporation into collagen model peptides (CMPs) and analyzed through a variety of computational methods including DFT and molecular dynamics calculations. Inspired by the success of generating multispectral imaging agents by using DNA as a scaffold for multichromophore assembly, the utilization of the distinctive self-assembly of collagen to template the arrangement of chromophores is also explored for the first time. Simple modifications regarding linker length, chromophore loading, chromophore spacing, and chromophore type are investigated and analyzed by computational methods to develop key insights in utilizing this novel scaffold for use in light harvesting applications. Separate projects regarding the development of novel photo-activatable probes based on the structure of xylopyridine, as well as chemical modifications to the pigment carbon black for the improvement of the jetness of coatings are also examined.

TABLE OF CONTENTS

ACKNOWLEDGMENTS	IV
ABSTRACT.....	VII
LIST OF TABLES	XIII
LIST OF ILLUSTRATIONS.....	XIV
CHAPTER 1: INTRODUCTION.....	1
1.1 Structure of Collagen.....	2
1.2 Biomaterials From Collagen	5
1.3 Studying Collagen	5
1.4 Chemical Modifications to Collagen	6
1.4.1 Conservation of the Glycine Residue.....	7
1.4.2 Proline Modifications.....	8
1.5 Non-traditional Applications for Biological Scaffolds	10
1.1.1 Interest in Multichromophore Systems	10
1.5.1 Advantages of Multichromophore Systems	11
1.5.2 Use of DNA as a Scaffold.....	14
1.5.3 Use of Collagen as a Scaffold for Multichromophore Assembly	17
1.6 Overview of Thesis.....	17

1.7	References.....	18
------------	------------------------	-----------

CHAPTER 2: A SINGLE STEREODYNAMIC CENTER MODULATES THE RATE OF SELF-ASSEMBLY IN A BIOMOLECULAR SYSTEM..... 27

2.1	Introduction.....	28
------------	--------------------------	-----------

2.2	Results and Discussion.....	30
------------	------------------------------------	-----------

2.3	Conclusions.....	41
------------	-------------------------	-----------

2.4	Acknowledgments	42
------------	------------------------------	-----------

2.5	Notes.....	42
------------	-------------------	-----------

2.6	References.....	42
------------	------------------------	-----------

2.7	Supplemental Information	48
------------	---------------------------------------	-----------

2.7.1	General Information.....	48
-------	--------------------------	----

2.7.2	Crystal Structure Analysis on Known Compounds Containing Aza-proline and Tertiary Amines	49
-------	--	----

2.7.3	DFT-B3LYP Calculated Conformations	57
-------	--	----

2.7.4	Coordinates of the DFT-B3LYP Stationary Points.....	63
-------	---	----

2.7.5	Frozen Conformation Energies	103
-------	------------------------------------	-----

2.7.6	Free Energy Conformations	104
-------	---------------------------------	-----

CHAPTER 3: AZA-GLYCINE INDUCES HYPERSTABILITY 106

3.1	Introduction.....	107
------------	--------------------------	------------

3.2	Results and Discussion.....	109
3.3	Conclusions.....	115
3.4	Acknowledgments	115
3.5	Notes.....	116
3.6	References.....	116
3.7	Supplemental Information	120
3.7.1	General information	120
3.7.2	MD Simulations	121
 CHAPTER 4: UTILIZATION OF COLLAGEN AS A SCAFFOLD FOR		
MULTICHROMOPHORE ASSEMBLY.....		138
4.1	Introduction.....	139
4.2	Results and Discussion.....	142
4.3	Conclusions.....	151
4.4	References.....	151
4.5	Supplemental Information	156
4.5.1	General Information.....	156
4.5.2	Experimental Procedures	157
4.5.3	General Protocols.....	165
4.5.4	Peptide solution preparation.....	168

4.5.5	CD Wavelength scan.....	168
4.5.6	CD Thermal denaturation experiment.....	169
4.5.7	Peptide Characterization, CD Spectra, and Fluorescence Spectra	170
4.5.8	Titration Data	200
 CHAPTER 5: INVESTIGATION OF DELTA-AZAPROLINE INCORPORATION		
INTO COLLAGEN		201
5.1	Introduction.....	202
5.2	Results and Discussion.....	203
5.3	Conclusions and Future Outlook.....	206
5.4	References.....	207
 Supporting Information		208
5.4.1	General Information.....	208
5.4.2	Experimental Procedures	209
5.4.3	General Protocols.....	213
5.4.4	Peptide solution preparation.....	217
5.4.5	CD Wavelength scan.....	217
5.4.6	CD Thermal denaturation experiment.....	217
5.4.7	Peptide Characterization and CD Spectra	218
5.4.8	Computational Coordinates.....	226
 CHAPTER 6: CHEMICAL MODIFICATIONS TO CARBON BLACK		233
6.1	Introduction.....	234

6.2	Results and Discussion.....	235
6.3	Conclusions and Future Outlook.....	239
6.4	References.....	240
	Supporting Information	241
6.4.1	General Information.....	241
6.4.2	Sedimentation Assay.....	241
6.4.3	Functionalization of Carbon Black	241
6.4.4	Sedimentation Assay Results.....	244
6.4.5	Table of Acronyms	244
6.4.6	DLS Measurements of Carbon Black Products	244
6.4.7	Characterization of Functionalized Carbon Black	246
	 CHAPTER 7: INSIGHTS INTO 2N-XYLOPYRIDINE DERIVATIVES.....	 260
7.1	Introduction.....	261
7.2	Results and Discussion.....	261
7.3	Conclusion and Future Outlook	264
7.4	References.....	264
7.5	Supporting Information	266
7.5.1	General Information.....	266
7.5.2	Experimental Procedures	267
7.5.3	Fluorescence Properties	271
7.5.4	NMR Spectra	275

LIST OF TABLES

TABLE 1.1 DIFFERENT TYPES OF COLLAGEN AND THEIR COMMON LOCATIONS IN THE HUMAN BODY	4
TABLE 4.1 THERMAL DENATURATION TEMPERATURES FOR UNSUBSTITUTED AND PYRENE-SUBSTITUTED CMPS	143
TABLE 4.2.....	149
TABLE 4.3 THERMAL DENATURATION TEMPERATURES FOR NON-PYRENE DYES	150
TABLE 5.1 THERMAL DENATURATION TEMPERATURES FOR SELECT CMPS.....	204
TABLE 6.1 SUMMARY OF TOP 10 PROMISING FUNCTIONALIZATIONS	238
TABLE 6.2 SUMMARY OF PARTICLE SIZES FOR FUNCTIONALIZED CARBON BLACK	244

LIST OF ILLUSTRATIONS

FIGURE 1.1. EXAMPLE OF PPI (LEFT) AND PPII (RIGHT) HELICES.....	2
FIGURE 1.2 CRYSTAL STRUCTURE OF COLLAGEN (3B0S) AND THE INTERCHAIN HYDROGEN BONDS	6
FIGURE 1.3 THE PUCKERED STATES OF PROLINE	9
FIGURE 1.4. ARRANGEMENT OF J- AND H- AGGREGATES	11
FIGURE 1.5 REPRESENTATION OF COVALENT LIGHT HARVESTING PORPHYRIN ARRAY OF OKADA	12
FIGURE 2.1 EXAMPLE OF CONFIGURATIONAL STABILITY AND STEREODYNAMICS WITH RESPECT TO THE PROLYL AMINO ACID.....	29
FIGURE 2.2 THE COLLAGEN TRIPLE HELIX AND AN EXPANDED VIEW OF THE -PROPRO-GLY- TRIPEPTIDE REPEAT WITH ADJACENT VIEW OF THE CHEMICAL STRUCTURE.....	30
FIGURE 2.3 DOCKING ANALYSIS OF AZPRO-PRO IN COLLAGEN AND DEGREE OF PYRAMIDALIZATION ANALYSIS.....	33
FIGURE 2.4 IMPACT OF REPLACING AN α -STEREOCENTER WITH A NITROGEN ATOM.	34
FIGURE 2.5 COMPUTATIONAL ANALYSIS OF THE AZPRO-PRO DIPEPTIDE.	36
FIGURE 2.6 UNFOLDING AND REFOLDING DATA FOR COLLAGEN MODEL PEPTIDES.	40
FIGURE 2.7 SURVEY OF KNOWN CRYSTAL STRUCTURE CONTAINING AZA-PROLINE AND OTHER PYRAMIDALIZED NITROGEN ATOMS WITH AT LEAST ONE CARBONYL CONTAINING SUBSTITUENT.....	50
FIGURE 2.8 EXAMINATION OF EXTENT OF PYRAMIDALIZATION OF NITROGEN CONTAINING COMPOUNDS IN THE CAMBRIDGE STRUCTURAL DATABASE	51
FIGURE 2.9. EXAMINATION OF EXTENT OF PYRAMIDALIZATION OF NITROGEN CONTAINING COMPOUNDS IN THE CAMBRIDGE STRUCTURAL DATABASE	54
FIGURE 2.10 EXAMINATION OF EXTENT OF PYRAMIDALIZATION OF NITROGEN CONTAINING COMPOUNDS IN THE CAMBRIDGE STRUCTURAL DATABASE	56
FIGURE 2.11 CALCULATED CONFORMATIONS USING 6-31G(D) BASIS SET WITH ENERGIES 0.00- 0.99 KCAL MOL ⁻¹	57
FIGURE 2.12 CALCULATED CONFORMATIONS USING 6-31G(D) BASIS SET WITH ENERGIES BETWEEN 1.00-1.99 KCAL MOL ⁻¹	58
FIGURE 2.13 CALCULATED CONFORMATIONS USING 6-31G(D) BASIS SET WITH ENERGIES 2.00- 2.99 KCAL MOL ⁻¹	59

FIGURE 2.14 CALCULATED CONFORMATIONS USING 6-31G(D) BASIS SET WITH ENERGIES BETWEEN 3.00-3.99 KCAL MOL ⁻¹	60
FIGURE 2.15 CALCULATED CONFORMATIONS USING 6-31G(D) BASIS SET WITH ENERGIES BETWEEN 4.00-6.99 KCAL MOL ⁻¹	61
FIGURE 2.16 CALCULATED CONFORMATIONS USING 6-31G(D) BASIS SET WITH ENERGIES BETWEEN 7.00-12.00 KCAL MOL ⁻¹	62
FIGURE 3.1 (TOP) GLYCYL VERSUS AZA-GLYCYL RESIDUES: AZGLY-CONTAINING COLLAGEN TRIPLE HELIX WITH AN EXPANDED VIEW OF THE -PRO-PRO-AZGLY- REPEAT SHOWING THE PROPOSED ADDITIONAL CROSS-STRAND H-BONDING INTERACTIONS. (BOTTOM) H-BOND MAP OF COLLAGEN CONTAINING THE UNNATURAL AZGLY MODIFICATION.	108
FIGURE 3.2 CHEMICAL STRUCTURES OF COLLAGEN MODEL CONTROL PEPTIDES 1, 2 AND AZGLY-CONTAINING PEPTIDES 3, 4.	110
FIGURE 3.3 (A) TABLE OF UNFOLDING AND REFOLDING DATA FOR COLLAGEN MODEL PEPTIDES.	111
FIGURE 3.4 MODEL OF THE COLLAGEN TRIPLE HELIX, WITH THE CENTRAL VARIABLE TRIPLET HIGHLIGHTED IN RED.	113
FIGURE 3.5 HYDROGEN BOND ANALYSIS FOR MD SIMULATIONS OF COLLAGEN MODEL PEPTIDE 4.	114
FIGURE 4.1 PROPOSED MODIFICATION TO COLLAGEN STRUCTURE.	141
FIGURE 4.2. STRUCTURES OF THE TWO UNNATURAL AMINO ACIDS INCORPORATED INTO CMPS	142
FIGURE 4.3. FRACTION FOLDED THERMAL DENATURATION PLOTS FOR VARIOUS CHROMOPHORE SUBSTITUTED CMPS.	144
FIGURE 4.4. EMISSION SPECTRA AT 20°C FOR CMPS CONTAINING THE (A) 2C LINKER AND (B) 3C LINKER	145
FIGURE 4.5. STRUCTURES USED TO CALCULATE POINT CHARGES IN THE MD SIMULATION	146
FIGURE 4.6. 50 NS MD SIMULATION PERFORMED WITH THE 2C LINKER AND 3C LINKER	147
FIGURE 4.7. HISTOGRAMS SUMMARIZING 9 SIMULATIONS DESCRIBING INTER- AND INTRA-STRAND INTERACTIONS	148
FIGURE 4.8 FAR-RED EXCIMER DYE C.	150
FIGURE 4.9 EMISSION SPECTRA AT 10°C AND 80°C OF CMP 30	150
FIGURE 4.10 FRACTION FOLDED THERMAL DENATURATION PLOTS FOR NON-PYRENE SUBSTITUTED CMPS	151

FIGURE 4.11 CD SPECTRA OF CMP 1.....	170
FIGURE 4.12 CD THERMAL OF CMP 1	170
FIGURE 4.13 CD SPECTRA OF CMP 2.....	170
FIGURE 4.14 CD THERMAL OF CMP 2	171
FIGURE 4.15 EMISSION SPECTRA OF CMP 2 ($\lambda_{\text{EX}} = 342 \text{ NM}$)	171
FIGURE 4.16 CD SPECTRA OF CMP 3.....	171
FIGURE 4.17 CD THERMAL OF CMP 3	172
FIGURE 4.18 CD SPECTRUM OF CMP 4.....	172
FIGURE 4.19 CD THERMAL OF CMP 4	172
FIGURE 4.20 EMISSION SPECTRA OF CMP 4 ($\lambda_{\text{EX}} = 342 \text{ NM}$)	173
FIGURE 4.21 FLUORESCENCE THERMAL OF CMP 4 ($\lambda_{\text{EX}} = 342 \text{ NM}$)	173
FIGURE 4.22 CD SPECTRA OF CMP 5.....	174
FIGURE 4.23 CD THERMAL OF CMP 5	174
FIGURE 4.24 CD SPECTRA OF CMP 6.....	174
FIGURE 4.25 CD THERMAL OF CMP 6	175
FIGURE 4.26 EMISSION SPECTRA FOR CMP 6 ($\lambda_{\text{EX}} = 342 \text{ NM}$)	175
FIGURE 4.27 FLUORESCENCE THERMAL OF CMP 6	175
FIGURE 4.28 CD SPECTRA OF CMP 7.....	176
FIGURE 4.29 CD THERMAL OF CMP 7	176
FIGURE 4.30 CD SPECTRA OF CMP 8.....	176
FIGURE 4.31 CD THERMAL OF CMP 8	177
FIGURE 4.32 EMISSION SPECTRA OF CMP 8	177
FIGURE 4.33 FLUORESCENCE THERMAL OF CMP 8	177
FIGURE 4.34 CD SPECTRA OF CMP 9.....	178
FIGURE 4.35 CD THERMAL OF CMP 9	178
FIGURE 4.36 CD SPECTRA OF CMP 10.....	178
FIGURE 4.37 CD THERMAL OF CMP 10	179
FIGURE 4.38 EMISSION SPECTRA OF CMP 10.....	179
FIGURE 4.39 CD SPECTRA OF CMP 11.....	179
FIGURE 4.40 CD THERMAL OF CMP 11	180
FIGURE 4.41 CD SPECTRA OF CMP 12.....	180
FIGURE 4.42 CD THERMAL OF CMP 12	180
FIGURE 4.43 EMISSION SPECTRA OF CMP 12.....	181

FIGURE 4.44 FLUORESCENCE THERMAL OF CMP 12	181
FIGURE 4.45 CD SPECTRA OF CMP 15.....	182
FIGURE 4.46 CD THERMAL OF CMP 15	182
FIGURE 4.47 CD SPECTRA OF CMP 16.....	182
FIGURE 4.48 CD THERMAL OF CMP 16	183
FIGURE 4.49 EMISSION SPECTRA OF CMP 16	183
FIGURE 4.50 FLUORESCENCE THERMAL OF CMP 16	183
FIGURE 4.51 CD SPECTRA OF CMP 17.....	184
FIGURE 4.52 CD THERMAL OF CMP 17	184
FIGURE 4.53 CD SPECTRA OF CMP 18.....	184
FIGURE 4.54 CD THERMAL OF CMP 18	185
FIGURE 4.55 EMISSION SPECTRA OF CMP 18	185
FIGURE 4.56 FLUORESCENCE THERMAL OF CMP 18	185
FIGURE 4.57 CD SPECTRA OF CMP 19.....	186
FIGURE 4.58 CD THERMAL OF CMP 19	186
FIGURE 4.59 CD SPECTRA OF CMP 20.....	186
FIGURE 4.60 CD THERMAL OF CMP 20	187
FIGURE 4.61 EMISSION SPECTRA OF CMP 20.....	187
FIGURE 4.62 FLUORESCENCE THERMAL OF CMP 20	187
FIGURE 4.63 CD SPECTRA OF CMP 21.....	188
FIGURE 4.64 CD THERMAL OF CMP 21	188
FIGURE 4.65 CD SPECTRA OF CMP 22.....	188
FIGURE 4.66 CD THERMAL OF CMP 22	189
FIGURE 4.67 EMISSION SPECTRA OF CMP 22.....	189
FIGURE 4.68 FLUORESCENCE THERMAL OF CMP 22	189
FIGURE 4.69 CD SPECTRA OF CMP 23.....	190
FIGURE 4.70 CD THERMAL OF CMP 23	190
FIGURE 4.71 CD SPECTRA OF CMP 24.....	190
FIGURE 4.72 CD THERMAL OF CMP 24	191
FIGURE 4.73 EMISSION SPECTRA OF CMP 24.....	191
FIGURE 4.74 FLUORESCENCE THERMAL OF CMP 24	191
FIGURE 4.75 CD SPECTRA OF CMP 25.....	192
FIGURE 4.76 CD THERMAL OF CMP 25	192

FIGURE 4.77 CD SPECTRA OF CMP 26.....	192
FIGURE 4.78 CD THERMAL OF CMP 26.....	193
FIGURE 4.79 EMISSION SPECTRA OF CMP 26.....	193
FIGURE 4.80 FLUORESCENCE THERMAL OF CMP 26	193
FIGURE 4.81 CD SPECTRA OF CMP 29.....	194
FIGURE 4.82 CD THERMAL OF CMP 29	194
FIGURE 4.83 EMISSION SPECTRA OF CMP 29.....	194
FIGURE 4.84 FLUORESCENCE THERMAL OF CMP 29	195
FIGURE 4.85 CD SPECTRA OF CMP 30.....	195
FIGURE 4.86 CD THERMAL OF CMP 30	195
FIGURE 4.87 EMISSION SPECTRA OF CMP 30.....	196
FIGURE 4.88 FLUORESCENCE THERMAL OF CMP 30	196
FIGURE 5.1 PROPOSED HYDROGEN BONDING INTERACTION FROM THE INCORPORATION OF A DELTA-AZAPROLINE	203
FIGURE 5.2 FINAL PRODUCTS FOR δ -AZAPROLINE INCORPORATION.....	204
FIGURE 5.3 FRACTION FOLDED THERMAL DENATURATION PLOT	204
FIGURE 5.4 SUMMARY OF COMPUTATIONAL ANALYSIS OF CIS-TRANS CONFORMATIONS OF δ - AZAPROLINE	205
FIGURE 5.5 CD SPECTRA OF A1 IN PH 2.6	218
FIGURE 5.6 CD THERMAL OF A1 IN PH 2.6.....	218
FIGURE 5.7 CD THERMAL OF A1 AT PH 7.4	219
FIGURE 5.8 CD SPECTRA OF A1 AT PH 10.6	219
FIGURE 5.9 CD THERMAL OF A1 AT PH 10.6	219
FIGURE 5.10 CD SPECTRA OF CMP A2 AT PH 2.6	220
FIGURE 5.11 CD THERMAL OF CMP A2 AT PH 2.6	220
FIGURE 5.12 CD SPECTRA OF A2 AT PH 7.4	220
FIGURE 5.13 CD THERMAL OF A2 AT PH 7.4	221
FIGURE 5.14 CD SPECTRA OF A2 AT PH 10.9	221
FIGURE 5.15 CD THERMAL OF A2 PH 10.9.....	221
FIGURE 5.16 CD SPECTRA OF A3	222
FIGURE 5.17 CD THERMAL OF A3	222
FIGURE 6.1. PROPOSED AMINE FUNCTIONALIZATION STRATEGY FOR CARBON BLACK.....	236
FIGURE 6.2 EFFECT OF FUNCTIONALIZATION WITH AMINE AND SUCCINIC ANHYDRIDE.....	237

FIGURE 6.3 RESULTS OF THE SEDIMENTATION ASSAY	244
FIGURE 7.1 STRUCTURES OF METHYLATED AND ALKYLATED DERIVATIVES	263
FIGURE 7.2 EMISSION SPECTRA OF COMPOUND 5, 8, 9, 10, AND 11	263
FIGURE 7.3 CELL IMAGING STUDIES FOR COMPOUNDS 5, 6, AND 7.....	263
FIGURE 7.4 EMISSION SPECTRA OF COMPOUND IN VARIOUS SOLVENTS ($\lambda_{\text{EX}} = 397 \text{ NM}$).....	271
FIGURE 7.5. EMISSION SPECTRA OF COMPOUND 6 IN VARIOUS SOLVENTS ($\lambda_{\text{EX}} = 397 \text{ NM}$)	272
FIGURE 7.6 EMISSION SPECTRA OF COMPOUND 7 IN VARIOUS SOLVENTS ($\lambda_{\text{EX}} = 397 \text{ NM}$).....	272
FIGURE 7.7 EMISSION SPECTRA OF 8 IN H_2O ($\lambda_{\text{EX}} = 466 \text{ NM}$)	272
FIGURE 7.8 EMISSION SPECTRA OF 9 IN H_2O ($\lambda_{\text{EX}} = 480 \text{ NM}$)	273
FIGURE 7.9 EMISSION SPECTRA OF 10 IN H_2O ($\lambda_{\text{EX}} = 423 \text{ NM}$)	273
FIGURE 7.10 EMISSION SPECTRA OF 11 IN H_2O ($\lambda_{\text{EX}} = 362 \text{ NM}$)	273
FIGURE 7.11 EMISSION SPECTRA OF 6 RECORDED IN THE PRESENCE OF DIFFERENT IONS ($\lambda_{\text{EX}} = 397$ NM).....	274
FIGURE 7.12. COMPOUND 6 PH SCREEN ($\lambda_{\text{EX}} = 397 \text{ NM}$).....	274

CHAPTER 1: INTRODUCTION

Collagen is the most abundant protein in mammals, making up a third of protein content in the body.¹ It is the main structural protein in the extracellular space in various connective tissues in the animal body, and is typically found in most fibrous tissues such as tendons, ligaments, and skin.² Additionally, it is found within the cornea, cartilage, bones, blood vessels, intervertebral discs, and dentin in the teeth.

1.1 Structure of Collagen

Structurally, collagen is a fibrillar protein characterized by a right handed bundle of three parallel, left-handed poly-L-proline II-type helices (PPII).³ This classification is derived from the unique structure that peptide chains with consecutive proline residues adopt. When the amide bonds in a poly-L-proline chain all adopt a *cis*- configuration, the unique structure is termed type-I. Similarly, when these amide bonds adopt a *trans*- configuration, the structure is termed type-II (Figure 1.1). Because L-proline prefers a

trans- amide bond conformation, PPII helices are much more numerous in comparison to PPI helices. Despite being less abundant compared to the α -helix and β -structures, PPII helices represent the third most frequently occurring regular structure in folded proteins. The PPII helix has also been shown to be an important recognition domain for protein-protein and protein-nucleic acid interactions, and is specifically found as the binding structure for SH3 domains.⁴ Collagen is a unique protein in that it consists of three independent strands which adopt this left-

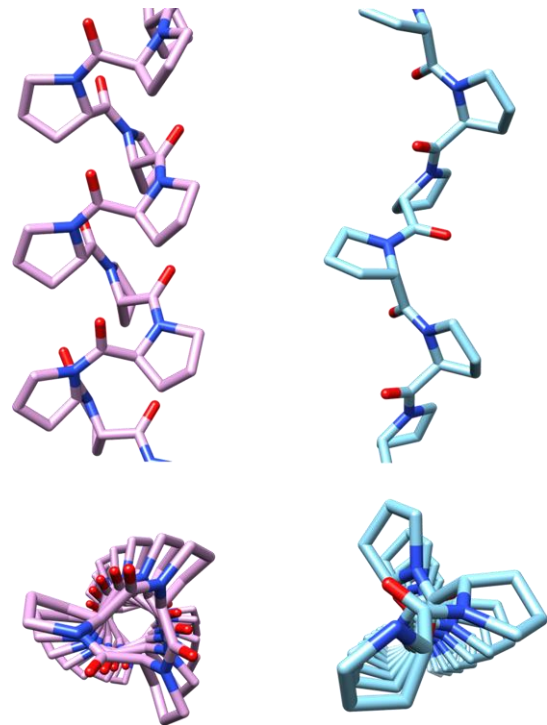


Figure 1.1. Example of PPI (left) and PPII (right) helices

The PPI helix is a tighter packed structure with more turns than a PPII helix

handed PPII-like geometry that pack tightly together through an internal network of hydrogen bonds to form a right handed triple helix.³

The diverse array of collagens can be attributed its basic composition of three strands, which are built in a repeating triplet sequence consisting of two amino acids (commonly labeled as Xaa and Yaa) and a glycine residue. Currently, 28 types of collagen have been found in vertebrates, and each type designated by a Roman numeral.² While the common structural feature of collagen is the presence of its unique triple helix, the actual percentage the helix composition varies between types, being 96% for collagen I and 10% for collagen XII.² The individual strands in each type of collagen are known as α chains, and can vary in size from 662 to 3152 amino acids in human $\alpha 1(X)$ and $\alpha 3(VI)$ chains, respectively.² When three identical α -chains interact with each other, for example in the case of collagen II, the collagen is termed a homotrimer. If one or two of these α -chains is replaced by a differing second or third α -chain, as in the case of collagen IX, these collagens are termed heterotrimers. The varying combinations of different α -chains give rise to a variety of diverse properties, affecting key attributes such as flexibility and molecular recognition. As seen by its incorporation in so many different bodily tissues (Table 1.1), collagen is an extremely versatile protein given its relatively simple structure.

Table 1.1 Different types of collagen and their common locations in the human body

Type of Collagen	Molecular Species	Common Tissues
<i>Fibril Forming Collagens</i>		
Collagen I	$[\alpha 1(I)]_2\alpha 2(I)$ $[\alpha 1(I)]_3$	Bones, dermis, tendon, ligaments, cornea
Collagen II	$[\alpha 1(II)]_3$	Cartilage, vitreous body, nucleus pulposus
Collagen III	$[\alpha 1(III)]_3$	Skin, vessel wall, reticular fibers of most tissues (lungs, liver, spleen, etc.)
Collagen V	$[\alpha 1(V)]_2\alpha 2(V)$ $[\alpha 1(V)]_3$ $[\alpha 1(V)]_2\alpha 4(V)$ $\alpha 1(XI)\alpha 1(V)\alpha 3(XI)$	Lung, cornea, bone, fetal membranes; together with type I collagen
Collagen XI	$\alpha 1(XI)\alpha 2(XI)\alpha 3(XI)$	Cartilage, vitreous body
<i>Basement Membrane Collagens</i>		
Collagen IV	$[\alpha 1(IV)]_2\alpha 2(IV)$; $\alpha 1-\alpha 6$	Basement membranes
<i>Microfibrillar Collagen</i>		
Collagen VI	$\alpha 1(VI), \alpha 2(VI), \alpha 3(VI)$	Widespread; dermis, cartilage, placenta, lungs, vessel wall, intervertebral disc
<i>Anchoring Fibrils</i>		
Collagen VII	$[\alpha 1(VIII)]_3$	Skin, dermal – epidermal junctions; oral mucosa, cervix
<i>Hexagonal Network-forming Collagens</i>		
Collagen VIII	$[\alpha 1(VIII)]_2\alpha 2(VIII)$	Endothelial cells, Descemet's membrane
Collagen X	$[\alpha 3(X)]_3$	Hypertrophic cartilage
<i>FACIT Collagens</i>		
Collagen IX	$\alpha 1(IX)\alpha 2(IX)\alpha 3(IX)$	Cartilage, vitreous humor, cornea
Collagen XII	$[\alpha 1(XII)]_3$	Pericardium, ligaments, tendon
Collagen XIV	$[\alpha 1(XIV)]_3$	Dermis, tendon, vessel wall, placenta, lungs, liver
Collagen XIX	$[\alpha 1(XIX)]_3$	Human rhabdomyosarcoma
Collagen XX	$[\alpha 1(XX)]_3$	Corneal epithelium, embryonic skin, sternal cartilage, tendon
Collagen XXI	$[\alpha 1(XXI)]_3$	Blood vessel wall
<i>Transmembrane Collagens</i>		
Collagen XIII	$[\alpha 1(XIII)]_3$	Epidermis, hair follicle, endomysium, intestine, chondrocytes, lungs, liver
Collagen XVII	$[\alpha 1(XVII)]_3$	Dermal – epidermal junctions
<i>Multiplexins</i>		
Collagen XV	$[\alpha 1(XV)]_3$	Fibroblasts, smooth muscle cells, kidney, pancreas
Collagen XVI	$[\alpha 1(XVI)]_3$	Fibroblasts, amnion, keratinocytes
Collagen XVIII	$[\alpha 1(XVIII)]_3$	Lungs, liver

1.2 Biomaterials From Collagen

The diversity of collagen has led to its use in a variety of biomaterials. Collagen is naturally biodegradable, and exogenous collagen is more biocompatible in comparison to other natural polymers.⁵ Additionally, it is only weakly antigenic, making it an ideal material for wound healing applications. Although there are many different types of collagen, only very few are used in making collagen-based biomaterials. Typically, only fibrillar collagen is used, as these can agglomerate and form larger structure fibers; this is commonly used in applications in wound healing and tissue engineering. The proteolytic resistance of collagen can be attributed to covalent crosslinks that can occur in larger collagen structures between free amino and acid residues. This has led to increased efforts to study modifications which can control the rate of degradation. Studying how modifications to the structure also has the potential to provide new information into how new types of materials can be made. Currently, a number of collagen-based biomaterials exist on the market, ranging from synthetic skins for burn victims to collagen-based sponges utilized in wound healing applications and bone repair.⁶

1.3 Studying Collagen

As stated previously, collagen fibers within the body are on the order of 662 to 3152 amino acids long. This can make studying the effect of small modifications on the structure and stability of the collagen triple helix increasingly difficult. As such, many researchers have turned to utilizing collagen model peptides (CMPs) to study collagen structure. These small peptides are approximately 21-30 amino acids in length, and have been used to gain greater insight on how small modifications perturb the triple helix folding. An essential technique to studying these CMPs involves circular dichroism (CD) spectroscopy. CMPs exhibit a unique CD signature, having an absorption max at typically 225 nm and an absorption minimum at approximately 200 nm. CMPs are commonly characterized by the ratio between this peak height and minimum, a term designated as the RPN (ratio positive negative) value.⁷ The absorption of the CD spectra

consists of a π - π^* amide transition at 200 ± 1 nm and a n - π^* transition at 225 nm.⁸ Much work has gone into the study of the structure of collagen utilizing these CMPs. The initial hypothesis of the collagen structure suggested it was comprised of all *cis*- amide bonds, however fiber diffraction data confirmed that the peptide bonds within collagen indeed favored a *trans*- configuration, and the bonds which held the triple helix together consisted of interstrand hydrogen bonds between the N-H_(Gly) and the carbonyl of the amino acid the Xaa position.³ The implementation of collagen model peptides allowed for the first crystal structure to be obtained by Berman and coworkers in 1994.⁹ Insight into the crystal structure first suggested the possibility of a weakly stabilizing effect between the C $_{\alpha}$ -H_(Gly) and the carbonyl of an interstrand Xaa position amino acid.

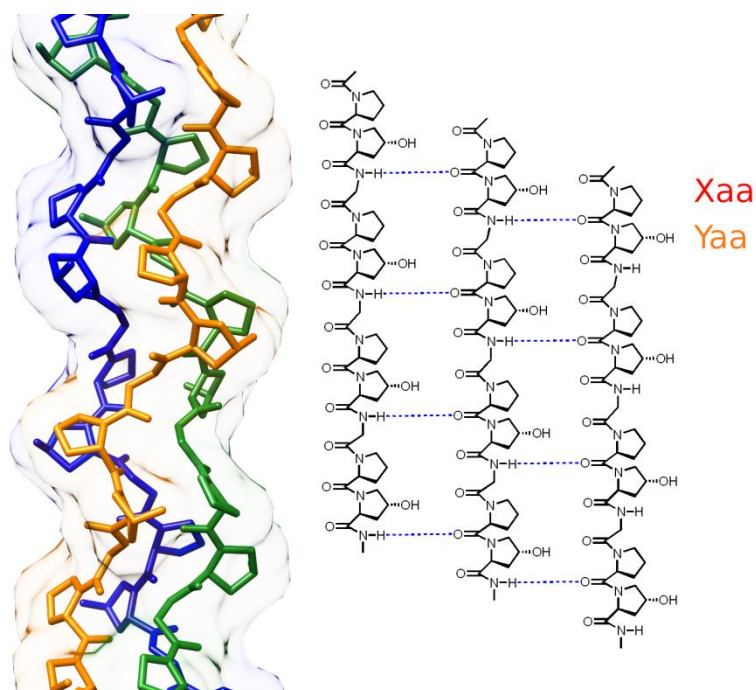


Figure 1.2 Crystal structure of collagen (3b0s) and the interchain hydrogen bonds

1.4 Chemical Modifications to Collagen

Collagen does have the potential to undergo a posttranslational modification of Pro residues in the Yaa position of collagen triplets by the enzyme prolyl 4-hydroxylase (P4H) in order to

stabilize the triple helix. This enzyme stereoselectively adds a 4-hydroxyl group to the proline in this position, the addition of which has a significant impact on the stability. Analysis of various CMPs containing these amino acids, termed hydroxyproline, shows an average increase of approximately 3°C in stabilization with each modification. Interestingly, this modification is applies only for the Yaa position of collagen, and is only conserved for the 4*R* configuration. Incorporation of 4*R* hydroxyproline in the Xaa position, or utilization of 4*S* hydroxyproline in the Yaa position, actually leads to destabilization of the triple helix.

1.4.1 Conservation of the Glycine Residue

Intrigued by these natural stabilizing modifications to the collagen triple helix, many researchers have endeavored to make various modifications to the natural structure of collagen to try and increase the stability. Dannenberg and coworkers attempted to use DFT calculations to predict that substitution of the glycine with D-alanine or D-serine would lead to stabilization of the collagen triple helix, however experimental results by Raines showed that these modifications were actually destabilizing.^{10,11} Berman and coworkers performed a substitution of glycine to L-alanine, and even obtained a crystal structure of this replacement. The melting temperature was found to be 33°C destabilizing, and the crystal structure emphasized the degree of perturbation that the alanine residue imparted to the assembled structure.⁹ In fact, most modifications to the glycine residue in collagen have been detrimental to triple helix formation. Brodsky and coworkers attempted to substitute the glycine residue with serine, cysteine, arginine, valine, glutamic acid, and aspartic acid, however each replacement was accompanied by a severe loss in thermal stability of the collagen triple helix.¹² In 2005, Raines and coworkers attempted to substitute the glycine amide bond with an ester. Although a relatively conservative replacement in theory, this replacement completely destabilized the triple helix.¹³ Raines and coworkers also investigated replacing the glycine residue with an (*E*)-alkene isostere, however this modification also completely destabilized the triple helix formation.¹³ Successful incorporation of thioamides

in CMPs was also performed by Raines and coworkers, which largely showed destabilization of the triple helix when replacing the Gly-Xaa peptide bonds; however interestingly a small degree of stabilization was observed through replacement of the Yaa-Gly peptide bond with a thioamide.¹⁴ This work clearly illustrates the importance of the glycine residue for the assembly of collagen.

1.4.2 Proline Modifications

While glycine replacements in the collagen structure have largely been destabilizing, modifications in the Xaa and Yaa positions have found more success. Specifically, several proline analogues have been synthesized and tested in collagen model peptides to assess their influence on collagen stability. Many of the analogues are substituted at the C-4 position, likely due to the similarity to natural hydroxyproline. Early hypotheses theorized that stabilization endowed by hydroxyproline in the Yaa position was due to a network of water bridges between the hydroxyproline residues. Later crystal structures seemed to confirm this notion. However, a seminal study by Raines and coworkers made a chemical modification switching the 4*R*-hydroxyproline for a 4*R*-fluoroproline (Flp), effectively removing the capability of the residue to participate in hydrogen bonding, as fluorine atoms are unable to participate in this type of intermolecular interaction.¹⁵ Raines proposed that rather than an extended hydrogen bonding matrix contributing to the stabilization of the collagen triple helix, the electronegativity of the hydroxyl group of hydroxyproline contributed to a favorable stereoelectronic effects. The electronegativity of the group in the C-4 position induced the proline ring to adopt a C γ -exo pucker due to the gauche effect, pre-organizing the collagen triple helix in its natural configuration and thus reducing the entropic cost of assembly. The epimer 4*S*-hydroxyproline actually favors a C γ -endo puckered conformation, which explains the destabilization observed with its incorporation in the Yaa position. This destabilization is conserved with the epimer 4*S*-fluoroproline (flp), which also favors the C γ -endo puckered conformation.¹⁶ Other derivatives

investigated by Raines and coworkers have included 4-methyl functionalized prolines.¹⁷

Interestingly, the 4*S*-methylproline (Mep) actually favors a C γ -exo conformation, and the

4*R*-methylproline (mep) favors a C γ -endo

conformation. As such, 4*R*-methylproline is

actually allowed in the Xaa position of collagen, and 4*S*-methylproline is allowed in the Yaa position of collagen, although both are destabilizing in comparison to native 4*R*-hydroxyproline.

With mep in the Xaa position and Mep in the Yaa position, the collagen stability is actually comparable to 4*R*-hydroxyproline. This data suggested that sterics also play a role in collagen assembly.

A particularly useful proline derivative was synthesized by Wennemers and coworkers. Their 4*R*-azidoproline derivative was shown to have comparable stability to native hydroxyproline, and also provided a functional handle for post-synthetic modification of the collagen triple helix.¹⁸ This derivative was also reduced to the free amine by Ganesh and coworkers to give 4*R/S*-aminoproline to form pH sensitive collagen triple helices.¹⁹ When the 4*S*-aminoproline residue was incorporated in the Xaa position of a collagen model peptide, the CMP displayed a thermal transition of 33°C at pH 10.7, however this would dramatically drop to 13°C at pH 3. Analysis of the structure by NMR and DFT calculations suggested the presence of a trans-annular hydrogen bond between the protonated amino group and the carbonyl of the amino acid. This interaction induced the proline ring to adopt a C γ -endo pucker. Interestingly, the 4*R*-aminoproline, while still having the capability of varying protonation states, did not perturb collagen stability as significantly as its epimer.^{20,21} These results also suggested sterics around the proline ring also influence the collagen stability. This work illustrated the importance of the interplay between

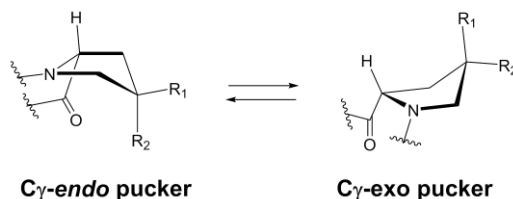


Figure 1.3 The puckered states of proline

hydrogen bonding, sterics, and stereoelectronic effects which all contribute to the thermal stability of collagen model peptides.

1.5 Non-traditional Applications for Biological Scaffolds

The unique structure and assembly of biological scaffolds has inspired their use in a variety of non-traditional applications. One such scaffold which has seen extensive use has been deoxyribonucleic acids (DNA). DNA is a naturally occurring biopolymer found in prokaryotic and eukaryotic cells used to encode genetic information.²² The biopolymer has a very unique structure, which consists of a phosphate group covalently attached to a five carbon sugar termed deoxyribose, which in turn is covalently attached to an aromatic nitrogenous base. Each nitrogenous base forms a stable hydrogen bond with a unique partner. It is precisely this unique pairing, along with help from hydrophobic stacking from the aromatic bases, which causes the DNA to typically fold into characteristic tertiary structures, including the idiosyncratic double helix. Given the versatility of DNA based structures and the degree of control offered to the assembly of supramolecular structures, many researchers have attempted to use it in a variety of applications.

1.1.1 Interest in Multichromophore Systems

One particular application for biological scaffolds which has garnered much interest in recent years has been in the area of multichromophic systems. As the name implies, these systems are covalent or noncovalent arrays of conjugated small molecules capable of π - π interactions. Multichromophoric systems are extremely versatile systems which are under investigation for use in synthetic photosystems and light harvesting antennae, synthetic ion channels, photovoltaic solar cells, organic semiconductors, and new types of supramolecular structures.²³ These systems hold much promise in the development of low-cost, lightweight, and environmentally friendly systems, in particular for light harvesting applications in solar cell research.

1.5.1 Advantages of Multichromophore Systems

The arraying of multiple chromophores in close proximity with one another has a number of different advantages. Firstly, a higher collective absorption in comparison to individual chromophores is observed. This is a desired attribute in solar cells, as the driving principle of utilizing solar energy demands high efficiency solar harvesting.²⁴ Other advantages brought about by these systems include the generation of entirely new photophysical properties. The interaction between chromophores in the ground state and excited state result in the formation of new complexes such as excited state dimers, termed excimers.²⁵ When a chromophore in the excited state interacts with a chromophore in the ground state of a different species, the complex is termed an exciplex. These types of interactions allows for a degree of tunability in multichromophore systems, as the use of different π -conjugated chromophores has the effect of changing the wavelengths of exciplex emission. Specifically, as excimer and exciplex systems decay, a red-shifted emission spectrum is typically observed. Other types of novel photophysical properties can result from the formation of J- or H- aggregates. The type of aggregate formed depends on the alignment of each small-molecule chromophore, typically determined by the dipole of the chromophore. In an H-aggregate, the molecules stack face-to-face, whereas in J-aggregation the molecules are arranged in a head-to-tail fashion (Figure 1.4).²⁶ The effect of aggregation on the ground state absorption spectra of a compound is a corresponding red-shift in the case of a J-aggregate, and a blue-shift in the case of an H-aggregate. Because the orientation and arrangement of the chromophores has a significant effect on the photophysical properties of these systems,

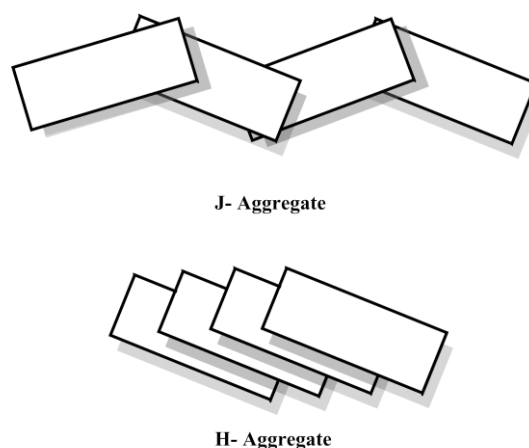


Figure 1.4. Arrangement of J- and H- Aggregates

multichromophore assemblies represent a versatile and tunable method for a number of different applications.

Much work has gone into the development of multichromophore systems. Typically, assembly is accomplished using either covalent methods or self-assembly methods. Covalent assemblies have an advantage where a well-defined structure can be generated.

Frechet and coworkers published one of the first uses of dye-labeled dendritic systems for light harvesting arrays.²⁷ The dendrimers consisted of a poly-aryl ether backbone

terminated by aminocoumarin dyes for light harvesting, shuttling the energy to a cyclic aminocoumarin dye positioned in the center of the dendrimer. The dendrimers displayed a high efficiency of energy transfer, only decreasing to approximately 86% by the fourth generation.

This technique was modified for more practical applications by using arrays of porphyrins as donor dyes and fullerenes as acceptor dyes.²⁸ Covalent assemblies were also developed by Okada and coworkers using poly-aromatic acetylenes as dendrimers, who was able to show >90% energy transfer from peripheral porphyrins to a central porphyrin (Figure 1.5).²⁹ While these systems allow for a great degree of control over chromophore placement and are the most commonly seen in literature, they can be tedious in construction and application.

Other methods by which multichromophore systems have been developed include the utilization of self-assembly by non-covalent interactions. Using simple principles of hydrogen bonding, π - π stacking, and strategic placement of water-solubilizing groups, various researchers have been able to control how chromophores assemble into larger structures. This method holds a great deal of

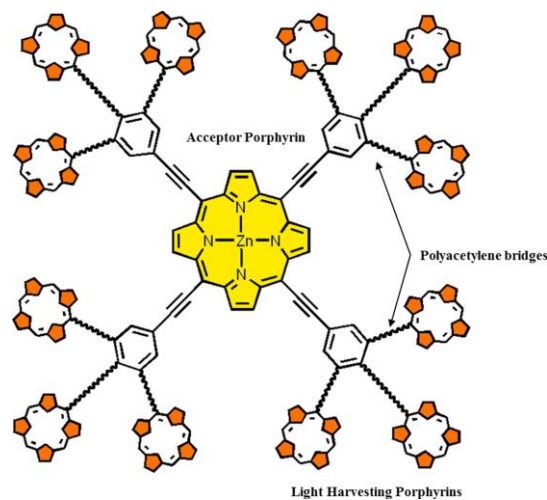


Figure 1.5 Representation of covalent light harvesting porphyrin array of Okada

promise for the development of light harvesting devices on a large scale. Because chromophores are characteristically planar and hydrophobic, they have a tendency to undergo uncontrolled aggregation. This often leads to quenching of fluorescence emission due to non-radiative decay by chromophore interactions. Controlling the assembly, however, can lead to interesting photophysical properties. In a seminal study by Wasielewski and coworkers, perylene-3,4:9,10-bis(dicarboximide) (PDI) chromophores substituted only with branched phenyl groups were able to be assembled into rod-like structures.³⁰ The emission of these assembled structures was found to be red-shifted in comparison to the monomers, and the assembled chromophores were found to display excimer-like interactions. Sautter and coworkers investigated supramolecular assembly of PDI chromophores and alkyl melamines, hypothesizing that hydrogen bonding between the imide group of the PDI and the melamine could direct assembly to higher order structures. The mixture of these two molecules was shown to produce mesoscopic structures by TEM imaging, and assembled systems were shown to be accompanied by a red-shift in the absorption in the UV-vis spectrum.³¹ In addition to perylene chromophores, porphyrins represent a highly investigated dye structure due to its similarity to the dyes found in photosynthetic systems, and have shown interesting photophysical properties after undergoing self-assembly. In recent work, Shelnutt and coworkers were able to self-assemble the porphyrins into nanotubes through functionalization of the porphyrin periphery with sulfates and pyridinium groups. Optical studies suggested that the chromophores underwent an offset J-aggregation, and that the morphology of the self-assembly could be controlled depending if the aggregates were stored in the presence or absence of light.³² In 2000, an elegant study carried out by Kuroda and coworkers developed a nonameric porphyrin assembly which could act as a light harvesting antenna. In this study, an acceptor porphyrin ring was functionalized with pyrazine moieties which served as coordination sites to assemble a donating zinc porphyrin ring functionalized with carboxylic acid moieties capable of forming hydrogen-bonded dimers. The self-assembled structure displayed an 82% efficient energy

transfer from the antenna system to the acceptor porphyrin dye, and exhibited an 18-fold enhancement of the fluorescence intensity of the acceptor dye. While self-assembly holds a lot of promise in the development of inexpensive light harvesting materials, this technique is often limited by the lack of methods for precisely placing different dyes within the greater structure.

1.5.2 Use of DNA as a Scaffold

Templating the assembly of chromophores using the structure of DNA possesses some unique benefits. Unlike most covalent assemblies, the assembly of DNA has been well studied and characterized. This allows for a greater degree of prediction of how a particular system will assemble, as oligomers and polymers of DNA are characteristically helical.³³ Several studies have demonstrated how the structure of DNA can be manipulated for the generation of well-defined nanostructures.^{34–36} The structure of DNA also intrinsically contains many advantages for multichromophore assembly. The backbone of DNA is comprised of phosphodiester bonds, which aids the water-solubility of the biopolymer. This counteracts the insolubility that can occur when chaining several hydrophobic chromophores together on a scaffold. Furthermore, base pairs in DNA naturally π - π stack and are optimally held apart at a distance of 3.4 Å, the distance at which excimers and exciplexes are favorably formed.²⁴ Using DNA as a templating scaffold, the position and orientation of chromophores can be precisely and predictably organized. DNA also presents a unique advantage in that automated synthesis is convenient. Solid phase phosphoramidite chemistry is a highly developed and optimized technique capable of generating oligonucleotides on the order of up to 150 nucleotides long.³⁷ In addition, the deoxyribose sugar backbone is easily derivatized for the introduction of chromophores with a variety of different post-synthetic chemical modifications.^{38–41} The incorporation of chromophores on to the DNA backbone is further facilitated by mutant DNA polymerases, although this has been met with only moderate success.²³ Martay and Kool were able to show that a pyrene modified nucleoside could act as a substrate to the Klenow fragment of *Escherichia coli* DNA Polymerase I.^{42,43}

Additionally, T7 RNA polymerase has been used by Tor and coworkers for the incorporation of furan-conjugated uridine, and further extended for the incorporation of 5'-thiophene uridine.^{44,45} These examples illustrate that utilization of DNA holds a great deal of promise for the non-traditional application of multichromophore assembly.

The many advantages that DNA presents for multichromophore assembly has inspired many researchers to investigate its use for this application. There are numerous approaches to this end, and one of the most common approaches has been simple replacement of nucleosides with mutants containing chromophores of interest. Letsinger and Wu were the first to implement this approach, incorporating a nucleosidic stilbene-4,4'-dicarboxamide residue in a short nucleotide sequence attached by a 3-carbon linker. Reversible excimer emission from the stilbene chromophore was observed when the DNA strands hybridized.^{46,47} This technique was adopted by Lewis and coworkers to study electron transfer within DNA with a number of different chromophores, including naphthalene-2,6-dicarboxamide, diphenylacetylene-4,4'-dicarboxamide, phenanthrene-2,7-dicarboxamide, 5,10-naphthalene diimide, and perylene-dicarboxamide.⁴⁶⁻⁵⁴ Häner and coworkers also utilized the same system, predominantly focusing on developing systems containing phenanthrenes and pyrenes.^{55,56} His work illustrated the relatively non-perturbing nature of phenanthrene and pyrene incorporation in the DNA duplex, and was also able to gain insight into chromophore interactions by monitoring changes in the absorbance and fluorescence spectra between assembled and non-assembled states. Later work built upon this success to apply the same principles to other DNA tertiary structures, namely 3-way junctions in the development of a modular light harvesting complex.⁵⁷ Use of a chiral linker was investigated by Komiyama and coworkers, who was able to construct multichromophore arrays which underwent H-aggregation.⁵⁸⁻⁶¹ A similar chiral linker, (*S*)-aminopropan-2,3-diol, was used by Wagenknecht and coworkers to generate arrays of perylene bisimides, which was shown to form interstrand excimers upon DNA hybridization.⁶²

In addition to chromophores covalently attached by various linkers, various researchers have investigated the use of simple base modifications to the DNA. Kool and coworkers have used this approach with a variety of chromophores using this approach including pyrene, benzopyrene, terphenyl, terthiophene, dimethylaminostilbene, binaphthyl, ternaphthyl, and quinacridone.^{63,64} The photophysical properties that arise from these chromophore interactions have been exceptionally interesting. In some cases, generation of Stokes shifts greater than 200 nm have been observed. Substituting these chromophores on a single stranded DNA backbone, Kool and coworkers were able to generate a variety of different systems capable of emitting in several wavelengths with a single excitation wavelength.⁶⁴ These systems have also been attached to antibodies for applications in multispectral labeling of cellular antigens.⁶⁵ Similar incorporation has been done with alkynyl substituted chromophores including pyrene, perylene, and anthracene by Inouye and coworkers.⁶⁶ The alkynyl substituent creates a more rigid aromatic system, and excimer and exciplex formation was observed within the system. The incorporation of these chromophores were able to increase the melting temperature of the DNA duplex by 6-9°C, likely due to increased hydrophobic interactions between chromophores with a large π - surface area. Chromophores have also been attached off of the DNA scaffold simply as side chains as a method by which to minimize the perturbation of the natural DNA base pairing. This method often requires the chromophores to be attached by a longer linker, as steric hindrance between the chromophore and the DNA backbone can cause complications during assembly. Wagenknecht and coworkers experimented with attaching chromophores to the 5-position of uridine.⁶⁷ A maximum of five chromophores were able to be attached to the DNA, and upon hybridization to cDNA, a 22-fold enhancement of fluorescence was observed. Kim and coworkers were able to synthesize a system consisting of ethynyl pyrene substituted on the C8 position of deoxyadenosine and the C5 position of uridine.⁶⁸ Excimer emission was observed for matched duplexes, and calculations suggested the chromophores reside in the major groove of the DNA

duplex. An interesting side-chain modification was developed by Stulz and coworkers involving the functionalization of the DNA duplex with diphenylporphyrin and tetraphenylporphyrin.^{69,70} Up to 11 chromophores were added to the scaffold, and energy minimized structures also suggested the chromophores sit in the major groove of DNA.

1.5.3 Use of Collagen as a Scaffold for Multichromophore Assembly

The wide expanse of research conducted on DNA as a scaffold for multichromophore assembly is an inspiration for the utilization of other biopolymers for a similar purpose, as new scaffolds may provide an avenue by which to develop materials with new and interesting photophysical properties. Collagen is one such biopolymer which has not been previously investigated for this application, and represents a scaffold with new and unique traits which could be advantageous for the assembly of chromophores. As alluded to previously, the structure of collagen has been well characterized and studied, aiding the prediction of chromophore interaction and spacing. Additionally, collagen shares the same advantage of DNA in that synthesis is facilitated through solid phase synthesis. Collagen has potential to generate devices with greater light harvesting capability, as unlike DNA it is comprised of three strands, allowing for a greater loading of chromophores.

1.6 Overview of Thesis

The work presented in this thesis explores a wide array of different topics. Chapter 2 describes the successful incorporation of the azapeptide alpha-azaproline into a CMP and undertakes a short computational study to gain insight into its non-perturbing nature in the Xaa position. Chapter 3 describes the incorporation of the aza peptide azaglycine into a CMP and turns to molecular dynamics to help explain the interesting increase in thermal stability of the triple helix. In Chapter 4, the functionalization of CMPs with various chromophores is explored using two different types of linkers. The fluorescence properties of these CMPs are investigated the influence of loading, spacing, arrangement, and type of chromophore are studied. CMPs are also

investigated via molecular dynamics simulations to gain further insight into how the chromophore interactions occur when the collagen is assembled. These results suggest that new photophysical effects can arise from chromophore interactions through collagen assembly, and have potential for use in light harvesting applications. The synthesis and incorporation of the aza-peptide delta-azaproline is discussed in Chapter 5, in addition to a short computational analysis to aid the explanation of the effects in thermal stability observed. Chapter 6 describes a separate project involving endeavors to functionalize the periphery of the compound carbon black to improve attributes such as jetness and dispersability. Lastly, Chapter 7 describes preliminary studies regarding a project to develop new photoactivatable probes based on a novel dixanthylidene scaffold.

1.7 References

- (1) Shoulders, M. D.; Raines, R. T. *Annu. Rev. Biochem.* **2009**, 78, 929–958.
- (2) Ricard-Blum, S. *Cold Spring Harb. Perspect. Biol.* **2011**, 3 (1), 1–19.
- (3) Shoulders, M. D.; Raines, R. T. *Annu. Rev. Biochem.* **2010**, 78, 929–958.
- (4) Adzhubei, A. A.; Sternberg, M. J. E.; Makarov, A. A. *J. Mol. Biol.* **2013**, 425 (12), 2100–2132.
- (5) Chattopadhyay, S.; Raines, R. T. *Biopolymers* **2014**, 101 (8), 821–833.
- (6) Parenteau-bareil, R.; Gauvin, R.; Berthod, F. *Materials (Basel)*. **2010**, 3, 1863–1887.
- (7) Parmar, A. S.; Nunes, A. M.; Baum, J.; Brodsky, B. *Biopolymers* **2012**, 97 (10), 795–806.
- (8) Gough, C. A. .; Bhatnagar, R. S. In *Circular Dichroism and the Conformational Analysis of Biomolecules*; 1996; pp 183–199.
- (9) Bella, J.; Eaton, M.; Brodsky, B.; Berman, H. *Science (80-.)*. **1994**, 266 (5182), 75–81.
- (10) Tsai, M.; Xu, Y.; Dannenberg, J. J. *J. Am. Chem. Soc.* **2005**, 127 (41), 14130–14131.
- (11) Horng, J.-C.; Kotch, F. W.; Raines, R. T. *Protein Sci.* **2006**, 16 (2), 208–215.

- (12) Beck, K.; Chan, V. C.; Shenoy, N.; Kirkpatrick, A.; Ramshaw, J. A. M.; Brodsky, B. *Proc. Natl. Acad. Sci.* **2000**, 97 (8), 4273–4278.
- (13) Jenkins, C. L.; Vasbinder, M. M.; Miller, S. J.; Raines, R. T. *Org. Lett.* **2005**, 7 (13), 2619–2622.
- (14) Newberry, R. W.; VanVeller, B.; Raines, R. T. *Chem. Commun.* **2015**, 51 (47), 9624–9627.
- (15) Holmgren, S. K.; Bretscher, L. E.; Taylor, K. M.; Raines, R. T. *Chem. Biol.* **1999**, 6 (2), 63–70.
- (16) Bretscher, L. E.; Jenkins, C. L.; Taylor, K. M.; DeRider, M. L.; Raines, R. T. *J. Am. Chem. Soc.* **2001**, 123 (4), 777–778.
- (17) Shoulders, M. D.; Hodges, J. A.; Raines, R. T. *J. Am. Chem. Soc.* **2006**, 128 (25), 8112–8113.
- (18) Erdmann, R. S.; Wennemers, H. *J. Am. Chem. Soc.* **2010**, 132 (40), 13957–13959.
- (19) Umashankara, M.; Babu, I. R.; Ganesh, K. N. *Chem. Commun. (Cambridge, United Kingdom)* **2003**, No. 20, 2606–2607.
- (20) Egli, J.; Siebler, C.; Maryasin, B.; Erdmann, R. S.; Bergande, C.; Ochsenfeld, C.; Wennemers, H. *Chem. - A Eur. J.* **2017**, 23 (33), 7938–7944.
- (21) Siebler, C.; Erdmann, R. S.; Wennemers, H. *Angew. Chem. Int. Ed. Engl.* **2014**, 53 (39), 10340–10344.
- (22) DNA <https://www.britannica.com/science/DNA> (accessed Oct 23, 2017).
- (23) Teo, Y. N.; Kool, E. T. *Chem. Rev.* **2012**, 112 (7), 4221–4245.
- (24) Jenekhe, S. A.; Osaheni, J. A. *Science (80-.)*. **1994**, 265 (5173), 765–768.
- (25) Lakowicz, J. *Principles of Fluorescence Spectroscopy*, 2nd ed.; Springer Science: New York, 1999.
- (26) Más-montoya, M.; Janssen, R. A. J. *Adv. Funct. Mater.* **2017**, 27, 1605779–1605791.

- (27) Gilat, S. L.; Adronov, A.; Fre, J. M. J. *Angew. Chemie Int. Ed.* **1999**, 38 (10), 1422–1427.
- (28) Guldi, D. M. *Chem. Soc. Rev.* **2002**, 31, 22–36.
- (29) Uetomo, A.; Kozaki, M.; Suzuki, S.; Yamanaka, K.; Ito, O.; Okada, K. *J. Am. Chem. Soc.* **2011**, 133, 13276–13279.
- (30) Rybtchinski, B.; Sinks, L. E.; Wasielewski, M. R. *J. Am. Chem. Soc.* **2004**, 126 (39), 12268–12269.
- (31) Würthner, F.; Thalacker, C.; Sautter, A. *Adv. Mater.* **1999**, 11 (9), 754–758.
- (32) Wang, Z.; Medforth, C. J.; Shelnutt, J. A. *J. Am. Chem. Soc.* **2004**, 126 (49), 15954–15955.
- (33) Sinden, R. R. *DNA Structure and Function*; Academic Press, Inc.: London, 1994.
- (34) Dutta, P. K.; Varghese, R.; Nangreave, J.; Lin, S.; Yan, H.; Liu, Y. *J. Am. Chem. Soc.* **2011**, 133 (31), 11985–11993.
- (35) Hemmig, E. A.; Creatore, C.; Wunsch, B.; Hecker, L.; Mair, P.; Parker, M. A.; Emmott, S.; Tinnefeld, P.; Keyser, U. F.; Chin, A. W. *Nano Lett.* **2016**, 16 (4), 2369–2374.
- (36) Han, D.; Pal, S.; Nangreave, J.; Deng, Z.; Liu, Y.; Yan, H. *Science* (80-.). **2011**, 332 (6027), 342–346.
- (37) Pon, R. T. In *Protocols for Oligonucleotides and Analogs*; Humana Press: New Jersey, 1993; pp 465–496.
- (38) Eördögh, Á.; Steinmeyer, J.; Peewasan, K.; Schepers, U.; Wagenknecht, H. A.; Kele, P. *Bioconjug. Chem.* **2016**, 27 (2), 457–464.
- (39) Berndt, S.; Herzig, N.; Kele, P.; Lachmann, D.; Li, X.; Wolfbeis, O. S.; Wagenknecht, H. A. *Bioconjug. Chem.* **2009**, 20 (3), 558–564.
- (40) Merkel, M.; Peewasan, K.; Arndt, S.; Ploschik, D.; Wagenknecht, H. A. *ChemBioChem* **2015**, 16 (11), 1541–1553.
- (41) Rieder, U.; Luedtke, N. W. *Angew. Chemie - Int. Ed.* **2014**, 53 (35), 9168–9172.

- (42) Matray, T. J.; Kool, E. T. *Nature* **1999**, 399 (June), 704–708.
- (43) Matray, T. J.; Kool, E. T. *J. Am. Chem. Soc.* **1998**, 120 (24), 6191–6192.
- (44) Srivatsan, S. G.; Tor, Y. *J. Am. Chem. Soc.* **2007**, 129 (7), 2044–2053.
- (45) Srivatsan, S. G.; Tor, Y. *Chem. - An Asian J.* **2009**, 4 (3), 419–427.
- (46) Letsinger, R. L.; Wu, T. *J. Am. Chem. Soc.* **1995**, 117 (28), 7323–7328.
- (47) Letsinger, R. L.; Wu, T. *J. Am. Chem. Soc.* **1994**, 116 (2), 811–812.
- (48) Hariharan, M.; Zheng, Y.; Long, H.; Zeidan, T. A.; Schatz, G. C.; Vura-Weis, J.; Wasielewski, M. R.; Zuo, X.; Tiede, D. M.; Lewis, F. D. *J. Am. Chem. Soc.* **2009**, 131 (16), 5920–5929.
- (49) Lewis, F. D.; Zhang, Y.; Liu, X.; Xu, N.; Letsinger, R. L. *J. Phys. Chem. B* **1999**, 103 (13), 2570–2578.
- (50) Zheng, Y.; Long, H.; Schatz, G. C.; Lewis, F. D. *Chem. Commun.* **2005**, 4795–4797.
- (51) Letsinger, R. L.; Wu, T.; Yang, J.-S.; Lewis, F. D. *Photochem. Photobiol. Sci.* **2008**, 7 (7), 854.
- (52) Daublain, P.; Siegmund, K.; Hariharan, M.; Vura-Weis, J.; Wasielewski, M. R.; Lewis, F. D.; Shafirovich, V.; Wang, Q.; Raytchev, M.; Fiebig, T. *Photochem. Photobiol. Sci.* **2008**, 7 (12), 1501–1508.
- (53) Lewis, F. D.; Kalgutkar, R. S.; Wu, Y.; Liu, X.; Liu, J.; Hayes, R. T.; Miller, S. E.; Wasielewski, M. R. *J. Am. Chem. Soc.* **2000**, 122 (49), 12346–12351.
- (54) Lewis, F. D.; Zhang, L.; Kelley, R. F.; Mccamant, D.; Wasielewski, M. R. *Tetrahedron* **2007**, 63, 3457–3464.
- (55) Langenegger, S. M.; Häner, R. *ChemBioChem* **2005**, 6 (12), 2149–2152.
- (56) Samain, F.; Malinovskii, V. L.; Langenegger, S. M.; Häner, R. *Bioorganic Med. Chem.* **2008**, 16 (1), 27–33.
- (57) Probst, M.; Langenegger, S. M.; Häner, R. *Chem. Commun.* **2014**, 50 (2), 159–161.

- (58) Kashida, H.; Komiyama, M.; Asanuma, H. *Chem. Lett.* **2006**, 35 (8), 934–935.
- (59) Fujii, T.; Kashida, H.; Asanuma, H. *Chem. - A Eur. J.* **2009**, 15 (39), 10092–10102.
- (60) Kashida, H.; Sekiguchi, K.; Liang, X.; Asanuma, H. *J. Am. Chem. Soc.* **2010**, 132 (17), 6223–6230.
- (61) Kashida, H.; Ito, H.; Fujii, T.; Hayashi, T.; Asanuma, H. *J. Am. Chem. Soc.* **2009**, 131 (29), 9928–9930.
- (62) Wagner, C.; Wagenknecht, H. A. *Org. Lett.* **2006**, 8 (19), 4191–4194.
- (63) Ren, R. X. F.; Chaudhuri, N. C.; Paris, P. L.; Rumney IV, S.; Kool, E. T. *J. Am. Chem. Soc.* **1996**, 118 (33), 7671–7678.
- (64) Gao, J.; Strässler, C.; Tahmassebi, D.; Kool, E. T. *J. Am. Chem. Soc.* **2002**, 124 (39), 11590–11591.
- (65) Guo, J.; Wang, S.; Dai, N.; Teo, Y. N.; Kool, E. T. *Proc. Natl. Acad. Sci.* **2011**, 108 (9), 3493–3498.
- (66) Chiba, J.; Takeshima, S.; Mishima, K.; Maeda, H.; Nanai, Y.; Mizuno, K.; Inouye, M. *Chem. - A Eur. J.* **2007**, 13 (29), 8124–8130.
- (67) Varghese, R.; Wagenknecht, H. A. *Chem. - A Eur. J.* **2010**, 16 (30), 9040–9046.
- (68) Hwang, G. T.; Seo, Y. J.; Kim, B. H. *Tetrahedron Lett.* **2005**, 46 (9), 1475–1477.
- (69) Bouamaied, I.; Nguyen, T.; Rühl, T.; Stulz, E. *Org. Biomol. Chem.* **2008**, 6 (21), 3888–3891.
- (70) Fendt, L. A.; Bouamaied, I.; Thöni, S.; Amiot, N.; Stulz, E. *J. Am. Chem. Soc.* **2007**, 129 (49), 15319–15329.
- (71) Wasielewski, M. R. *Acc. Chem. Res.* **2009**, 42 (12), 1910–1921.
- (72) Benveniste, A. L.; Creeger, Y.; Fisher, G. W.; Ballou, B.; Waggoner, A. S.; Armitage, B. A. *J. Am. Chem. Soc.* **2007**, 129 (7), 2025–2034.
- (73) Jana, B.; Ghosh, A.; Patra, A. *J. Phys. Chem. Lett.* **2017**, 4608–4620.

- (74) Frischmann, P. D.; Mahata, K.; Würthner, F. *Chem. Soc. Rev.* **2013**, 42 (4), 1847–1870.
- (75) Waggoner, A. S. *Curr. Opin. Chem. Biol.* **2006**, 10 (1), 62–66.
- (76) Gombert, A. *Photonics for Solar Energy Systems*; SPIE: Bas-Rhin, 2006.
- (77) García-Parajó, M. F.; Hernando, J.; Mosteiro, G. S.; Hoogenboom, J. P.; van Dijk, E. M. H. P.; van Hulst, N. F. *ChemPhysChem* **2005**, 6 (5), 819–827.
- (78) Scholes, G. D.; Rumbles, G. *Nat. Mater.* **2006**, 5 (9), 683–696.
- (79) Benveniste, A. L.; Creeger, Y.; Fisher, G. W.; Ballou, B.; Waggoner, A. S.; Armitage, B. a. *J. Am. Chem. Soc.* **2007**, 129 (7), 2025–2034.
- (80) Balakrishnan, K.; Datar, A.; Naddo, T.; Huang, J.; Oitker, R.; Yen, M.; Zhao, J.; Zang, L. *J. Am. Chem. Soc.* **2006**, 128 (22), 7390–7398.
- (81) Peng, H.-S.; Chiu, D. T. *Chem. Soc. Rev.* **2015**, 44 (14), 4699–4722.
- (82) Foster, S.; Finlayson, C. E.; Keivanidis, P. E.; Huang, Y.-S.; Hwang, I.; Friend, R. H.; Otten, M. B. J.; Lu, L.-P.; Schwartz, E.; Nolte, R. J. M.; Rowan, A. E. *Macromolecules* **2009**, 42 (6), 2023–2030.
- (83) Frischmann, P. D.; Mahata, K.; Würthner, F. *Chem. Soc. Rev.* **2013**, 42 (4), 1847–1870.
- (84) Leo, K.; Universita, T.; Riede, M.; Lu, B. *Compr. Semicond. Sci. Technol.* **2011**, 4, 448–507.
- (85) Jurchescu, O. D.; Popinciuc, M.; van Wees, B. J.; Palstra, T. T. M. *Adv. Mater.* **2007**, 19 (5), 688–692.
- (86) Li, S.-L.; Xiao, T.; Lin, C.; Wang, L. *Chem. Soc. Rev.* **2012**, 41 (18), 5950–5968.
- (87) González-Rodríguez, D.; Schenning, A. P. H. J. *Chem. Mater.* **2011**, 23 (3), 310–325.
- (88) Elemans, J. A. A. W.; van Hameren, R.; Nolte, R. J. M.; Rowan, A. E. *Adv. Mater.* **2006**, 18 (10), 1251–1266.
- (89) Szent-Gyorgyi, C.; Schmidt, B. F.; Fitzpatrick, J. a J.; Bruchez, M. P. *J. Am. Chem. Soc.* **2010**, 132 (32), 11103–11109.

- (90) Hindin, E.; Forties, R. A.; Loewe, R. S.; Ambroise, A.; Kirmaier, C.; Bocian, D. F.; Lindsey, J. S.; Holten, D.; Knox, R. S. *J. Phys. Chem. B* **2004**, *108* (34), 12821–12832.
- (91) Malinovskii, V. L.; Wenger, D.; Häner, R. *Chem. Soc. Rev.* **2010**, *39* (2), 410–422.
- (92) Janssen, P. G. a; Vandenbergh, J.; van Dongen, J. L. J.; Meijer, E. W.; Schenning, A. P. H. *J. J. Am. Chem. Soc.* **2007**, *129* (19), 6078–6079.
- (93) Teo, Y. N.; Kool, E. T. *Chem. Rev.* **2012**, *112* (7), 4221–4245.
- (94) Spillmann, C. M.; Medintz, I. L. *J. Photochem. Photobiol. C Photochem. Rev.* **2015**, *23*, 1–24.
- (95) Lewis, F. D.; Zhang, L.; Zuo, X. *J. Am. Chem. Soc.* **2005**, *127* (28), 10002–10003.
- (96) Lewis, F. D.; Liu, X.; Miller, S. E.; Wasielewski, M. R. *J. Am. Chem. Soc.* **1999**, *121* (41), 9746–9747.
- (97) Würthner, F.; Kaiser, T. E.; Saha-Möller, C. R. *Angew. Chemie - Int. Ed.* **2011**, *50* (15), 3376–3410.
- (98) Zhang, Y.; Malamakal, R. M.; Chenoweth, D. M. *Angew. Chemie Int. Ed.* **2015**, *54* (37), 10826–10832.
- (99) Zhang, Y.; Malamakal, R. M.; Chenoweth, D. M. *J. Am. Chem. Soc.* **2015**, *137* (39), 12422–12425.
- (100) Okuyama, K.; Miyama, K.; Mizuno, K.; Bächinger, H. P. *Biopolymers* **2012**, *97* (8), 607–616.
- (101) Fillon, Y. A.; Anderson, J. P.; Chmielewski, J. *J. Am. Chem. Soc.* **2005**, *127* (33), 11798–11803.
- (102) Gauba, V.; Hartgerink, J. D. *J. Am. Chem. Soc.* **2007**, *129* (48), 15034–15041.
- (103) Hornak, V.; Abel, R.; Okur, A.; Strockbine, B.; Roitberg, A.; Simmerling, C. *Proteins Struct. Funct. Bioinforma.* **2006**, *65* (3), 712–725.
- (104) Senes, A.; Ubarretxena-Belandia, I.; Engelman, D. M. *Proc. Natl. Acad. Sci.* **2001**, *98*

- (16), 9056–9061.
- (105) Duttagupta, I.; Misra, D.; Bhunya, S.; Paul, A.; Sinha, S. *J. Org. Chem.* **2015**, *80*, 10585–10604.
- (106) Donnet, J.-B.; Bansal, R. C.; Wang, M.-J. *Carbon Black: Science and Technology*, 2nd ed.; Marcel Dekker, Inc.: New York, 1993.
- (107) Yang, J.; Tang, B.; Qiu, W.; Zhang, S. *Carbon N. Y.* **2012**, *50* (15), 5621–5624.
- (108) Li, H. Y.; Chen, H. Z.; Xu, W. J.; Yuan, F.; Wang, J. R.; Wang, M. *Colloids Surfaces A Physicochem. Eng. Asp.* **2005**, *254* (1–3), 173–178.
- (109) Tiarks, F.; Landfester, K.; Antonietti, M. *Macromol. Chem. Phys.* **2001**, *202* (1), 51–60.
- (110) He, H.; Zhong, M.; Konkolewicz, D.; Yacatto, K.; Rappold, T.; Sugar, G.; David, N. E.; Matyjaszewski, K. *J. Mater. Chem. A* **2013**, *1* (23), 6810.
- (111) Liu, T.; Casado-Portilla, R.; Belmont, J.; Matyjaszewski, K. *J. Polym. Sci. Part A Polym. Chem.* **2005**, *43* (20), 4695–4709.
- (112) Guo, C.; Zhou, L.; Lv, J. *Polym. Polym. Compos.* **2013**, *21* (7), 449–456.
- (113) Fu, S.; Zhang, L.; Tian, A.; Xu, Y.; Du, C.; Xu, C. *Ind. Eng. Chem. Res.* **2014**, *53* (24), 10007–10014.
- (114) Bergemann, K.; Fanghänel, E.; Knackfuß, B.; Lüthge, T.; Schukat, G. *Carbon N. Y.* **2004**, *42* (11), 2338–2340.
- (115) Huang, J. F.; Shen, F.; Li, X. H.; Zhou, X. Q.; Li, B. Y.; Xu, R. L.; Wu, C. F. *J. Colloid Interface Sci.* **2008**, *328* (1), 92–97.
- (116) Tsubokawa, N.; Satoh, T.; Murota, M.; Sato, S.; Shimizu, H. *Polym. Adv. Technol.* **2001**, *602* (December 2000), 596–602.
- (117) Ichioka, H.; Satoh, T.; Hayashi, S.; Fujiki, K.; Tsubokawa, N. *React. Funct. Polym.* **1998**, *37*, 75–82.
- (118) Taniguchi, Y.; Ogawa, M.; Gang, W.; Saitoh, H.; Fujiki, K.; Yamauchi, T.; Tsubokawa,

- N. *Mater. Chem. Phys.* **2008**, *108* (2–3), 397–402.
- (119) Zhou, X.; Li, Q.; Wu, C. *Appl. Organomet. Chem.* **2008**, *22*, 78–81.
- (120) Gagey, N.; Neveu, P.; Benbrahim, C.; Goetz, B.; Aujard, I.; Baudin, J.-B.; Jullien, L. *J. Am. Chem. Soc.* **2007**, *129* (32), 9986–9998.
- (121) Cho, S.-Y.; Song, Y.-K.; Kim, J.-G.; Oh, S.-Y.; Chung, C.-M. *Tetrahedron Lett.* **2009**, *50* (33), 4769–4772.
- (122) Kobayashi, T.; Komatsu, T.; Kamiya, M.; Campos, C.; González-Gaitán, M.; Terai, T.; Hanaoka, K.; Nagano, T.; Urano, Y. *J. Am. Chem. Soc.* **2012**, *134* (27), 11153–11160.
- (123) Faal, T.; Wong, P. T.; Tang, S.; Coulter, A.; Chen, Y.; Tu, C. H.; Baker, J. R.; Choi, S. K.; Inlay, M. A. *Mol. BioSyst.* **2015**, *11* (3), 783–790.
- (124) Ballister, E. R.; Aonbangkhen, C.; Mayo, A. M.; Lampson, M. A.; Chenoweth, D. M. *Nat. Commun.* **2014**, *5*, 5475.
- (125) Lord, S. J.; Conley, N. R.; Lee, H. D.; Samuel, R.; Liu, N.; Twieg, R. J.; Moerner, W. E. *J. Am. Chem. Soc.* **2008**, *130* (29), 9204–9205.
- (126) An, P.; Yu, Z.; Lin, Q. *Org. Lett.* **2013**, *15* (21), 5496–5499.
- (127) Yu, Z.; Ho, L. Y.; Lin, Q. *J. Am. Chem. Soc.* **2011**, *133* (31), 11912–11915.
- (128) Lim, R. K. V.; Lin, Q. *Acc. Chem. Res.* **2011**, *44* (9), 828–839.
- (129) Rarig, R.-A. F.; Tran, N. M.; Chenoweth, D. M. *J. Am. Chem. Soc.* **2013**, *135* (24), 9213–9219.
- (130) Tran, M. N.; Chenoweth, D. M. *Angew. Chemie Int. Ed.* **2015**, *54* (22), 6442–6446.
- (131) Tran, M. N.; Rarig, R.-A. F.; Chenoweth, D. M. *Chem. Sci.* **2015**, *6* (8), 4508–4512.

CHAPTER 2: A SINGLE STEREODYNAMIC CENTER MODULATES THE RATE OF SELF-ASSEMBLY IN A BIOMOLECULAR SYSTEM

The content of this chapter was originally published in *Angewandte Chemie International Edition*. It is adapted with permission by the publisher:

Zhang, Y., Malamakal, R. M., Chenoweth, D. M. A Single Stereodynamic Center Modulates the Rates of Assembly in a Biomolecular System. *Angew. Chem. Int. Ed.* **2015**, *54*, 10826-10832.
Copyright 2015 Wiley-VCH Verlag GmbH & Co. KGaA, Weinheim.

The work presented in this thesis constitutes of the computational and Crystal Structure Database analysis of azaproline. CD, NMR, and Hysteresis data can be found in the dissertation of Yitao Zhang.

2.1 Introduction

One of the most ubiquitous chiral elements in nature is the sp³-hybridized tertiary carbon stereocenter, exemplified by its presence in the α -amino acid building blocks of biomolecules.^{1,2} Chirality³ in molecular systems can be thought of as a form of stereochemical preorganization that limits the conformational space. Understanding how molecular systems respond to perturbations in their chiral building blocks can provide insight into diverse areas, such as biomolecule self-assembly, protein folding, drug design, materials, and catalysis.⁴⁻⁷ Biomolecular structure is governed by a delicate balance of non-covalent intra- and intermolecular interactions that drive macromolecular assembly and recognition events that are critical to all life processes. These events are intimately coupled to stereochemistry, which is a property that is hard-wired into the building blocks of life.^{1,2,8-12} For proteins and peptides, the building blocks are amino acids with sp³-hybridized tertiary carbon stereocenters in the L-configuration. Natural amino acid building blocks are typically enantiopure and lack the ability to interconvert readily between D and L forms in the absence of enzymatic or harsh chemical conditions.¹¹⁻¹² The C-H bond of an sp³-hybridized tertiary carbon requires more than 80 kcal mol⁻¹ for thermal homolysis (Figure 2.1).¹³ The unique asymmetry imposed by the configurationally stable stereocenters of amino acids also restricts conformational mobility, as shown in Ramachandran maps.¹⁴ Nitrogen atoms in their sp³-hybridized form can adopt a pyramidalized geometry that is very similar to a tertiary carbon stereocenter, with the exception of a lone pair of electrons occupying the position once held by a hydrogen atom on the tertiary carbon.¹⁵ Despite a similar electron pair geometry between sp³-hybridized nitrogen and sp³-hybridized carbon, there is a striking difference in the energy of activation required for interconversion between the two mirror image forms in each case (Figure 2.1). A typical activation barrier for pyramidal inversion of sp³-hybridized nitrogen ranges from 5–10 kcal mol⁻¹, corresponding to interconversion between the two mirror image forms.¹⁵

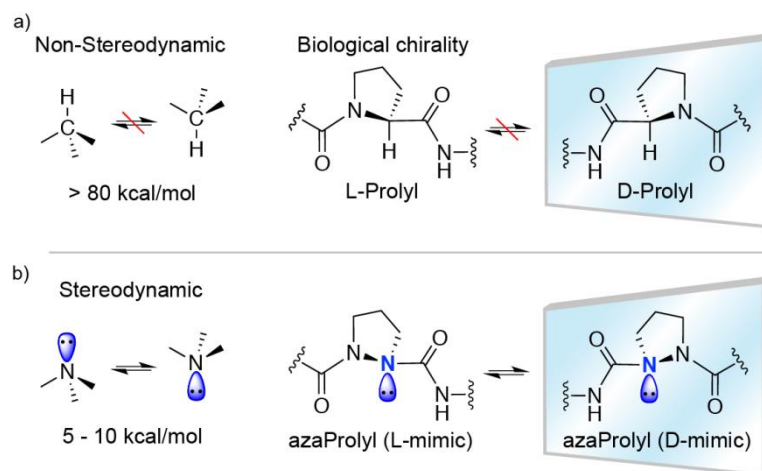


Figure 2.1 Example of configurational stability and stereodynamics with respect to the prolyl amino acid.

a) Configurationally stable sp^3 hybridized tertiary carbon stereocenter and the prolyl amino acid example. b) A stereodynamic sp^3 -hybridized tertiary nitrogen center and an example of how a stereodynamic pyramidalized nitrogen (as in aza-proline, AzPro) could potentially mimic both prolyl stereochemical configurations.

In addition to the conformational constraints imposed by amino acid stereochemistry, living systems have proline at their disposal. Proline is a unique amino acid representing a limiting case in the continuum of preorganization.^{8-10,14,16} Proline has a privileged structure, where side chain cyclization to form the pyrrolidine ring results in the most conformationally restricted amino acid building block present in nature (Figure 2.1). The pyrrolidine ring constraint has a dramatic impact on biomolecular conformation, folding, assembly, and recognition events. Collagen represents one of the most striking examples of a highly preorganized, proline-rich, self-assembling protein structure in nature.¹⁷⁻²¹ Collagen adopts a densely packed triple helical structure requiring a precise backbone conformation for proper self-assembly (Figure 2.1).¹⁷⁻²⁸ A major gap in our understanding of biomolecular folding and self-assembly involves grasping the importance of stereochemistry and its impact on these processes. The achiral nature of aza-proline (AzPro or AzP) and the ability of nitrogen to adopt either of two pyramidalized forms readily provides a unique opportunity to glean insight into the vital role that stereochemistry plays in biomolecular assembly (Figure 2.1 b). Prior studies have not examined the effect of AzPro modifications on folding or self-assembly in the context of longer peptide chains, prompting our

investigation of the impact of AzPro in a collagen model peptide system²⁶ to assess the influence of stereodynamics on the triple helix self-assembly process.

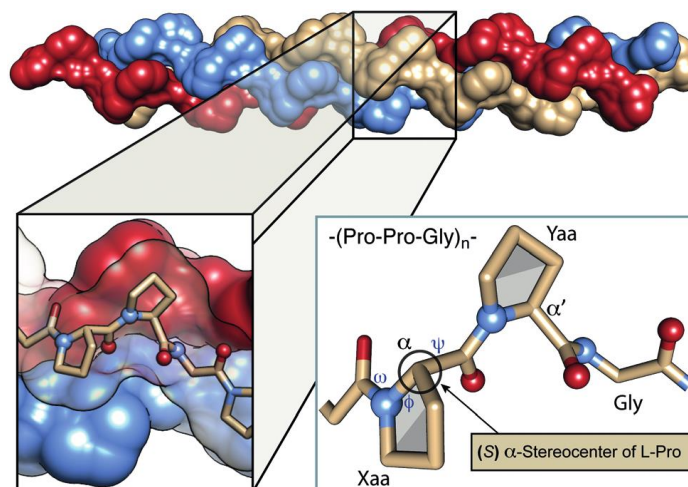


Figure 2.2 The collagen triple helix and an expanded view of the -ProPro-Gly-tripeptide repeat with adjacent view of the chemical structure.

Individual polypeptide chains are differentially colored red, blue, and beige. Detailed view of the tripeptide repeat (Xaa-Yaa-Gly) showing designated torsional descriptors and proline stereocenters. Heteroatoms are differentially colored red = oxygen, blue = nitrogen, and beige = carbon

Herein, we demonstrate that replacing a single amino acid stereocenter with a nitrogen atom results in a fluxional system with the capacity to mimic amino acid stereochemistry. First, we evaluated a proline rich dipeptide by replacing a single stereocenter with a nitrogen atom to create a stereodynamic perturbation at a central location. Next, this perturbation was assessed in the context of a triple helix forming collagen model peptide system. We demonstrate that a single stereodynamic atom dramatically alters the rate of triple helix self-assembly with little to no effect on the thermal unfolding, highlighting the vital importance of stereochemistry as a pre-organizing element in biomolecular folding and assembly events.

2.2 Results and Discussion

The tertiary structural motif adopted by collagen is a right-handed triple helix composed of three staggered polypeptide chains in a left-handed polyproline type-II (PPII) helical conformation (Figure 2.2). Over the past several decades, collagen has been the focus of many

research efforts aimed at developing a molecular level understanding of its self-assembling properties and for the development of designed materials.²²⁻³⁸ The most common repeating amino acid motif is XaaYaaGly, where Xaa is proline 28 % of the time, Yaa is either hydroxyproline (Hyp) or proline 38 % of the time, with the glycine remaining intolerant to substitution.¹⁹ To date, nearly all amino acid substitutions beyond the ProHypGly motif have led to significant destabilization of the collagen triple helix except for a few rare examples. The few instances of stabilizing amino acid substitutions that have been discovered to date have led to significant insight into protein structure, such as the stereoelectronic effects and $n \rightarrow \pi^*$ interactions pioneered by the Raines group.³⁹⁻⁴⁴ These studies have revealed that side-chain modification using unnatural amino acids can modulate the self-assembly properties of the triple-helical structure, pointing to a delicate balance of noncovalent interactions.⁴⁵⁻⁵⁸ Seminal studies on peptoid substitutions have also shown that N-alkylated glycine can be substituted for proline when a bulky hydrophobic side chain is used. This is the one example of an achiral proline replacement that has led to collagen triple helix stabilization.⁵⁹⁻⁶² In contrast to side chain modifications, collagen backbone modifications have resulted in significantly destabilized structures, often resulting in a complete inability to form a triple helical structure.⁶³⁻⁶⁵ Backbone modifications in the form of stereochemical inversion (L to D amino acids) and heteroatom replacement have all resulted in either severe destabilization or a complete lack of triple helix formation.⁶³⁻⁶⁸ Amide-to-ester substitutions also have a detrimental impact on collagen triple helix stability and many other protein secondary structures.⁶⁶ In addition, trans-alkene amide bond isosteres greatly destabilize the triple helical structure of collagen irrespective of positioning and involvement in hydrogen bonding.^{67,68} A recent example of thioamide substitution in collagen was demonstrated to have a minimally perturbing and modest stabilizing effect on the triple helix structure, depending on position, highlighting the importance of minimally perturbing backbone substitutions in proteins.⁶⁹⁻⁷² To date, these seminal studies have revealed a wealth of fundamental

insight into protein structure and point to a general intolerance of the collagen peptide backbone to molecular editing.^{19,63-68}

Intrigued by the possibility of nitrogen serving as a stereodynamic stereochemical mimic, we analyzed a model of the collagen triple helix based on existing crystal structures.²¹ The model revealed that aza-proline substitution in the Xaa position would potentially result in a solvent exposed nitrogen devoid of any deleterious electronic effects with main chain functional groups (Figure 2.3). In contrast, substitution at the Yaa position revealed a potential detrimental interstrand electrostatic interaction. After determining a strategic position for nitrogen backbone incorporation, we conducted a thorough survey of pyramidalized nitrogen containing small molecule crystal structures in the Cambridge Structural Database (see Figure 2.8 in Supplemental Information). This survey revealed that small molecule crystal structures containing AzPro and other tri-substituted amines display a broad range of pyramidal character (Figure 2.3 c, entry 1–26; Figure 2.8). To quantify the extent of pyramidalization (d), a triangular pyramid was defined with nitrogen at the apex and the substituent atoms positioned at the remaining vertices of the base. The distance from the apex normal to the base plane was measured as the d value, in angstroms, for each structure. The d value of aza-proline and other nitrogen containing small molecules was found to range from 0 to 0.6 Å (Figure 2.3 c). Applying this same measure to the proline α carbon in high-resolution crystal structures of triple helical collagen reveals an average pyramidalization distance of 0.53 ± 0.02 Å ($n = 36$) for effectively mimicking the stereogenic center with a nitrogen atom (Figure 2.3 c, top marker in entry “27”).

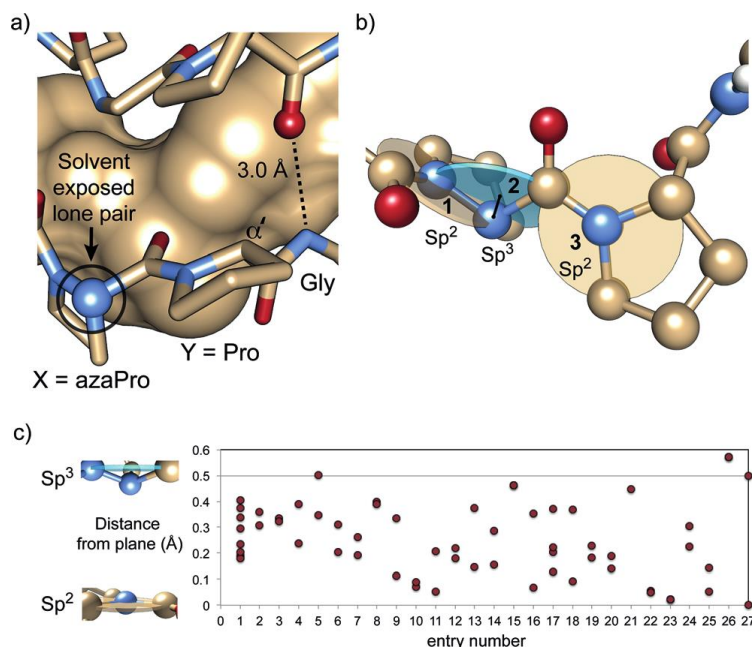


Figure 2.3 Docking analysis of AzPro-Pro in collagen and degree of pyramidalization analysis.

a) Model showing the position of AzPro containing collagen model peptide peptide **5**. b) ball-stick model of the di-propyl urea moiety in CMP **5**; black arrow and cyan plate show the distance d between N and the plane defined by its three connecting atoms, indicating the degree of pyramidalization c) Survey of the degree of pyramidalization of nitrogen atoms in AzPro-containing small molecule crystal structures found in the CCDC and other trisubstituted nitrogen containing small molecules. Details for entry numbers can be found in Figure 2.8 of the Supplemental Information.

To gauge the impact of AzPro incorporation we synthesized two small molecule model systems:

Ac-Pro-Pro-OMe (**1**) containing natural L-proline residues and Ac-AzPro-Pro-OMe (**2**)

containing a single AzPro residue in which the alpha-CH stereocenter has been replaced by

nitrogen, rendering the residue achiral (Figure 2.4, Scheme 2.1). AzPro has been previously

incorporated into small peptide systems and pioneering work on aza-amino acids has led to the

development of many important bioactive aza-peptides often showing increased biological

activity and/or improved pharmacokinetic properties.⁷³⁻⁸⁷ The proton NMR spectra of our

dipeptide model systems provide a striking picture of the difference in the conformational

dynamics between the parent dipeptide (**1**) and the AzPro containing dipeptide (**2**) (Figure 2.4).

The parent dipeptide system (**1**) exhibits well-resolved ^1H resonances in the NMR with visible

spin-spin splitting patterns. In contrast, the NMR spectrum of the dipeptide containing AzPro (**2**)

is severely line broadened and featureless, illustrating the fluxional nature of the nitrogen atom replacement (Figure 2.4).

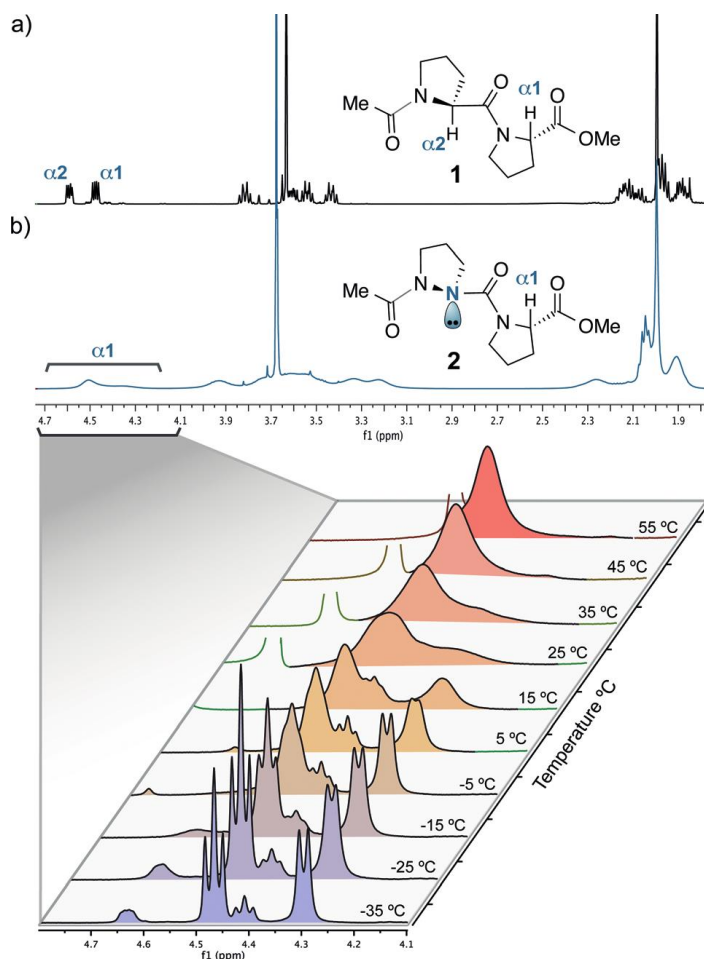


Figure 2.4 Impact of replacing an α -stereocenter with a nitrogen atom.

Prolyl dipeptide model system and the nitrogen substituted analogue shown with ^1H NMR data (taken in CDCl_3). a) Chemical structures of the Ac-Pro-Pro-OMe (**1**) dipeptide model system and ^1H NMR spectrum. b) Chemical structure of the Ac-AzPro-Pro-OMe (**2**) dipeptide model system and ^1H NMR spectrum. NMR spectra show severe broadening after replacement of the carbon stereocenter with a nitrogen atom. The nitrogen atom replacement is shown in blue with the lone pair. The α_1 proton region is expanded and shown at variable temperatures. Upon cooling, distinct conformer populations are observed.

We performed variable temperature ^1H NMR experiments to gain insight into the dynamics of the AzPro containing dipeptide **2**. Upon cooling dipeptide **2**, we observed that the broad α_1 proton signal split into four broad but defined conformer populations. Coalescence of the α_1 proton peaks begins at $-15\text{ }^\circ\text{C}$ and continues until all of the peaks coalesce near $40\text{ }^\circ\text{C}$. At temperatures of $-15\text{ }^\circ\text{C}$, discrete sets of signals were observed as exemplified by the expanded α_1

proton region shown in Figure 2.4 b. At $-35\text{ }^{\circ}\text{C}$, the apparent triplet and doublet peaks could be observed together with peaks that are still relatively broad in the aliphatic region, suggesting sub-populations of fluxional conformers with a certain degree of dynamism even at low temperature. Therefore, only qualitative conclusions could be drawn from the low temperature NMR experiments regarding the four different conformer populations in solution. The rate constants for the interconversion between conformer populations were estimated to be between $k_{tc} = 60\text{--}200\text{ s}^{-1}$ for the $\alpha 1$ conformer sub-populations with activation energies ranging from $\Delta G^{\ddagger} = 13\text{--}16\text{ kcal mol}^{-1}$ and relative ground state energies of $\leq 1\text{ kcal mol}^{-1}$. The dynamic nature of dipeptide 2 is extraordinary given the perturbation of only a single atom, providing a qualitative representation of the AzPro stereodynamics.

To gain insight into the accessible conformational space and the pyramidalization preference of AzPro dipeptide 2, we employed DFT calculations utilizing the 6-31g(d) basis sets to assess the possible low energy conformations available to the AzPro-Pro dipeptide (Figure 2.5). Nine low energy conformers (CE1) were determined with relative ground state energies less than 1 kcal mol^{-1} with approximately half of the population occupying a conformation mimicking D-proline and the other half of the population occupying a conformation mimicking L-proline. The full calculated ground state conformational ensemble (CE2) contained a total of 48 structures with relative energies less than 12 kcal mol^{-1} (Figure 2.5 a,b). The results in Figure 2.5 b provide an overlay of all 48 ground state structures colored according to their relative energies and a glimpse into the stereodynamic nature of aza-proline in the context of the sterically congested proline containing peptide 2 (Figure 2.5 b), which is in contrast to the stereostatic nature of the adjacent proline residue with locked alpha carbon stereochemistry. A subset of 35 conformers with relative energies less than 4 kcal mol^{-1} were further analyzed for pyramidal character and nitrogen-carbonyl bond lengths at each of the three nitrogen atoms shown in Figure 2.5 a. In general, N2 exhibited a clear preference for adopting a highly pyramidalized form and a longer

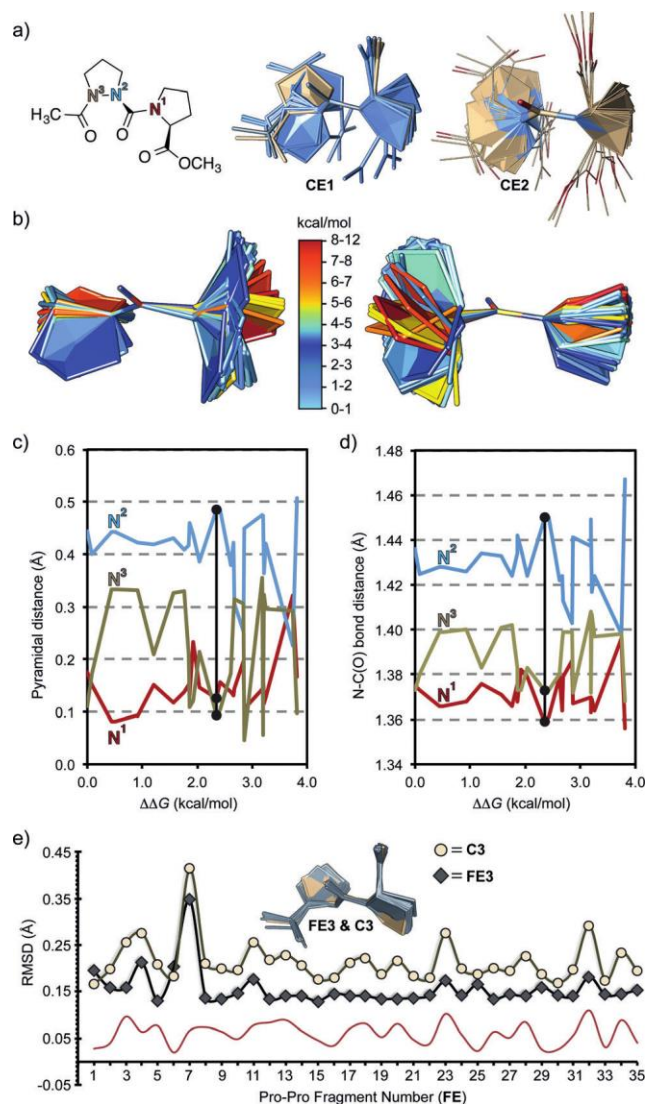


Figure 2.5 Computational analysis of the AzPro-Pro dipeptide.

a) (left) Chemical structure with labeled nitrogen atoms. (middle) Ensemble (CE1) of lowest energy conformers with relative energies less than 4 kcal/mol. (right) Ensemble (CE2) of all conformers found for the AzPro-Pro dipeptide **2** by DFT. b) Front and back view of the conformational ensemble calculated for the AzPro-Pro dipeptide color-coded by relative ground state energy shows the stereodynamic nature of AzPro (oriented toward middle) versus the stereostatic nature of proline (oriented toward left or right side). Low energy conformers exhibit both *D*- and *L*- proline mimicking conformations. Conformations where N^2 is planarized correlate with higher relative ground state energies. c) Pyramidalization distance for conformer ensemble CE1 plotted as a function of relative conformer energy for each nitrogen atom. Pyramidalization is defined as the distance *d* between N and the plane defined by its three connecting atoms, indicating the degree of pyramidalization. d) Plot of the nitrogen-carbonyl bond length for each of the three nitrogen atoms. e) Comparison of Pro-Pro dipeptide units from collagen crystal structures (FE3) to the conformer (C3) showing the small structural RMSD. Deviation between C3 and each member of FE3 is shown as the bottom line.

N-CO bond, which is consistent with the capacity to mimic both *D* and *L* forms of proline.

Nitrogen atoms N1 and N3 exhibited less pyramidal character with N1 showing a propensity

toward a more sp² amide-like geometry. The pyramidalization preferences paralleled the expectations for N-CO bond length trends, where structures with less pyramidal character exhibited shorter N-CO bond lengths (Figure 2.5 d). A comparison of the RMSD between the calculated structures and their dipeptide analogues found in the crystal structure of collagen yielded several low energy conformations capable of mimicking orientations compatible with the collagen triple helix, implying the feasibility of proline with AzPro. The calculated structure (C3) with the lowest average pairwise RMSD compared to the ensemble of fragments from the crystal structures is shown in Figure 2.5 e, and conformer C3 is indicated with black markers on the plots in Figure 2.5 c and d. The presence of additional low energy calculated structures suggest the conformationally dynamic nature of the dipeptide with the capacity to mimic both the D and L stereochemistry of proline.

Previous studies of small molecule and short peptide systems containing AzPro reveal that substitution of the alpha-CH by a nitrogen atom in the prolyl ring can result in perturbations to ring puckering, backbone conformation, and rotational barriers of the cis–trans amide bond preceding the prolyl residue compared to that of proline. Crystallography and computational studies have demonstrated the ability of both nitrogen atoms in AzPro to adopt a pyramidalized geometry; the bond lengths of CO-N and N α -CO are longer by up to 0.1 Å and shorter by 0.01–0.03 Å compared to a Pro residue, respectively, although this result most certainly varies with dihedral angle and molecular environment.⁸⁸⁻⁹⁷ NMR, IR, X-ray and computational studies support a cis amide bond preference for AzPro in certain situations, such as short peptides prone to adopt a type VI β -turn structure in organic solvents.⁸⁸⁻⁹⁵ Preference for the cis geometry in organic solvents has been attributed to the potential for a lp–lp interaction between N α and the preceding carbonyl in the trans conformation. This repulsive interaction is reported to be reduced in water resulting in a significant decrease in the cis amide preference.^{89,90} Simulations on tetrapeptides containing AzPro indicate that the cis–trans preference is highly variable and

context dependent.⁸⁸ Rotational barriers for cis–trans isomerization of the aza-prolyl amide bond have been calculated to be 16.7 kcal mol⁻¹ in water, which is 2.1–4.3 kcal mol⁻¹ lower than estimates of the cognate proline dipeptide.⁹¹ Building on previous studies and our current observations of AzPro incorporation into peptide 2, AzPro appears well suited as a stereodynamic mimic for proline at the X position within collagen model peptide systems.

Next, we focused on the impact of stereodynamics in the context of a full-length collagen model peptide system. Guided by insights gained from analysis of dipeptide fragments, we targeted the alpha stereocenter of proline in the Xaa position of the collagen peptide for replacement with a stereodynamic probe. Inspection of the Xaa position revealed a minimally perturbing solvent exposed environment, providing a logical choice for AzPro replacement (Figure 2.3 a). We synthesized peptides 3, 4 and 5, where peptide 5 constitutes replacement of a single stereogenic carbon atom with a single nitrogen atom at the central Xaa location in a 260 atom (21 amino acid) peptide system (Figure 2.6 a). Circular dichroism (CD) spectroscopy was used to evaluate self-assembly of the triple helix for each of our collagen model peptides. CD measurements of solutions containing collagen model peptides 3 and 5 exhibit characteristic maxima at approximately 224 nm, which is typical for the collagen triple helix structure (see Supplemental Information, SI).

Control peptide 4 containing D-proline exhibits a CD spectrum at 4 °C similar to that of 3 and 5, but with a reduced ellipticity maximum and a shallower minimum, indicating a lower propensity toward triple helix formation (Supplemental Information).²²⁻²⁸ Thermal CD denaturation experiments revealed that peptide 5 underwent a cooperative unfolding transition upon heating (Figure 2.6 and SI). In contrast, peptide 4 lacked the ability to self-assemble into a triple-helix structure, as evidenced by a linear decrease in molar ellipticity as a function of temperature. These results indicate that replacement of the stereocenter between two proline residues with a nitrogen atom (peptide 5) results in a stable triple helix that cooperatively unfolds

in a manner similar to the parent all L-amino acid configured collagen model peptide, 3, and at a similar unfolding temperature. The data from CD thermal denaturation experiments were fitted to a two-state model, as previously described.^{98,55,56} For peptide 3 and 5, the melting temperatures, at which 50 % of the triple helix unfolds, are nearly identical (<1 °C) (Figure 2.6 d). This observation reveals that an sp³-hybridized nitrogen atom can effectively mimic the geometry of a tertiary carbon stereogenic center in the context of a collagen model peptide system. The implication is that the L-proline conformation is effectively mimicked by the stereodynamic nitrogen in peptide 5, further supported by data from compound 4, showing that D-amino acids are detrimental to the formation of a stable triple helix in addition to previous reports.⁶³⁻⁶⁵

To probe the impact of stereodynamics on the kinetics of triple helix self-assembly, we monitored triple helix formation for peptides 3 and 5 using isothermal CD refolding experiments over a time course of 600 min. Peptides 3 and 5, at a concentration of 0.2 mM in PBS buffer, were denatured at 80 °C for 15 min, and their CD profiles were monitored at 4 °C until both peptides recovered >50 % ellipticity at 224 nm. A major difference was observed as peptide 5 approached 50 % recovery at a rate approximately 7 times slower than that of control peptide 3 (Figure 2.6 c). Hysteresis studies were performed to gain further insight into the stability of peptide 5.^{55,56,99} The free energy difference between peptides 3 and 5 is relatively large compared to the difference in T_m (Figure 2.6 b,d). Based on the hysteresis data and refolding studies, the origin of the free energy difference is consistent with an increase in the entropy term for peptide 5. There appears to be a compensatory effect in the enthalpy term even though the overall ΔG is less favorable. The ΔG was found to be -10.5 kcal mol⁻¹ for peptide 3 and -7.7 kcal mol⁻¹ for peptide 5 with a $\Delta\Delta G$ of 2.8 kcal mol⁻¹. The difference appears to be primarily rooted in the entropy term, considering the observed enthalpic benefit after replacing the stereocenter with nitrogen, although further calorimetric data is needed to reach a firm conclusion. The large difference in half time values for triple helix self-assembly is a striking demonstration of the

important role that stereochemistry plays in biopolymer preorganization; however, there are several other factors pertaining to AzPro that must be taken into consideration.

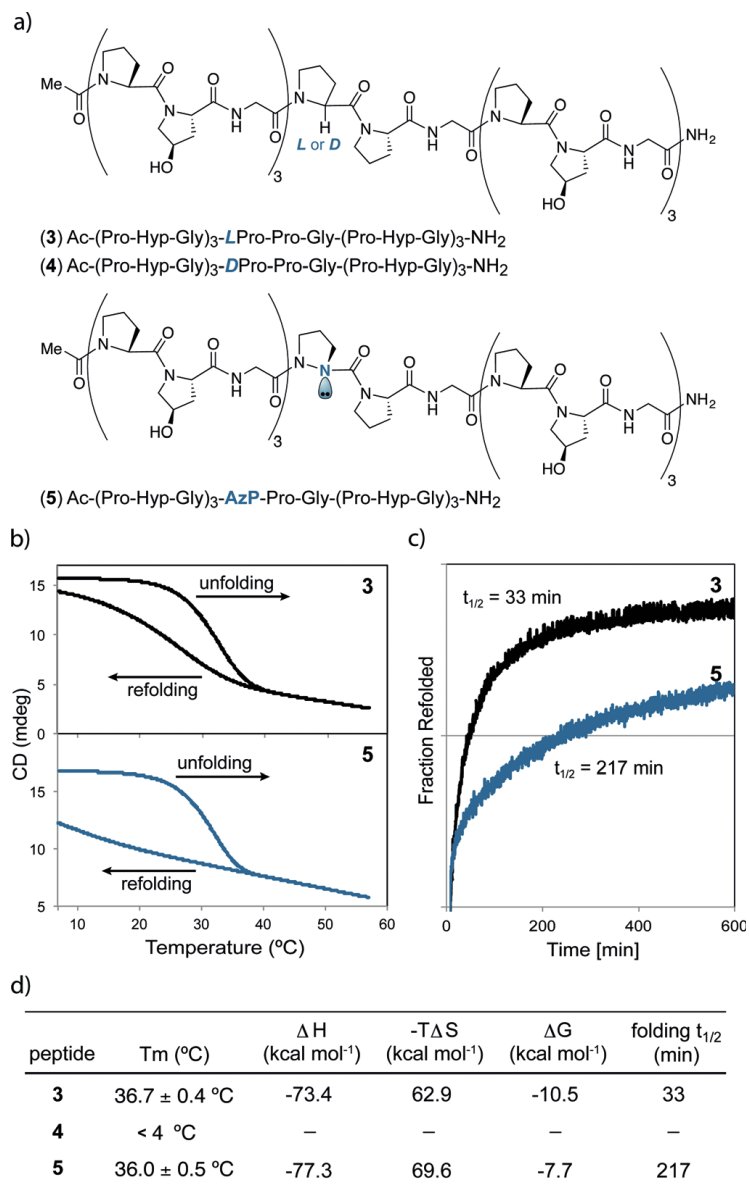


Figure 2.6 Unfolding and refolding data for collagen model peptides.

a) Chemical structure of collagen model peptides **3**, **4** and model peptide **5** containing a stereodynamic nitrogen atom. b) Unfolding and folding data for collagen model peptides showing the hysteresis difference. c) Kinetic refolding showing a 7-fold decrease in folding half time. d) Table of thermodynamic data and refolding half-times.

Taken collectively, the results reported herein support the notion that the nitrogen atom of the AzPro system can adopt an sp³-hybridized form, with a pyramidalized geometry effectively mimicking the stereocenter of proline in the context of a collagen triple helix. Substitution at the

Xaa position places the AzPro residue in the most sterically congested environment possible among the naturally occurring amino acids between two proline residues. A pyramidalized geometry implies decreased resonance stabilization when there is an electron withdrawing carbonyl substituent on nitrogen. However, in the case where the AzPro residue is adjacent to another proline residue, a ground state destabilized situation is created with enough steric congestion to preclude a planarized resonance stabilized pseudo-urea as supported by our calculations (Figure 2.5 d,e). This destabilized ground state may decrease the N-C(O) rotational barrier, allowing easy access to fluxional conformations spanning the continuum between fully delocalized and fully pyramidalized. In addition to a subtle but intricate balance of electronic, steric, and stereoelectronic effects, the fluxional nature of a stereodynamic perturbation also exerts an entropic cost during the process of triple-helix self-assembly, as reflected in the refolding kinetics of peptide 5 (Figure 2.6).

2.3 Conclusions

In conclusion, our study suggests that configurationally stable sp^3 -hybridized tertiary carbon stereocenters serve as preorganizing elements to lower the entropic barrier of biomolecular folding and self-assembly events. Pyramidalized nitrogen is able to mimic stereogenic carbon atoms effectively in biomolecular systems. The low nitrogen pyramidalization barrier creates a fluxional system capable of sampling conformational space. Conformational sampling can allow for enthalpic tuning of inter- and intramolecular interactions albeit with an entropic cost. In addition to insight into the fundamental importance of stereochemistry as a preorganizing element in natural systems, these studies may provide insight into diverse areas ranging from self-assembling materials and drug design to catalysis and synthetic receptors. Despite increased entropy being manifest in dynamic systems, herein lies the first experimental realization of the impact of stereodynamics in the context of a self-assembling biopolymer system utilizing a

stereodynamic single atom probe as an atomic mimic of an sp³-hybridized tertiary carbon stereocenter.

2.4 Acknowledgments

This work was supported by funding from the University of Pennsylvania. Instruments were supported by the National Science Foundation and the National Institutes of Health including HRMS (NIH RR-023444) and MALDI-MS (NSF MRI-0820996). We thank Prof. Dr. Helma Wennemers, Prof. Dr. Peter Bächinger and Dr. Roman Erdmann for advice on hysteresis studies.

2.5 Notes

Yitao Zhang performed the synthesis and characterization of the dipeptide and incorporation into collagen model peptides. Detailed analysis is discussed in his dissertation.

2.6 References

- (1) Srinivasan, R.; Rose, G. D. *Proc. Natl. Acad. Sci. USA* **1999**, *96*, 14258.
- (2) Anfinsen, C. B. *Science* **1973**, *181*, 223.
- (3) Eliel, E. L.; Wilen, S. *Stereochemistry of Organic Compounds*, Wiley Interscience: New York, 1994.
- (4) He, M.; Bode, J. W. *Proc. Natl. Acad. Sci. USA* **2011**, *108*, 14752.
- (5) Barrett, K. T.; Metrano, A. J.; Rablen, P. R.; Miller, S. J. *Nature* **2014**, *509*, 71.
- (6) Wang, J.; Feringa, B. L. *Science* **2011**, *331*, 1429.
- (7) Clayden, J.; Lund, A.; Vallverdú, L.; Helliwell, M. *Nature* **2004**, *431*, 966.
- (8) Kay, B. K.; Williamson, M. P.; Sudol, M. *FASEB J.* **2000**, *14*, 231.
- (9) MacArthur, M. W.; Thornton, J. M. *J. Mol. Biol.* **1991**, *218*, 397.
- (10) Pauling, L.; Corey, R. B. *Nature* **1951**, *168*, 550.
- (11) Hazen, A. R. M. *Genesis: The Scientific Quest for Life's Origin*, Henry: Washington, 2005.

- (12) Joyce, G. F.; Visser, G. M.; Van Boeckel, C. A. A.; Van Boom, J. H.; Orgel, L. E.; Van Westrenen, J. *Nature* **1984**, *310*, 602.
- (13) Pauling, L. *The Nature of the Chemical Bond*, 3rd ed., Cornell University Press: Ithaca, 1960.
- (14) Ramachandran, G. N.; Ramakrishnan, C.; Sasisekharan, V. *J. Mol. Biol.* **1963**, *7*, 95.
- (15) Lambert, J. B. *Organonitrogen Stereodynamics*, Vol. 1, 1st ed., VCH: New York, 1992.
- (16) O'Neil, K. T.; DeGrado, W. F. *Science* **1990**, *250*, 646.
- (17) Ramachandran, G. N.; Kartha, G. *Nature* **1954**, *174*, 269.
- (18) Rich, A.; Crick, F. H. *J. Mol. Biol.* **1961**, *3*, 483.
- (19) Shoulders, M. D.; Raines, R. T. *Annu. Rev. Biochem.* **2009**, *78*, 929.
- (20) Bella, J.; Eaton, M.; Brodsky, B.; Berman, H. M. *Science* **1994**, *266*, 75.
- (21) Brodsky, B.; Thiagarajan, G.; Madhan, B.; Kar, K. *Biopolymers* **2008**, *89*, 345.
- (22) Holmgren, S. K.; Taylor, K. M.; Bretscher, L. E.; Raines, R. T. *Nature* **1998**, *392*, 666.
- (23) Fields G. B.; Prockop, D. J. *Biopolymers* **1996**, *40*, 345.
- (24) Engel, J. Bächinger, H. P. *Top. Curr. Chem.* **2005**, *247*, 7.
- (25) Ackerman, M. S.; Bhate, M.; Shenoy, N.; Beck, K.; Ramshaw, J. A. M.; Brodsky, B. *J. Biol. Chem.* **1999**, *274*, 7668.
- (26) Persikov, A. V.; Ramshaw, J. A. M.; Kirkpatrick, A.; Brodsky, B. *Biochemistry* **2000**, *39*, 14960.
- (27) Vitagliano, L.; Berisio, R.; Mazzarella, L.; Zagari, A. *Biopolymers* **2001**, *58*, 459.
- (28) Berisio, R.; Vitagliano, L.; Mazzarella, L.; Zagari, A. *Protein Sci.* **2002**, *11*, 262.
- (29) Kusebauch, U.; Cadamuro, S. A.; Musiol, H.-J.; Lenz, M. O.; Wachtveitl, J.; Moroder, L.; Renner, C. *Angew. Chem. Int. Ed.* **2006**, *45*, 7015.
- (30) Cejas, M. A.; Kinney, W. A.; Chen, C.; Leo, G. C.; Tounge, B. A.; Vinter, J. G.; Joshi, P. P.; Maryanoff, B. E. *J. Am. Chem. Soc.* **2007**, *129*, 2202.

- (31) Rele, S.; Song, Y.; Apkarian, R. P.; Qu, Z.; Conticello, V. P.; Chaikof, E. L. *J. Am. Chem. Soc.* **2007**, *129*, 14780.
- (32) Yamazaki, C. M.; Asada, S.; Kitagawa, K.; Koide, T. *Biopolymers* **2008**, *90*, 816.
- (33) Pires, M. M.; Przybyla, D. E.; Chmielewski, J. *Angew. Chem. Int. Ed.* **2009**, *48*, 7813.
- (34) Lee, S.-G.; Lee, J. Y.; Chmielewski, J. *Angew. Chem. Int. Ed.* **2008**, *47*, 8429.
- (35) Fallas, J. A.; Gauba, V.; Hartgerink, J. D. *J. Biol. Chem.* **2009**, *284*, 26851.
- (36) Fields, G. B. *Org. Biomol. Chem.* **2010**, *8*, 1237.
- (37) Jiang, T.; Xu, C.; Zuo, X.; Conticello, V. P. *Angew. Chem. Int. Ed.* **2014**, *53*, 8367.
- (38) Tanrikulu, I. C.; Raines, R. T. *J. Am. Chem. Soc.* **2014**, *136*, 13490.
- (39) Bartlett, G. J.; Choudhary, A.; Raines, R. T.; Woolfson, D. N. *Nat. Chem. Biol.* **2010**, *6*, 615.
- (40) Choudhary, A.; Gandla, D.; Krow, G. R.; Raines, R. T. *J. Am. Chem. Soc.* **2009**, *131*, 7244.
- (41) Jakobsche, C. E.; Choudhary, A.; Miller, S. J.; Raines, R. T. *J. Am. Chem. Soc.* **2010**, *132*, 6651.
- (42) Newberry, R. W.; VanVeller, B.; Guzei, I. A.; Raines, R. T. *J. Am. Chem. Soc.* **2013**, *135*, 7843.
- (43) Choudhary, A.; Newberry, R. W.; Raines, R. T. *Org. Lett.* **2014**, *16*, 3421.
- (44) Newberry, R. W.; Bartlett, G. J.; VanVeller, B.; Woolfson, D. N.; Raines, R. T. *Protein Sci.* **2014**, *23*, 284.
- (45) Holmgren, S. K.; Taylor, K. M.; Bretscher, L. E.; Raines, R. T. *Nature* **1998**, *392*, 666.
- (46) Holmgren, S. K.; Bretscher, L. E.; Taylor, K. M.; Raines, R. T. *Chem. Biol.* **1999**, *6*, 63.
- (47) Bretscher, L. E.; Jenkins, C. L.; Taylor, K. M.; DeRider, M. L.; Raines, R. T. *J. Am. Chem. Soc.* **2001**, *123*, 777.
- (48) Hodges, J. A.; Raines, R. T. *J. Am. Chem. Soc.* **2003**, *125*, 9262.

- (49) Shoulders, M. D.; Hodges, J. A.; Raines, R. T. *J. Am. Chem. Soc.* **2006**, *128*, 8112.
- (50) Kotch, F. W.; Guzei, I. A.; Raines, R. T. *J. Am. Chem. Soc.* **2008**, *130*, 2952.
- (51) Cadamuro, S. A.; Reichold, R.; Kusebauch, U.; Musiol, H.-J.; Renner, C.; Tavan, P.; Moroder, L. *Angew. Chem. Int. Ed.* **2008**, *47*, 2143.
- (52) Umashankara, M.; Babu, I. R.; Ganesh, K. N. *Chem. Commun.* **2003**, 2606.
- (53) Erdmann, R. S.; Wennemers, H. *J. Am. Chem. Soc.* **2010**, *132*, 13957.
- (54) Shoulders, M. D.; Satyshur, K. A.; Forest, K. T.; Raines, R. T. *Proc. Natl. Acad. Sci. USA* **2010**, *107*, 559.
- (55) Erdmann, R. S.; Wennemers, H. *Angew. Chem. Int. Ed.* **2011**, *50*, 6835.
- (56) Erdmann, R. S.; Wennemers, H. *J. Am. Chem. Soc.* **2012**, *134*, 17117.
- (57) Siebler, C.; Erdmann, R. S.; Wennemers, H. *Chimia* **2013**, *67*, 891.
- (58) Siebler, C.; Erdmann, R. S.; Wennemers, H. *Angew. Chem. Int. Ed.* **2014**, *53*, 10340.
- (59) Goodman, M.; Melacini, G.; Feng, Y. *J. Am. Chem. Soc.* **1996**, *118*, 10928.
- (60) Feng, Y.; Melacini, G.; Taulane, J. P.; Goodman, M. *Biopolymers* **1996**, *39*, 859.
- (61) Feng, Y.; Melacini, G.; Goodman, M. *Biochemistry* **1997**, *36*, 8716.
- (62) Goodman, M.; Bhumralkar, M.; Jefferson, E. A.; Kwak, J.; Locardi, E. *Biopolymers* **1998**, *47*, 127.
- (63) Frey, P.; Nitschmann, H. *Helv. Chim. Acta* **1976**, *59*, 1401.
- (64) Shah, N. K.; Brodsky, B.; Kirkpatrick, A.; Ramshaw, J. A. M. *Biopolymers* **1999**, *49*, 297.
- (65) Horng, J. C.; Kotch, F. W.; Raines, R. T. *Protein Sci.* **2007**, *16*, 208.
- (66) Jenkins, C. L.; Vasbinder, M. M.; Miller, S. J.; Raines, R. T. *Org. Lett.* **2005**, *7*, 2619.
- (67) Dai, N.; Wang, X. J.; Etzkorn, F. A. *J. Am. Chem. Soc.* **2008**, *130*, 5396.
- (68) Dai, N.; Etzkorn, F. A. *J. Am. Chem. Soc.* **2009**, *131*, 13728.
- (69) Newberry, R. W.; VanVeller, B.; Raines, R. T. *Chem. Commun.* **2015**, *51*, 9624.
- (70) Goldberg, J. M.; Batjargal, S.; Petersson, E. J. *J. Am. Chem. Soc.* **2010**, *132*, 14718.

- (71) Batjargal, S.; Wang, Y. J.; Goldberg, J. M.; Wissner, R. F.; Petersson, E. J. *J. Am. Chem. Soc.* **2012**, *134*, 9172.
- (72) Petersson, E. J.; Goldberg, J. M.; Wissner, R. F. *Phys. Chem. Chem. Phys.* **2014**, *16*, 6827.
- (73) Hess, H.-J.; Moreland, W. T.; Laubach, G. D. *J. Am. Chem. Soc.* **1963**, *85*, 4040.
- (74) Niedrich, H.; Oehme, C. J. *J. Prakt. Chem.* **1972**, *314*, 759.
- (75) Ho, T. L.; Nestor, J. J.; McCrae, G. I.; Vickery, B. H. *Int. J. Pept. Protein Res.* **1984**, *24*, 79.
- (76) Dutta, A. S.; Furr, B. J. A. *Annu. Rep. Med. Chem.* **1985**, *20*, 203.
- (77) Zega, A. *Curr. Med. Chem.* **2005**, *12*, 589.
- (78) Dutta, A. S.; Furr, B. J. A.; Giles, M. B.; Valcaccia, B. J. *Med. Chem.* **1978**, *21*, 1018.
- (79) Han, H.; Yoon, J.; Janda, K. D. *Bioorg. Med. Chem. Lett.* **1998**, *8*, 117.
- (80) Boeglin, D.; Lubell, W. D. *J. Comb. Chem.* **2005**, *7*, 864.
- (81) Gante, J. *Angew. Chem. Int. Ed. Engl.* **1994**, *33*, 1699.
- (82) Melendez, R. E.; Lubell, W. D. *J. Am. Chem. Soc.* **2004**, *126*, 6759.
- (83) Proulx, C.; Sabatino, D.; Hopewell, R.; Spiegel, J.; Gaicía Ramos, Y.; Lubell, W. D. *Future Med. Chem.* **2011**, *3*, 1139.
- (84) Gante, J. *Synthesis* **1989**, 405.
- (85) Freeman, N. S.; Hurevich, M.; Gilon, C. *Tetrahedron* **2009**, *65*, 1737.
- (86) Sabatino, D.; Proulx, C.; Kloczek, S.; Bourguet, C. B.; Boeglin, D.; Ong, H.; Lubell, W. D. *Org. Lett.* **2009**, *11*, 3650.
- (87) Freeman, N. S.; Tal-Gan, Y.; Klein, S.; Levitzki, A.; Gilon, C. *J. Org. Chem.* **2011**, *76*, 3078.
- (88) Zhang, W. J.; Berglund, A.; Kao, J. L.; Couty, J. P.; Gershengorn, M. C.; Marshall, G. R. *J. Am. Chem. Soc.* **2003**, *125*, 1221.
- (89) Che, Y.; Marshall, G. R. *J. Org. Chem.* **2004**, *69*, 9030.

- (90) Che, Y.; Marshall, G. R. *Biopolymers* **2006**, *81*, 392.
- (91) Kang, Y. K.; Byun, B. J. *J. Phys. Chem. B* **2007**, *111*, 5377.
- (92) Didierjean, C.; Duca, V. D.; Benedetti, E.; Aubry, A.; Zouikri, M.; Marraud, M.; Boussard, G. *J. Pept. Res.* **1997**, *50*, 451.
- (93) Lecoq, A.; Boussard, G.; Marraud, M. *Tetrahedron Lett.* **1992**, *33*, 5209.
- (94) Lecoq, A.; Boussard, G.; Marraud, M.; Aubry, A. *Biopolymers* **1993**, *33*, 1051.
- (95) Zouikri, M.; Vicherat, A.; Aubry, A.; Marraud, M.; Boussard, G. *J. Pept. Res.* **1998**, *52*, 19.
- (96) Lee, H.-J.; Ahn, I.-A.; Ro, S.; Choi, K.-H.; Choi, Y.-S.; Lee, K.-B. *J. Pept. Res.* **2000**, *56*, 35.
- (97) Lee, H.-J.; Song, J.-W.; Choi, Y.-S.; Park, H.-M.; Lee, K.-B. *J. Am. Chem. Soc.* **2002**, *124*, 11881.
- (98) Engel, J.; Chen, H. T.; Prockop, D. J.; Klump, H. *Biopolymers* **1977**, *16*, 601.
- (99) Mizuno, K.; Boudko, S. P.; Engel, J.; Bächinger, H. P. *Biophys. J.* **2010**, *98*, 3004.

2.7 Supplemental Information

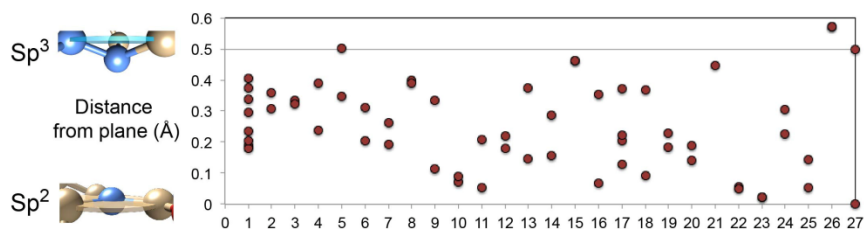
2.7.1 General Information

All commercial reagents and solvents were used as received. Fmoc-Pro-OH, Fmoc-Gly-OH, HBTU and Rink Amide AM Resin (100-200 mesh) were purchased from Novabiochem. Fmoc-Hyp(tBu)-OH and Fmoc-D-Pro-OH were purchased from Advanced Chemtech. Piperidine was purchased from American Bioanalytical. Triphosgene was purchased from Acros Organics. All remaining chemicals were purchased from Sigma Aldrich. Flash column chromatography was performed using Silicycle silica gel (55–65 Å pore diameter). Thin-layer chromatography was performed on Sorbent Technologies silica plates (250 µm thickness). Infrared (IR) spectra were obtained on PerkinElmer FT-IR Spectrum BX system and reported as wavenumber of the absorption maxima between 4000 cm⁻¹ and 800 cm⁻¹ of only major peaks. Proton nuclear magnetic resonance spectroscopy (¹H NMR) and carbon nuclear magnetic resonance spectroscopy (¹³C NMR) spectra were recorded on a Bruker UNI 500 ¹H NMR. High-resolution mass spectra were obtained at the University of Pennsylvania's Mass Spectrometry Service Center on a Micromass AutoSpec electrospray/chemical ionization spectrometer. Mass of long peptides were obtained via a Bruker Ultraflex III Matrix-assisted laser desorption/ionization(MALDI) mass spectrometer. Ultraviolet absorption spectrophotometry was performed on a JASCO V-650 spectrophotometer with a PAC-743R multichannel Peltier using quartz cells with a 1 cm cell path length. High performance liquid chromatography analysis was performed using a Jasco HPLC instrument equipped with a Phenomenex column (Luna 5u C18(2) 100A; 250 × 4.60 mm, 5 µm). Circular dichroism experiments were performed with an Aviv 410 CD Spectrometer at University of Pennsylvania Biochemistry/Chemistry Resource Center. All calculations were performed using Gaussian 09.1 All local minima were optimized in gas phase using DFT-B3LYP 6-31G(d) basis set, which were then confirmed to be stable and

have no imaginary frequencies by stability and frequency calculations, respectively, on the same basis set.

2.7.2 Crystal Structure Analysis on Known Compounds Containing Aza-proline and Tertiary Amines

Crystal structure analysis was performed on compounds within the Cambridge Structural Database. Analysis was conducted using ConQuest Version 1.17 (Build RC5) with the database CSD Version 5.36 (November 2014) on 2015-02-25, implementing the substructure search outlined in the figures below. In each search, the distance from a nitrogen atom to the plane formed by its three adjacent atoms was measured, and the number of structures found by a particular search was also recorded and graphed alongside the aforementioned pyramidalization distance.



CCDC #	Entry #	distance (Ang)	distance (Ang)	distance (Ang)	distance (Ang)	distance (Ang)	distance (Ang)	distance (Ang)	distance (Ang)
LINFUJ	1	0.374	0.404	0.337	0.294	0.189	0.179	0.205	0.236
PILCUI	2	0.307	0.359						
PILCOC	3	0.336	0.322						
PILDAP	4	0.389	0.239						
AXOWAM	5	0.502	0.346						
BAFTEI	6	0.31	0.204						
BAGNIH	7	0.262	0.192						
BAGZOA	8	0.399	0.388						
BAGZOZ	9	0.335	0.113						
BCZNON	10	0.07	0.088						
BEMHPO	11	0.207	0.052						
BIVWEJ	12	0.219	0.18						
BOSFEV	13	0.373	0.148						
BUFWEE	14	0.285	0.155						
BUGJUU	15	0.462	0.462						
BZLPRZ	16	0.353	0.069						
CEZDER	17	0.37	0.128	0.204	0.224				
DELDAZ	18	0.368	0.091						
DIFZAU	19	0.182	0.228						
DIFZEY	20	0.188	0.142						
QIHBAM	21	0.447							
DUVWOG	22	0.055	0.051						
DUXYUQ	23	0.022	0.022						
DUZCAD	24	0.305	0.227						
DUZFEK	25	0.052	0.145						
EHAJUS	26	0.57	0.572						
Collagen	27	0.5	0						

Figure 2.7 Survey of known crystal structure containing aza-proline and other pyramidalized nitrogen atoms with at least one carbonyl containing substituent

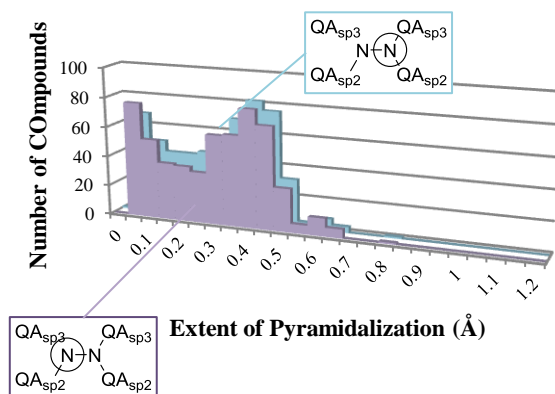
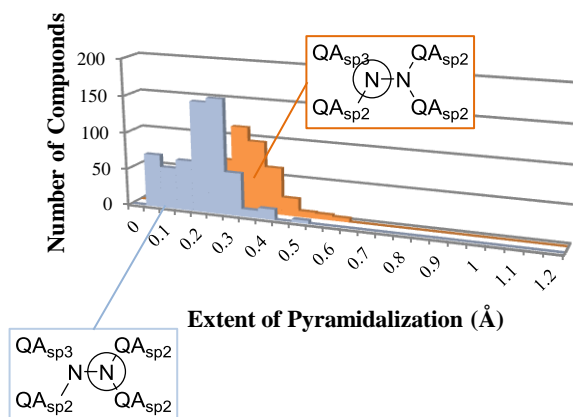
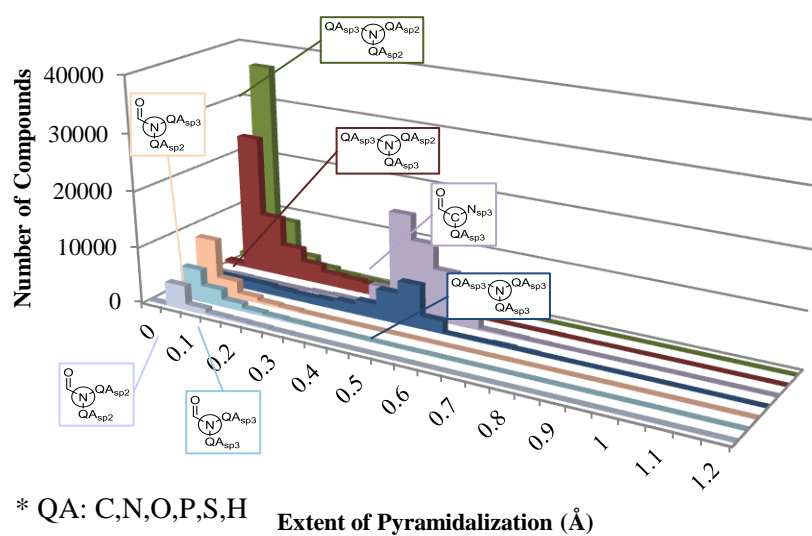
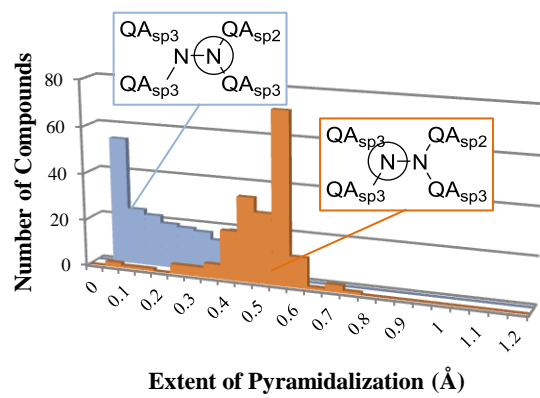
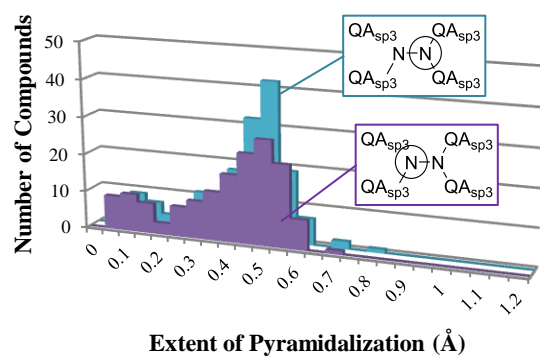
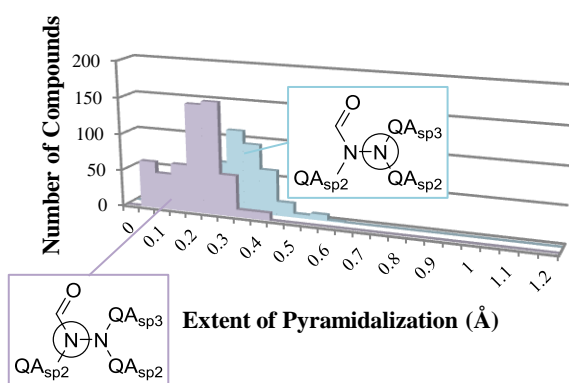
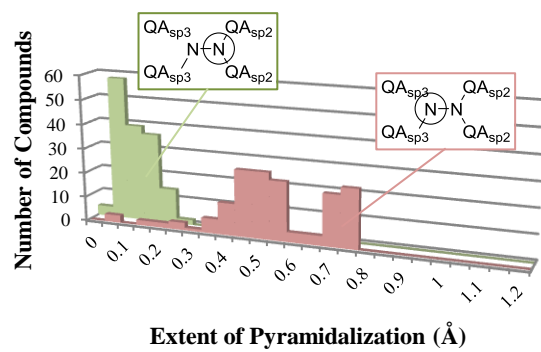


Figure 2.8 Examination of extent of pyramidalization of nitrogen containing compounds in the Cambridge Structural Database





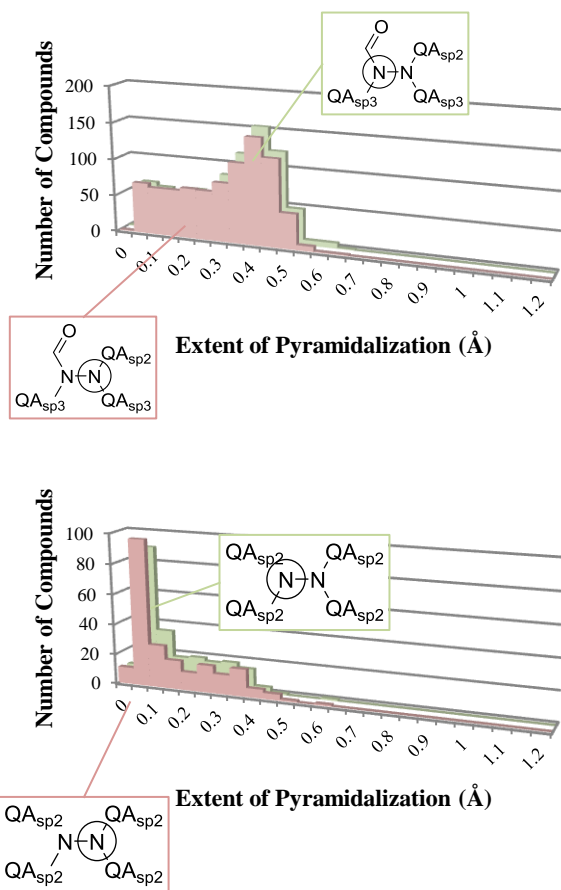
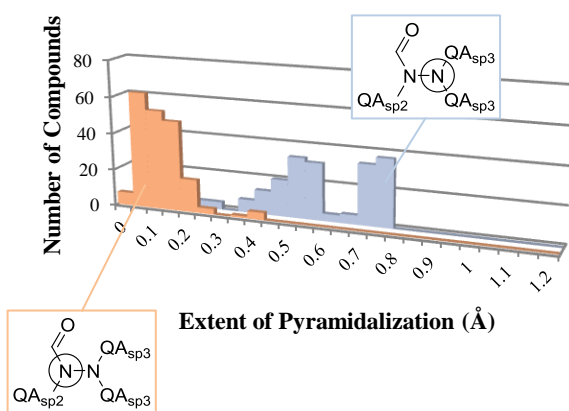
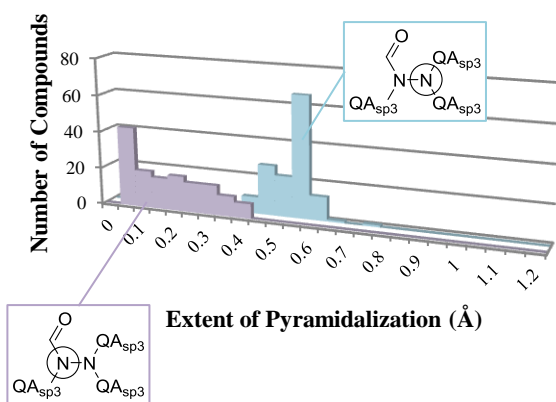


Figure 2.9. Examination of extent of pyramidalization of nitrogen containing compounds in the Cambridge Structural Database



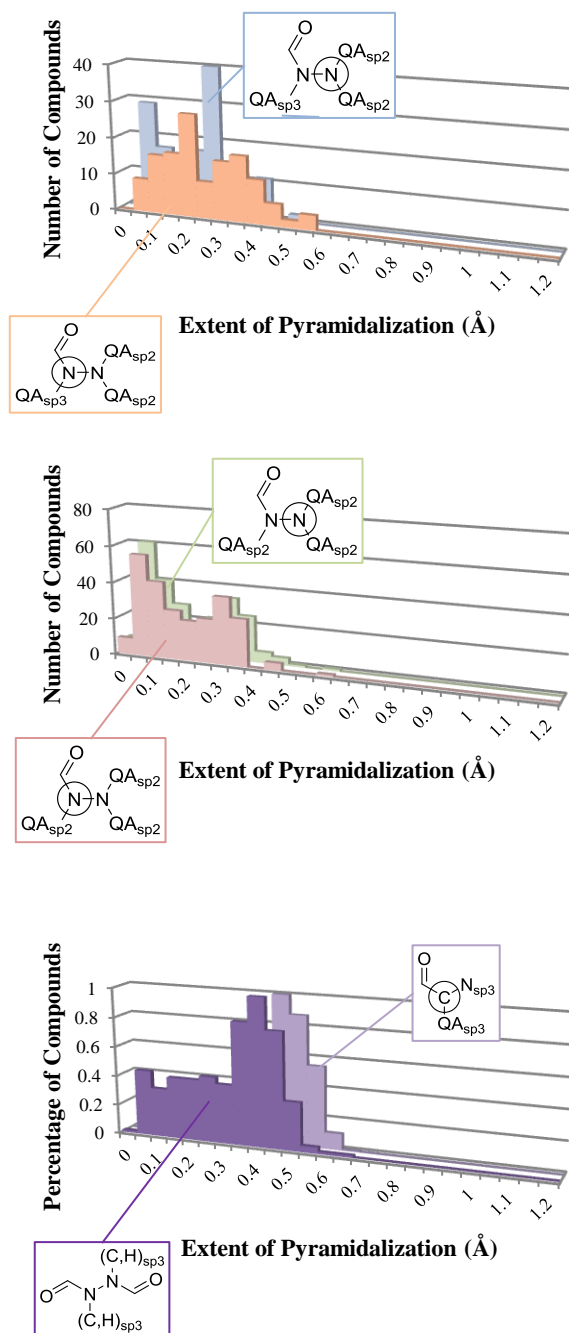


Figure 2.10 Examination of extent of pyramidalization of nitrogen containing compounds in the Cambridge Structural Database

2.7.3 DFT-B3LYP Calculated Conformations

Conformations 0.00-0.99 kcal mol⁻¹

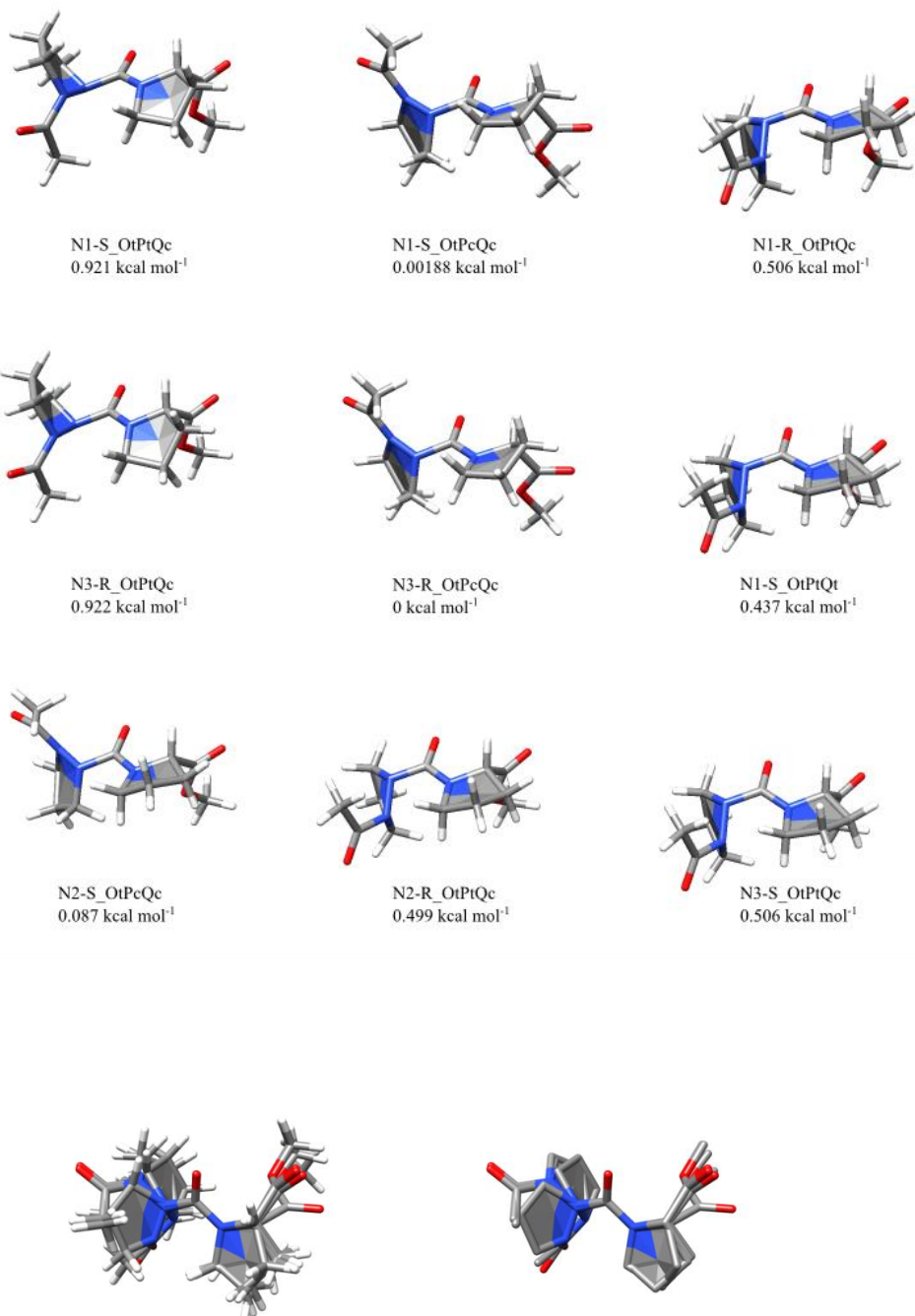


Figure 2.11 Calculated conformations using 6-31G(d) basis set with energies 0.00-0.99 kcal mol⁻¹

Conformations 1.00-1.99 kcal mol⁻¹

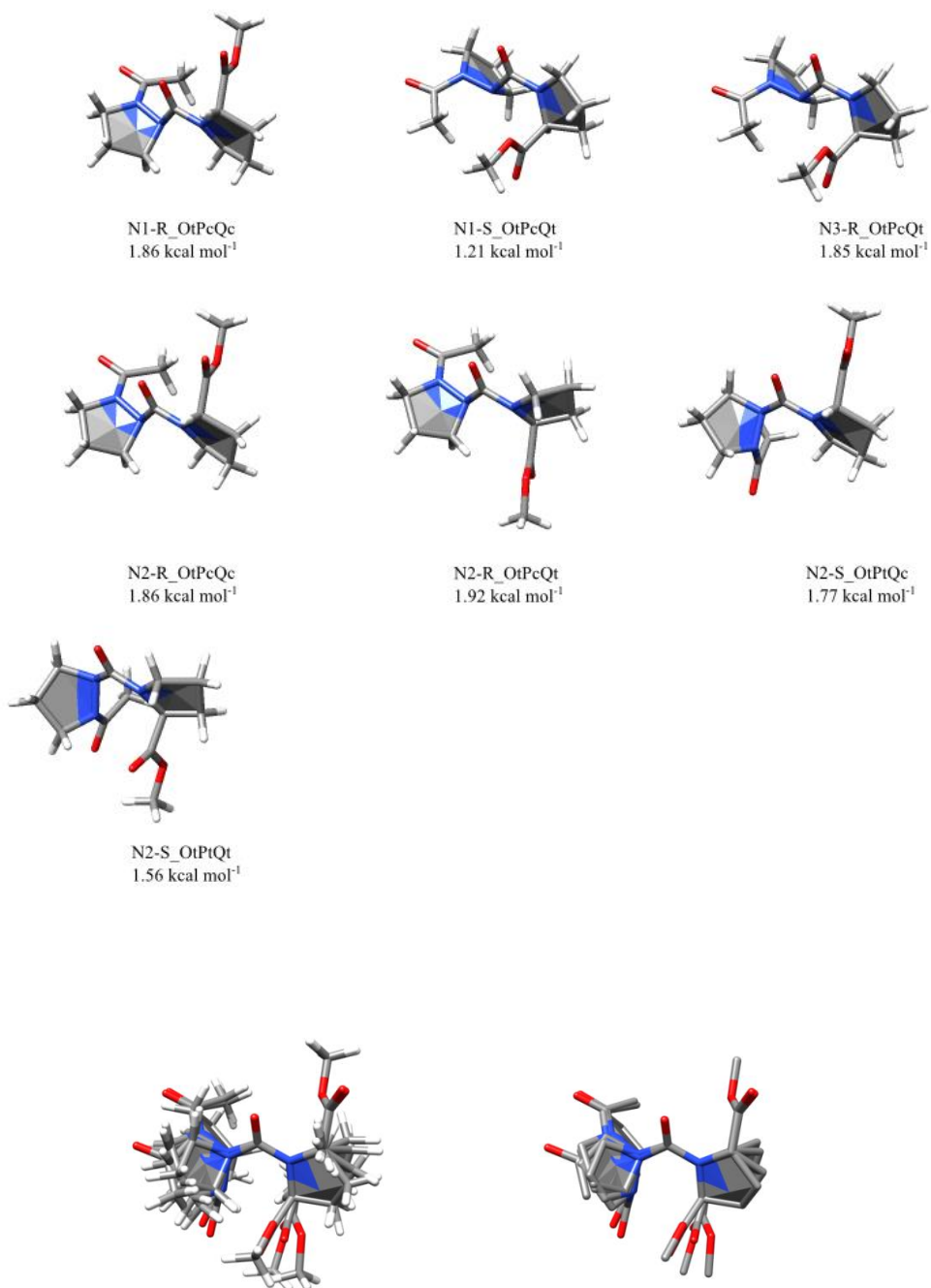


Figure 2.12 Calculated conformations using 6-31G(d) basis set with energies between 1.00-1.99 kcal mol⁻¹

Conformations 2.00-2.99 kcal mol⁻¹

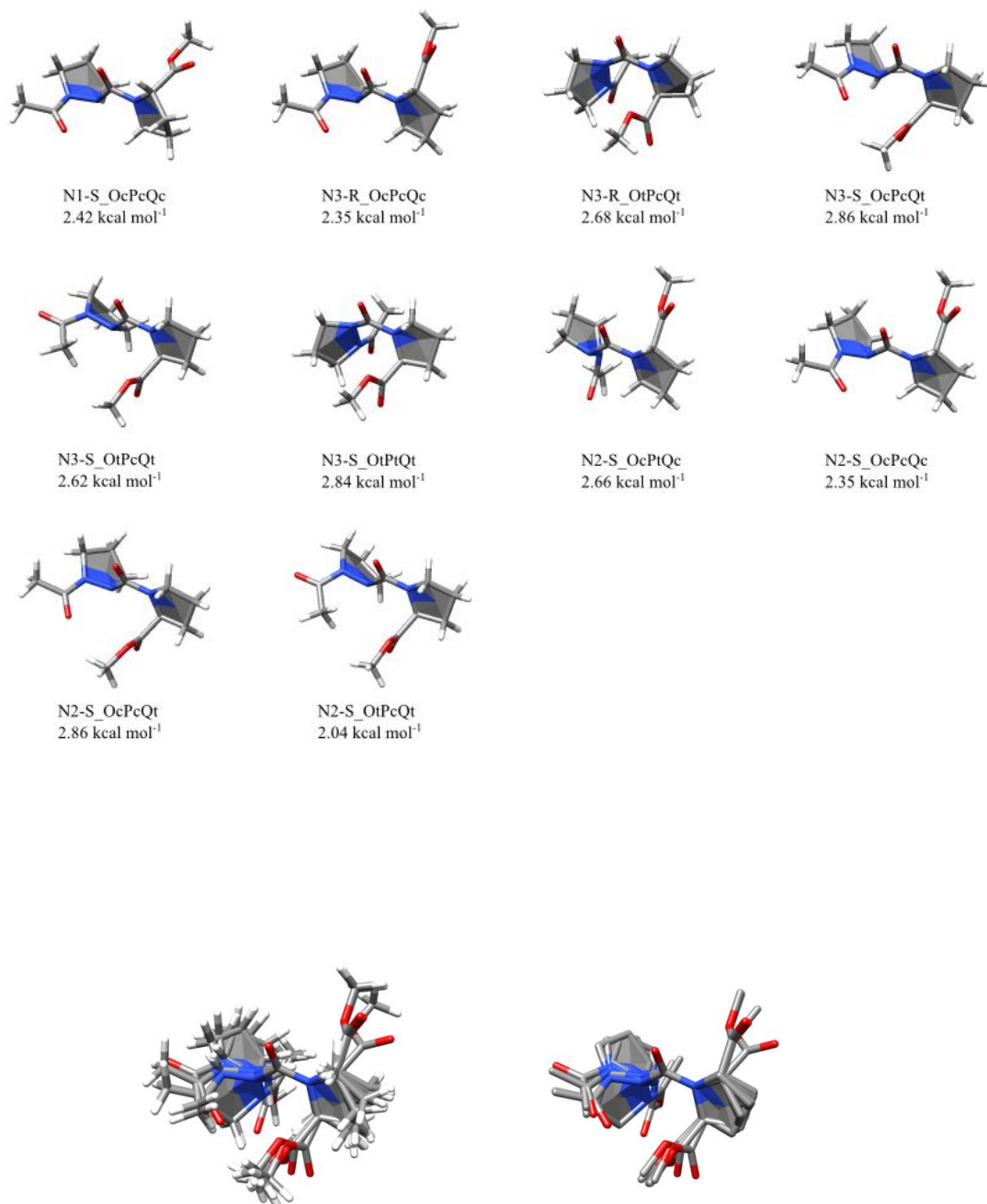


Figure 2.13 Calculated conformations using 6-31G(d) basis set with energies 2.00-2.99 kcal mol⁻¹

Conformations 3.00-3.99 kcal mol⁻¹

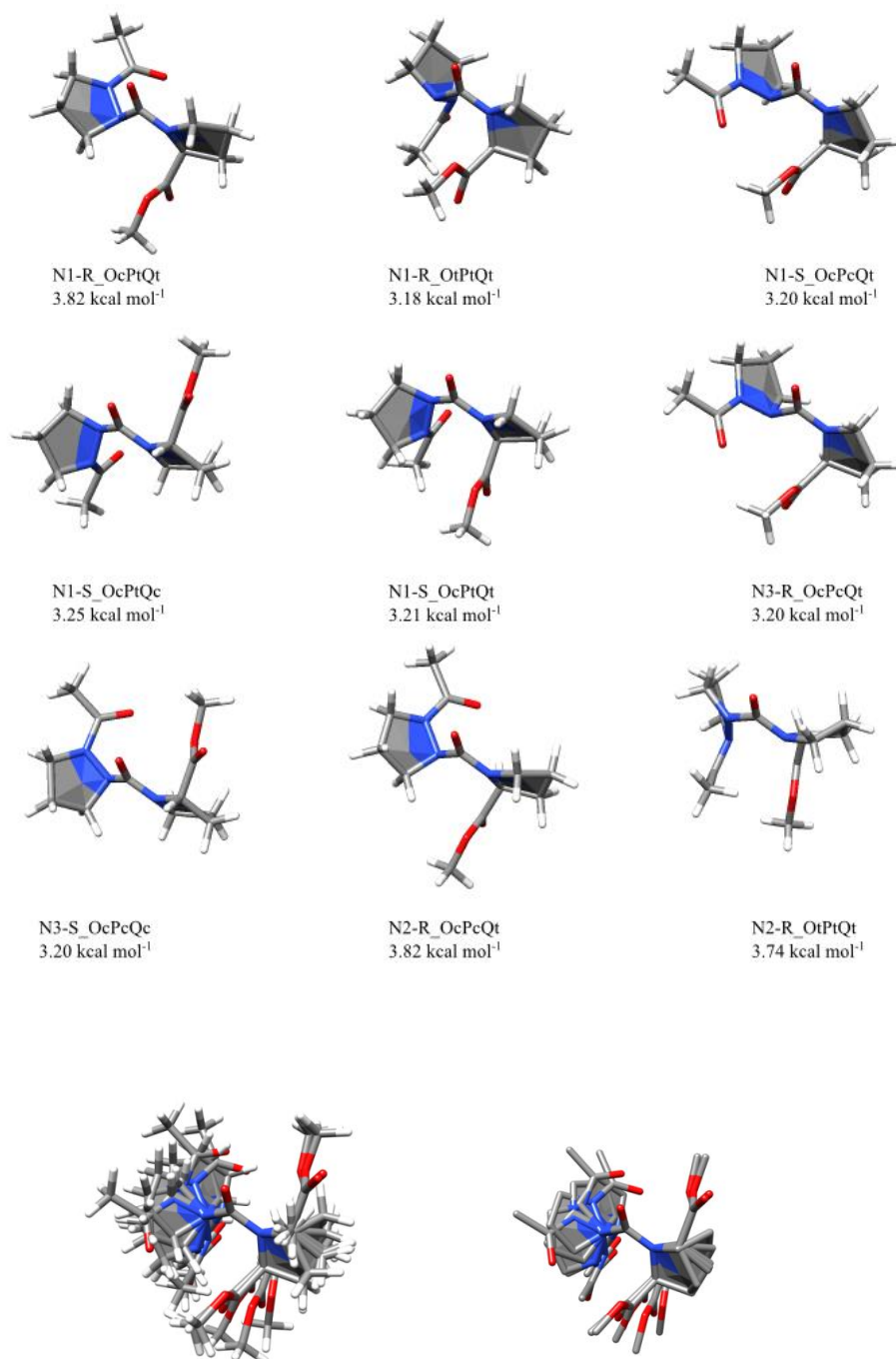


Figure 2.14 Calculated conformations using 6-31G(d) basis set with energies between 3.00-3.99 kcal mol⁻¹

Conformations 4.00-6.99 kcal mol⁻¹

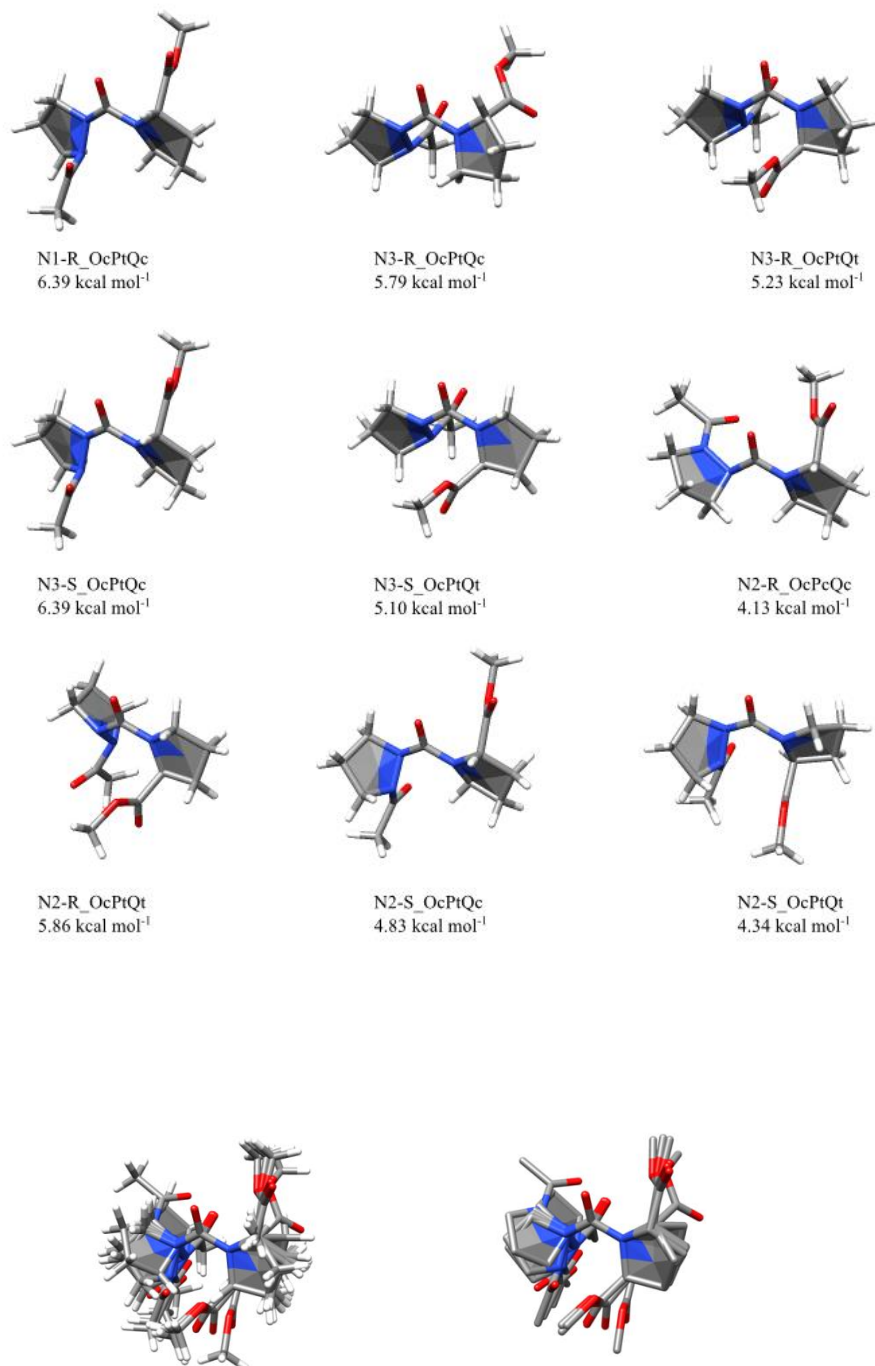
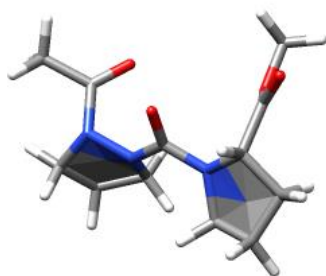
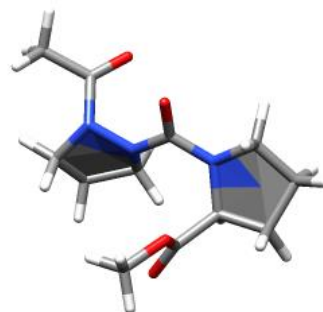


Figure 2.15 Calculated conformations using 6-31G(d) basis set with energies between 4.00-6.99 kcal mol⁻¹

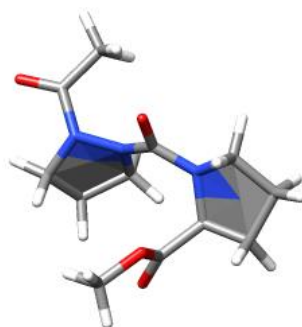
Conformations 7.00-12.00 kcal mol⁻¹



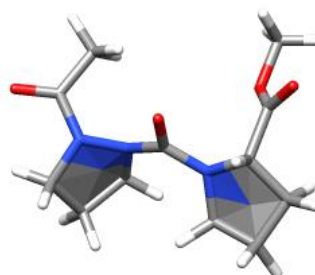
N1-R_OcPcQc
11.03 kcal mol⁻¹



N1-R_OcPcQt
11.63 kcal mol⁻¹



N1-R_OtPcQt
8.04 kcal mol⁻¹



N3-S_OtPcQc
7.11 kcal mol⁻¹

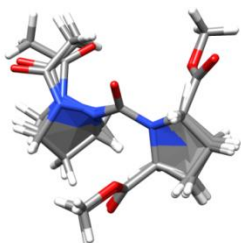


Figure 2.16 Calculated conformations using 6-31G(d) basis set with energies between 7.00-12.00 kcal mol⁻¹

2.7.4 Coordinates of the DFT-B3LYP Stationary Points

N1-R_OcPcQc free

C	-1.208	-2.169	-1.269	H	-0.429	-2.094	-2.035
C	-2.613	-1.884	-1.824	H	-1.168	-3.180	-0.838
N	-1.023	-1.141	-0.232	H	-3.090	-2.781	-2.231
C	-3.348	-1.300	-0.611	H	-2.557	-1.137	-2.625
C	-2.268	-0.411	0.037	H	-4.243	-0.728	-0.866
C	0.146	-0.452	0.047	H	-3.638	-2.102	0.080
C	-2.546	-0.147	1.512	H	-2.247	0.578	-0.435
O	0.130	0.711	0.424	H	1.508	-2.870	1.087
N	1.334	-1.159	-0.153	H	0.940	-3.209	-0.561
O	-3.263	0.754	1.891	H	-1.776	0.148	4.013
O	-1.973	-1.054	2.323	H	-1.627	-1.626	4.232
C	1.614	-2.594	0.031	H	-3.238	-0.870	3.977
N	2.534	-0.458	0.110	H	3.699	-3.211	0.310
C	-2.174	-0.829	3.728	H	3.175	-3.280	-1.376
C	3.087	-2.710	-0.446	H	4.538	-1.030	-0.282
C	3.530	-1.233	-0.647	H	3.473	-0.943	-1.700
C	2.794	-0.179	1.477	H	4.471	1.087	0.863
O	2.004	-0.443	2.361	H	4.873	-0.168	2.063
C	4.105	0.545	1.738	H	3.939	1.246	2.559

N1-R_OcPcQc frozen

C	-1.276	-2.415	-0.889	H	-0.720	-2.500	-1.827
C	-2.790	-2.382	-1.154	H	-1.007	-3.266	-0.248
N	-1.022	-1.130	-0.228	H	-3.222	-3.386	-1.212
C	-3.335	-1.553	0.015	H	-2.988	-1.873	-2.104
C	-2.257	-0.465	0.211	H	-4.320	-1.120	-0.176
C	0.154	-0.459	0.045	H	-3.401	-2.172	0.917
C	-2.212	0.029	1.657	H	-2.466	0.421	-0.398
O	0.120	0.708	0.423	H	1.526	-3.223	0.336
N	1.369	-1.131	-0.068	H	1.232	-2.803	-1.364
O	-2.789	1.021	2.041	H	-0.718	0.536	3.791
O	-1.537	-0.822	2.451	H	-0.779	-1.179	4.291
C	1.752	-2.499	-0.456	H	-2.276	-0.180	4.298
N	2.518	-0.395	0.275	H	3.831	-2.903	0.093
C	-1.323	-0.373	3.798	H	3.578	-2.836	-1.658
C	3.280	-2.392	-0.703	H	4.548	-0.626	-0.281
C	3.551	-0.873	-0.645	H	3.405	-0.402	-1.624
C	2.759	-0.213	1.648	H	4.337	1.241	1.221
O	1.957	-0.542	2.500	H	4.882	-0.212	2.089
C	4.059	0.505	1.980	H	3.924	1.006	2.941

N1-R_OcPcQc free

C	-2.278	-0.427	0.067	H	-2.319	-0.182	1.130
C	-3.348	-1.421	-0.384	H	-2.334	0.514	-0.496
N	-1.026	-1.143	-0.233	H	-4.313	-0.942	-0.575
C	-2.728	-2.025	-1.651	H	-3.496	-2.194	0.380
C	-1.215	-2.129	-1.310	H	-3.142	-2.999	-1.929
C	0.148	-0.450	0.048	H	-2.867	-1.342	-2.494
C	-0.340	-1.887	-2.542	H	-0.982	-3.143	-0.969
O	0.131	0.711	0.424	H	1.526	-2.887	1.072
N	1.337	-1.159	-0.142	H	0.966	-3.207	-0.591
O	0.354	-2.736	-3.061	H	1.406	-0.419	-3.902
O	-0.461	-0.628	-2.999	H	0.122	0.744	-4.366
C	1.626	-2.596	0.020	H	0.094	-0.941	-4.988
N	2.535	-0.454	0.117	H	3.715	-3.210	0.273
C	0.346	-0.298	-4.141	H	3.167	-3.248	-1.411
C	3.095	-2.698	-0.469	H	4.540	-1.015	-0.281
C	3.534	-1.218	-0.649	H	3.476	-0.916	-1.699
C	2.793	-0.179	1.484	H	4.475	1.089	0.880
O	2.001	-0.440	2.365	H	4.874	-0.179	2.066
C	4.107	0.539	1.750	H	3.945	1.232	2.579

N1-R_OcPcQt frozen

C	-2.276	-0.494	0.203	H	-2.085	0.113	1.088
C	-3.192	-1.693	0.448	H	-2.674	0.166	-0.580
N	-1.025	-1.133	-0.229	H	-4.254	-1.430	0.420
C	-2.800	-2.663	-0.677	H	-2.974	-2.133	1.428
C	-1.275	-2.409	-0.896	H	-2.994	-3.713	-0.442
C	0.157	-0.457	0.046	H	-3.351	-2.417	-1.590
C	-0.955	-2.392	-2.395	H	-0.690	-3.222	-0.461
O	0.121	0.708	0.423	H	1.658	-3.183	0.411
N	1.375	-1.126	-0.065	H	1.233	-2.866	-1.286
O	-0.323	-3.255	-2.971	H	-0.165	-1.189	-4.624
O	-1.481	-1.316	-3.007	H	-1.718	-0.297	-4.739
C	1.792	-2.492	-0.431	H	-1.672	-2.081	-4.942
N	2.515	-0.369	0.260	H	3.919	-2.860	-0.055
C	-1.239	-1.223	-4.422	H	3.529	-2.731	-1.776
C	3.297	-2.332	-0.784	H	4.536	-0.547	-0.348
C	3.535	-0.808	-0.693	H	3.357	-0.318	-1.656
C	2.784	-0.216	1.632	H	4.325	1.279	1.217
O	2.003	-0.578	2.490	H	4.917	-0.194	2.016
C	4.079	0.513	1.957	H	3.961	0.975	2.938

N1-R_OcPtQc free

C	-1.248	-2.583	-0.292	H	-0.444	-3.090	-0.825
C	-2.598	-2.662	-1.012	H	-1.313	-3.009	0.721
N	-1.016	-1.138	-0.231	H	-3.114	-3.611	-0.839
C	-3.363	-1.453	-0.447	H	-2.444	-2.547	-2.091
C	-2.268	-0.376	-0.208	H	-4.149	-1.085	-1.112
C	0.138	-0.457	0.045	H	-3.832	-1.724	0.505
C	-2.531	0.378	1.094	H	-2.258	0.382	-0.996
O	0.131	0.713	0.425	H	2.745	0.428	-0.343
N	1.354	-1.148	-0.024	H	2.527	-0.069	1.343
O	-3.107	1.441	1.154	H	-1.780	1.252	3.473
O	-2.144	-0.335	2.175	H	-1.991	-0.379	4.192
C	2.595	-0.435	0.317	H	-3.409	0.542	3.589
N	1.666	-2.106	-1.023	H	4.466	-1.165	-0.559
C	-2.350	0.319	3.435	H	4.155	-1.816	1.053
C	3.680	-1.523	0.113	H	3.450	-3.213	-1.319
C	2.907	-2.714	-0.516	H	2.643	-3.456	0.243
C	1.520	-1.712	-2.366	H	2.005	-3.721	-3.097
O	0.891	-0.718	-2.678	H	3.149	-2.454	-3.583
C	2.090	-2.673	-3.399	H	1.548	-2.515	-4.333

N1-R_OcPtQc frozen

C	-1.265	-2.493	-0.719	H	-0.596	-2.741	-1.541
C	-2.725	-2.431	-1.190	H	-1.133	-3.235	0.081
N	-1.018	-1.131	-0.228	H	-3.208	-3.413	-1.178
C	-3.369	-1.431	-0.223	H	-2.763	-2.047	-2.215
C	-2.259	-0.379	0.004	H	-4.285	-0.974	-0.605
C	0.148	-0.463	0.044	H	-3.607	-1.926	0.726
C	-2.380	0.245	1.390	H	-2.343	0.454	-0.701
O	0.123	0.712	0.424	H	2.965	0.283	-0.394
N	1.380	-1.090	-0.037	H	2.377	0.200	1.273
O	-2.973	1.277	1.609	H	-1.403	0.938	3.746
O	-1.857	-0.544	2.355	H	-1.490	-0.756	4.334
C	2.602	-0.395	0.387	H	-2.990	0.161	3.965
N	1.699	-2.372	-0.520	H	4.434	-1.519	-0.050
C	-1.946	-0.008	3.683	H	4.006	-1.533	1.664
C	3.595	-1.558	0.651	H	3.314	-3.661	-0.013
C	2.748	-2.831	0.408	H	2.263	-3.169	1.329
C	1.838	-2.497	-1.916	H	2.195	-4.652	-1.833
O	1.358	-1.677	-2.677	H	3.595	-3.693	-2.346
C	2.503	-3.774	-2.408	H	2.231	-3.907	-3.456

N1-R_OcPtQt free

C	-2.331	-0.552	0.013	H	-2.217	0.317	0.662
C	-3.124	-1.709	0.631	H	-2.777	-0.222	-0.935
N	-1.010	-1.148	-0.234	H	-4.205	-1.591	0.514
C	-2.574	-2.936	-0.111	H	-2.900	-1.780	1.702
C	-1.063	-2.620	-0.286	H	-2.720	-3.879	0.421
C	0.118	-0.449	0.047	H	-3.056	-3.025	-1.092
C	-0.547	-3.259	-1.566	H	-0.471	-3.030	0.535
O	0.145	0.715	0.426	H	2.692	-1.693	-1.690
N	1.326	-1.252	-0.168	H	1.358	-0.624	-2.181
O	-0.195	-4.416	-1.633	H	0.805	-3.389	-3.845
O	-0.607	-2.432	-2.636	H	-0.335	-2.247	-4.634
C	2.065	-0.848	-1.381	H	-0.882	-3.877	-4.119
N	2.262	-1.006	0.875	H	3.825	0.470	-1.556
C	-0.228	-3.033	-3.886	H	2.339	1.274	-1.002
C	2.925	0.355	-0.946	H	4.266	-0.371	0.643
C	3.252	0.031	0.525	H	3.148	0.912	1.166
C	1.992	-1.528	2.110	H	2.906	-0.142	3.499
O	0.994	-2.209	2.332	H	4.036	-1.347	2.861
C	3.004	-1.191	3.193	H	2.797	-1.827	4.055

N1-R_OcPtQt frozen

C	-2.292	-0.408	-0.139	H	-2.165	0.453	0.516
C	-3.244	-1.479	0.399	H	-2.603	-0.052	-1.131
N	-1.021	-1.138	-0.231	H	-4.294	-1.258	0.187
C	-2.767	-2.771	-0.291	H	-3.127	-1.560	1.486
C	-1.253	-2.528	-0.623	H	-2.891	-3.660	0.333
C	0.146	-0.457	0.045	H	-3.330	-2.941	-1.214
C	-1.016	-2.831	-2.104	H	-0.607	-3.207	-0.066
O	0.128	0.714	0.425	H	3.027	0.225	-0.167
N	1.374	-1.100	-0.005	H	2.304	0.090	1.442
O	-0.552	-3.877	-2.511	H	-0.126	-1.961	-4.487
O	-1.447	-1.835	-2.894	H	-1.700	-1.156	-4.783
C	2.578	-0.472	0.549	H	-1.611	-2.947	-4.658
N	1.704	-2.345	-0.568	H	4.419	-1.625	0.232
C	-1.201	-1.998	-4.303	H	3.801	-1.748	1.883
C	3.505	-1.687	0.832	H	3.240	-3.720	-0.037
C	2.657	-2.911	0.405	H	2.086	-3.312	1.248
C	1.995	-2.336	-1.952	H	2.183	-4.495	-2.078
O	1.657	-1.404	-2.659	H	3.716	-3.611	-2.284
C	2.640	-3.596	-2.499	H	2.504	-3.597	-3.581

N1-R_OtPcQc free

C	-1.178	-2.601	-0.300	H	-0.421	-3.062	-0.936
C	-2.594	-2.742	-0.865	H	-1.097	-3.045	0.702
N	-1.015	-1.141	-0.231	H	-3.036	-3.719	-0.650
C	-3.354	-1.584	-0.198	H	-2.573	-2.611	-1.953
C	-2.301	-0.448	-0.069	H	-4.232	-1.256	-0.760
C	0.133	-0.451	0.047	H	-3.691	-1.888	0.799
C	-2.461	0.290	1.260	H	-2.420	0.311	-0.847
O	0.135	0.711	0.424	H	2.321	-2.447	-1.519
N	1.332	-1.238	-0.108	H	0.843	-1.666	-2.133
O	-3.068	1.329	1.378	H	-1.516	1.173	3.572
O	-1.946	-0.413	2.291	H	-1.614	-0.470	4.289
C	1.727	-1.526	-1.509	H	-3.108	0.411	3.821
N	2.466	-0.588	0.424	H	3.300	-0.543	-2.697
C	-2.059	0.225	3.576	H	1.921	0.492	-2.295
C	2.572	-0.302	-1.917	H	4.289	-0.175	-0.518
C	3.242	0.130	-0.596	H	3.187	1.211	-0.436
C	2.961	-0.865	1.674	H	1.892	-2.707	2.088
O	4.032	-0.388	2.030	H	1.137	-1.264	2.769
C	2.101	-1.743	2.564	H	2.637	-1.898	3.501

N1-R_OtPcQc frozen

C	-1.275	-2.390	-0.927	H	-0.637	-2.484	-1.811
C	-2.761	-2.282	-1.299	H	-1.107	-3.263	-0.278
N	-1.021	-1.129	-0.228	H	-3.222	-3.261	-1.464
C	-3.355	-1.527	-0.104	H	-2.872	-1.694	-2.217
C	-2.257	-0.497	0.253	H	-4.309	-1.040	-0.319
C	0.155	-0.461	0.045	H	-3.508	-2.216	0.735
C	-2.277	-0.170	1.744	H	-2.424	0.456	-0.257
O	0.119	0.708	0.423	H	2.111	-2.916	0.718
N	1.365	-1.130	-0.106	H	0.967	-3.168	-0.607
O	-2.940	0.724	2.216	H	-1.148	0.180	4.113
O	-1.558	-1.048	2.477	H	-0.960	-1.592	4.334
C	1.773	-2.532	-0.254	H	-2.593	-0.846	4.282
N	2.557	-0.378	-0.109	H	3.771	-3.107	-0.958
C	-1.572	-0.804	3.894	H	2.642	-2.717	-2.262
C	2.957	-2.439	-1.252	H	4.425	-0.781	-0.943
C	3.376	-0.941	-1.192	H	3.147	-0.426	-2.129
C	3.191	-0.019	1.093	H	1.819	-0.936	2.502
O	4.369	0.304	1.082	H	1.569	0.785	2.241
C	2.338	0.015	2.341	H	2.993	0.229	3.187

N1-R_OtPcQt free

C	-2.267	-0.432	0.145	H	-2.275	-0.250	1.222
C	-3.360	-1.385	-0.331	H	-2.328	0.541	-0.359
N	-1.028	-1.142	-0.232	H	-4.327	-0.889	-0.450
C	-2.791	-1.896	-1.662	H	-3.484	-2.211	0.379
C	-1.267	-2.029	-1.388	H	-3.220	-2.844	-1.996
C	0.153	-0.453	0.047	H	-2.960	-1.150	-2.446
C	-0.452	-1.684	-2.635	H	-1.030	-3.071	-1.150
O	0.128	0.713	0.425	H	1.949	-3.060	0.694
N	1.347	-1.168	0.008	H	0.827	-3.123	-0.671
O	0.177	-2.496	-3.282	H	1.254	-0.140	-3.980
O	-0.543	-0.379	-2.943	H	-0.010	1.113	-4.202
C	1.668	-2.579	-0.253	H	-0.167	-0.493	-4.995
N	2.556	-0.450	-0.064	H	3.676	-3.179	-0.894
C	0.184	0.045	-4.110	H	2.577	-2.807	-2.234
C	2.875	-2.512	-1.226	H	4.377	-0.875	-0.982
C	3.317	-1.024	-1.181	H	3.052	-0.503	-2.108
C	3.232	-0.063	1.101	H	2.000	-0.979	2.626
O	4.411	0.251	1.045	H	1.570	0.688	2.237
C	2.413	0.005	2.371	H	3.066	0.346	3.175

N1-R_OtPcQt frozen

C	-2.263	-0.532	0.304	H	-2.100	-0.179	1.325
C	-3.275	-1.674	0.196	H	-2.560	0.335	-0.300
N	-1.023	-1.129	-0.228	H	-4.306	-1.316	0.127
C	-2.820	-2.415	-1.069	H	-3.203	-2.333	1.070
C	-1.272	-2.360	-0.975	H	-3.180	-3.445	-1.138
C	0.157	-0.461	0.045	H	-3.152	-1.874	-1.961
C	-0.635	-2.383	-2.366	H	-0.912	-3.253	-0.452
O	0.118	0.708	0.422	H	2.109	-2.883	0.800
N	1.372	-1.127	-0.101	H	1.015	-3.192	-0.559
O	-0.030	-3.335	-2.816	H	0.777	-1.286	-4.339
O	-0.857	-1.243	-3.040	H	-0.595	-0.209	-4.759
C	1.796	-2.534	-0.193	H	-0.726	-1.987	-4.988
N	2.552	-0.355	-0.165	H	3.837	-3.065	-0.794
C	-0.311	-1.187	-4.370	H	2.717	-2.866	-2.151
C	2.999	-2.472	-1.171	H	4.397	-0.732	-1.061
C	3.348	-0.959	-1.243	H	3.046	-0.525	-2.201
C	3.218	0.051	1.005	H	2.000	-0.896	2.525
O	4.386	0.400	0.945	H	1.568	0.776	2.173
C	2.412	0.091	2.283	H	3.076	0.414	3.086

N1-R_OtPtQc free

C	-1.237	-2.389	-0.959	H	-0.504	-2.509	-1.758
C	-2.666	-2.230	-1.499	H	-1.155	-3.252	-0.289
N	-1.015	-1.130	-0.228	H	-3.150	-3.195	-1.680
C	-3.360	-1.403	-0.409	H	-2.652	-1.675	-2.444
C	-2.265	-0.401	0.021	H	-4.263	-0.891	-0.747
C	0.144	-0.460	0.044	H	-3.629	-2.047	0.437
C	-2.464	0.052	1.464	H	-2.304	0.512	-0.581
O	0.124	0.709	0.423	H	3.431	-0.754	0.106
N	1.389	-1.136	-0.142	H	2.357	0.528	0.725
O	-3.142	1.007	1.767	H	-1.654	0.575	3.927
O	-1.888	-0.781	2.358	H	-1.567	-1.176	4.318
C	2.501	-0.547	0.643	H	-3.147	-0.392	3.981
N	1.399	-2.510	0.222	H	3.452	-1.521	2.372
C	-2.082	-0.412	3.734	H	1.934	-0.691	2.749
C	2.449	-1.295	1.998	H	2.174	-3.515	1.888
C	1.644	-2.586	1.681	H	0.682	-2.597	2.202
C	2.073	-3.404	-0.617	H	3.011	-2.091	-2.062
O	2.404	-4.505	-0.206	H	1.425	-2.651	-2.563
C	2.338	-2.955	-2.044	H	2.800	-3.791	-2.571

N1-R_OtPtQc frozen

C	-1.278	-2.551	-0.529	H	-0.489	-2.983	-1.140
C	-2.636	-2.506	-1.238	H	-1.338	-3.133	0.402
N	-1.019	-1.133	-0.229	H	-3.169	-3.460	-1.177
C	-3.366	-1.362	-0.523	H	-2.493	-2.267	-2.299
C	-2.250	-0.329	-0.229	H	-4.176	-0.921	-1.110
C	0.147	-0.461	0.044	H	-3.790	-1.724	0.420
C	-2.526	0.413	1.076	H	-2.199	0.446	-1.001
O	0.125	0.713	0.424	H	3.076	0.183	-0.150
N	1.375	-1.091	-0.077	H	2.331	-0.014	1.442
O	-3.083	1.485	1.130	H	-1.829	1.243	3.489
O	-2.181	-0.319	2.157	H	-2.094	-0.394	4.177
C	2.594	-0.538	0.523	H	-3.474	0.564	3.541
N	1.694	-2.274	-0.767	H	4.446	-1.681	0.239
C	-2.415	0.323	3.420	H	3.670	-1.983	1.797
C	3.479	-1.798	0.737	H	3.264	-3.638	-0.511
C	2.669	-2.960	0.099	H	2.124	-3.532	0.856
C	1.964	-2.207	-2.150	H	1.694	-0.085	-2.514
O	2.601	-3.090	-2.697	H	0.248	-1.048	-2.799
C	1.338	-1.047	-2.900	H	1.606	-1.145	-3.952

N1-R_OtPtQt free

C	-2.296	-0.473	0.053	H	-2.248	0.022	1.024
C	-3.279	-1.642	-0.010	H	-2.516	0.292	-0.705
N	-1.016	-1.136	-0.230	H	-4.310	-1.319	-0.178
C	-2.737	-2.500	-1.166	H	-3.247	-2.203	0.931
C	-1.190	-2.257	-1.155	H	-2.968	-3.563	-1.066
C	0.140	-0.456	0.046	H	-3.162	-2.161	-2.117
C	-0.728	-1.980	-2.585	H	-0.653	-3.140	-0.807
O	0.129	0.710	0.424	H	3.430	-0.817	-0.004
N	1.376	-1.173	-0.114	H	2.420	0.610	0.350
O	-0.385	-2.850	-3.359	H	0.589	-0.641	-4.450
O	-0.819	-0.678	-2.910	H	-0.562	0.734	-4.337
C	2.525	-0.461	0.499	H	-1.099	-0.859	-4.973
N	1.380	-2.445	0.540	H	3.504	-1.064	2.375
C	-0.447	-0.347	-4.260	H	2.022	-0.118	2.597
C	2.496	-0.890	1.986	H	2.154	-3.065	2.386
C	1.647	-2.192	1.978	H	0.696	-2.057	2.499
C	2.087	-3.502	-0.065	H	2.717	-2.435	-1.857
O	2.420	-4.465	0.607	H	1.451	-3.627	-2.130
C	2.358	-3.421	-1.552	H	3.101	-4.184	-1.786

N1-R_OtPtQt frozen

C	-1.278	-2.551	-0.529	H	-0.489	-2.983	-1.140
C	-2.636	-2.506	-1.239	H	-1.338	-3.133	0.402
N	-1.019	-1.133	-0.229	H	-3.169	-3.459	-1.178
C	-3.366	-1.362	-0.523	H	-2.493	-2.266	-2.299
C	-2.250	-0.329	-0.229	H	-4.176	-0.921	-1.109
C	0.147	-0.461	0.044	H	-3.790	-1.724	0.420
C	-2.526	0.413	1.076	H	-2.199	0.446	-1.001
O	0.125	0.713	0.424	H	3.076	0.183	-0.151
N	1.375	-1.091	-0.077	H	2.331	-0.014	1.442
O	-3.083	1.485	1.130	H	-1.829	1.242	3.489
O	-2.181	-0.319	2.157	H	-2.094	-0.394	4.177
C	2.594	-0.538	0.522	H	-3.474	0.563	3.542
N	1.694	-2.274	-0.767	H	4.446	-1.681	0.240
C	-2.415	0.322	3.420	H	3.669	-1.984	1.798
C	3.479	-1.798	0.737	H	3.264	-3.638	-0.512
C	2.669	-2.960	0.098	H	2.124	-3.532	0.855
C	1.963	-2.206	-2.150	H	1.694	-0.085	-2.514
O	2.601	-3.090	-2.697	H	0.248	-1.047	-2.799
C	1.338	-1.046	-2.900	H	1.606	-1.144	-3.952

N1-S_OcPcQc free

C	-1.057	-2.342	-1.109	H	-0.655	-3.225	-0.602
C	-2.555	-2.495	-1.434	H	-0.447	-2.155	-1.998
N	-1.012	-1.149	-0.234	H	-2.714	-2.921	-2.428
C	-3.116	-1.070	-1.292	H	-3.035	-3.161	-0.707
C	-2.314	-0.502	-0.106	H	-4.192	-1.033	-1.109
C	0.120	-0.448	0.047	H	-2.894	-0.479	-2.187
C	-3.022	-0.764	1.229	H	-2.183	0.583	-0.169
O	0.145	0.715	0.426	H	2.302	-2.898	0.678
N	1.311	-1.250	-0.160	H	0.783	-2.449	1.495
O	-4.180	-0.464	1.428	H	-3.716	-2.195	3.344
O	-2.227	-1.337	2.155	H	-2.078	-2.010	4.058
C	1.683	-2.060	1.015	H	-3.159	-0.588	3.868
N	2.448	-0.435	-0.366	H	3.213	-1.606	2.543
C	-2.844	-1.543	3.438	H	1.808	-0.523	2.551
C	2.487	-1.089	1.909	H	4.228	-0.359	0.771
C	3.161	-0.143	0.890	H	3.045	0.907	1.180
C	2.579	0.187	-1.583	H	3.625	2.018	-1.098
O	1.786	0.007	-2.498	H	4.707	0.642	-1.369
C	3.777	1.116	-1.703	H	3.872	1.407	-2.750

N1-S_OcPcQc frozen

C	-1.185	-2.366	-1.029	H	-0.787	-3.255	-0.530
C	-2.720	-2.497	-1.206	H	-0.657	-2.243	-1.982
N	-1.019	-1.143	-0.232	H	-2.990	-2.756	-2.234
C	-3.294	-1.136	-0.768	H	-3.103	-3.293	-0.558
C	-2.285	-0.659	0.293	H	-4.310	-1.198	-0.372
C	0.139	-0.452	0.047	H	-3.288	-0.425	-1.600
C	-2.652	-1.185	1.687	H	-2.249	0.430	0.376
O	0.134	0.713	0.425	H	1.537	-3.114	-0.968
N	1.330	-1.157	-0.136	H	1.046	-3.040	0.743
O	-3.723	-0.970	2.213	H	-2.819	-3.022	3.598
O	-1.664	-1.898	2.267	H	-1.058	-2.892	3.925
C	1.670	-2.573	-0.022	H	-2.155	-1.511	4.259
N	2.469	-0.449	-0.531	H	3.766	-3.162	-0.298
C	-1.951	-2.358	3.599	H	3.337	-2.890	1.395
C	3.176	-2.532	0.375	H	4.524	-0.889	-0.271
C	3.571	-1.034	0.239	H	3.619	-0.549	1.219
C	2.539	-0.078	-1.875	H	4.308	1.162	-1.539
O	1.578	-0.177	-2.619	H	4.575	-0.239	-2.597
C	3.856	0.541	-2.317	H	3.657	1.149	-3.201

N1-S_OcPcQt free

C	-2.317	-0.466	-0.121	H	-2.204	0.589	-0.382
C	-3.227	-1.244	-1.081	H	-2.676	-0.518	0.916
N	-1.014	-1.146	-0.233	H	-4.269	-1.258	-0.748
C	-2.598	-2.646	-1.120	H	-3.191	-0.791	-2.076
C	-1.076	-2.371	-1.043	H	-2.865	-3.226	-2.007
C	0.126	-0.448	0.047	H	-2.898	-3.226	-0.239
C	-0.453	-2.243	-2.438	H	-0.555	-3.205	-0.568
O	0.141	0.713	0.425	H	2.258	-2.998	0.481
N	1.328	-1.230	-0.158	H	0.683	-2.681	1.245
O	0.102	-3.165	-2.994	H	-0.380	-1.588	-4.974
O	-0.673	-1.036	-2.979	H	-0.432	0.167	-4.588
C	1.610	-2.222	0.900	H	1.013	-0.798	-4.161
N	2.484	-0.419	-0.144	H	3.016	-2.025	2.589
C	-0.071	-0.811	-4.270	H	1.598	-0.967	2.680
C	2.330	-1.411	1.999	H	4.141	-0.471	1.165
C	3.060	-0.303	1.207	H	2.873	0.688	1.635
C	2.845	0.266	-1.277	H	3.886	1.959	-0.403
O	2.230	0.177	-2.331	H	4.944	0.589	-0.772
C	4.071	1.153	-1.122	H	4.292	1.588	-2.097

N1-S_OcPcQt frozen

C	-2.294	-0.570	0.239	H	-2.282	0.512	0.105
C	-3.340	-1.287	-0.619	H	-2.436	-0.779	1.309
N	-1.021	-1.139	-0.231	H	-4.318	-1.337	-0.132
C	-2.718	-2.674	-0.839	H	-3.454	-0.771	-1.577
C	-1.194	-2.403	-0.952	H	-3.111	-3.197	-1.717
C	0.144	-0.454	0.047	H	-2.895	-3.314	0.034
C	-0.714	-2.318	-2.408	H	-0.638	-3.230	-0.508
O	0.130	0.711	0.424	H	1.525	-3.097	-0.985
N	1.349	-1.145	-0.119	H	1.163	-3.044	0.761
O	0.054	-3.116	-2.906	H	-0.885	-1.959	-5.004
O	-1.269	-1.289	-3.060	H	-1.399	-0.250	-4.792
C	1.721	-2.565	-0.048	H	0.264	-0.750	-4.345
N	2.483	-0.391	-0.447	H	3.804	-3.008	-0.548
C	-0.782	-1.056	-4.396	H	3.500	-3.011	1.194
C	3.247	-2.514	0.254	H	4.545	-0.761	-0.146
C	3.581	-1.001	0.302	H	3.564	-0.622	1.330
C	2.567	0.129	-1.734	H	4.312	1.353	-1.248
O	1.615	0.116	-2.499	H	4.622	0.055	-2.419
C	3.886	0.798	-2.089	H	3.697	1.481	-2.918

N1-S_OcPtQc free

C	-1.200	-2.596	-0.311	H	-0.475	-3.112	0.322
C	-2.659	-2.794	0.122	H	-1.051	-2.939	-1.343
N	-1.014	-1.135	-0.230	H	-3.103	-3.692	-0.317
C	-3.340	-1.498	-0.346	H	-2.718	-2.878	1.212
C	-2.278	-0.411	-0.061	H	-4.288	-1.288	0.156
C	0.138	-0.458	0.045	H	-3.534	-1.534	-1.425
C	-2.476	0.207	1.327	H	-2.345	0.427	-0.758
O	0.130	0.712	0.424	H	3.364	-1.027	0.441
N	1.356	-1.185	-0.079	H	2.401	0.449	0.734
O	-3.127	1.210	1.518	H	-3.128	0.109	3.897
O	-1.932	-0.540	2.310	H	-1.582	-0.715	4.295
C	2.579	-0.375	0.047	H	-1.586	0.977	3.695
N	1.526	-1.903	-1.293	H	3.958	0.112	-1.603
C	-2.072	0.000	3.634	H	2.471	1.076	-1.578
C	2.884	0.079	-1.398	H	2.831	-1.523	-2.931
C	2.155	-0.978	-2.272	H	1.375	-0.519	-2.889
C	1.872	-3.252	-1.181	H	1.730	-3.593	-3.344
O	1.770	-3.871	-0.137	H	3.366	-3.739	-2.676
C	2.305	-3.929	-2.475	H	2.174	-5.004	-2.342

N1-S_OcPtQc frozen

C	-1.262	-2.528	-0.626	H	-0.755	-3.221	0.046
C	-2.790	-2.666	-0.523	H	-0.914	-2.712	-1.651
N	-1.018	-1.132	-0.229	H	-3.185	-3.413	-1.218
C	-3.302	-1.247	-0.802	H	-3.064	-2.970	0.493
C	-2.250	-0.350	-0.116	H	-4.312	-1.057	-0.429
C	0.147	-0.461	0.044	H	-3.298	-1.042	-1.879
C	-2.657	-0.005	1.320	H	-2.143	0.613	-0.620
O	0.124	0.712	0.424	H	2.913	-0.255	1.077
N	1.382	-1.056	-0.161	H	2.464	0.725	-0.326
O	-3.416	0.901	1.588	H	-3.557	-0.615	3.747
O	-2.141	-0.852	2.229	H	-1.965	-1.323	4.187
C	2.624	-0.296	0.020	H	-2.126	0.436	3.867
N	1.682	-2.383	-0.516	H	4.442	-1.505	-0.196
C	-2.476	-0.563	3.595	H	4.126	-0.473	-1.595
C	3.650	-1.092	-0.829	H	3.356	-3.167	-1.572
C	2.810	-2.232	-1.456	H	2.405	-1.939	-2.429
C	1.730	-3.317	0.540	H	2.093	-5.003	-0.804
O	1.214	-3.087	1.617	H	3.444	-4.617	0.277
C	2.351	-4.664	0.203	H	1.992	-5.388	0.937

N1-S_OcPtQt free

C	-2.282	-0.406	-0.013	H	-2.370	0.430	-0.714
C	-3.364	-1.477	-0.210	H	-2.293	0.014	1.000
N	-1.016	-1.133	-0.229	H	-4.248	-1.284	0.406
C	-2.649	-2.783	0.167	H	-3.684	-1.508	-1.257
C	-1.214	-2.573	-0.379	H	-3.119	-3.684	-0.237
C	0.143	-0.459	0.045	H	-2.593	-2.892	1.256
C	-1.126	-3.077	-1.821	H	-0.484	-3.141	0.201
O	0.126	0.710	0.424	H	3.332	-0.853	0.596
N	1.369	-1.165	-0.055	H	2.362	0.627	0.376
O	-0.909	-4.235	-2.112	H	-2.148	-3.360	-4.234
O	-1.386	-2.117	-2.736	H	-1.680	-1.687	-4.692
C	2.597	-0.350	-0.040	H	-0.429	-2.941	-4.403
N	1.534	-2.099	-1.106	H	4.126	-0.571	-1.607
C	-1.411	-2.564	-4.102	H	2.931	0.684	-1.960
C	3.067	-0.308	-1.519	H	2.701	-2.027	-2.885
C	2.161	-1.354	-2.220	H	1.365	-0.869	-2.794
C	1.936	-3.390	-0.716	H	1.791	-4.283	-2.693
O	1.794	-3.779	0.429	H	3.459	-4.001	-2.142
C	2.452	-4.294	-1.822	H	2.495	-5.307	-1.419

N1-S_OcPtQt frozen

C	-2.267	-0.350	-0.146	H	-2.148	0.603	-0.667
C	-3.315	-1.269	-0.781	H	-2.500	-0.122	0.902
N	-1.020	-1.134	-0.230	H	-4.319	-1.089	-0.385
C	-2.790	-2.673	-0.457	H	-3.346	-1.116	-1.865
C	-1.251	-2.528	-0.598	H	-3.190	-3.463	-1.099
C	0.148	-0.460	0.045	H	-3.019	-2.937	0.582
C	-0.809	-2.931	-2.005	H	-0.756	-3.214	0.089
O	0.125	0.712	0.424	H	2.922	-0.332	1.114
N	1.380	-1.061	-0.154	H	2.490	0.706	-0.255
O	-0.594	-4.081	-2.329	H	-1.178	-2.912	-4.634
O	-0.752	-1.891	-2.862	H	-0.423	-1.288	-4.765
C	2.633	-0.330	0.056	H	0.551	-2.714	-4.273
N	1.655	-2.377	-0.560	H	4.424	-1.573	-0.203
C	-0.429	-2.232	-4.220	H	4.140	-0.476	-1.560
C	3.646	-1.115	-0.822	H	3.305	-3.149	-1.664
C	2.781	-2.208	-1.498	H	2.375	-1.858	-2.452
C	1.681	-3.362	0.451	H	1.809	-5.014	-0.945
O	1.185	-3.158	1.544	H	3.311	-4.717	-0.039
C	2.217	-4.719	0.027	H	1.919	-5.444	0.785

N1-S_OtPcQc free

C	-1.116	-2.260	-1.205	H	-0.692	-3.189	-0.811
C	-2.627	-2.388	-1.465	H	-0.563	-2.005	-2.118
N	-1.018	-1.149	-0.234	H	-2.838	-2.750	-2.476
C	-3.171	-0.976	-1.199	H	-3.072	-3.100	-0.759
C	-2.310	-0.497	-0.017	H	-4.235	-0.950	-0.959
C	0.130	-0.447	0.048	H	-2.993	-0.325	-2.062
C	-2.961	-0.838	1.330	H	-2.165	0.588	-0.014
O	0.142	0.714	0.426	H	2.131	-3.124	0.125
N	1.321	-1.208	-0.201	H	0.577	-2.830	0.949
O	-4.138	-0.662	1.559	H	-3.424	-2.315	3.487
O	-2.084	-1.311	2.236	H	-1.800	-1.920	4.146
C	1.534	-2.388	0.672	H	-3.049	-0.643	3.964
N	2.502	-0.453	-0.038	H	2.926	-2.569	2.371
C	-2.634	-1.561	3.542	H	1.594	-1.427	2.618
C	2.303	-1.815	1.881	H	4.184	-0.927	1.112
C	3.134	-0.668	1.270	H	3.095	0.243	1.875
C	3.163	0.143	-1.083	H	2.106	-0.822	-2.719
O	4.265	0.647	-0.903	H	1.555	0.819	-2.353
C	2.440	0.175	-2.417	H	3.126	0.582	-3.161

N1-S_OtPcQc frozen

C	-1.304	-2.547	-0.473	H	-0.804	-3.183	0.265
C	-2.833	-2.631	-0.353	H	-0.981	-2.858	-1.477
N	-1.021	-1.128	-0.228	H	-3.246	-3.466	-0.927
C	-3.294	-1.257	-0.859	H	-3.114	-2.760	0.696
C	-2.226	-0.295	-0.293	H	-4.304	-0.986	-0.543
C	0.156	-0.462	0.044	H	-3.265	-1.222	-1.955
C	-2.659	0.289	1.055	H	-2.067	0.571	-0.940
O	0.118	0.708	0.423	H	2.209	-2.168	-1.745
N	1.371	-1.119	-0.121	H	1.002	-3.095	-0.840
O	-3.317	1.301	1.153	H	-3.761	0.154	3.458
O	-2.306	-0.487	2.100	H	-2.328	-0.711	4.112
C	1.808	-2.375	-0.743	H	-2.193	0.992	3.562
N	2.539	-0.504	0.372	H	3.780	-3.255	-0.350
C	-2.677	0.028	3.389	H	2.568	-3.643	0.879
C	2.931	-2.855	0.213	H	4.366	-1.314	0.964
C	3.310	-1.578	1.016	H	3.012	-1.664	2.065
C	3.230	0.460	-0.380	H	2.038	0.483	-2.191
O	4.393	0.716	-0.112	H	1.614	1.725	-1.013
C	2.453	1.184	-1.457	H	3.136	1.872	-1.956

N1-S_OtPcQt free

C	-2.314	-0.459	-0.047	H	-2.219	0.593	-0.322
C	-3.287	-1.238	-0.945	H	-2.603	-0.503	1.010
N	-1.018	-1.145	-0.233	H	-4.293	-1.289	-0.519
C	-2.636	-2.623	-1.083	H	-3.359	-0.758	-1.925
C	-1.118	-2.315	-1.109	H	-2.960	-3.180	-1.967
C	0.135	-0.448	0.048	H	-2.849	-3.240	-0.203
C	-0.622	-2.097	-2.542	H	-0.547	-3.166	-0.735
O	0.137	0.711	0.425	H	1.806	-3.273	-0.014
N	1.331	-1.207	-0.175	H	0.579	-2.700	1.134
O	-0.102	-2.969	-3.203	H	-1.079	-1.313	-5.034
O	-0.893	-0.859	-3.003	H	-0.836	0.409	-4.581
C	1.520	-2.445	0.642	H	0.532	-0.751	-4.527
N	2.500	-0.443	0.009	H	3.514	-2.754	1.490
C	-0.542	-0.621	-4.380	H	2.317	-2.257	2.693
C	2.646	-2.110	1.660	H	4.062	-0.414	1.387
C	2.995	-0.635	1.368	H	2.468	0.049	2.042
C	3.328	-0.129	-1.053	H	2.427	-1.299	-2.643
O	4.464	0.284	-0.859	H	1.826	0.359	-2.527
C	2.722	-0.265	-2.437	H	3.471	0.060	-3.161

N1-S_OtPcQt frozen

C	-2.267	-0.535	0.304	H	-2.314	0.525	0.046
C	-3.394	-1.361	-0.327	H	-2.267	-0.606	1.400
N	-1.026	-1.134	-0.230	H	-4.259	-1.450	0.338
C	-2.737	-2.719	-0.617	H	-3.727	-0.900	-1.259
C	-1.277	-2.374	-0.978	H	-3.238	-3.285	-1.408
C	0.157	-0.458	0.046	H	-2.728	-3.341	0.285
C	-1.026	-2.158	-2.479	H	-0.609	-3.183	-0.688
O	0.122	0.710	0.423	H	1.522	-2.946	-1.231
N	1.362	-1.131	-0.106	H	1.095	-3.132	0.491
O	-0.052	-2.581	-3.070	H	-1.686	-2.039	-5.037
O	-1.985	-1.419	-3.063	H	-2.665	-0.557	-4.765
C	1.700	-2.564	-0.221	H	-0.880	-0.515	-4.588
N	2.550	-0.376	-0.177	H	3.802	-2.908	-0.712
C	-1.782	-1.118	-4.457	H	3.406	-3.321	0.962
C	3.207	-2.609	0.156	H	4.539	-0.829	0.258
C	3.544	-1.155	0.558	H	3.409	-0.990	1.632
C	2.926	0.323	-1.328	H	1.365	-0.237	-2.716
O	4.086	0.677	-1.475	H	1.046	1.261	-1.818
C	1.826	0.670	-2.309	H	2.276	1.244	-3.120

N1-S_OtPtQc free

C	-1.269	-2.574	-0.406	H	-0.675	-3.166	0.293
C	-2.777	-2.717	-0.139	H	-1.010	-2.890	-1.421
N	-1.016	-1.131	-0.228	H	-3.215	-3.544	-0.705
C	-3.342	-1.347	-0.539	H	-2.954	-2.901	0.926
C	-2.254	-0.363	-0.058	H	-4.319	-1.126	-0.101
C	0.145	-0.460	0.044	H	-3.437	-1.271	-1.628
C	-2.520	0.104	1.376	H	-2.227	0.549	-0.657
O	0.124	0.709	0.423	H	3.432	-0.733	0.131
N	1.391	-1.143	-0.081	H	2.373	0.701	0.208
O	-3.219	1.056	1.641	H	-3.246	-0.276	3.895
O	-1.964	-0.706	2.301	H	-1.672	-1.055	4.274
C	2.550	-0.246	-0.296	H	-1.748	0.685	3.839
N	1.493	-2.103	-1.121	H	3.696	-0.090	-2.170
C	-2.178	-0.305	3.665	H	2.151	0.771	-2.186
C	2.656	-0.133	-1.836	H	2.566	-2.090	-2.918
C	1.931	-1.407	-2.354	H	1.058	-1.156	-2.964
C	2.075	-3.338	-0.813	H	2.893	-3.098	1.168
O	2.482	-4.066	-1.705	H	1.210	-3.590	1.182
C	2.156	-3.724	0.653	H	2.471	-4.767	0.704

N1-S_OtPtQc frozen

C	-1.238	-2.490	-0.776	H	-0.720	-3.256	-0.198
C	-2.766	-2.667	-0.712	H	-0.866	-2.549	-1.807
N	-1.020	-1.137	-0.231	H	-3.139	-3.302	-1.520
C	-3.310	-1.233	-0.767	H	-3.044	-3.138	0.238
C	-2.271	-0.433	0.048	H	-4.321	-1.125	-0.365
C	0.146	-0.459	0.045	H	-3.313	-0.860	-1.798
C	-2.667	-0.357	1.525	H	-2.203	0.605	-0.283
O	0.128	0.714	0.425	H	3.068	-0.230	0.801
N	1.370	-1.076	-0.156	H	2.437	0.673	-0.583
O	-3.519	0.399	1.935	H	-3.440	-1.407	3.831
O	-2.019	-1.247	2.307	H	-1.772	-1.972	4.183
C	2.630	-0.329	-0.201	H	-2.147	-0.217	4.118
N	1.645	-2.445	-0.314	H	4.469	-1.443	-0.644
C	-2.375	-1.202	3.701	H	3.737	-0.705	-2.071
C	3.516	-1.209	-1.126	H	3.241	-3.425	-1.250
C	2.679	-2.499	-1.362	H	2.191	-2.485	-2.340
C	1.826	-3.242	0.836	H	1.668	-1.791	2.430
O	2.407	-4.311	0.755	H	0.130	-2.531	2.010
C	1.200	-2.732	2.119	H	1.360	-3.489	2.888

N1-S_OtPtQt free

C	-1.237	-2.389	-0.959	H	-0.504	-2.510	-1.757
C	-2.666	-2.231	-1.498	H	-1.155	-3.252	-0.288
N	-1.015	-1.130	-0.228	H	-3.150	-3.196	-1.679
C	-3.360	-1.404	-0.409	H	-2.652	-1.676	-2.444
C	-2.265	-0.401	0.021	H	-4.263	-0.891	-0.747
C	0.144	-0.460	0.044	H	-3.630	-2.046	0.437
C	-2.464	0.052	1.464	H	-2.304	0.512	-0.581
O	0.124	0.709	0.423	H	3.431	-0.754	0.106
N	1.389	-1.136	-0.142	H	2.357	0.528	0.726
O	-3.141	1.007	1.767	H	-1.654	0.576	3.926
O	-1.888	-0.780	2.358	H	-1.567	-1.175	4.318
C	2.501	-0.547	0.644	H	-3.147	-0.391	3.981
N	1.399	-2.510	0.221	H	3.451	-1.521	2.373
C	-2.082	-0.411	3.734	H	1.933	-0.692	2.749
C	2.449	-1.296	1.998	H	2.175	-3.516	1.887
C	1.644	-2.587	1.680	H	0.682	-2.598	2.201
C	2.073	-3.404	-0.619	H	3.017	-2.095	-2.062
O	2.403	-4.505	-0.208	H	1.427	-2.642	-2.562
C	2.338	-2.954	-2.044	H	2.793	-3.792	-2.574

N1-S_OtPtQt frozen

C	-1.278	-2.551	-0.529	H	-0.489	-2.983	-1.140
C	-2.636	-2.506	-1.239	H	-1.338	-3.133	0.402
N	-1.019	-1.133	-0.229	H	-3.169	-3.459	-1.178
C	-3.366	-1.362	-0.523	H	-2.493	-2.266	-2.299
C	-2.250	-0.329	-0.229	H	-4.176	-0.921	-1.109
C	0.147	-0.461	0.044	H	-3.790	-1.724	0.420
C	-2.526	0.413	1.076	H	-2.199	0.446	-1.001
O	0.125	0.713	0.424	H	3.076	0.183	-0.151
N	1.375	-1.091	-0.077	H	2.331	-0.014	1.442
O	-3.083	1.485	1.130	H	-1.829	1.242	3.489
O	-2.181	-0.319	2.157	H	-2.094	-0.394	4.177
C	2.594	-0.538	0.522	H	-3.474	0.563	3.542
N	1.694	-2.274	-0.767	H	4.446	-1.681	0.240
C	-2.415	0.322	3.420	H	3.669	-1.984	1.798
C	3.479	-1.798	0.737	H	3.264	-3.638	-0.512
C	2.669	-2.960	0.098	H	2.124	-3.532	0.855
C	1.963	-2.206	-2.150	H	1.694	-0.085	-2.514
O	2.601	-3.090	-2.697	H	0.248	-1.047	-2.799
C	1.338	-1.046	-2.900	H	1.606	-1.144	-3.952

N3-R_OcPcQc free

C	-1.101	-2.359	-1.059	H	-0.274	-2.379	-1.770
C	-2.485	-2.225	-1.710	H	-1.046	-3.261	-0.434
N	-1.011	-1.143	-0.232	H	-2.912	-3.192	-1.992
C	-3.310	-1.497	-0.636	H	-2.412	-1.609	-2.613
C	-2.303	-0.483	-0.044	H	-4.203	-0.999	-1.023
C	0.125	-0.451	0.046	H	-3.625	-2.205	0.140
C	-2.637	-0.137	1.403	H	-2.328	0.466	-0.589
O	0.139	0.712	0.425	H	0.758	-2.457	1.500
N	1.317	-1.253	-0.143	H	2.292	-2.905	0.710
O	-3.408	0.743	1.711	H	-2.051	0.309	3.942
O	-2.045	-0.967	2.290	H	-1.812	-1.445	4.243
C	1.667	-2.067	1.038	H	-3.438	-0.801	3.839
N	2.458	-0.440	-0.326	H	1.758	-0.525	2.568
C	-2.363	-0.702	3.667	H	3.160	-1.612	2.602
C	2.452	-1.096	1.947	H	3.048	0.893	1.232
C	3.155	-0.157	0.941	H	4.221	-0.387	0.839
C	2.623	0.170	-1.546	H	4.746	0.620	-1.287
O	1.852	-0.016	-2.478	H	3.664	2.001	-1.048
C	3.826	1.094	-1.644	H	3.945	1.379	-2.690

N3-R_OcPcQc frozen

C	-1.139	-2.093	-1.367	H	-0.323	-1.931	-2.077
C	-2.518	-1.776	-1.966	H	-1.096	-3.135	-1.020
N	-1.022	-1.151	-0.235	H	-2.967	-2.640	-2.465
C	-3.324	-1.295	-0.751	H	-2.428	-0.967	-2.700
C	-2.286	-0.459	0.030	H	-4.207	-0.704	-1.007
C	0.134	-0.447	0.048	H	-3.648	-2.151	-0.147
C	-2.658	-0.334	1.502	H	-2.249	0.567	-0.353
O	0.141	0.716	0.426	H	0.776	-3.074	0.724
N	1.296	-1.208	-0.065	H	1.567	-3.158	-0.873
O	-3.469	0.470	1.906	H	-2.138	-0.190	4.084
O	-2.048	-1.246	2.286	H	-1.815	-1.954	4.168
C	1.547	-2.631	0.091	H	-3.466	-1.343	3.818
N	2.518	-0.620	-0.382	H	2.899	-2.871	1.819
C	-2.395	-1.172	3.678	H	3.613	-3.375	0.281
C	2.961	-2.635	0.754	H	3.501	-0.623	1.490
C	3.495	-1.181	0.546	H	4.496	-1.157	0.111
C	2.633	0.299	-1.398	H	4.773	0.237	-1.804
O	1.700	0.556	-2.146	H	4.305	1.429	-0.577
C	3.998	0.959	-1.518	H	3.927	1.722	-2.295

N3-R_OcPcQt free

C	-2.317	-0.466	-0.120	H	-2.204	0.589	-0.381
C	-3.227	-1.244	-1.082	H	-2.676	-0.519	0.916
N	-1.014	-1.146	-0.233	H	-4.269	-1.257	-0.749
C	-2.598	-2.646	-1.120	H	-3.190	-0.791	-2.076
C	-1.077	-2.371	-1.043	H	-2.865	-3.226	-2.008
C	0.126	-0.448	0.047	H	-2.898	-3.226	-0.239
C	-0.452	-2.243	-2.438	H	-0.556	-3.205	-0.568
O	0.141	0.713	0.425	H	2.259	-2.998	0.479
N	1.328	-1.229	-0.158	H	0.683	-2.682	1.244
O	0.102	-3.166	-2.994	H	3.016	-2.025	2.589
O	-0.673	-1.037	-2.980	H	1.598	-0.968	2.679
C	1.610	-2.222	0.899	H	4.141	-0.471	1.165
N	2.484	-0.419	-0.144	H	2.874	0.687	1.635
C	-0.071	-0.812	-4.270	H	-0.380	-1.588	-4.974
C	2.330	-1.411	1.999	H	-0.430	0.167	-4.588
C	3.060	-0.304	1.206	H	1.013	-0.800	-4.160
C	2.844	0.267	-1.277	H	3.884	1.961	-0.403
O	2.229	0.178	-2.330	H	4.943	0.590	-0.772
C	4.071	1.154	-1.121	H	4.291	1.589	-2.096

N3-R_OcPcQt frozen

C	-2.309	-0.466	0.017	H	-2.156	0.614	-0.014
C	-3.247	-0.983	-1.080	H	-2.675	-0.730	1.019
N	-1.024	-1.152	-0.236	H	-4.289	-1.030	-0.749
C	-2.675	-2.366	-1.419	H	-3.193	-0.331	-1.956
C	-1.144	-2.194	-1.271	H	-2.955	-2.725	-2.414
C	0.137	-0.446	0.049	H	-3.013	-3.112	-0.690
C	-0.454	-1.830	-2.593	H	-0.688	-3.135	-0.960
O	0.141	0.716	0.426	H	1.620	-3.088	-0.953
N	1.315	-1.186	-0.058	H	0.857	-3.100	0.664
O	0.391	-2.528	-3.118	H	3.699	-3.278	0.137
O	-0.921	-0.684	-3.107	H	2.987	-2.969	1.726
C	1.606	-2.614	0.036	H	4.510	-1.034	0.244
N	2.532	-0.549	-0.304	H	3.426	-0.654	1.606
C	-0.264	-0.213	-4.302	H	-0.268	-0.991	-5.070
C	3.023	-2.621	0.691	H	-0.842	0.653	-4.624
C	3.493	-1.137	0.624	H	0.758	0.078	-4.054
C	2.681	0.425	-1.258	H	4.323	1.496	-0.300
O	1.782	0.725	-2.033	H	4.830	0.412	-1.610
C	4.043	1.103	-1.284	H	3.985	1.926	-1.997

N3-R_OcPtQc free

C	-1.152	-2.188	-1.278	H	-0.673	-3.124	-0.982
C	-2.672	-2.347	-1.457	H	-0.666	-1.845	-2.203
N	-1.020	-1.153	-0.236	H	-2.935	-2.612	-2.486
C	-3.247	-0.990	-1.017	H	-3.047	-3.129	-0.792
C	-2.320	-0.560	0.126	H	-4.291	-1.058	-0.701
C	0.129	-0.447	0.048	H	-3.176	-0.255	-1.827
C	-2.733	-1.157	1.479	H	-2.204	0.520	0.227
O	0.144	0.718	0.427	H	2.695	-0.110	1.080
N	1.333	-1.111	-0.206	H	2.657	0.471	-0.592
O	-3.411	-2.154	1.623	H	-1.687	-1.961	3.829
O	-2.189	-0.460	2.488	H	-1.910	-0.308	4.485
C	2.610	-0.422	0.032	H	-3.338	-1.298	4.022
N	1.523	-2.492	0.046	H	4.352	-1.671	0.483
C	-2.297	-1.055	3.792	H	4.243	-1.224	-1.223
C	3.655	-1.503	-0.344	H	3.252	-3.690	-0.233
C	2.805	-2.774	-0.620	H	2.619	-2.898	-1.691
C	1.232	-2.964	1.338	H	1.589	-5.041	0.735
O	0.605	-2.297	2.142	H	2.673	-4.433	2.004
C	1.646	-4.400	1.620	H	0.985	-4.790	2.396

N3-R_OcPtQc frozen

C	-1.177	-2.125	-1.328	H	-0.767	-3.107	-1.071
C	-2.702	-2.206	-1.553	H	-0.651	-1.766	-2.224
N	-1.020	-1.153	-0.236	H	-2.948	-2.352	-2.609
C	-3.247	-0.887	-0.979	H	-3.117	-3.044	-0.986
C	-2.314	-0.604	0.202	H	-4.292	-0.966	-0.673
C	0.130	-0.448	0.048	H	-3.154	-0.075	-1.709
C	-2.728	-1.354	1.476	H	-2.187	0.456	0.427
O	0.144	0.719	0.427	H	3.143	-0.287	0.585
N	1.336	-1.108	-0.150	H	2.410	0.564	-0.788
O	-3.542	-2.254	1.524	H	-1.655	-2.675	3.558
O	-2.021	-0.913	2.527	H	-1.574	-1.143	4.486
C	2.604	-0.420	-0.361	H	-3.166	-1.831	4.017
N	1.601	-2.481	-0.188	H	4.377	-1.580	-0.950
C	-2.121	-1.701	3.725	H	3.444	-0.980	-2.326
C	3.364	-1.389	-1.314	H	3.108	-3.590	-1.163
C	2.510	-2.691	-1.315	H	1.946	-2.796	-2.251
C	1.063	-3.377	0.707	H	1.242	-5.155	-0.561
O	0.336	-3.030	1.626	H	2.504	-5.007	0.673
C	1.441	-4.834	0.467	H	0.850	-5.440	1.154

N3-R_OcPtQt free

C	-2.316	-0.491	0.003	H	-2.205	0.589	-0.104
C	-3.245	-1.123	-1.040	H	-2.654	-0.696	1.027
N	-1.019	-1.148	-0.234	H	-4.286	-1.158	-0.705
C	-2.646	-2.522	-1.251	H	-3.206	-0.551	-1.973
C	-1.117	-2.302	-1.128	H	-2.924	-2.983	-2.204
C	0.133	-0.450	0.047	H	-2.963	-3.199	-0.450
C	-0.457	-2.085	-2.494	H	-0.627	-3.185	-0.715
O	0.139	0.716	0.426	H	2.767	-0.100	0.980
N	1.342	-1.101	-0.233	H	2.601	0.520	-0.672
O	0.190	-2.932	-3.074	H	-0.502	-1.305	-5.034
O	-0.717	-0.864	-3.003	H	-0.444	0.422	-4.541
C	2.615	-0.388	-0.067	H	0.953	-0.663	-4.235
N	1.580	-2.471	0.045	H	4.445	-1.565	0.202
C	-0.137	-0.594	-4.289	H	4.119	-1.161	-1.486
C	3.650	-1.442	-0.539	H	3.319	-3.631	-0.304
C	2.819	-2.747	-0.700	H	2.552	-2.928	-1.744
C	1.370	-2.907	1.363	H	1.764	-4.995	0.832
O	0.744	-2.241	2.168	H	2.926	-4.285	1.970
C	1.869	-4.310	1.678	H	1.293	-4.683	2.527

N3-R_OcPtQt frozen

C	-2.303	-0.513	0.131	H	-2.237	0.568	-0.005
C	-3.325	-1.182	-0.797	H	-2.519	-0.710	1.189
N	-1.020	-1.143	-0.232	H	-4.312	-1.271	-0.333
C	-2.695	-2.549	-1.102	H	-3.433	-0.603	-1.719
C	-1.175	-2.256	-1.160	H	-3.066	-3.014	-2.020
C	0.138	-0.454	0.046	H	-2.872	-3.247	-0.276
C	-0.709	-1.951	-2.588	H	-0.613	-3.138	-0.855
O	0.134	0.715	0.426	H	3.164	-0.246	0.583
N	1.365	-1.088	-0.139	H	2.371	0.643	-0.732
O	-0.096	-2.738	-3.281	H	-1.152	-1.072	-5.064
O	-1.082	-0.726	-3.004	H	-1.067	0.633	-4.503
C	2.604	-0.352	-0.354	H	0.387	-0.418	-4.456
N	1.703	-2.448	-0.162	H	4.424	-1.326	-1.119
C	-0.700	-0.381	-4.347	H	3.278	-0.862	-2.382
C	3.361	-1.256	-1.365	H	3.345	-3.447	-1.024
C	2.652	-2.640	-1.267	H	2.120	-2.890	-2.191
C	1.190	-3.360	0.728	H	1.510	-5.146	-0.495
O	0.396	-3.046	1.605	H	2.739	-4.890	0.754
C	1.670	-4.793	0.530	H	1.110	-5.423	1.221

N3-R_OtPcQc free

C	-1.116	-2.261	-1.204	H	-0.692	-3.189	-0.809
C	-2.627	-2.389	-1.464	H	-0.563	-2.007	-2.117
N	-1.018	-1.149	-0.234	H	-2.838	-2.752	-2.474
C	-3.171	-0.977	-1.198	H	-3.072	-3.101	-0.757
C	-2.310	-0.497	-0.017	H	-4.235	-0.951	-0.958
C	0.129	-0.447	0.048	H	-2.993	-0.327	-2.062
C	-2.960	-0.838	1.331	H	-2.165	0.588	-0.015
O	0.142	0.714	0.426	H	2.131	-3.124	0.127
N	1.321	-1.208	-0.201	H	0.577	-2.829	0.951
O	-4.138	-0.662	1.560	H	-3.424	-2.313	3.487
O	-2.083	-1.310	2.236	H	-1.799	-1.921	4.146
C	1.534	-2.387	0.674	H	-3.046	-0.641	3.965
N	2.502	-0.452	-0.039	H	2.926	-2.566	2.373
C	-2.633	-1.561	3.542	H	1.594	-1.424	2.618
C	2.303	-1.813	1.881	H	4.185	-0.925	1.112
C	3.134	-0.666	1.269	H	3.095	0.246	1.873
C	3.162	0.145	-1.084	H	2.106	-0.822	-2.719
O	4.263	0.650	-0.904	H	1.553	0.818	-2.353
C	2.438	0.176	-2.417	H	3.124	0.584	-3.162

N3-R_OtPcQc frozen

C	-1.303	-2.579	-0.107	H	-0.719	-3.029	0.703
C	-2.815	-2.654	0.173	H	-1.062	-3.102	-1.041
N	-1.024	-1.135	-0.230	H	-3.268	-3.549	-0.264
C	-3.358	-1.349	-0.427	H	-2.993	-2.674	1.252
C	-2.246	-0.331	-0.107	H	-4.325	-1.047	-0.018
C	0.153	-0.458	0.045	H	-3.463	-1.437	-1.515
C	-2.460	0.310	1.268	H	-2.231	0.502	-0.813
O	0.124	0.712	0.424	H	2.144	-2.281	-1.721
N	1.361	-1.110	-0.160	H	0.957	-3.130	-0.714
O	-3.086	1.333	1.432	H	-3.153	0.305	3.823
O	-1.961	-0.440	2.275	H	-1.660	-0.589	4.272
C	1.769	-2.412	-0.698	H	-1.562	1.085	3.635
N	2.575	-0.497	0.180	H	3.745	-3.282	-0.272
C	-2.099	0.135	3.585	H	2.561	-3.536	1.018
C	2.917	-2.819	0.273	H	4.397	-1.245	0.858
C	3.337	-1.478	0.947	H	3.060	-1.454	2.007
C	3.031	0.774	-0.116	H	1.756	0.938	-1.881
O	4.050	1.175	0.433	H	1.597	2.253	-0.714
C	2.309	1.570	-1.181	H	3.065	2.149	-1.717

N3-R_OtPcQt free

C	-2.313	-0.459	-0.047	H	-2.218	0.594	-0.321
C	-3.287	-1.237	-0.947	H	-2.604	-0.503	1.010
N	-1.018	-1.145	-0.233	H	-4.293	-1.287	-0.522
C	-2.636	-2.622	-1.085	H	-3.357	-0.756	-1.927
C	-1.119	-2.315	-1.109	H	-2.960	-3.178	-1.969
C	0.135	-0.449	0.048	H	-2.850	-3.240	-0.205
C	-0.620	-2.097	-2.542	H	-0.548	-3.166	-0.734
O	0.137	0.711	0.425	H	1.792	-3.278	-0.022
N	1.331	-1.207	-0.175	H	0.580	-2.696	1.138
O	-0.097	-2.969	-3.201	H	3.524	-2.761	1.455
O	-0.892	-0.860	-3.004	H	2.342	-2.286	2.681
C	1.518	-2.448	0.637	H	4.063	-0.417	1.389
N	2.500	-0.443	0.011	H	2.466	0.031	2.048
C	-0.539	-0.623	-4.380	H	-1.074	-1.316	-5.035
C	2.656	-2.123	1.646	H	-0.835	0.406	-4.582
C	2.997	-0.643	1.368	H	0.536	-0.751	-4.526
C	3.327	-0.123	-1.050	H	2.426	-1.285	-2.645
O	4.463	0.288	-0.855	H	1.822	0.370	-2.519
C	2.719	-0.252	-2.433	H	3.467	0.078	-3.156

N3-R_OtPcQt frozen

C	-2.294	-0.437	0.061	H	-2.154	0.637	-0.069
C	-3.313	-1.040	-0.915	H	-2.576	-0.614	1.107
N	-1.027	-1.145	-0.234	H	-4.319	-1.083	-0.489
C	-2.743	-2.432	-1.219	H	-3.356	-0.443	-1.830
C	-1.210	-2.217	-1.220	H	-3.102	-2.863	-2.159
C	0.147	-0.452	0.047	H	-2.991	-3.134	-0.415
C	-0.690	-1.908	-2.629	H	-0.709	-3.142	-0.934
O	0.133	0.716	0.426	H	1.593	-2.975	-1.162
N	1.332	-1.165	-0.059	H	0.854	-3.143	0.453
O	-0.082	-2.711	-3.304	H	3.703	-3.234	-0.189
O	-1.027	-0.673	-3.050	H	3.003	-3.306	1.433
C	1.605	-2.608	-0.130	H	4.502	-1.058	0.464
N	2.577	-0.520	-0.121	H	3.327	-0.969	1.798
C	-0.642	-0.352	-4.401	H	-1.124	-1.035	-5.105
C	3.025	-2.729	0.504	H	-0.979	0.672	-4.563
C	3.472	-1.266	0.752	H	0.441	-0.424	-4.517
C	2.956	0.596	-0.838	H	1.386	0.398	-2.335
O	4.075	1.065	-0.661	H	1.284	1.843	-1.331
C	1.980	1.170	-1.839	H	2.561	1.729	-2.575

N3-R_OtPtQc free

C	-1.269	-2.574	-0.406	H	-0.674	-3.166	0.292
C	-2.777	-2.717	-0.139	H	-1.010	-2.889	-1.422
N	-1.016	-1.131	-0.228	H	-3.215	-3.544	-0.704
C	-3.342	-1.347	-0.539	H	-2.954	-2.900	0.926
C	-2.254	-0.363	-0.058	H	-4.319	-1.125	-0.100
C	0.145	-0.460	0.044	H	-3.437	-1.271	-1.628
C	-2.520	0.104	1.376	H	-2.227	0.549	-0.657
O	0.124	0.709	0.423	H	3.432	-0.733	0.131
N	1.391	-1.143	-0.081	H	2.373	0.701	0.207
O	-3.219	1.056	1.641	H	-3.246	-0.273	3.895
O	-1.964	-0.706	2.302	H	-1.674	-1.056	4.274
C	2.550	-0.246	-0.297	H	-1.746	0.684	3.840
N	1.493	-2.103	-1.121	H	3.696	-0.090	-2.170
C	-2.178	-0.305	3.665	H	2.151	0.771	-2.187
C	2.656	-0.134	-1.836	H	2.566	-2.091	-2.918
C	1.931	-1.407	-2.354	H	1.057	-1.157	-2.964
C	2.075	-3.338	-0.813	H	1.210	-3.590	1.183
O	2.482	-4.066	-1.704	H	2.472	-4.766	0.705
C	2.156	-3.723	0.654	H	2.893	-3.097	1.169

N3-R_OtPtQc frozen

C	-1.109	-2.149	-1.335	H	-0.819	-3.150	-1.004
C	-2.580	-2.099	-1.783	H	-0.436	-1.858	-2.151
N	-1.025	-1.154	-0.236	H	-2.690	-2.341	-2.844
C	-3.023	-0.672	-1.431	H	-3.174	-2.824	-1.214
C	-2.291	-0.411	-0.107	H	-4.103	-0.564	-1.324
C	0.136	-0.448	0.048	H	-2.670	0.040	-2.186
C	-3.136	-0.836	1.100	H	-2.051	0.646	0.046
O	0.142	0.721	0.428	H	3.167	-0.379	0.649
N	1.343	-1.103	-0.142	H	2.448	0.602	-0.647
O	-4.350	-0.838	1.111	H	-3.757	-2.334	3.206
O	-2.383	-1.146	2.172	H	-2.361	-1.677	4.124
C	2.623	-0.417	-0.303	H	-3.736	-0.616	3.671
N	1.628	-2.470	-0.220	H	4.385	-1.514	-1.039
C	-3.116	-1.463	3.368	H	3.368	-0.862	-2.329
C	3.350	-1.328	-1.340	H	3.107	-3.553	-1.216
C	2.518	-2.647	-1.364	H	1.946	-2.749	-2.294
C	1.180	-3.481	0.601	H	-0.556	-2.814	1.715
O	1.382	-4.649	0.285	H	0.545	-3.926	2.567
C	0.492	-3.073	1.887	H	0.968	-2.199	2.343

N3-R_OtPtQt free

C	-2.266	-0.349	-0.040	H	-2.132	0.666	-0.419
C	-3.344	-1.139	-0.798	H	-2.483	-0.273	1.032
N	-1.021	-1.135	-0.230	H	-4.316	-1.095	-0.298
C	-2.775	-2.561	-0.874	H	-3.473	-0.731	-1.807
C	-1.260	-2.322	-1.056	H	-3.188	-3.170	-1.682
C	0.149	-0.458	0.045	H	-2.934	-3.094	0.071
C	-0.931	-2.165	-2.546	H	-0.693	-3.186	-0.717
O	0.125	0.711	0.424	H	3.383	-0.627	0.477
N	1.390	-1.133	0.052	H	2.365	0.720	-0.093
O	-0.985	-3.086	-3.332	H	-1.225	-0.995	-4.887
O	-0.612	-0.900	-2.893	H	-0.170	0.375	-4.401
C	2.595	-0.335	-0.227	H	0.510	-1.273	-4.617
N	1.597	-2.382	-0.578	H	4.019	-0.638	-1.885
C	-0.359	-0.693	-4.294	H	2.399	-0.112	-2.375
C	2.952	-0.740	-1.670	H	3.290	-2.936	-1.682
C	2.479	-2.209	-1.762	H	1.930	-2.420	-2.684
C	1.794	-3.503	0.236	H	1.834	-2.666	2.226
O	2.319	-4.507	-0.217	H	0.219	-3.091	1.680
C	1.266	-3.407	1.654	H	1.370	-4.389	2.119

N3-R_OtPtQt frozen

C	-2.310	-0.472	0.042	H	-2.198	0.605	-0.092
C	-3.305	-1.102	-0.947	H	-2.598	-0.654	1.085
N	-1.024	-1.152	-0.235	H	-4.300	-1.225	-0.511
C	-2.660	-2.444	-1.326	H	-3.404	-0.468	-1.833
C	-1.144	-2.141	-1.313	H	-2.995	-2.841	-2.288
C	0.137	-0.449	0.048	H	-2.864	-3.204	-0.563
C	-0.664	-1.647	-2.683	H	-0.571	-3.047	-1.111
O	0.140	0.718	0.427	H	3.181	-0.366	0.615
N	1.343	-1.122	-0.107	H	2.458	0.534	-0.735
O	-0.143	-2.365	-3.511	H	-1.050	-0.326	-4.966
O	-0.919	-0.339	-2.881	H	-0.780	1.244	-4.134
C	2.627	-0.463	-0.327	H	0.557	0.057	-4.304
N	1.610	-2.495	-0.091	H	4.380	-1.596	-1.025
C	-0.519	0.186	-4.159	H	3.314	-1.061	-2.330
C	3.334	-1.446	-1.307	H	3.115	-3.648	-0.962
C	2.516	-2.771	-1.209	H	1.953	-2.971	-2.126
C	1.133	-3.434	0.793	H	0.747	-1.940	2.343
O	1.329	-4.626	0.578	H	-0.671	-2.869	1.836
C	0.406	-2.929	2.025	H	0.574	-3.659	2.820

N3-S_OcPcQc free

C	-1.124	-2.614	-0.292	H	-0.388	-3.069	0.374
C	-2.579	-2.889	0.122	H	-0.930	-2.970	-1.313
N	-1.013	-1.142	-0.232	H	-2.988	-3.779	-0.367
C	-3.320	-1.599	-0.270	H	-2.634	-3.039	1.204
C	-2.295	-0.489	0.050	H	-4.263	-1.453	0.263
C	0.128	-0.452	0.046	H	-3.536	-1.588	-1.345
C	-2.419	0.000	1.500	H	-2.431	0.397	-0.574
O	0.138	0.712	0.425	H	0.924	-1.513	-2.182
N	1.329	-1.239	-0.124	H	2.414	-2.283	-1.585
O	-3.127	0.925	1.831	H	-2.547	-0.547	4.238
O	-1.700	-0.759	2.343	H	-0.774	-0.847	4.133
C	1.783	-1.390	-1.519	H	-1.451	0.767	3.736
N	2.436	-0.631	0.509	H	1.928	0.693	-2.138
C	-1.620	-0.311	3.706	H	3.370	-0.251	-2.550
C	2.594	-0.104	-1.794	H	3.012	1.309	-0.164
C	3.177	0.254	-0.408	H	4.249	0.041	-0.344
C	2.510	-0.677	1.882	H	4.628	-0.151	2.011
O	1.705	-1.295	2.564	H	3.515	1.179	2.367
C	3.671	0.100	2.483	H	3.718	-0.137	3.546

N3-S_OcPcQc frozen

C	-1.195	-2.596	0.012	H	-0.543	-2.923	0.828
C	-2.688	-2.749	0.360	H	-0.943	-3.175	-0.885
N	-1.021	-1.148	-0.234	H	-3.105	-3.688	-0.017
C	-3.341	-1.508	-0.272	H	-2.819	-2.727	1.445
C	-2.279	-0.409	-0.070	H	-4.302	-1.242	0.177
C	0.137	-0.449	0.048	H	-3.501	-1.658	-1.346
C	-2.425	0.280	1.293	H	-2.359	0.389	-0.812
O	0.138	0.715	0.426	H	0.963	-2.220	-1.960
N	1.317	-1.149	-0.195	H	1.596	-3.216	-0.623
O	-3.034	1.314	1.457	H	-2.801	0.334	3.980
O	-1.865	-0.442	2.281	H	-1.199	-0.462	4.188
C	1.647	-2.233	-1.108	H	-1.312	1.172	3.465
N	2.483	-0.848	0.507	H	3.175	-1.506	-2.530
C	-1.799	0.200	3.564	H	3.755	-2.772	-1.440
C	3.117	-1.886	-1.507	H	3.589	0.199	-0.959
C	3.551	-0.790	-0.486	H	4.518	-1.001	-0.026
C	2.490	-0.663	1.870	H	4.597	-0.958	2.339
O	1.500	-0.865	2.558	H	4.171	0.721	1.961
C	3.817	-0.194	2.447	H	3.663	-0.001	3.510

N3-S_OcPcQt free

C	-2.309	-0.471	-0.040	H	-2.365	-0.046	0.965
C	-3.317	-1.593	-0.299	H	-2.417	0.354	-0.756
N	-1.014	-1.142	-0.232	H	-4.296	-1.213	-0.605
C	-2.632	-2.424	-1.394	H	-3.456	-2.193	0.608
C	-1.131	-2.389	-1.009	H	-3.004	-3.450	-1.468
C	0.131	-0.451	0.047	H	-2.765	-1.941	-2.367
C	-0.219	-2.462	-2.238	H	-0.876	-3.262	-0.399
O	0.137	0.711	0.425	H	0.656	-2.794	1.075
N	1.333	-1.215	-0.166	H	2.222	-3.059	0.280
O	0.466	-3.427	-2.498	H	1.534	-1.200	-3.852
O	-0.351	-1.374	-3.007	H	0.172	-0.438	-4.722
C	1.591	-2.318	0.780	H	0.376	-2.224	-4.771
N	2.493	-0.421	-0.059	H	1.596	-1.294	2.706
C	0.499	-1.320	-4.171	H	3.018	-2.319	2.462
C	2.320	-1.641	1.962	H	2.809	0.500	1.834
C	3.035	-0.435	1.309	H	4.120	-0.566	1.277
C	2.904	0.338	-1.126	H	4.993	0.614	-0.557
O	2.340	0.322	-2.211	H	3.922	1.933	-0.056
C	4.122	1.209	-0.855	H	4.356	1.747	-1.775

N3-S_OcPcQt frozen

C	-2.293	-0.464	0.054	H	-2.313	-0.145	1.099
C	-3.326	-1.537	-0.290	H	-2.407	0.430	-0.573
N	-1.024	-1.149	-0.234	H	-4.322	-1.121	-0.471
C	-2.726	-2.196	-1.543	H	-3.404	-2.261	0.529
C	-1.188	-2.143	-1.316	H	-3.069	-3.222	-1.704
C	0.140	-0.448	0.048	H	-2.984	-1.610	-2.429
C	-0.425	-1.782	-2.597	H	-0.812	-3.123	-1.011
O	0.137	0.714	0.426	H	0.774	-3.112	0.635
N	1.308	-1.201	-0.037	H	1.571	-3.095	-0.964
O	0.408	-2.501	-3.111	H	0.919	0.133	-3.948
O	-0.817	-0.598	-3.083	H	-0.638	0.779	-4.554
C	1.553	-2.640	0.032	H	-0.107	-0.871	-5.028
N	2.549	-0.590	-0.221	H	2.891	-3.100	1.734
C	-0.102	-0.116	-4.239	H	3.629	-3.352	0.147
C	2.955	-2.706	0.716	H	3.360	-0.783	1.719
C	3.458	-1.233	0.723	H	4.492	-1.138	0.390
C	2.761	0.410	-1.136	H	4.922	0.355	-1.395
O	1.904	0.757	-1.938	H	4.384	1.409	-0.073
C	4.138	1.055	-1.080	H	4.130	1.901	-1.767

N3-S_OcPtQc free

C	-1.248	-2.583	-0.293	H	-0.444	-3.090	-0.827
C	-2.598	-2.661	-1.013	H	-1.312	-3.009	0.720
N	-1.016	-1.138	-0.231	H	-3.114	-3.611	-0.840
C	-3.363	-1.453	-0.448	H	-2.443	-2.546	-2.092
C	-2.268	-0.376	-0.208	H	-4.148	-1.085	-1.112
C	0.138	-0.457	0.045	H	-3.832	-1.724	0.505
C	-2.531	0.378	1.094	H	-2.258	0.382	-0.995
O	0.131	0.713	0.425	H	2.745	0.427	-0.343
N	1.354	-1.148	-0.023	H	2.527	-0.068	1.343
O	-3.108	1.440	1.154	H	-1.781	1.251	3.474
O	-2.144	-0.336	2.175	H	-1.992	-0.380	4.192
C	2.595	-0.435	0.318	H	-3.410	0.541	3.589
N	1.666	-2.106	-1.023	H	4.467	-1.166	-0.556
C	-2.350	0.319	3.435	H	4.152	-1.817	1.055
C	3.680	-1.523	0.114	H	3.451	-3.212	-1.319
C	2.907	-2.714	-0.516	H	2.643	-3.457	0.242
C	1.520	-1.712	-2.366	H	2.006	-3.719	-3.098
O	0.891	-0.718	-2.677	H	3.150	-2.453	-3.582
C	2.091	-2.671	-3.400	H	1.550	-2.513	-4.334

N3-S_OcPtQc frozen

C	-1.291	-2.573	-0.185	H	-0.477	-3.156	-0.613
C	-2.586	-2.675	-0.995	H	-1.443	-2.904	0.854
N	-1.017	-1.137	-0.230	H	-3.140	-3.597	-0.798
C	-3.358	-1.413	-0.571	H	-2.339	-2.635	-2.061
C	-2.254	-0.353	-0.282	H	-4.059	-1.060	-1.331
C	0.140	-0.458	0.045	H	-3.930	-1.614	0.341
C	-2.569	0.418	0.997	H	-2.184	0.396	-1.075
O	0.130	0.714	0.425	H	3.149	0.043	-0.039
N	1.366	-1.100	-0.090	H	2.281	-0.105	1.500
O	-3.133	1.488	1.022	H	-1.934	1.305	3.407
O	-2.244	-0.290	2.103	H	-2.197	-0.319	4.127
C	2.569	-0.640	0.595	H	-3.573	0.610	3.442
N	1.727	-2.228	-0.837	H	4.385	-1.877	0.533
C	-2.509	0.377	3.346	H	3.348	-2.225	1.921
C	3.345	-1.963	0.860	H	3.246	-3.667	-0.562
C	2.582	-3.037	0.032	H	1.971	-3.678	0.680
C	1.308	-2.440	-2.131	H	1.562	-4.615	-2.164
O	0.581	-1.652	-2.719	H	2.890	-3.714	-2.915
C	1.803	-3.733	-2.767	H	1.320	-3.821	-3.741

N3-S_OcPtQt free

C	-2.303	-0.515	0.090	H	-2.295	-0.166	1.125
C	-3.299	-1.646	-0.175	H	-2.488	0.353	-0.557
N	-1.018	-1.144	-0.233	H	-4.312	-1.280	-0.369
C	-2.688	-2.364	-1.388	H	-3.339	-2.320	0.689
C	-1.157	-2.293	-1.131	H	-3.025	-3.397	-1.508
C	0.135	-0.452	0.047	H	-2.933	-1.818	-2.305
C	-0.379	-2.155	-2.441	H	-0.794	-3.214	-0.667
O	0.136	0.714	0.425	H	2.635	0.485	-0.628
N	1.341	-1.114	-0.213	H	2.757	-0.134	1.028
O	0.275	-3.045	-2.944	H	1.215	-0.831	-4.105
O	-0.551	-0.941	-3.001	H	-0.116	0.287	-4.547
C	2.621	-0.422	-0.022	H	-0.196	-1.451	-4.995
N	1.546	-2.488	0.065	H	4.142	-1.223	-1.408
C	0.135	-0.729	-4.244	H	4.425	-1.628	0.288
C	3.648	-1.494	-0.470	H	2.557	-2.971	-1.696
C	2.800	-2.787	-0.647	H	3.275	-3.676	-0.233
C	1.291	-2.929	1.373	H	2.787	-4.353	2.021
O	0.662	-2.254	2.169	H	1.657	-5.018	0.825
C	1.742	-4.348	1.685	H	1.124	-4.720	2.505

N3-S_OcPtQt frozen

C	-2.284	-0.514	0.178	H	-2.210	-0.175	1.213
C	-3.293	-1.643	-0.035	H	-2.511	0.360	-0.448
N	-1.019	-1.138	-0.231	H	-4.317	-1.279	-0.153
C	-2.763	-2.336	-1.299	H	-3.267	-2.333	0.817
C	-1.217	-2.269	-1.134	H	-3.106	-3.368	-1.418
C	0.142	-0.457	0.045	H	-3.065	-1.771	-2.187
C	-0.542	-2.126	-2.495	H	-0.849	-3.202	-0.702
O	0.130	0.713	0.425	H	2.393	0.657	-0.627
N	1.370	-1.092	-0.120	H	3.168	-0.300	0.653
O	0.021	-3.034	-3.073	H	0.961	-0.850	-4.292
O	-0.685	-0.888	-3.006	H	-0.341	0.355	-4.564
C	2.614	-0.356	-0.293	H	-0.571	-1.363	-5.038
N	1.708	-2.452	-0.164	H	3.223	-0.818	-2.344
C	-0.120	-0.682	-4.311	H	4.440	-1.254	-1.138
C	3.365	-1.221	-1.337	H	2.232	-2.932	-2.164
C	2.709	-2.629	-1.228	H	3.425	-3.398	-0.930
C	1.155	-3.391	0.673	H	2.676	-4.950	0.646
O	0.346	-3.100	1.545	H	1.453	-5.119	-0.625
C	1.611	-4.821	0.417	H	1.032	-5.472	1.074

N3-S_OtPcQc free

C	-1.257	-2.134	-1.294	H	-0.504	-2.057	-2.084
C	-2.669	-1.808	-1.805	H	-1.230	-3.156	-0.891
N	-1.023	-1.137	-0.231	H	-3.166	-2.683	-2.234
C	-3.366	-1.261	-0.554	H	-2.619	-1.033	-2.579
C	-2.259	-0.406	0.093	H	-4.260	-0.670	-0.765
C	0.150	-0.456	0.046	H	-3.648	-2.083	0.114
C	-2.509	-0.187	1.580	H	-2.240	0.596	-0.349
O	0.126	0.711	0.424	H	2.289	-2.997	0.352
N	1.363	-1.162	0.028	H	0.803	-3.124	-0.589
O	-3.259	0.668	1.994	H	-1.781	0.073	4.098
O	-1.876	-1.082	2.363	H	-1.508	-1.694	4.256
C	1.688	-2.516	-0.430	H	-3.163	-1.043	4.009
N	2.531	-0.407	-0.199	H	3.293	-3.056	-1.835
C	-2.103	-0.919	3.773	H	1.906	-2.258	-2.588
C	2.540	-2.275	-1.694	H	4.250	-0.907	-1.270
C	3.172	-0.881	-1.440	H	2.971	-0.188	-2.263
C	3.314	0.043	0.863	H	2.320	-0.900	2.535
O	4.462	0.410	0.658	H	1.754	0.730	2.169
C	2.644	0.098	2.218	H	3.364	0.496	2.934

N3-S_OtPcQc frozen

C	-1.244	-2.082	-1.349	H	-0.487	-1.950	-2.129
C	-2.659	-1.748	-1.848	H	-1.202	-3.124	-1.002
N	-1.026	-1.141	-0.232	H	-3.151	-2.609	-2.310
C	-3.362	-1.253	-0.578	H	-2.616	-0.943	-2.591
C	-2.260	-0.417	0.101	H	-4.258	-0.659	-0.767
C	0.150	-0.454	0.047	H	-3.640	-2.102	0.059
C	-2.523	-0.237	1.591	H	-2.240	0.597	-0.314
O	0.129	0.714	0.425	H	1.964	-3.037	0.632
N	1.337	-1.158	-0.065	H	0.854	-3.120	-0.746
O	-3.310	0.580	2.016	H	-1.825	0.012	4.124
O	-1.853	-1.114	2.365	H	-1.483	-1.746	4.252
C	1.679	-2.562	-0.314	H	-3.160	-1.158	3.996
N	2.581	-0.528	0.066	H	3.675	-3.165	-1.015
C	-2.103	-0.986	3.776	H	2.607	-2.606	-2.309
C	2.902	-2.435	-1.270	H	4.445	-0.883	-0.794
C	3.393	-0.969	-1.064	H	3.206	-0.352	-1.951
C	3.024	0.346	1.042	H	1.562	-0.385	2.496
O	4.089	0.925	0.873	H	1.603	1.366	2.282
C	2.223	0.468	2.320	H	2.941	0.563	3.139

N3-S_OtPcQt free

C	-2.296	-0.450	0.016	H	-2.302	-0.032	1.024
C	-3.322	-1.560	-0.206	H	-2.430	0.380	-0.691
N	-1.020	-1.140	-0.231	H	-4.319	-1.173	-0.435
C	-2.717	-2.357	-1.372	H	-3.399	-2.188	0.690
C	-1.184	-2.305	-1.114	H	-3.076	-3.387	-1.438
C	0.142	-0.452	0.047	H	-2.946	-1.857	-2.319
C	-0.415	-2.234	-2.435	H	-0.851	-3.227	-0.629
O	0.131	0.710	0.424	H	0.634	-2.774	1.024
N	1.343	-1.177	-0.181	H	1.500	-3.294	-0.440
O	0.221	-3.160	-2.891	H	1.055	-1.148	-4.342
O	-0.598	-1.057	-3.063	H	-0.220	0.060	-4.709
C	1.486	-2.562	0.371	H	-0.487	-1.683	-5.051
N	2.506	-0.462	0.186	H	2.731	-3.112	2.100
C	-0.020	-0.959	-4.378	H	3.618	-2.983	0.571
C	2.810	-2.547	1.168	H	2.554	-0.668	2.275
C	3.077	-1.050	1.389	H	4.131	-0.779	1.447
C	3.242	0.284	-0.712	H	1.642	1.140	-1.879
O	4.351	0.705	-0.410	H	2.323	-0.341	-2.564
C	2.572	0.585	-2.037	H	3.263	1.180	-2.634

N3-S_OtPcQt frozen

C	-2.281	-0.455	0.115	H	-2.242	-0.119	1.153
C	-3.329	-1.534	-0.151	H	-2.434	0.428	-0.518
N	-1.027	-1.144	-0.233	H	-4.334	-1.123	-0.285
C	-2.799	-2.215	-1.422	H	-3.360	-2.244	0.684
C	-1.248	-2.162	-1.274	H	-3.148	-3.243	-1.551
C	0.149	-0.453	0.047	H	-3.105	-1.643	-2.303
C	-0.596	-1.871	-2.628	H	-0.866	-3.139	-0.971
O	0.131	0.714	0.425	H	0.765	-3.147	0.437
N	1.322	-1.184	-0.039	H	1.541	-2.988	-1.160
O	0.031	-2.691	-3.265	H	0.720	-0.425	-4.424
O	-0.850	-0.619	-3.056	H	-0.640	0.740	-4.542
C	1.548	-2.633	-0.124	H	-0.834	-0.952	-5.117
N	2.585	-0.573	-0.055	H	2.895	-3.407	1.448
C	-0.364	-0.301	-4.374	H	3.628	-3.319	-0.158
C	2.950	-2.811	0.533	H	3.272	-1.089	1.871
C	3.435	-1.367	0.823	H	4.477	-1.184	0.566
C	3.018	0.549	-0.730	H	1.412	1.880	-1.219
O	4.147	0.975	-0.515	H	1.461	0.454	-2.252
C	2.084	1.187	-1.733	H	2.700	1.734	-2.449

N3-S_OtPtQc free

C	-1.237	-2.389	-0.959	H	-0.504	-2.509	-1.758
C	-2.666	-2.230	-1.499	H	-1.155	-3.252	-0.290
N	-1.015	-1.130	-0.228	H	-3.150	-3.195	-1.680
C	-3.360	-1.404	-0.409	H	-2.652	-1.675	-2.444
C	-2.265	-0.401	0.022	H	-4.263	-0.891	-0.747
C	0.144	-0.460	0.044	H	-3.629	-2.047	0.437
C	-2.464	0.052	1.464	H	-2.304	0.512	-0.581
O	0.124	0.709	0.423	H	3.431	-0.754	0.105
N	1.389	-1.136	-0.142	H	2.357	0.528	0.724
O	-3.142	1.007	1.767	H	-1.654	0.575	3.927
O	-1.888	-0.781	2.358	H	-1.566	-1.176	4.318
C	2.501	-0.546	0.643	H	-3.147	-0.393	3.981
N	1.399	-2.510	0.222	H	3.452	-1.520	2.372
C	-2.082	-0.412	3.734	H	1.935	-0.690	2.749
C	2.450	-1.295	1.998	H	2.174	-3.515	1.889
C	1.644	-2.586	1.681	H	0.682	-2.596	2.202
C	2.073	-3.404	-0.617	H	1.425	-2.652	-2.563
O	2.404	-4.505	-0.206	H	2.800	-3.792	-2.570
C	2.338	-2.955	-2.043	H	3.011	-2.092	-2.062

N3-S_OtPtQc frozen

C	-1.255	-2.586	-0.044	H	-0.504	-3.188	-0.556
C	-2.654	-2.763	-0.638	H	-1.239	-2.842	1.025
N	-1.022	-1.144	-0.233	H	-3.149	-3.670	-0.278
C	-3.390	-1.477	-0.219	H	-2.582	-2.830	-1.730
C	-2.280	-0.390	-0.106	H	-4.168	-1.180	-0.927
C	0.141	-0.454	0.046	H	-3.869	-1.622	0.754
C	-2.431	0.385	1.204	H	-2.347	0.357	-0.900
O	0.134	0.716	0.426	H	3.201	-0.072	-0.111
N	1.354	-1.107	-0.113	H	2.347	-0.125	1.446
O	-2.981	1.457	1.295	H	-1.463	1.243	3.519
O	-1.983	-0.332	2.261	H	-1.698	-0.373	4.265
C	2.589	-0.698	0.550	H	-3.112	0.608	3.749
N	1.680	-2.226	-0.884	H	4.334	-2.040	0.561
C	-2.075	0.338	3.528	H	3.211	-2.332	1.894
C	3.276	-2.069	0.835	H	3.120	-3.721	-0.673
C	2.492	-3.096	-0.038	H	1.856	-3.746	0.577
C	1.326	-2.489	-2.189	H	-0.395	-1.356	-2.835
O	1.554	-3.594	-2.667	H	0.903	-1.540	-4.031
C	0.690	-1.359	-2.976	H	1.068	-0.377	-2.678

N3-S_OtPtQt free

C	-2.272	-0.420	0.073	H	-2.241	-0.048	1.099
C	-3.335	-1.488	-0.173	H	-2.401	0.445	-0.592
N	-1.024	-1.141	-0.232	H	-4.331	-1.064	-0.328
C	-2.804	-2.212	-1.418	H	-3.385	-2.174	0.681
C	-1.250	-2.171	-1.263	H	-3.161	-3.239	-1.522
C	0.147	-0.454	0.047	H	-3.103	-1.664	-2.319
C	-0.631	-1.887	-2.628	H	-0.866	-3.143	-0.952
O	0.130	0.713	0.425	H	2.415	0.640	-0.194
N	1.365	-1.152	0.065	H	3.337	-0.660	0.599
O	-0.320	-2.750	-3.420	H	0.940	-0.600	-4.359
O	-0.541	-0.564	-2.884	H	-0.080	0.872	-4.233
C	2.614	-0.430	-0.194	H	-0.733	-0.635	-4.963
N	1.530	-2.463	-0.437	H	2.610	-0.435	-2.364
C	-0.072	-0.217	-4.199	H	4.154	-0.967	-1.680
C	3.069	-1.005	-1.549	H	2.076	-2.752	-2.475
C	2.538	-2.456	-1.531	H	3.304	-3.194	-1.282
C	1.541	-3.531	0.466	H	-0.140	-2.929	1.700
O	2.012	-4.607	0.133	H	1.433	-2.518	2.372
C	0.889	-3.286	1.812	H	0.900	-4.225	2.367

N3-S_OtPtQt frozen

C	-2.300	-0.490	0.077	H	-2.311	-0.180	1.125
C	-3.314	-1.583	-0.259	H	-2.443	0.407	-0.541
N	-1.024	-1.150	-0.235	H	-4.320	-1.188	-0.427
C	-2.721	-2.235	-1.522	H	-3.367	-2.310	0.559
C	-1.175	-2.093	-1.357	H	-3.010	-3.281	-1.647
C	0.139	-0.449	0.048	H	-3.052	-1.689	-2.411
C	-0.548	-1.607	-2.665	H	-0.711	-3.057	-1.136
O	0.138	0.717	0.426	H	2.490	0.508	-0.687
N	1.337	-1.136	-0.093	H	3.192	-0.441	0.642
O	0.075	-2.310	-3.432	H	0.801	0.149	-4.139
O	-0.810	-0.303	-2.889	H	-0.589	1.285	-4.123
C	2.634	-0.501	-0.301	H	-0.707	-0.293	-4.975
N	1.580	-2.513	-0.075	H	3.237	-1.099	-2.325
C	-0.289	0.237	-4.115	H	4.372	-1.615	-1.071
C	3.312	-1.481	-1.303	H	1.974	-3.061	-2.086
C	2.513	-2.814	-1.167	H	3.122	-3.668	-0.872
C	1.060	-3.449	0.789	H	-0.751	-2.891	1.820
O	1.234	-4.642	0.565	H	0.659	-1.953	2.335
C	0.324	-2.943	2.015	H	0.492	-3.671	2.813

N2-R_OcPcQc free

C	-1.125	-2.608	-0.321	H	-0.412	-3.018	-1.038
C	-2.580	-2.794	-0.763	H	-0.927	-3.063	0.658
N	-1.013	-1.143	-0.232	H	-2.964	-3.791	-0.529
C	-3.325	-1.677	-0.013	H	-2.660	-2.647	-1.847
C	-2.306	-0.507	0.068	H	-4.253	-1.370	-0.502
C	0.128	-0.451	0.047	H	-3.576	-2.015	0.998
C	-2.348	0.159	1.446	H	-2.522	0.281	-0.659
O	0.138	0.712	0.425	H	2.399	-2.289	-1.596
N	1.330	-1.238	-0.124	H	0.951	-1.444	-2.195
O	-2.946	1.183	1.687	H	-1.186	1.007	3.577
O	-1.707	-0.594	2.357	H	-0.818	-0.647	4.168
C	1.802	-1.374	-1.514	H	-2.506	-0.020	4.198
N	2.424	-0.646	0.546	H	3.419	-0.254	-2.523
C	-1.552	-0.019	3.663	H	2.027	0.726	-2.025
C	2.664	-0.116	-1.743	H	4.320	-0.236	-0.300
C	3.288	0.132	-0.355	H	3.284	1.196	-0.094
C	2.560	-0.848	1.897	H	3.737	0.898	2.430
O	1.746	-1.484	2.553	H	4.715	-0.525	2.042
C	3.785	-0.194	2.519	H	3.808	-0.464	3.575

N2-R_OcPcQt free

C	-2.331	-0.552	0.013	H	-2.216	0.317	0.662
C	-3.123	-1.709	0.632	H	-2.777	-0.222	-0.935
N	-1.010	-1.148	-0.234	H	-4.205	-1.591	0.515
C	-2.574	-2.936	-0.110	H	-2.899	-1.780	1.703
C	-1.063	-2.621	-0.285	H	-2.720	-3.879	0.423
C	0.118	-0.449	0.047	H	-3.057	-3.025	-1.091
C	-0.547	-3.260	-1.565	H	-0.470	-3.029	0.536
O	0.145	0.715	0.426	H	2.691	-1.693	-1.691
N	1.326	-1.252	-0.168	H	1.358	-0.625	-2.182
O	-0.195	-4.416	-1.632	H	0.804	-3.391	-3.844
O	-0.607	-2.433	-2.635	H	-0.336	-2.249	-4.633
C	2.065	-0.849	-1.382	H	-0.883	-3.879	-4.117
N	2.262	-1.005	0.874	H	3.825	0.470	-1.558
C	-0.229	-3.035	-3.885	H	2.338	1.274	-1.003
C	2.925	0.355	-0.947	H	4.266	-0.370	0.642
C	3.252	0.031	0.524	H	3.148	0.913	1.164
C	1.992	-1.526	2.110	H	2.905	-0.140	3.499
O	0.994	-2.207	2.332	H	4.037	-1.344	2.861
C	3.004	-1.189	3.192	H	2.798	-1.825	4.054

N2-R_OcPtQc free

C	-1.175	-2.347	-1.051	H	-0.348	-2.445	-1.757
C	-2.542	-2.132	-1.714	H	-1.188	-3.242	-0.415
N	-1.014	-1.135	-0.230	H	-3.015	-3.073	-2.010
C	-3.331	-1.375	-0.636	H	-2.431	-1.511	-2.610
C	-2.275	-0.414	-0.041	H	-4.199	-0.831	-1.016
C	0.138	-0.458	0.045	H	-3.679	-2.072	0.135
C	-2.598	-0.046	1.402	H	-2.257	0.536	-0.586
O	0.130	0.711	0.424	H	3.400	-0.774	-0.297
N	1.357	-1.161	-0.169	H	2.418	0.589	0.309
O	-3.341	0.863	1.699	H	-2.003	0.407	3.938
O	-2.040	-0.886	2.300	H	-1.837	-1.352	4.260
C	2.563	-0.488	0.347	H	-3.434	-0.646	3.840
N	1.409	-2.467	0.383	H	3.781	-1.266	2.010
C	-2.355	-0.593	3.672	H	2.374	-0.321	2.524
C	2.734	-1.040	1.784	H	2.381	-3.209	2.126
C	1.850	-2.318	1.790	H	0.965	-2.185	2.420
C	1.820	-3.497	-0.463	H	1.435	-5.068	1.015
O	1.855	-3.374	-1.676	H	3.149	-4.803	0.651
C	2.142	-4.821	0.217	H	2.116	-5.597	-0.549

N2-R_OcPtQt free

C	-2.268	-0.383	0.005	H	-2.233	0.103	0.982
C	-3.344	-1.462	-0.115	H	-2.392	0.404	-0.750
N	-1.019	-1.131	-0.229	H	-4.327	-1.048	-0.358
C	-2.789	-2.368	-1.220	H	-3.433	-2.015	0.828
C	-1.258	-2.388	-0.952	H	-3.205	-3.379	-1.225
C	0.149	-0.460	0.045	H	-2.985	-1.917	-2.200
C	-0.522	-2.570	-2.277	H	-0.990	-3.253	-0.341
O	0.123	0.709	0.423	H	3.415	-0.610	-0.055
N	1.391	-1.114	-0.132	H	2.326	0.520	0.796
O	-0.243	-3.667	-2.714	H	1.427	-1.922	-3.937
O	-0.306	-1.411	-2.912	H	0.510	-0.490	-4.519
C	2.536	-0.527	0.590	H	-0.091	-2.149	-4.857
N	1.455	-2.507	0.120	H	3.720	-1.695	2.035
C	0.437	-1.511	-4.144	H	2.329	-0.876	2.755
C	2.680	-1.404	1.864	H	2.268	-3.591	1.768
C	1.782	-2.637	1.565	H	0.849	-2.598	2.135
C	2.212	-3.229	-0.831	H	1.621	-5.117	0.110
O	2.627	-2.722	-1.855	H	3.377	-4.858	-0.021
C	2.413	-4.702	-0.519	H	2.436	-5.235	-1.471

N2-R_OtPcQc free

C	-1.178	-2.601	-0.300	H	-1.095	-3.045	0.702
C	-2.594	-2.742	-0.864	H	-0.421	-3.062	-0.937
N	-1.015	-1.141	-0.232	H	-2.574	-2.612	-1.953
C	-3.354	-1.584	-0.196	H	-3.036	-3.720	-0.649
C	-2.301	-0.449	-0.068	H	-3.690	-1.889	0.800
C	0.133	-0.451	0.047	H	-4.232	-1.257	-0.758
C	-2.461	0.290	1.260	H	-2.421	0.311	-0.846
N	1.332	-1.238	-0.108	H	2.321	-2.446	-1.520
O	0.135	0.711	0.424	H	0.843	-1.665	-2.134
O	-3.067	1.329	1.379	H	-1.514	1.172	3.572
O	-1.946	-0.414	2.292	H	-1.613	-0.470	4.289
C	1.727	-1.526	-1.510	H	-3.106	0.411	3.822
N	2.466	-0.588	0.424	H	3.300	-0.541	-2.697
C	-2.058	0.224	3.576	H	1.920	0.493	-2.294
C	2.572	-0.301	-1.917	H	4.289	-0.174	-0.518
C	3.242	0.131	-0.596	H	3.187	1.211	-0.435
C	2.962	-0.866	1.674	H	1.137	-1.266	2.768
C	2.101	-1.745	2.563	H	2.637	-1.899	3.500
O	4.032	-0.389	2.030	H	1.893	-2.708	2.087

N2-R_OtPcQt free

C	-2.319	-0.493	-0.016	H	-2.877	-0.461	-0.961
C	-3.007	-1.405	1.004	H	-2.146	0.525	0.333
N	-1.021	-1.152	-0.235	H	-2.628	-1.185	2.008
C	-2.574	-2.811	0.556	H	-4.095	-1.287	1.018
C	-1.145	-2.608	-0.050	H	-3.256	-3.184	-0.215
C	0.132	-0.445	0.049	H	-2.556	-3.544	1.366
C	-1.014	-3.448	-1.318	H	-0.366	-2.963	0.627
O	0.143	0.715	0.426	H	2.231	-2.599	-1.419
N	1.324	-1.231	-0.098	H	0.774	-1.805	-2.067
O	-0.501	-4.545	-1.349	H	3.266	-0.841	-2.763
O	-1.594	-2.856	-2.386	H	1.923	0.270	-2.454
C	1.677	-1.657	-1.475	H	4.295	-0.283	-0.647
N	2.482	-0.564	0.357	H	3.225	1.128	-0.681
C	-1.587	-3.632	-3.598	H	-0.561	-3.858	-3.902
C	2.554	-0.503	-2.005	H	-2.081	-3.011	-4.345
C	3.253	0.036	-0.739	H	-2.129	-4.570	-3.455
C	3.015	-0.758	1.607	H	1.248	-0.983	2.829
O	4.109	-0.284	1.887	H	2.749	-1.661	3.511
C	2.166	-1.534	2.597	H	1.879	-2.513	2.199

N2-R_OtPtQc free

C	-1.237	-2.389	-0.959	H	-1.155	-3.252	-0.289
C	-2.666	-2.230	-1.499	H	-0.504	-2.509	-1.758
N	-1.015	-1.130	-0.228	H	-2.652	-1.675	-2.444
C	-3.360	-1.403	-0.409	H	-3.150	-3.195	-1.680
C	-2.265	-0.401	0.021	H	-3.629	-2.047	0.437
C	0.144	-0.460	0.044	H	-4.263	-0.890	-0.747
C	-2.464	0.052	1.464	H	-2.304	0.512	-0.581
O	0.124	0.709	0.423	H	3.431	-0.754	0.106
N	1.389	-1.136	-0.141	H	2.357	0.528	0.725
O	-3.142	1.007	1.767	H	3.450	-1.519	2.374
C	2.501	-0.547	0.644	H	1.932	-0.691	2.749
O	-1.888	-0.780	2.358	H	2.175	-3.515	1.888
N	1.399	-2.510	0.222	H	0.682	-2.598	2.202
C	-2.082	-0.412	3.734	H	-1.654	0.576	3.926
C	2.448	-1.295	1.998	H	-1.567	-1.175	4.318
C	1.644	-2.587	1.681	H	-3.147	-0.392	3.981
C	2.073	-3.404	-0.618	H	1.426	-2.650	-2.563
O	2.404	-4.505	-0.207	H	2.799	-3.791	-2.571
C	2.338	-2.955	-2.044	H	3.012	-2.092	-2.062

N2-R_OtPtQt free

C	-2.290	-0.392	-0.189	H	-2.062	0.669	-0.092
C	-3.041	-0.983	1.005	H	-2.842	-0.561	-1.122
N	-1.028	-1.160	-0.238	H	-4.118	-0.789	0.975
C	-2.706	-2.475	0.891	H	-2.642	-0.563	1.936
C	-1.239	-2.500	0.354	H	-2.790	-3.028	1.830
C	0.136	-0.444	0.049	H	-3.372	-2.952	0.163
C	-1.060	-3.700	-0.568	H	-0.545	-2.659	1.185
O	0.146	0.722	0.428	H	3.373	-0.513	-0.078
N	1.352	-1.076	-0.224	H	2.338	0.010	1.271
O	-0.706	-4.786	-0.159	H	-0.286	-4.864	-2.845
O	-1.440	-3.453	-1.834	H	-1.737	-4.221	-3.685
C	2.546	-0.806	0.580	H	-1.914	-5.422	-2.361
N	1.459	-2.393	-0.709	H	3.880	-2.329	1.454
C	-1.333	-4.576	-2.736	H	2.281	-2.232	2.203
C	2.818	-2.171	1.250	H	3.032	-3.723	-0.329
C	2.258	-3.205	0.242	H	1.625	-3.961	0.715
C	1.614	-2.600	-2.083	H	1.709	-0.537	-2.747
O	2.012	-3.680	-2.492	H	0.114	-1.284	-2.882
C	1.187	-1.468	-2.992	H	1.407	-1.762	-4.019

N2-S_OcPcQc free

C	-1.101	-2.358	-1.060	H	-0.274	-2.378	-1.771
C	-2.485	-2.224	-1.711	H	-1.046	-3.261	-0.436
N	-1.011	-1.143	-0.232	H	-2.911	-3.191	-1.994
C	-3.310	-1.497	-0.638	H	-2.412	-1.607	-2.614
C	-2.303	-0.482	-0.044	H	-4.203	-0.998	-1.024
C	0.125	-0.451	0.046	H	-3.625	-2.205	0.138
C	-2.638	-0.137	1.402	H	-2.328	0.467	-0.590
O	0.139	0.712	0.425	H	0.758	-2.457	1.501
N	1.317	-1.253	-0.143	H	2.292	-2.904	0.711
O	-3.408	0.744	1.710	H	-2.052	0.309	3.941
O	-2.046	-0.967	2.289	H	-1.814	-1.446	4.243
C	1.667	-2.066	1.038	H	-3.440	-0.800	3.838
N	2.458	-0.440	-0.327	H	1.758	-0.523	2.567
C	-2.365	-0.702	3.666	H	3.160	-1.611	2.602
C	2.453	-1.095	1.946	H	3.048	0.894	1.230
C	3.155	-0.157	0.940	H	4.221	-0.386	0.838
C	2.622	0.170	-1.547	H	4.746	0.619	-1.289
O	1.850	-0.017	-2.479	H	3.664	2.001	-1.050
C	3.825	1.094	-1.646	H	3.944	1.378	-2.693

N2-S_OcPcQt free

C	-2.309	-0.471	-0.040	H	-2.365	-0.046	0.965
C	-3.317	-1.593	-0.299	H	-2.417	0.354	-0.757
N	-1.014	-1.142	-0.232	H	-4.296	-1.213	-0.606
C	-2.632	-2.424	-1.395	H	-3.456	-2.193	0.608
C	-1.131	-2.389	-1.009	H	-3.004	-3.450	-1.468
C	0.131	-0.451	0.047	H	-2.765	-1.941	-2.368
C	-0.219	-2.461	-2.238	H	-0.876	-3.262	-0.399
O	0.137	0.711	0.425	H	0.656	-2.794	1.075
N	1.333	-1.215	-0.166	H	2.222	-3.059	0.280
O	0.466	-3.427	-2.499	H	1.534	-1.198	-3.852
O	-0.350	-1.374	-3.007	H	0.172	-0.437	-4.722
C	1.591	-2.318	0.780	H	0.377	-2.223	-4.771
N	2.493	-0.421	-0.059	H	1.596	-1.296	2.706
C	0.499	-1.319	-4.170	H	3.019	-2.319	2.461
C	2.320	-1.641	1.963	H	2.806	0.500	1.835
C	3.033	-0.434	1.310	H	4.119	-0.563	1.279
C	2.904	0.338	-1.125	H	4.992	0.615	-0.555
O	2.340	0.323	-2.210	H	3.921	1.934	-0.055
C	4.121	1.211	-0.853	H	4.355	1.748	-1.773

N2-S_OcPtQc free

C	-1.233	-2.588	-0.265	H	-0.494	-3.087	-0.885
C	-2.650	-2.689	-0.835	H	-1.169	-3.010	0.747
N	-1.015	-1.134	-0.229	H	-3.128	-3.645	-0.599
C	-3.374	-1.489	-0.204	H	-2.617	-2.588	-1.926
C	-2.278	-0.396	-0.069	H	-4.224	-1.134	-0.791
C	0.140	-0.459	0.045	H	-3.746	-1.762	0.790
C	-2.421	0.343	1.261	H	-2.365	0.370	-0.845
O	0.128	0.711	0.424	H	2.335	0.480	0.752
N	1.362	-1.180	-0.086	H	3.290	-1.027	0.706
O	-2.988	1.416	1.385	H	-1.453	1.159	3.586
O	-1.949	-0.394	2.291	H	-1.620	-0.486	4.285
C	2.590	-0.393	0.155	H	-3.075	0.464	3.829
N	1.563	-1.831	-1.334	H	3.089	1.037	-1.455
C	-2.035	0.234	3.579	H	4.178	-0.354	-1.365
C	3.136	-0.036	-1.255	H	1.424	-0.182	-2.622
C	2.207	-0.826	-2.209	H	2.730	-1.300	-3.040
C	1.992	-3.165	-1.269	H	3.536	-3.457	-2.768
O	1.892	-3.832	-0.257	H	1.895	-3.453	-3.439
C	2.498	-3.758	-2.578	H	2.472	-4.844	-2.478

N2-S_OcPtQt free

C	-2.303	-0.481	0.050	H	-2.121	0.435	0.610
C	-3.076	-1.555	0.819	H	-2.807	-0.225	-0.892
N	-1.019	-1.140	-0.231	H	-4.159	-1.397	0.800
C	-2.657	-2.855	0.114	H	-2.751	-1.563	1.866
C	-1.192	-2.589	-0.369	H	-2.703	-3.738	0.756
C	0.140	-0.456	0.046	H	-3.310	-3.040	-0.746
C	-1.049	-3.113	-1.794	H	-0.473	-3.127	0.251
O	0.131	0.713	0.425	H	2.357	0.644	0.366
N	1.367	-1.155	-0.051	H	3.324	-0.834	0.611
O	-0.762	-4.260	-2.066	H	-0.391	-2.986	-4.383
O	-1.376	-2.186	-2.721	H	-1.706	-1.801	-4.680
C	2.595	-0.338	-0.037	H	-2.086	-3.488	-4.194
N	1.548	-2.107	-1.084	H	2.937	0.670	-1.968
C	-1.388	-2.655	-4.079	H	4.136	-0.574	-1.590
C	3.075	-0.315	-1.513	H	1.383	-0.901	-2.789
C	2.179	-1.374	-2.204	H	2.725	-2.055	-2.857
C	1.974	-3.382	-0.662	H	3.526	-3.993	-2.056
O	1.833	-3.747	0.490	H	1.869	-4.318	-2.622
C	2.520	-4.298	-1.744	H	2.578	-5.301	-1.320

N2-S_OtPcQc free

C	-1.155	-2.299	-1.130	H	-0.332	-2.320	-1.851
C	-2.530	-2.079	-1.776	H	-1.136	-3.243	-0.568
N	-1.017	-1.141	-0.232	H	-2.986	-3.013	-2.120
C	-3.329	-1.394	-0.658	H	-2.436	-1.409	-2.639
C	-2.289	-0.449	-0.013	H	-4.206	-0.846	-1.009
C	0.137	-0.452	0.047	H	-3.665	-2.138	0.075
C	-2.619	-0.163	1.448	H	-2.283	0.528	-0.508
O	0.134	0.711	0.424	H	0.564	-2.709	1.088
N	1.327	-1.199	-0.188	H	1.592	-3.320	-0.224
O	-3.389	0.707	1.789	H	-2.005	0.194	3.994
O	-2.026	-1.025	2.300	H	-1.776	-1.571	4.234
C	1.470	-2.516	0.508	H	-3.402	-0.902	3.869
N	2.502	-0.470	0.076	H	2.538	-2.736	2.426
C	-2.328	-0.805	3.689	H	3.558	-2.945	0.994
C	2.723	-2.373	1.411	H	2.521	-0.318	2.165
C	3.040	-0.866	1.369	H	4.103	-0.627	1.398
C	3.262	0.097	-0.928	H	1.717	0.894	-2.204
O	4.389	0.514	-0.699	H	2.234	-0.736	-2.652
C	2.586	0.231	-2.280	H	3.310	0.658	-2.975

N2-S_OtPcQt free

C	-2.301	-0.463	0.014	H	-2.309	-0.040	1.020
C	-3.314	-1.588	-0.199	H	-2.447	0.361	-0.697
N	-1.020	-1.142	-0.232	H	-4.318	-1.214	-0.423
C	-2.707	-2.382	-1.367	H	-3.377	-2.212	0.700
C	-1.169	-2.291	-1.139	H	-3.041	-3.422	-1.412
C	0.140	-0.451	0.047	H	-2.966	-1.901	-2.315
C	-0.426	-2.152	-2.470	H	-0.795	-3.212	-0.686
O	0.133	0.710	0.424	H	0.580	-2.763	1.034
N	1.337	-1.190	-0.172	H	1.571	-3.306	-0.339
O	0.270	-3.020	-2.951	H	0.934	-0.829	-4.370
O	-0.700	-0.978	-3.073	H	-0.516	0.160	-4.736
C	1.475	-2.548	0.444	H	-0.514	-1.609	-5.054
N	2.504	-0.468	0.157	H	2.579	-2.930	2.313
C	-0.158	-0.812	-4.396	H	3.579	-2.972	0.852
C	2.739	-2.465	1.336	H	2.467	-0.486	2.252
C	3.019	-0.955	1.430	H	4.075	-0.696	1.505
C	3.321	0.076	-0.818	H	1.777	0.775	-2.162
O	4.449	0.461	-0.543	H	2.487	-0.782	-2.613
C	2.712	0.207	-2.199	H	3.434	0.720	-2.836

N2-S_OtPtQc free

C	-1.233	-2.588	-0.265	H	-0.494	-3.087	-0.885
C	-2.650	-2.689	-0.835	H	-1.169	-3.010	0.747
N	-1.015	-1.134	-0.229	H	-3.128	-3.645	-0.599
C	-3.374	-1.489	-0.204	H	-2.617	-2.588	-1.926
C	-2.278	-0.396	-0.069	H	-4.224	-1.134	-0.792
C	0.140	-0.459	0.045	H	-3.746	-1.762	0.789
C	-2.421	0.343	1.261	H	-2.365	0.370	-0.845
O	0.128	0.711	0.424	H	2.335	0.480	0.752
N	1.362	-1.180	-0.086	H	3.290	-1.027	0.706
O	-2.988	1.416	1.385	H	-1.453	1.159	3.586
O	-1.949	-0.394	2.291	H	-1.620	-0.486	4.285
C	2.590	-0.393	0.155	H	-3.075	0.464	3.829
N	1.563	-1.831	-1.334	H	3.089	1.038	-1.454
C	-2.035	0.234	3.579	H	4.178	-0.354	-1.365
C	3.136	-0.036	-1.255	H	1.424	-0.181	-2.622
C	2.208	-0.826	-2.209	H	2.730	-1.300	-3.039
C	1.992	-3.165	-1.269	H	1.351	-3.994	0.633
O	2.200	-3.831	-2.266	H	2.787	-2.963	0.762
C	2.279	-3.697	0.129	H	2.905	-4.583	0.021

N2-S_OtPtQt free

C	-2.299	-0.449	0.005	H	-2.127	0.434	0.618
C	-3.152	-1.530	0.671	H	-2.732	-0.133	-0.954
N	-1.017	-1.137	-0.230	H	-4.225	-1.336	0.586
C	-2.724	-2.805	-0.070	H	-2.901	-1.598	1.736
C	-1.214	-2.578	-0.400	H	-2.869	-3.723	0.504
C	0.141	-0.456	0.046	H	-3.293	-2.900	-1.002
C	-0.939	-3.055	-1.825	H	-0.583	-3.136	0.294
O	0.129	0.711	0.424	H	2.373	0.674	0.380
N	1.392	-1.148	-0.049	H	3.424	-0.762	0.243
O	-1.069	-2.387	-2.827	H	-1.103	-4.699	-3.819
O	-0.626	-4.366	-1.810	H	-0.315	-6.038	-2.914
C	2.558	-0.241	-0.177	H	0.645	-4.619	-3.433
N	1.552	-2.055	-1.133	H	2.201	0.887	-2.010
C	-0.333	-4.962	-3.091	H	3.754	0.037	-2.003
C	2.705	-0.034	-1.702	H	1.131	-1.013	-2.915
C	2.006	-1.277	-2.315	H	2.662	-1.915	-2.906
C	2.152	-3.297	-0.891	H	1.235	-4.525	0.593
O	2.634	-3.935	-1.816	H	2.015	-3.085	1.287
C	2.099	-3.854	0.518	H	2.996	-4.458	0.670

2.7.5 Frozen Conformation Energies

	Energy (kJ mol ⁻¹)	Relative Energy (Hartree)	Relative Energy (kcal mol ⁻¹)
N1_R_OcPcQc	-933.583453	0.020263	12.7152244
N1_R_OcPcQt	-933.581904	0.021812	13.6872365
N1_R_OcPtQc	-933.590905	0.012811	8.0390238
N1_R_OcPtQt	-933.589265	0.014451	9.0681393
N1_R_OtPcQc	-933.590343	0.013373	8.3916841
N1_R_OtPcQt	-933.588494	0.015222	9.5519491
N1_R_OtPtQc	-933.595120	0.008596	5.3940714
N1_R_OtPtQt	-933.595122	0.008594	5.3928164
N1_S_OcPcQc	-933.587350	0.016366	10.2698200
N1_S_OcPcQt	-933.585993	0.017723	11.1213503
N1_S_OcPtQc	-933.591614	0.012102	7.5941196
N1_S_OcPtQt	-933.592802	0.010914	6.8486383
N1_S_OtPcQc	-933.587954	0.015762	9.8908043
N1_S_OtPcQt	-933.589020	0.014696	9.2218792
N1_S_OtPtQc	-933.596715	0.007001	4.3931938
N1_S_OtPtQt	-933.595122	0.008594	5.3928164
N3_R_OcPcQc	-933.587416	0.016300	10.2284043
N3_R_OcPcQt	-933.585554	0.018162	11.3968270
N3_R_OcPtQc	-933.587439	0.016277	10.2139716
N3_R_OcPtQt	-933.588671	0.015045	9.4408800
N3_R_OtPcQc	-933.584372	0.019344	12.1385432
N3_R_OtPcQt	-933.586561	0.017155	10.7649249
N3_R_OtPtQc	-933.592139	0.011577	7.2646771
N3_R_OtPtQt	-933.591121	0.012595	7.9034818
N3_S_OcPcQc	-933.586247	0.017469	10.9619629
N3_S_OcPcQt	-933.586105	0.017611	11.0510693
N3_S_OcPtQc	-933.586276	0.017440	10.9437651
N3_S_OcPtQt	-933.588591	0.015125	9.4910807
N3_S_OtPcQc	-933.585398	0.018318	11.4947185
N3_S_OtPcQt	-933.590093	0.013623	8.5485615
N3_S_OtPtQc	-933.590001	0.013715	8.6062924
N3_S_OtPtQt	-933.591006	0.012710	7.9756454

2.7.6 Free Energy Conformations

	Energy (kJ mol ⁻¹)	Relative Energy (Hartree)	Relative Energy (kcal mol ⁻¹)
N1_R_OcPcQc	-933.586129	0.017587	11.036009
N1_R_OcPcQt	-933.585178	0.018538	11.632771
N1_R_OcPtQc	-933.593526	0.010190	6.394321
N1_R_OcPtQt	-933.597636	0.006080	3.815258
N1_R_OtPcQc	-933.600758	0.002958	1.856173
N1_R_OtPcQt	-933.590906	0.012810	8.038396
N1_R_OtPtQc	-933.602909	0.000807	0.506400
N1_R_OtPtQt	-933.598643	0.005073	3.183356
N1_S_OcPcQc	-933.59986	0.003856	2.419677
N1_S_OcPcQt	-933.598622	0.005094	3.196533
N1_S_OcPtQc	-933.598539	0.005177	3.248617
N1_S_OcPtQt	-933.598602	0.005114	3.209083
N1_S_OtPcQc	-933.603713	0.000003	0.001883
N1_S_OtPcQt	-933.601784	0.001932	1.212348
N1_S_OtPtQc	-933.602249	0.001467	0.920556
N1_S_OtPtQt	-933.603019	0.000697	0.437374
N3_R_OcPcQc	-933.599976	0.003740	2.346885
N3_R_OcPcQt	-933.598620	0.005096	3.197788
N3_R_OcPtQc	-933.594486	0.009230	5.791912
N3_R_OcPtQt	-933.595380	0.008336	5.230919
N3_R_OtPcQc	-933.603716	0.000000	0.000000
N3_R_OtPcQt	-933.600766	0.002950	1.851153
N3_R_OtPtQc	-933.602247	0.001469	0.921811
N3_R_OtPtQt	-933.599445	0.004271	2.680093
N3_S_OcPcQc	-933.598620	0.005096	3.197788
N3_S_OcPcQt	-933.599156	0.004560	2.861443
N3_S_OcPtQc	-933.593525	0.010191	6.394949
N3_S_OcPtQt	-933.595585	0.008131	5.102279
N3_S_OtPcQc	-933.592382	0.011334	7.112192
N3_S_OtPcQt	-933.599545	0.004171	2.617342
N3_S_OtPtQc	-933.602910	0.000806	0.505773
N3_S_OtPtQt	-933.599185	0.004531	2.843245
N2_R_OcPcQc	-933.597137	0.006579	4.128385
N2_R_OcPcQt	-933.597634	0.006082	3.816513
N2_R_OcPtQc	-933.599473	0.004243	2.662523
N2_R_OcPtQt	-933.594377	0.009339	5.860311

N2_R_OtPcQc	-933.600759	0.002957	1.855545
N2_R_OtPcQt	-933.600656	0.003060	1.920179
N2_R_OtPtQc	-933.602921	0.000795	0.498870
N2_R_OtPtQt	-933.597752	0.005964	3.742466
N2_S_OcPcQc	-933.599975	0.003741	2.347513
N2_S_OcPcQt	-933.599159	0.004557	2.859561
N2_S_OcPtQc	-933.596023	0.007693	4.827430
N2_S_OcPtQt	-933.596804	0.006912	4.337345
N2_S_OtPcQc	-933.603577	0.000139	0.087224
N2_S_OtPcQt	-933.600462	0.003254	2.041916
N2_S_OtPtQc	-933.600902	0.002814	1.765812
N2_S_OtPtQt	-933.601225	0.002491	1.563126

CHAPTER 3: AZA-GLYCINE INDUCES HYPERSTABILITY

The content of this chapter was originally published in *Journal of the American Chemical Society*. It is adapted with permission by the publisher:

From: Y. Zhang, R. M. Malamakal, D. M. Chenoweth. Aza-Glycine Induces Collagen Hyperstability. *J. Am. Chem. Soc.* **2015**, *137*, 12422-12425. Copyright 2015 American Chemical Society.

The work in this thesis consists of the MD simulations performed on azaglycine incorporated collagen. CD and synthesis data can be found in the dissertation of Yitao Zhang.

3.1 Introduction

Biomolecular structure is governed by a delicate balance of non-covalent intra- and intermolecular interactions.¹ These interactions drive macromolecular assembly and intermolecular recognition events critical to all life processes.^{2,3} The hydrogen bond is a ubiquitous non-covalent interaction in nature.^{2,4,5} Hydrogen bonds are often found at subunit interfaces in helical biopolymer assemblies. Historically, speculative model building by pioneers such as Pauling, Watson, and Crick has led to some of the greatest achievements in structural biology, many of which hinged on the correct pairing or maximizing of H-bonds in biopolymers.⁶ Understanding how molecular systems respond to perturbations in their building blocks can provide insight into biomolecule self-assembly, protein folding, drug design, materials and catalysis, in addition to modulating or enhancing the properties of biopolymers to create new biomimetic materials with superior properties.⁷ Collagen adopts a densely packed H-bonded structure requiring a precise backbone conformation for proper self-assembly into its right handed triple-helical form.⁸ The tertiary structural motif is composed of three staggered polypeptide chains, each chain adopting a left-handed polyproline type-II helical conformation. A single cross-strand H-bond is present at each amino acid triplet repeat. In recent decades, collagen has been the focus of many research efforts aimed at developing a molecular-level understanding of its self-assembly properties⁹ for designing new materials.¹⁰ Collagen triple-helix assembly depends on a balance of non-covalent interactions and amino acid side-chain modifications that can modulate the stability.¹¹ In contrast, collagen backbone modifications, with the exception of a peptoid residue,¹² have typically resulted in significantly destabilized structures.¹³ To date, the glycine (Gly) residue in collagen has remained largely intolerant to substitution, with the exception of a recent thioamide substitution by Raines et al.^{13d}

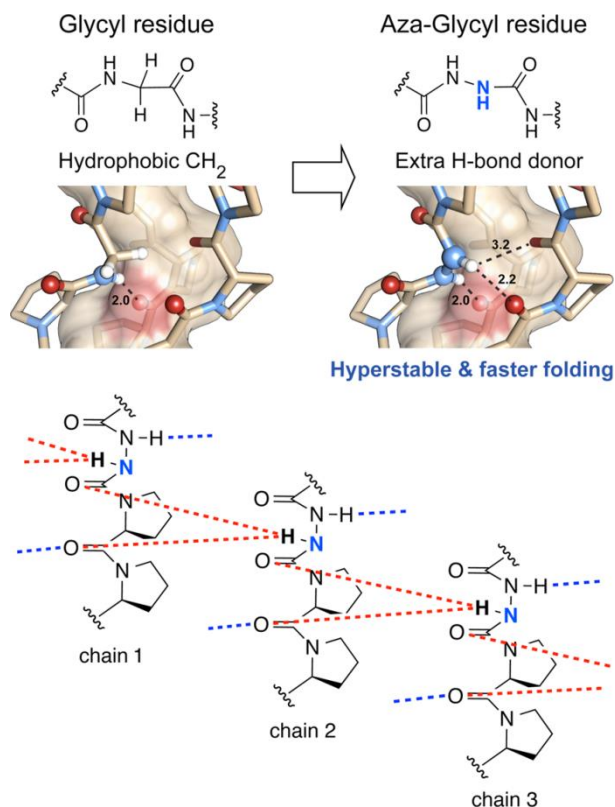


Figure 3.1 (Top) Glycyl versus aza-glycyl residues: azGly-containing collagen triple helix with an expanded view of the -Pro-Pro-azGly- repeat showing the proposed additional cross-strand H-bonding interactions. (Bottom) H-bond map of collagen containing the unnatural azGly modification. Natural collagen H-bonds are shown as blue dashed lines between strands. Proposed additional H-bonds from azGly substitution are shown as red dashed lines. AzGly N-atom is shown in blue.

Recently, we provided new insight into the fundamental importance of stereochemistry as a pre-organizing element in biomolecular folding using stereodynamic probes.¹⁴ We demonstrated that the rate of triple-helix self-assembly in a stereodynamic collagen model peptide is dramatically altered, with little to no effect on the thermal unfolding. Here we replace the α -C of Gly with a N-atom and show that addition of an extra H-bond donor in the backbone can lead to a hyperstable collagen triple helix (Figure 3.1). This Communication details the first atomic modification to the main-chain backbone of collagen that has resulted in significant triple-helix hyperstability and significantly faster folding kinetics. These results have important implications for the design of new biomimetic materials.

3.2 Results and Discussion

We synthesized peptides 1–4 to assess the effects of substituting Gly with aza-glycine (azGly)^{15,16} in the context of a collagen model peptide system. Our design constitutes replacement of a single CH with a single N-atom at the central location in a 260-atom (21 amino acid) peptide system (Figure 3.2). We used circular dichroism (CD) spectroscopy to evaluate self-assembly of the triple helix for each collagen peptide. CD spectra of solutions containing 3 and 4 both exhibit characteristic maxima at ~224 nm, indicating the presence of triple-helix structure. Thermal denaturation experiments showed cooperative unfolding transitions for all peptides (see Supplemental Information (SI)). The data from CD thermal denaturation experiments were fitted to a two-state model, as previously described.¹⁷ The melting temperatures (T_m), at which 50% of the triple helix unfolds, are shown in Figure 3.3a for 1–4. A striking increase in T_m of ~10 °C was observed for 3 and 4 compared to the corresponding control compounds 1 and 2. The results show that replacement of a single Gly α -CH with a N-atom results in a significant increase in triple-helix thermal stability. In addition to being the first favorable replacement for a Gly residue in a collagen model peptide,^{8c,18} this substitution results in the highest stabilizing effect of any single-residue mutation in a collagen PPG or POG peptide system.¹⁹ Raines et al. reported a seminal study where replacement of a single proline (Pro) residue with a fluorinated Pro residue resulted in a 5 °C increase in thermal stability.²⁰ Pairing the azGly residue with the fluoroproline discovery of Raines could result in extremely stable collagen peptide systems with unique, new material properties.

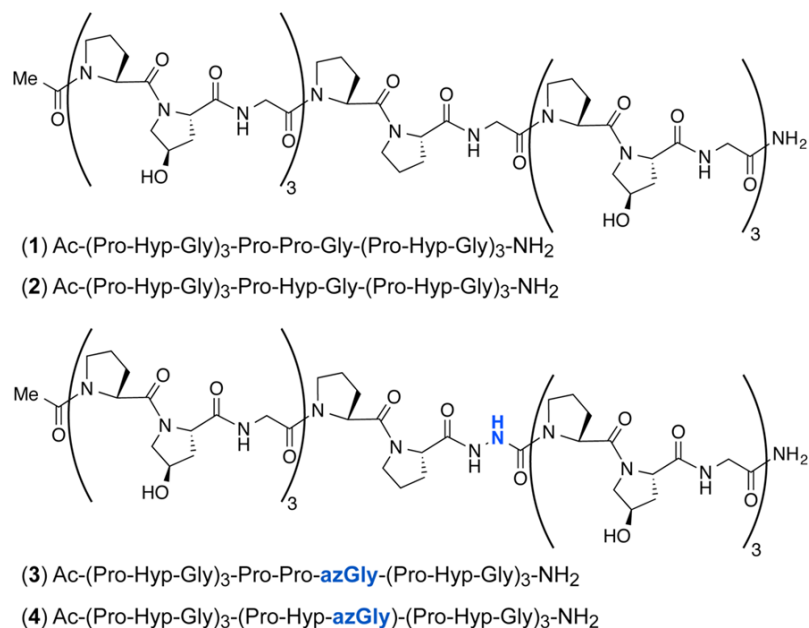


Figure 3.2 Chemical structures of collagen model control peptides 1, 2 and azGly-containing peptides 3 , 4.

A model based on a known collagen crystal structure in which a Gly was substituted by azGly shows the azGly α -NH is 2.2 Å from the carbonyl of Gly and 3.2 Å from the carbonyl of Pro in a neighboring peptide chain. This distance is similar to the key canonical interstrand H-bond from the Gly amide NH to the carbonyl preceding Pro in the Yaa position. Additional H-bonding from azGly could increase the number of interchain H-bonds within a triplet of Xaa-Yaa-Gly, providing a connection between all three peptide chains through multiple dynamic H-bonds (Figure 3.1, bottom).

Next, we assessed the kinetics of triple-helix formation for peptides 1–4. The peptides, at 0.2 mM in PBS buffer, were denatured at 80 °C for 15 min, and their CD profiles were monitored at 4 °C until they recovered (>50%) ellipticity at 224 nm. The refolding rate of peptides containing the azGly moiety was enhanced in both comparisons. The presence of trimers was confirmed for 1–4 by size exclusion chromatography with multi-angle light scattering (SEC-MALS) analysis using a D-Pro-containing collagen peptide (5) as a monomeric control (Figure 3.3 e).¹⁴ The

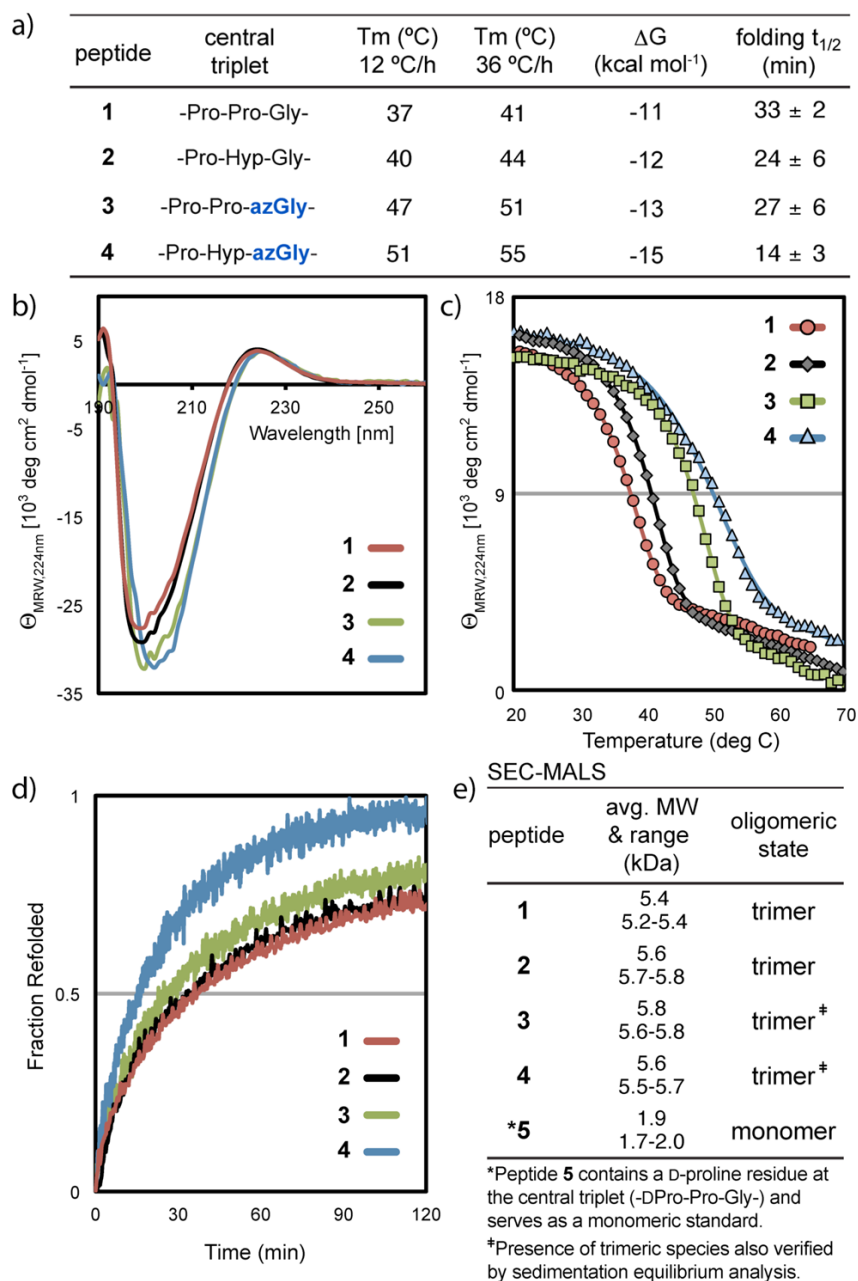


Figure 3.3 (a) Table of unfolding and refolding data for collagen model peptides.

Values of T_m (standard error <1 °C) were determined in triplicate by CD spectroscopy at scan rates of 12 and 36 °C/h. (b) CD wavelength scans of homotrimers formed by 1–4. (c) Unfolding curves for the thermal transition of 1–4 at 12 °C/h. (d) Refolding of peptides was observed by monitoring the recovery of ellipticity after thermal denaturation. (e) SEC-MALS analysis confirming the presence of the trimeric peptide assemblies for 1–4. The presence of the trimeric state for 3 and 4 was also verified by sedimentation equilibrium analysis using AUC. Control peptide 5 contains a central D-Pro and serves as a monomeric standard for SEC-MALS analysis.

trimeric state of azGly-containing 3 and 4 was also verified by sedimentation equilibrium analysis using analytical ultracentrifugation (AUC).

A hysteresis study was performed to gain further insight into the stability of 3 and 4. The free energy differences between the peptides were in accord with the differences in T_m and previous reports using this method: $\Delta G = -11, -12, -13$, and -15 kcal/mol for peptides 1–4, respectively. The origin of ΔG is primarily consistent with an increase in the enthalpic gain from the ability of azGly to form extra H-bonds, although this will require verification by calorimetric methods. The large differences in half-time values for triple-helix self-assembly for azGly-containing peptides are striking in comparison to our previous results with aza-proline, where we elucidated the role of stereochemistry with respect to biopolymer pre-organization and self-assembly.¹⁴

Our model suggests the incorporation of azGly into the triplet adds the possibility for extra H-bonding between the new α -NH and two different amide carbonyls on an adjacent peptide strand in addition to the already present amide H-bond. To gain further insight into the azGly substitution, we performed molecular dynamics (MD) calculations using GROMACS (see SI for details). Simulations on full triple-helical models of 1–4 revealed heavy-atom root-mean-square deviation (RMSD) values of <0.07 for the central 5-amino-acid triplets of 1 and 2 and slightly higher RMSD values for the N- (0.2) and C-terminal (0.14) triplets compared to a common starting model (Figure 4.4).

The azGly-containing triple-helical structures 3 and 4 showed RMSD values similar to those of the parent systems, except at the azGly position near the central triplet, where the RMSD increased to 0.10 for 3 and 0.08 for 4. Analysis of the azGly H-bonding parameters revealed the possibility of three different H-bonds at each azGly residue, with the new α -NH participating in up to two H-bonds (Figure 3.5). H-bond distances are shown in Figure 3.5c with angles shown in Figure 3.5d, revealing the possibility for three dynamic H-bonds with slightly less optimal

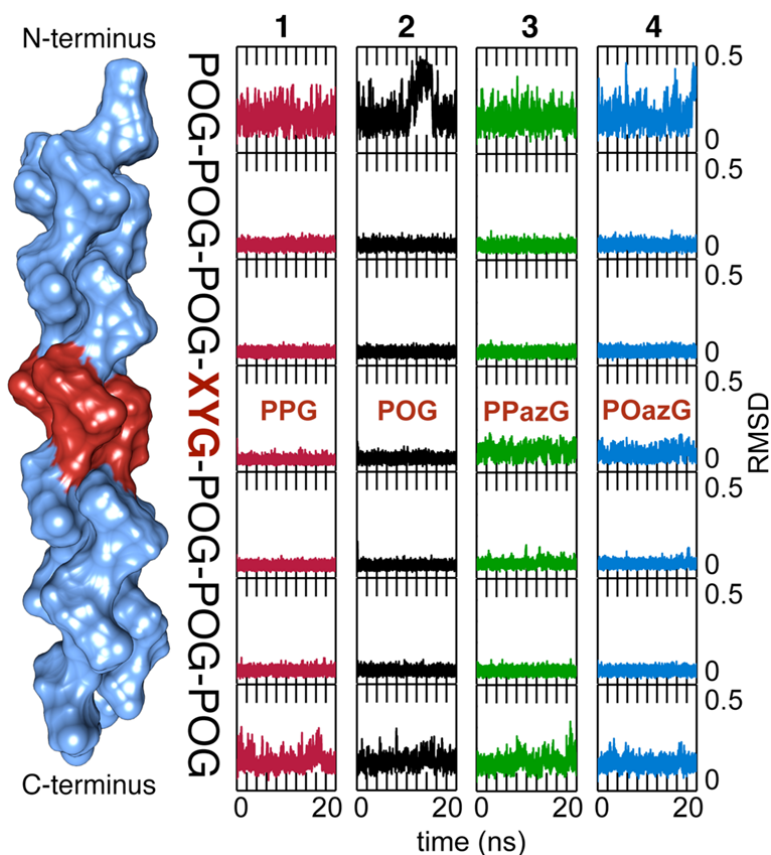


Figure 3.4 Model of the collagen triple helix, with the central variable triplet highlighted in red.

Plot of RMSD for the heavy atoms of each trimeric triplet of each simulated collagen peptide system compared to a common reference crystal structure used to build all starting MD models. Reference crystal structure used was PDB 3B0S.

parameters than the standard amide H-bond present in collagen. The MD simulation data imply that multiple dynamic but weak H-bonds with non-optimal distance and angle parameters may be more favorable in certain cases than strong H-bonds.

Peptide backbone substitutions have provided a wealth of insightful information regarding protein structure, and have led to the discovery of fundamentally important interactions such as the gauche effect in collagen and $n-\pi^*$ interactions. Previous reports of heteroatom replacement in the collagen peptide backbone have resulted in either severe destabilization or a complete lack of triple-helix formation. Amide-to-ester substitutions have provided a wealth of information regarding H-bond strength and have a detrimental impact on collagen triple-helix stability. In

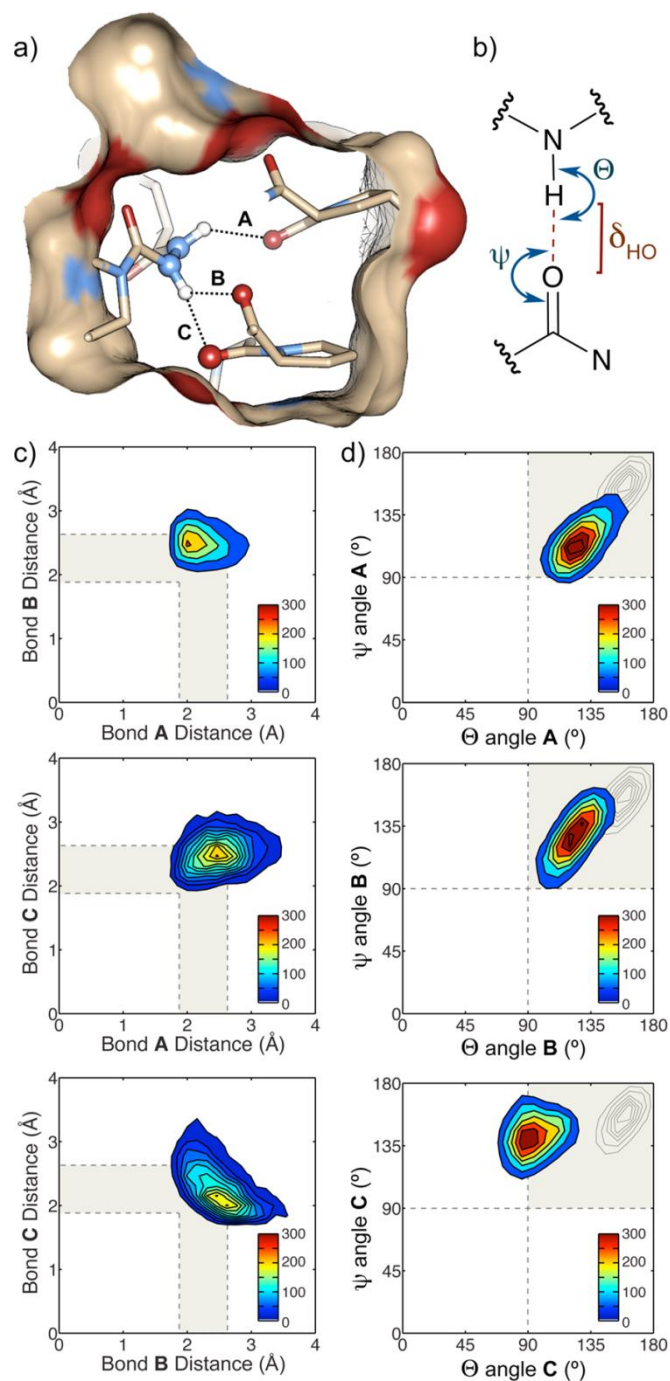


Figure 3.5 Hydrogen bond analysis for MD simulations of collagen model peptide 4.

(a) Cross section through collagen triple helix showing possible azGly H-bonds. (b) Schematic of H-bond parameters. (c) H-bond distance measurements and correlations for A, B, and C from (a). (d) H-bond angle measurements for A, B, and C. Gray watermark on plots designates H-bond angles for non-azGly peptide system. Shaded regions on plots designate optimal H-bond parameters.

addition, trans alkene amide bond isosteres greatly destabilize the triple-helical structure of collagen irrespective of positioning and involvement in H-bonding. To date, these efforts have demonstrated an intolerance of the collagen peptide backbone to molecular editing.¹³

3.3 Conclusions

In summary, our study suggests that nature's limited set of building blocks are not sufficient for optimizing the stability of self-assembled biopolymer systems such as collagen, and there is much to be gained from judicious synthetic modifications such as azGly incorporation. In addition to insight into the fundamental importance of hydrogen bonding as a stabilizing element in natural systems, these studies may provide insight into optimization of self-assembling biomimetic materials. Beyond collagen, these studies suggest the opportunity for protein stabilization in a broader context via azGly scanning, which could identify unique positions for increasing thermal stability in addition to decreasing proteolytic degradation, as already reported for aza-amino acids. Current studies incorporating multiple azGly residues and assessing synergistic effects with other unnatural residues in addition to structural studies are under way and will be reported in due course.

3.4 Acknowledgments

This work was supported by funding from the University of Pennsylvania. Instruments supported by the National Science Foundation and the National Institutes of Health including HRMS (NIH RR-023444) and MALDI-MS (NSF MRI-0820996). We thank Prof. Dr. Helma Wennemers, Prof. Dr. Peter Bachinger and Dr. Roman Erdmann for advice on hysteresis studies. We thank Dr. Ewa Folta-Stogniew of the Keck Foundation Biotechnology Resource Laboratory at Yale University for SEC-MALS analysis. The SEC-LS/UV/RI instrumentation was supported by NIH Award Number 1S10RR023748-01. We thank Jeffrey Lary at the AU Facility of the Biotechnology-Bioservices Center, University of Connecticut for AUC analysis. We thank Prof. Jessica Anna and Stephen Meloni for advice on MD simulations.

3.5 Notes

Yitao Zhang performed the synthesis and characterization of the CMPs investigated in this work.

Detailed analysis and discussion is found in his dissertation

3.6 References

- (1) Srinivasan, R.; Rose, G. D. *Proc. Natl. Acad. Sci. USA* **1999**, *96*, 14258.
- (2) Anfinsen, C. B. *Science* **1973**, *181*, 223.
- (3) (a) Černý, J.; Hobza, P. *Phys. Chem. Chem. Phys.* **2007**, *9*, 5291. (b) Dunitz, J. D. *Chem. Biol.* **1995**, *2*, 709. (c) Schneider, H. -J. *Angew. Chem. Int. Ed.* **2009**, *48*, 3924. (d) Williams, D. H.; Stephens, E.; O'Brien, D. P.; Zhou, M. *Angew. Chem. Int. Ed.* **2004**, *43*, 6596.
- (4) (a) Mirsky, A. E.; Pauling, L. *Proc. Natl. Acad. Sci. USA* **1936**, *22*, 439. (b) Pauling, L.; Corey, R. B.; Branson, H. R. *Proc. Natl. Acad. Sci. USA* **1951**, *37*, 205. (c) Pauling, L.; Corey, R. B. *Proc. Natl. Acad. Sci. USA* **1951**, *37*, 729.
- (5) (a) Hubbard, R. E.; Kamran Haider, M. In *eLS*; John Wiley & Sons, Ltd: 2001. (b) Deechongkit, S.; Nguyen, H.; Powers, E. T.; Dawson, P. E.; Gruebele, M.; Kelly, J. W. *Nature* **2004**, *430*, 101. (c) Pace, C. N. *Nat. Struct. Mol. Biol.* **2009**, *16*, 681. (d) Gao, J.; Bosco, D. A.; Powers, E. T.; Kelly, J. W. *Nat. Struct. Mol. Biol.* **2009**, *16*, 684. (e) Bowie, J. U. *Curr. Opin. Struc. Biol.* **2011**, *21*, 42.
- (6) (a) Pauling, L.; Corey, R. B. *Nature* **1951**, *168*, 550. (b) Pauling, L.; Corey, R. B. *Proc. Natl. Acad. Sci. USA* **1951**, *37*, 241. (c) Crick, F. H. C. *Nature* **1952**, *170*, 882. (d) Watson, J. D.; Crick, F. H. C. *Nature* **1953**, *171*, 737.
- (7) (a) He, M.; Bode, J. W. *Proc. Natl. Acad. Sci. USA* **2011**, *108*, 14752. (b) Barrett, K. T.; Metrano, A. J.; Rablen, P. R.; Miller, S. J. *Nature* **2014**, *509*, 71. (c) Wang, J.; Feringa, B. L. *Science* **2011**, *331*, 1429. (d) Clayden, J.; Lund, A.; Vallverdú, L.; Helliwell, M. *Nature* **2004**, *431*, 966.

- (8) (a) Ramachandran, G. N.; Kartha, G. *Nature* **1954**, *174*, 269. (b) Rich, A.; Crick, F. H. *J. Mol. Biol.* **1961**, *3*, 483. (c) Shoulders, M. D.; Raines, R. T. *Annu. Rev. Biochem.* **2009**, *78*, 929.
- (9) (a) Bella, J.; Eaton, M.; Brodsky, B.; Berman, H. M. *Science* **1994**, *266*, 75. (b) Holmgren, S. K.; Taylor, K. M.; Bretscher, L. E.; Raines, R. T. *Nature* **1998**, *392*, 666. (c) Fields, G. B.; Prockop, D. J. *Biopolymers* **1996**, *40*, 345. (f) Schumacher, M.; Mizuno, K.; Bächinger, H. P. *J. Mol. Biol.* **2005**, *280*, 20397. (d) Goodman, M.; Melacini, G.; Feng, Y. *J. Am. Chem. Soc.* **1996**, *118*, 10928. (e) Kawahara, K.; Nishi, Y.; Nakamura, S.; Uchiyama, S.; Nishiuchi, Y.; Nakazawa, T.; Ohkubo, T.; Kobayashi, Y. *Biochemistry* **2005**, *44*, 15812. (f) Berisio, R.; Vitagliano, L.; Mazzarella, L.; Zagari, A. *Protein Sci.* **2002**, *11*, 262. (m) Gauba, V.; Hartgerink, J. D. *J. Am. Chem. Soc.* **2007**, *129*, 2683. (g) Gauba, V.; Hartgerink, J. D. *J. Am. Chem. Soc.* **2007**, *129*, 15034. (h) Lee, S.-G.; Lee, J. Y.; Chmielewski, J. *Angew. Chem. Int. Ed.* **2008**, *47*, 8429.
- (10) (a) Kusebauch, U.; Cadamuro, S. A.; Musiol, H. -J.; Lenz, M. O.; Wachtveitl, J.; Moroder, L.; Renner, C. *Angew. Chem. Int. Ed.* **2006**, *45*, 7015. (b) Cejas, M. A.; Kinney, W. A.; Chen, C.; Leo, G. C.; Tounge, B. A.; Vinter, J. G.; Joshi, P. P.; Maryanoff, B. E. *J. Am. Chem. Soc.* **2007**, *129*, 2202. (c) Rele, S.; Song, Y.; Apkarian, R. P.; Qu, Z.; Conticello, V. P.; Chaikof, E. L. *J. Am. Chem. Soc.* **2007**, *129*, 14780. (d) Wang, A. Y.; Mo, X.; Chen, C. S.; Yu, S. M. *J. Am. Chem. Soc.* **2005**, *127*, 4130. (e) Przybyla, D. E.; Chmielewski, J. *J. Am. Chem. Soc.* **2008**, *130*, 12610. (f) Fallas, J. A.; Gauba, V.; Hartgerink, J. D. *J. Biol. Chem.* **2009**, *284*, 26851.
- (11) (a) Holmgren, S. K.; Taylor, K. M.; Bretscher, L. E.; Raines, R. T. *Nature* **1998**, *392*, 666. (b) Bretscher, L. E.; Jenkins, C. L.; Taylor, K. M.; DeRider, M. L.; Raines, R. T. *J. Am. Chem. Soc.* **2001**, *123*, 777. (c) Hodges, J. A.; Raines, R. T. *J. Am. Chem. Soc.* **2003**, *125*, 9262. (d) Shoulders, M. D.; Hodges, J. A.; Raines, R. T. *J. Am. Chem. Soc.* **2006**, *128*,

8112. (e) Kotch, F. W.; Guzei, I. A.; Raines, R. T. *J. Am. Chem. Soc.* **2008**, *130*, 2952. (f) Cadamuro, S. A.; Reichold, R.; Kusebauch, U.; Musiol, H. -J.; Renner, C.; Tavan, P.; Moroder, L. *Angew. Chem.* **2008**, *120*, 2174. (g) Umashankara, M.; Babu, I. R.; Ganesh, K. N.; *Chem. Commun.* **2003**, 2606. (h) Erdmann, R. S.; Wennemers, H. *J. Am. Chem. Soc.* **2010**, *132*, 13957. (i) Shoulders, M. D.; Satyshur, K. A.; Forest, K. T.; Raines, R. T. *Proc. Natl. Acad. Sci. USA* **2010**, *107*, 559. (j) Bartlett, G. J.; Choudhary, A.; Raines, R. T.; Woolfson, D. N. *Nat. Chem. Biol.* **2010**, *6*, 615. (k) Choudhary, A. Gandla, D.; Krow, G. R.; Raines, R. T. *J. Am. Chem. Soc.* **2009**, *131*, 7244. (l) Jakobsche, C. E.; Choudhary, A.; Miller, S. J.; Raines, R. T. *J. Am. Chem. Soc.* **2010**, *132*, 6651. (m) Erdmann, R. S.; Wennemers, H. *Angew. Chem. Int. Ed.* **2011**, *50*, 6835. (n) Erdmann, R. S.; Wennemers, H. *J. Am. Chem. Soc.* **2012**, *134*, 17117. (o) Siebler, C.; Erdmann, R. S.; Wennemers, H. *Angew. Chem. Int. Ed.* **2014**, *53*, 10340. (p) Newberry, R. W.; Bartlett, G. J.; VanVeller, B.; Woolfson, D. N.; Raines, R. T. *Protein Sci.* **2014**, *23*, 284.
- (12) Goodman, M.; Bhumralkar, M.; Jefferson, E. A.; Kwak, J.; Locardi, E. *Biopolymers* **1998**, *47*, 127.
- (13) (a) Frey, P.; Nitschmann, H. *Helv. Chim. Acta* **1976**, *59*, 1401. (b) Shah, N. K.; Brodsky, B.; Kirkpatrick, A. Ramshaw, J. A. M. *Biopolymers* **1999**, *49*, 297-302; (c) Jenkins, C. L.; Vasbinder, M. M.; Miller, S. J.; Raines, R. T. *Org. Lett.* **2005**, *7*, 2619. (d) Dai, N.; Wang, X. J.; Etzkorn, F. A. *J. Am. Chem. Soc.* **2008**, *130*, 5396. (e) Dai, N.; Etzkorn, F. A. *J. Am. Chem. Soc.* **2009**, *131*, 13728. (f) Newberry, R. W.; VanVeller, B.; Raines, R. T. *Chem. Commun.* **2015**, *51*, 9624.
- (14) Zhang, Y.; Malamakal, R. M.; Chenoweth, D. M. *Angew. Chem. Int. Ed.* **2015**, *54*, 10826.
- (15) Sabatino, D.; Proulx, C.; Kloczek, S.; Bourguet, C. B.; Boeglin, D.; Ong, H.; Lubell, W. D. *Org. Lett.* **2009**, *11*, 3650.

- (16) Reviews and selected work on incorporating azGly into biologically active peptides: (a) Zega, A. *Cur. Med. Chem.* **2005**, *12*, 589. (b) Proulx, C.; Sabatino, D.; Hopewell, R.; Spiegel, J.; Garcia Ramos, Y.; Lubell, W. D. *Chem. Med. Chem.* **2011**, *3*, 1139.
- (17) Engel, J.; Chen, H. T.; Prockop, D. J.; Klump, H. *Biopolymers* **1977**, *16*, 601.
- (18) Replacing Gly by Ala, Arg, Asp, Glu, Cys, Ser, Val, or selected _D-amino acid all lead to dramatic destabilization of the model host-guest system. (a) Beck, K.; Chan, V. C.; Shenoy, N.; Kirkpatrick, A.; Ramshaw, J. A. M.; Brodsky, B. *Proc. Natl. Acad. Sci. USA*, **2000**, *97*, 4273. (b) Horng, J. C.; Kotch, F. W.; Raines, R. T. *Protein Sci.* **2007**, *16*, 208. (c) Chen, Y. S.; Chen, C. C.; Horng, J. C. *Biopolymers* **2011**, *96*, 60.
- (19) Natural amino acids do not outcompete Pro in X and Hyp in Y: (a) Persikov, A. V.; Ramshaw, J. A. M.; Kirkpatrick, A.; Brodsky, B. *Biochemistry* **2000**, *39*, 14940. (b) Jenkins, C. L.; Bretscher, L. E.; Guzei, I. A.; Raines, R. T. *J. Am. Chem. Soc.* **2003**, *125*, 6422.
- (20) Shoulders, M. D.; Kamer, K. J.; Raines, R. T. *Bioorg. Med. Chem. Lett.* **2009**, *19*, 3859.

3.7 Supplemental Information

3.7.1 General information

All commercial reagents and solvents were used as received. Fmoc-Pro-OH, Fmoc-Gly-OH, HATU and Rink Amide AM Resin (100-200 mesh) were purchased from Novabiochem. Fmoc-Hyp(tBu)-OH was purchased from Advanced Chemtech. Piperidine was purchased from American Bioanalytical. All remaining chemicals were purchased from Sigma Aldrich. Flash column chromatography was performed using Silicycle silica gel (55–65 Å pore diameter). Thin-layer chromatography was performed on Sorbent Technologies silica plates (250 µm thickness). High-resolution mass spectra were obtained at the University of Pennsylvania's Mass Spectrometry Service Center on a Micromass AutoSpec electrospray/chemical ionization spectrometer. Mass of long peptides were obtained via a Bruker Ultraflex III Matrix-assisted laser desorption/ionization(MALDI) mass spectrometer. Ultraviolet absorption spectrophotometry was performed on a JASCO V-650 spectrophotometer with a PAC-743R multichannel Peltier using quartz cells with a 1 cm cell path length. High performance liquid chromatography analysis was performed using a Jasco HPLC instrument equipped with a Phenomenex column (Luna 5u C18(2) 100A; 250 × 4.60 mm, 5 µm). Circular dichroism experiments were performed with a Jasco J-1500 CD Spectrometer.

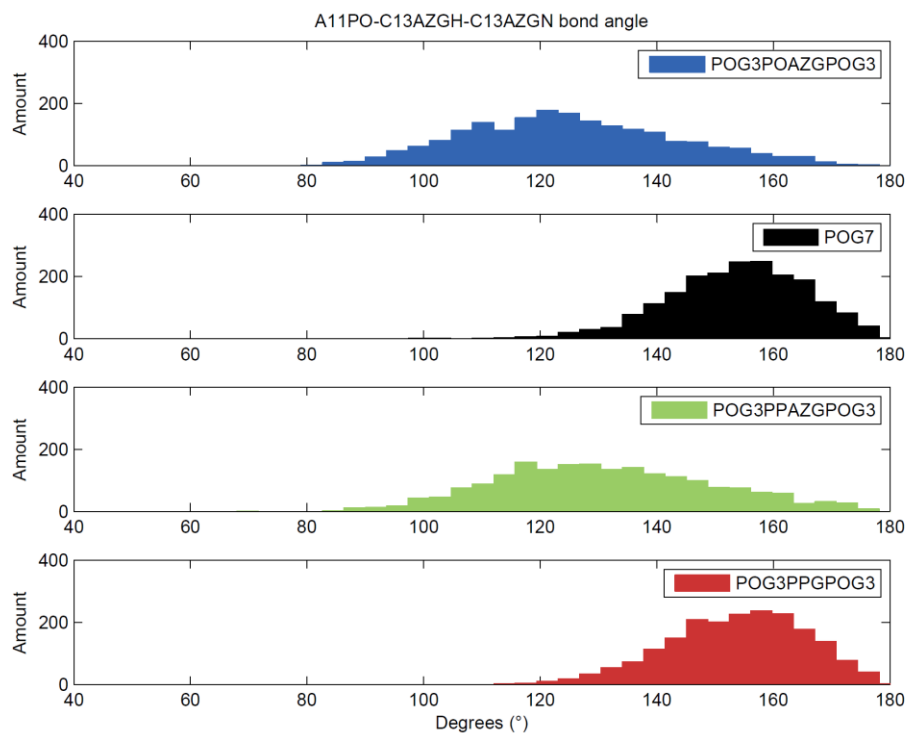
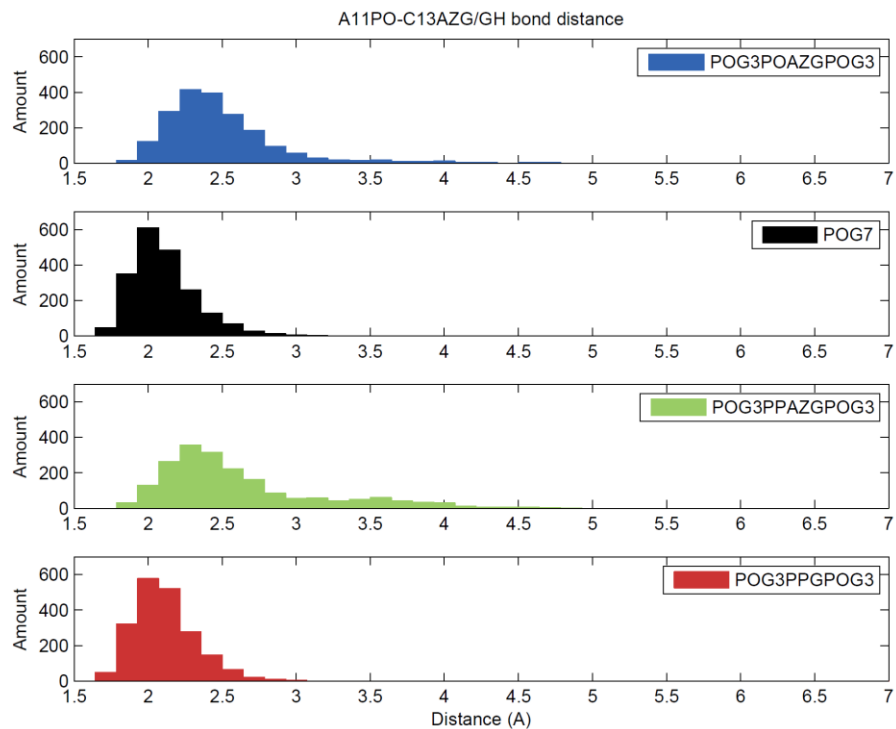
3.7.2 MD Simulations

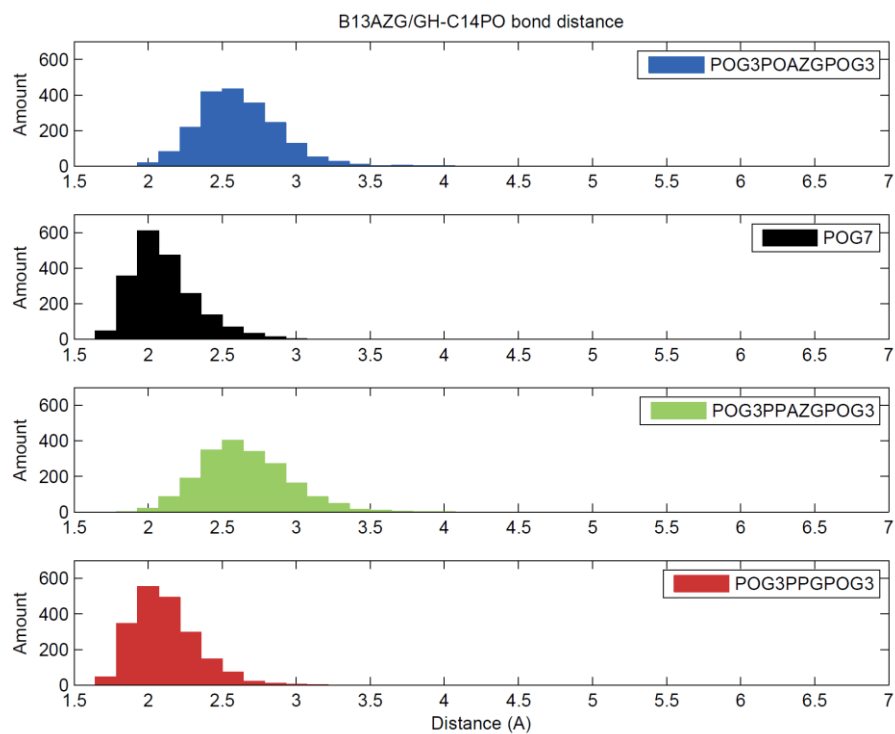
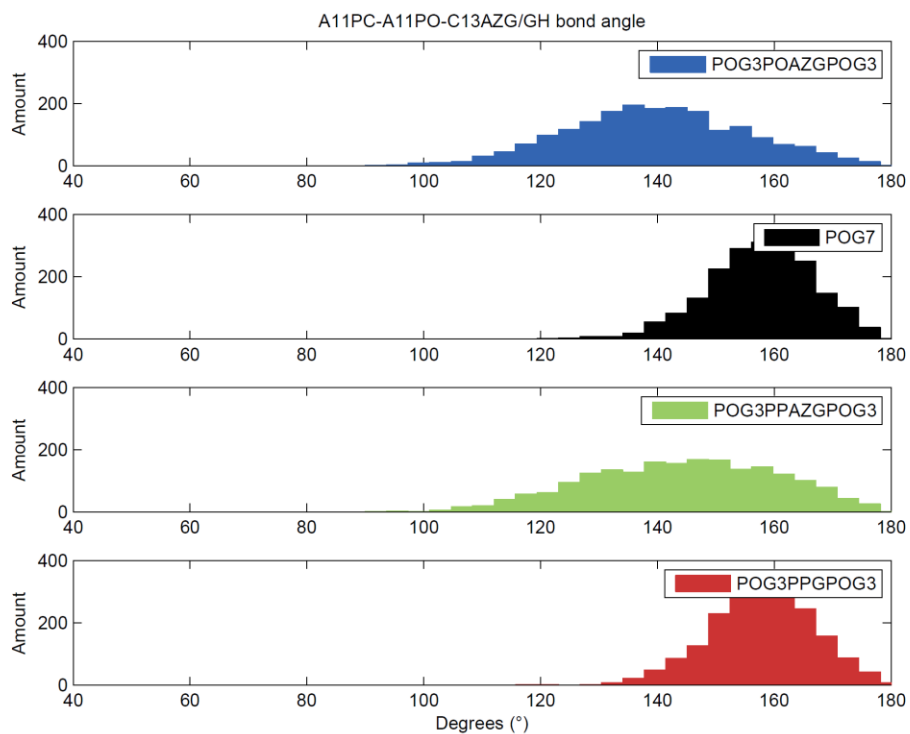
Molecular dynamics were performed using GROMACS 5.0.5¹⁻⁵ utilizing the AMBER99SB force field.⁶ All systems were solvated using the TIP3P water model. The AZG parameters were generated with AmberTools 15⁷ utilizing the restrained electrostatic potential (RESP) approach to determine partial charges. Quantum mechanical optimizations were performed using the Gaussian 09 software package⁸ using B3LYP/6-31g(d) basis set for geometry optimizations, and HF/6-31g(d) basis set to calculate electrostatic potentials. Bond force constants were imported into GROMACS from the general amber force field (GAFF). All systems were subjected to an energy minimization of maximum 50000 steps using the steepest descent algorithm. This step was followed by a solvent equilibration and equilibration of the entire system for 100 ps. The production run was carried out for all peptides for 20 nanoseconds (ns) using 2 femtosecond (fs) time steps, saving coordinates every picosecond (ps) at 300 K and at a pressure of one bar. The velocity rescaling (V-rescale) thermostat and Parrinello–Rahman were used to control the temperature and pressure, respectively.⁹ The particle mesh Ewald (PME) method was used to calculate the electrostatic interactions. Post processing was performed using GROMACS analysis tools, UCSF Chimera¹⁰, and Matlab (MATLAB 8.3, The MathWorks Inc., Natick, MA, 2000).

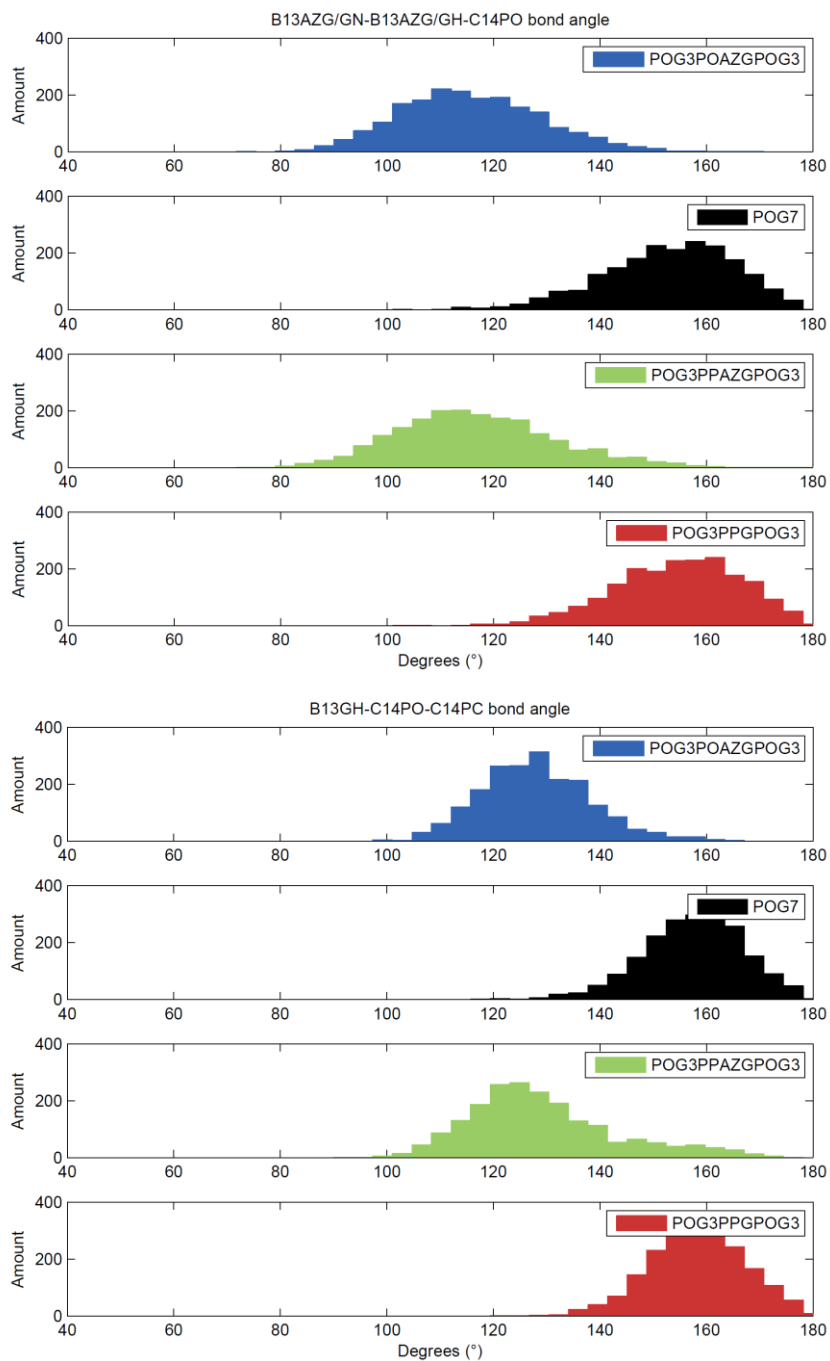
- (1) Bekker, H., Berendsen, H. J. C., Dijkstra, E. J., Achterop, S., van Drunen, R., van der Spoel, D., Sijbers, A., Keegstra, H., Reitsma, B., Renardus, M. K. R. Gromacs: A parallel computer for molecular dynamics simulations. In *Physics Computing 92* (Singapore, 1993). de Groot, R. A., Nadrchal, J., eds. . World Scientific.
- (2) Berendsen, H. J. C., van der Spoel, D., van Drunen, R. GROMACS: A message-passing parallel molecular dynamics implementation. *Comp. Phys. Comm.* 91:43–56, 1995.

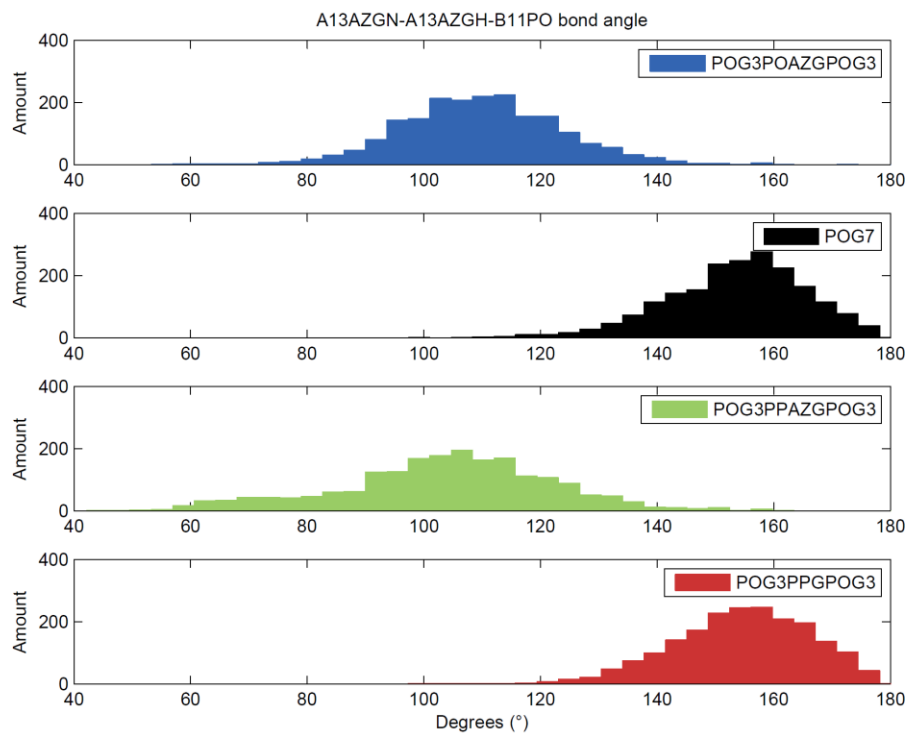
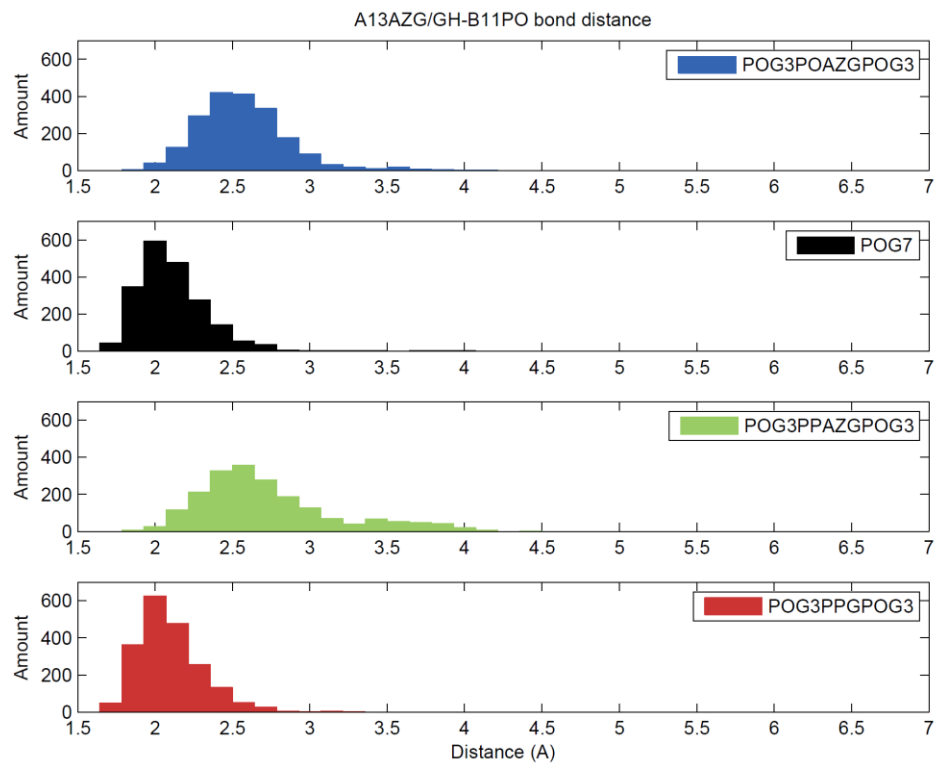
- (3) Lindahl, E., Hess, B., van der Spoel, D. GROMACS 3.0: A package for molecular simulation and trajectory analysis. *J. Mol. Mod.* 7:306–317, 2001.
- (4) van der Spoel, D., Lindahl, E., Hess, B., Groenhof, G., Mark, A. E., Berendsen, H. J. C. GROMACS: Fast, Flexible and Free. *J. Comp. Chem.* 26:1701–1718, 2005.
- (5) Hess, B., Kutzner, C., van der Spoel, D., Lindahl, E. GROMACS 4: Algorithms for Highly Efficient, Load-Balanced, and Scalable Molecular Simulation. *J. Chem. Theory Comput.* 4(3):435–447, 2008. Pronk, S., Páll, S., Schulz, R., Larsson, P., Bjelkmar, P., Apostolov, R., Shirts, M. R., Smith, J. C., Kasson, P. M., van der Spoel, D., Hess, B., Lindahl, E. GROMACS 4.5: a highthroughput and highly parallel open source molecular simulation toolkit. *Bioinformatics* 29(7):845–854, 2013
- (6) V. Hornak, R. Abel, A. Okur, B. Strockbine, A. Roitberg and C. Simmerling, *Proteins: Struct., Funct., Bioinf.*, **2006**, 65, 712.
- (7) D.A. Case, J.T. Berryman, R.M. Betz, D.S. Cerutti, T.E. Cheatham, III, T.A. Darden, R.E. Duke, T.J. Giese, H. Gohlke, A.W. Goetz, N. Homeyer, S. Izadi, P. Janowski, J. Kaus, A. Kovalenko, T.S. Lee, S. LeGrand, P. Li, T. Luchko, R. Luo, B. Madej, K.M. Merz, G. Monard, P. Needham, H. Nguyen, H.T. Nguyen, I. Omelyan, A. Onufriev, D.R. Roe, A. Roitberg, R. Salomon-Ferrer, C.L. Simmerling, W. Smith, J. Swails, R.C. Walker, J. Wang, R.M. Wolf, X. Wu, D.M. York and P.A. Kollman (2015), AMBER 2015, University of California, San Francisco.
- (8) Frisch, M. J.; Trucks, G. W.; Schlegel, H. B.; Scuseria, G. E.; Robb, M. A.; Cheeseman, J. R.; Scalmani, G.; Barone, V.; Mennucci, B.; Petersson, G. A.; Nakatsuji, H.; Caricato, M.; Li, X.; Hratchian, H. P.; Izmaylov, A. F.; Bloino, J.; Zheng, G.; Sonnenberg, J. L.; Hada, M.; Ehara, M.; Toyota, K.; Fukuda, R.; Hasegawa, J.; Ishida, M.; Nakajima, T.; Honda, Y.; Kitao, O.; Nakai, H.; Vreven, T.;

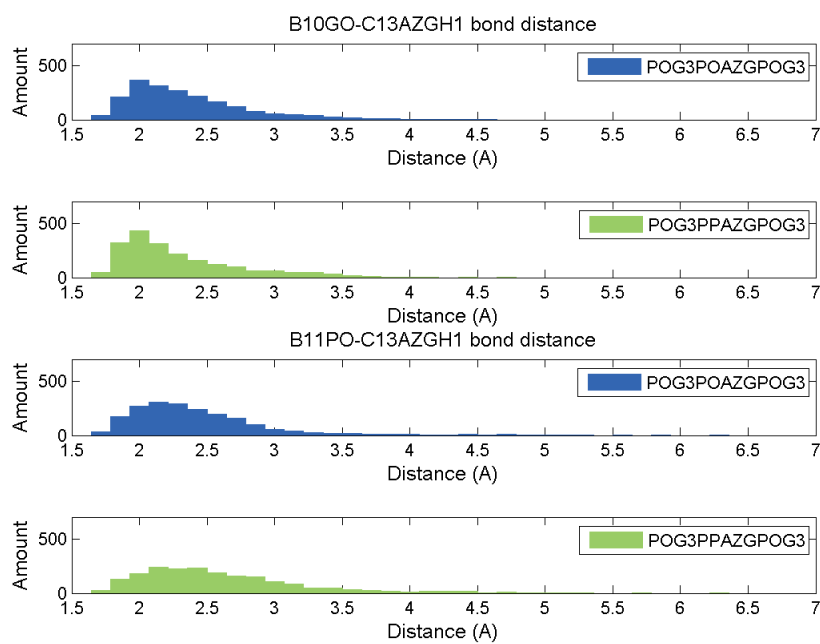
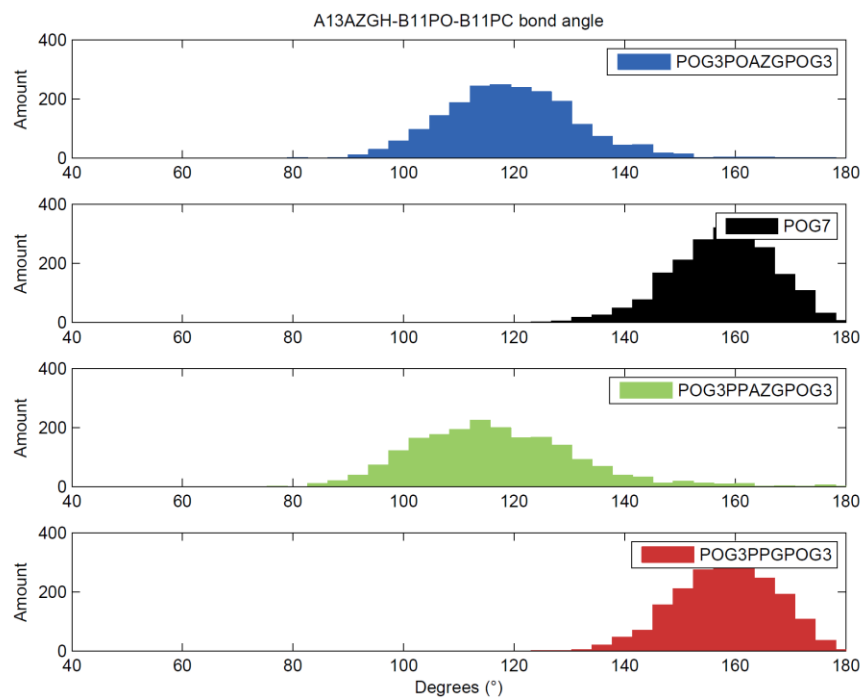
- J. A. Montgomery, J.; Peralta, J. E.; Ogliaro, F.; Bearpark, M.; Heyd, J. J.; Brothers, E.; Kudin, K. N.; Staroverov, V. N.; Kobayashi, R.; Normand, J.; Raghavachari, K.; Rendell, A.; Burant, J. C.; Iyengar, S. S.; Tomasi, J.; Cossi, M.; Rega, N.; Millam, J. M.; Klene, M.; Knox, J. E.; Cross, J. B.; Bakken, V.; Adamo, C.; Jaramillo, J.; Gomperts, R.; Stratmann, R. E.; Yazyev, O.; Austin, A. J.; Cammi, R.; Pomelli, C.; Ochterski, J. W.; Martin, R. L.; Morokuma, K.; Zakrzewski, V. G.; Voth, G. A.; Salvador, P.; Dannenberg, J. J.; Dapprich, S.; Daniels, A. D.; Farkas, Ö.; Foresman, J. B.; Ortiz, J. V.; Cioslowski, J.; Fox, D. J. Gaussian 09, Revision B.01.; Gaussian, Inc.: Wallingford, CT, **2009**
- (9) Gopalakrishnan, R.; Azhagiya Singam, E.R.; Sundar, J.V.; Subramanian, V. *Phys. Chem. Chem. Phys.* **2015**, 17 5172-5186
- (10) Pettersen EF, Goddard TD, Huang CC, Couch GS, Greenblatt DM, Meng EC, Ferrin TE. *J Comput Chem.* **2004** Oct; 25(13):1605-12.

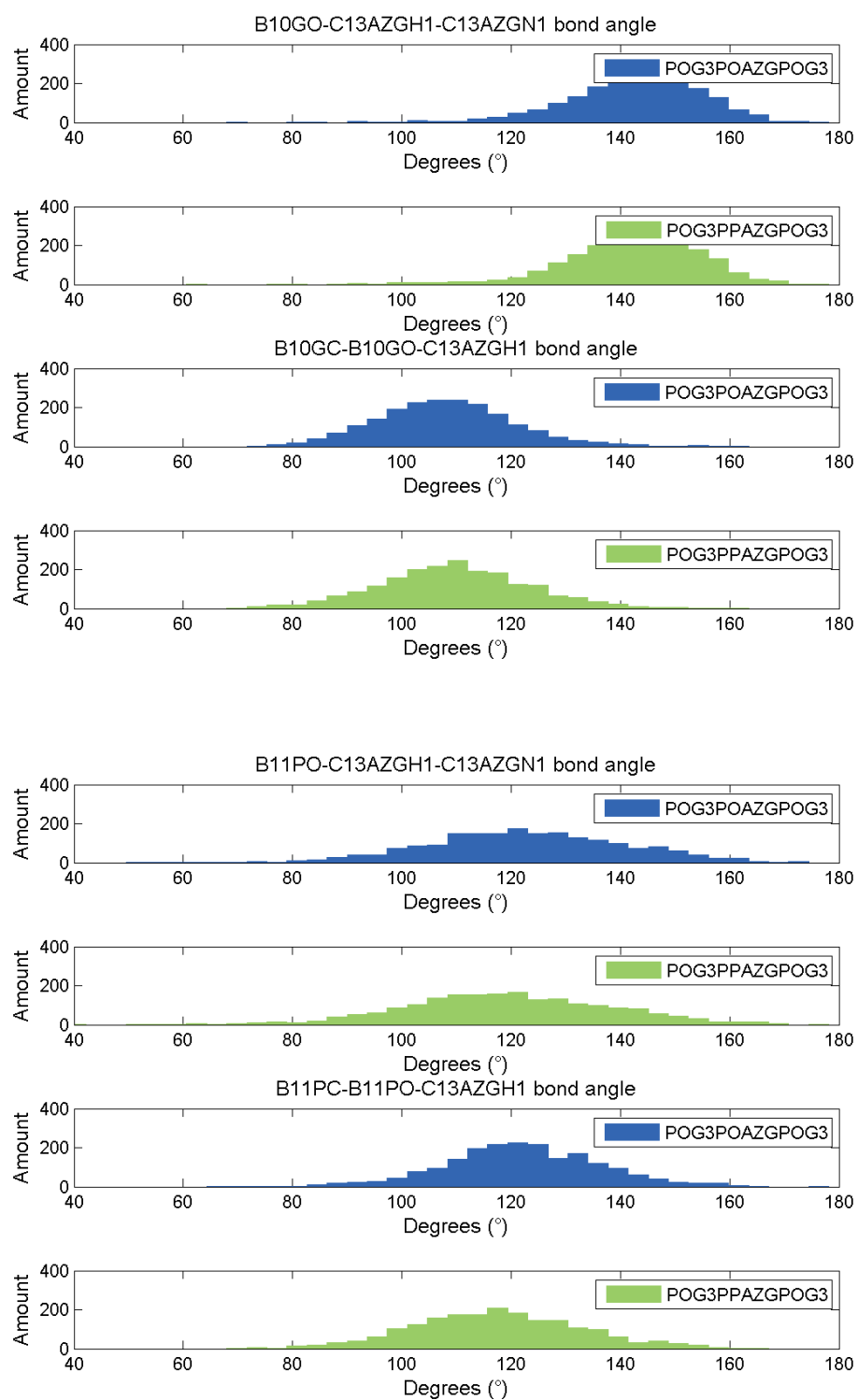


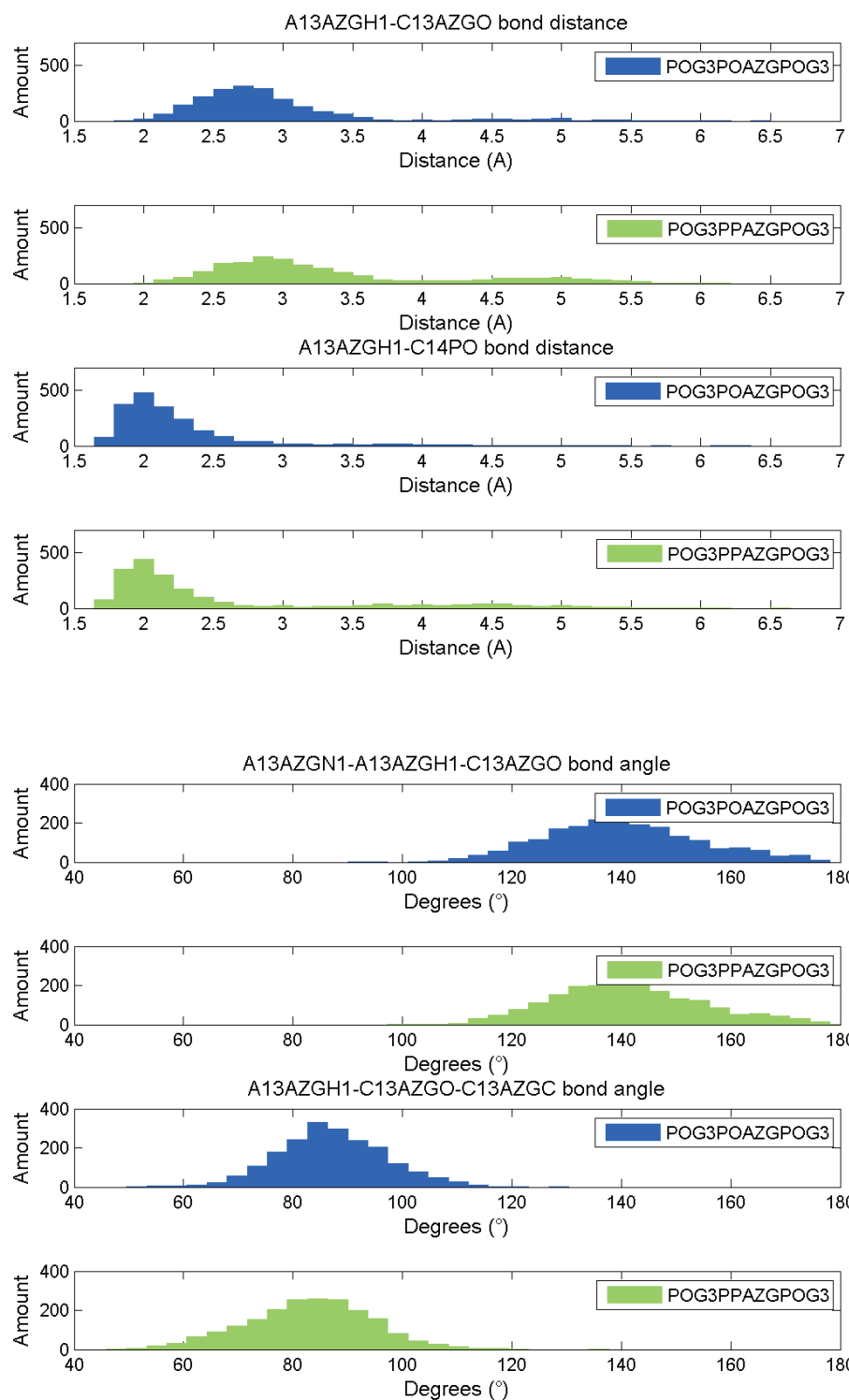


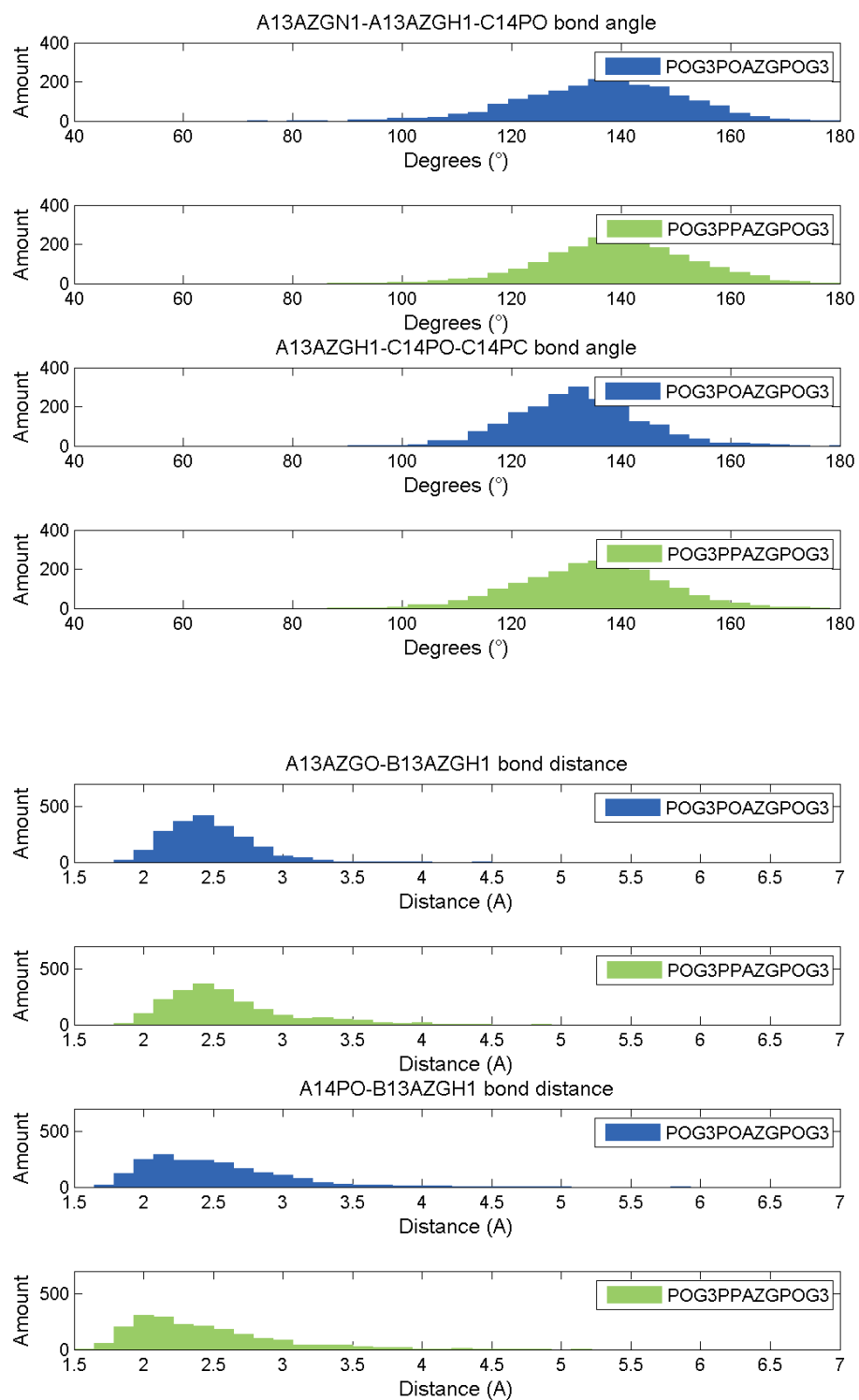


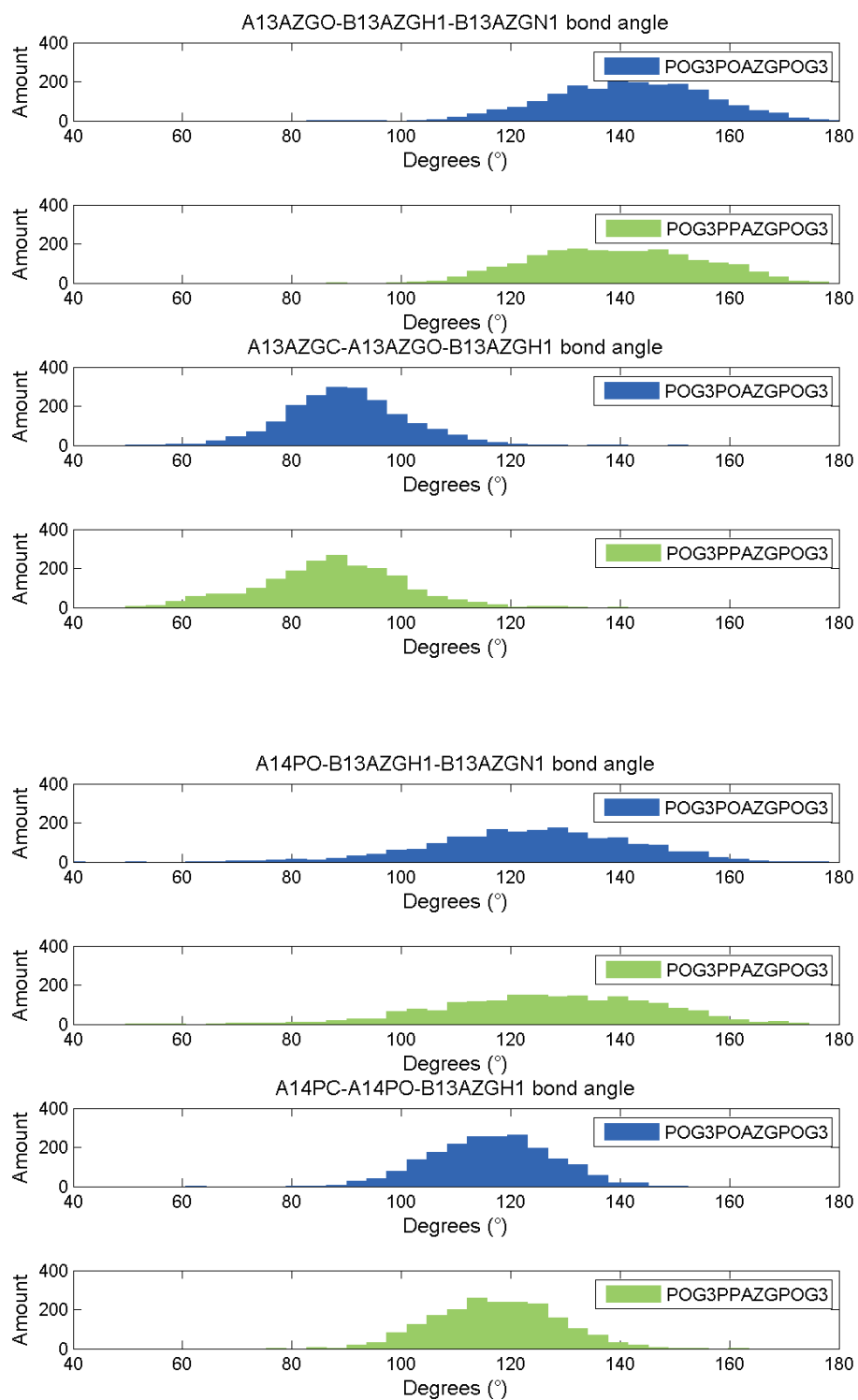


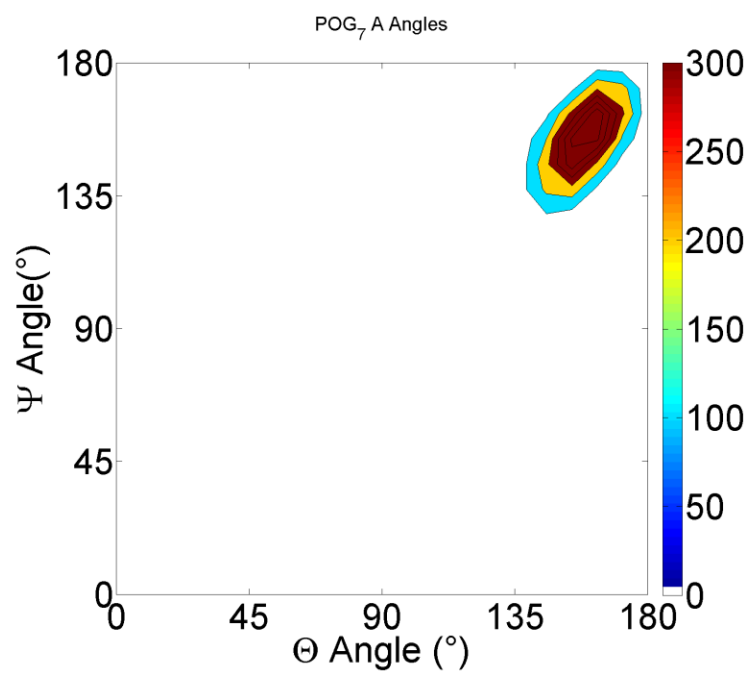
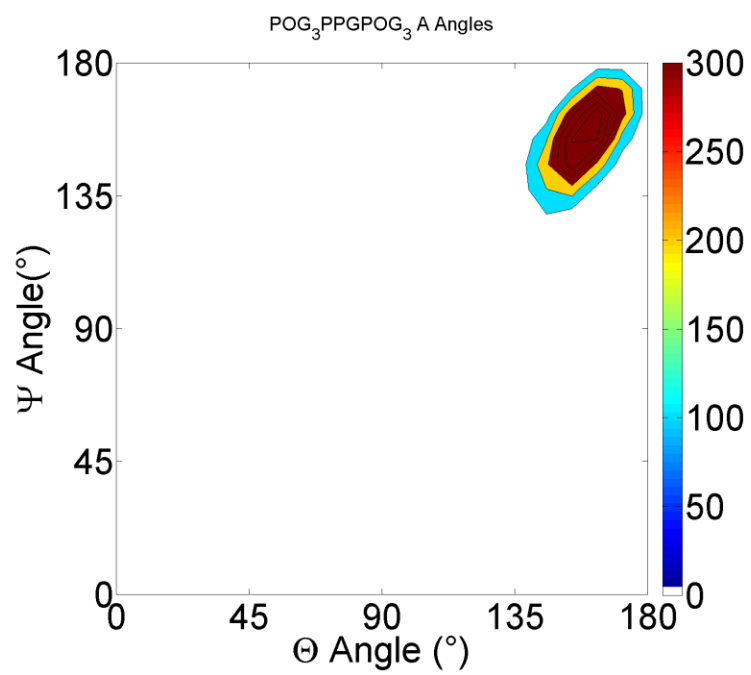


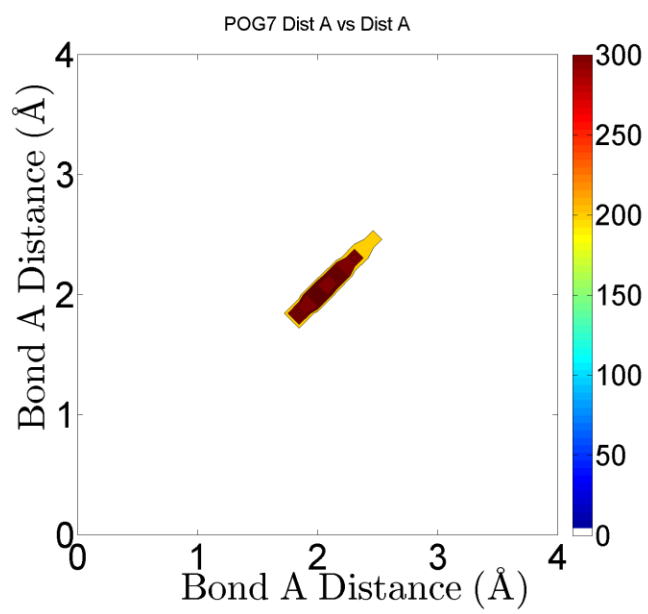
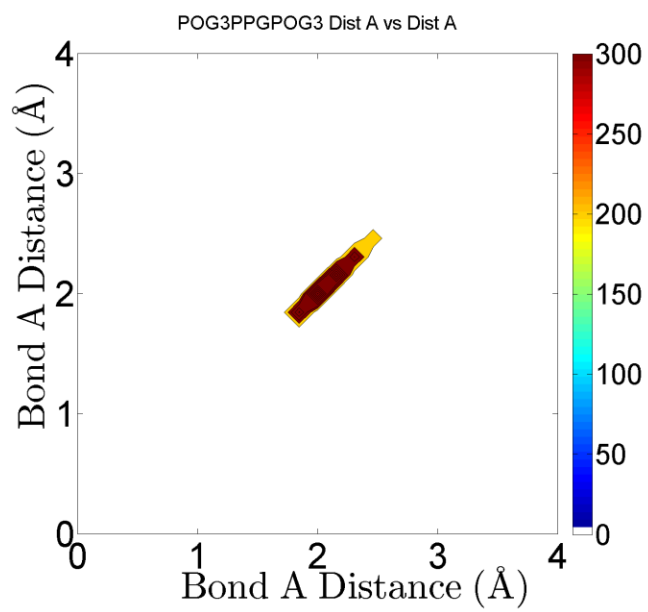


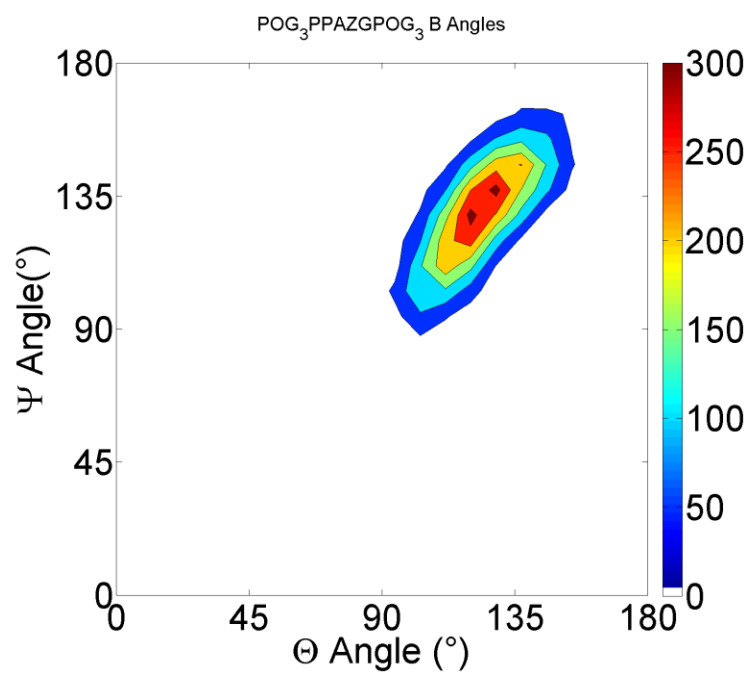
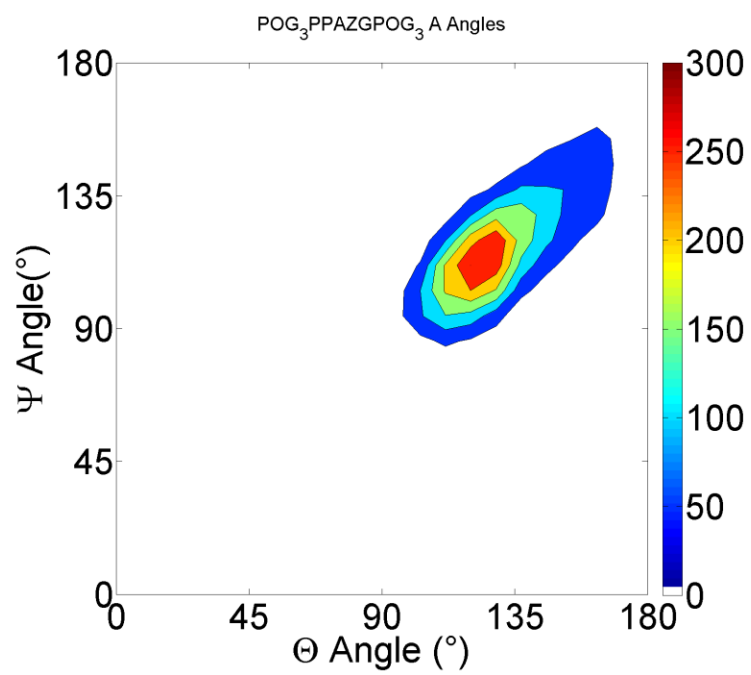


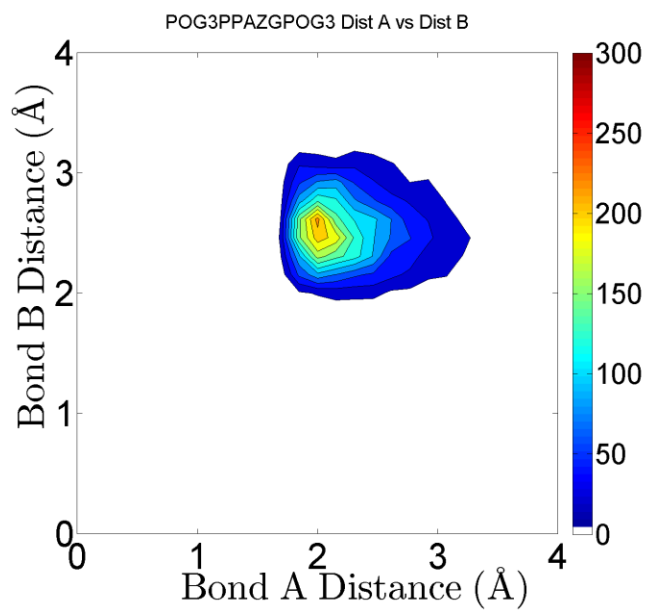
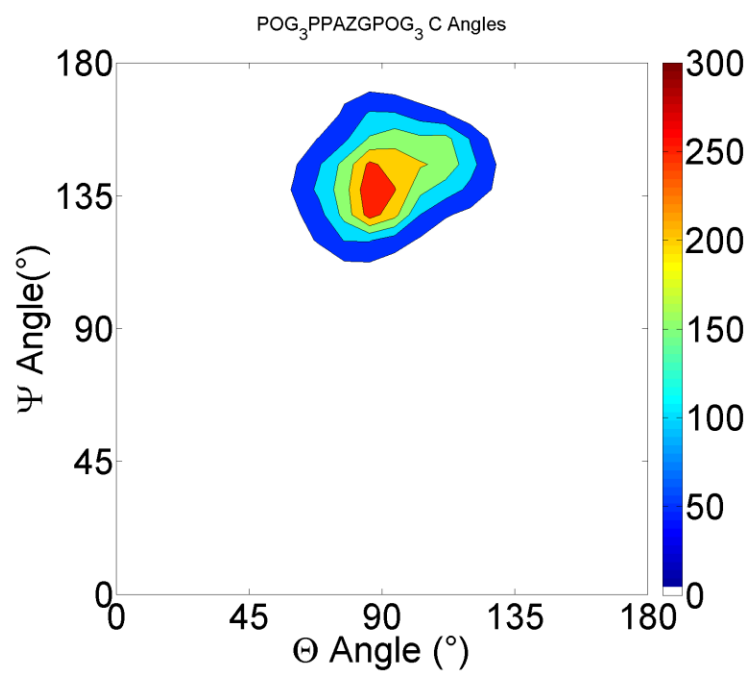


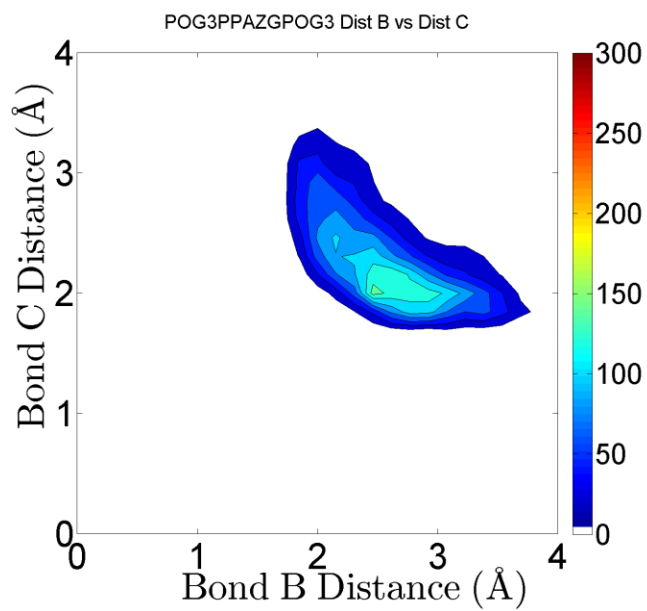
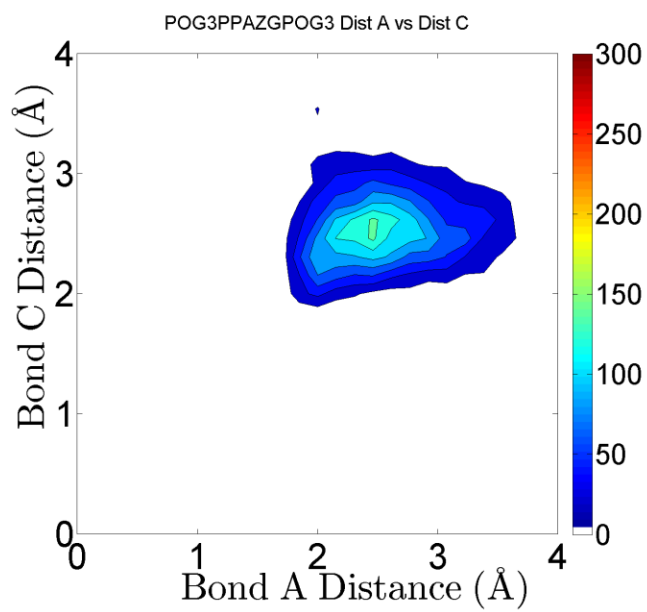












CHAPTER 4: UTILIZATION OF COLLAGEN AS A SCAFFOLD FOR
MULTICHROMOPHORE ASSEMBLY

4.1 Introduction

The ability to mimic the efficiency of light harvesting in nature has been a goal which has eluded researchers over the last several decades.¹⁻⁴ While nature primarily uses light harvesting systems in photosynthesis, researchers are primarily interested in studying these systems for applications in photonic wires, solar energy conversion, and fluorescence imaging.⁵⁻⁷ One of the most well studied light harvesting proteins found in nature is phycoerythrin, a protein isolated from photosynthetic purple bacteria. The spatial orientation of the tetrapyrrole phycoerythrobilin dyes within the protein leads to highly efficient redistribution of the excitation energy by optimizing dye spacing. This, in turn, results in a minimal loss of energy due to self-quenching despite the high dye loading.⁸ This and other natural multichromophore systems have inspired many researchers to investigate synthetic alternatives in an effort to match or improve upon their light harvesting capabilities.

Multichromophore arrays are defined as systems of multiple dye molecules which are arranged into precise supramolecular structures.⁹ These assemblies can employ covalent or noncovalent attachment of the dyes, each strategy having their own unique advantages. Noncovalent approaches are generally synthetically facile, but often lack the precision found in covalent assemblies. Despite this drawback, researchers have developed self-assembling systems with considerable morphological control,¹⁰ created fluorescent nanoparticles for bioimaging¹¹, and generated systems for applications in photovoltaics¹²⁻¹⁴ and semiconductors.^{15,16}

A number of different methods have been utilized for constructing covalent multichromophore assemblies. Typically, dyes are covalently bound to a scaffold which is capable of assembling into a larger supramolecular structure. In the past, these scaffolds have been comprised of dendritic polymers¹⁷⁻²⁰, hydrocarbons²¹, and self-assembling biomolecules including nucleic acids and proteins^{9,22-24}. Of the many different kinds of biopolymers available, use of DNA for multichromophore assembly has been the most extensively studied.^{25,26} Several studies have been

conducted involving replacing nucleosides with chromophores^{27–37}, attachment of chromophores on the DNA backbone^{27–29,31–35,38–40,37}, or as side chains off of nucleobases.^{41–44} DNA, being a highly versatile biopolymer, has also been used in noncovalent assembly of chromophores through the intercalation of dyes within base pairs.⁹ Biological scaffolds which have been far less studied include those based on proteins. Utilization of proteins holds promise to develop compounds with novel chromophore orientations, as proteins have the potential to adopt more complicated three-dimensional structures.

Interesting photophysical properties can be generated from the interactions of π -conjugated systems. The most notable includes the formation of J-aggregates, where the collective absorption of the interacting chromophores becomes red-shifted, and are sometimes accompanied by an increase in fluorescence quantum yield.⁴⁵ Common dyes which have been investigated for the generation of J-aggregates have included cyanines, merocyanines, squaraines, and perylene bisimides.⁴⁵ Another common interaction resulting from chromophore assembly includes excimer and exciplex formation, where chromophores form excited state dimers which result in red-shifted emission when decayed.⁴⁶ Elegant work by Kool and workers have shown a variety of multispectral imaging agents with significant Stokes Shifts can be generated through select chromophore interactions covalently attached along a DNA scaffold.^{47,48} This powerful control of photophysical properties inspired the idea that collagen, one of nature's most abundant proteins, could be utilized as a similar scaffold for the development of new types of materials.

Collagen consists of three polypeptide chains consisting of a repeating sequence of XaaYaaG, where Xaa and Yaa can be any amino acid, but typically are proline or hydroxyproline residues.⁴⁹ Each individual strand forms a left-handed polyproline-II-type helix, and these helices supercoil to form a right-handed triple helix. Native collagen can vary in size from 662 to 3152 amino acids long, and the sheer size of the protein hinders the study of point modifications to the structure.⁵⁰ Rather, collagen model peptides (CMPs), which are on the order of 21-30 amino

acids long, are a much simpler system to study the basic structure of collagen.⁴⁹ Several modifications to CMPs have provided insight into various factors which influence the collagen stability, including stereodynamism,⁵¹ stereoelectronic effects,^{52,53} and internal hydrogen bonding mechanisms.^{54,55}

Incorporation of 4*R*-hydroxyproline into the Yaa position of CMPs is a common strategy by which to increase the stability of the triple helix. The crystal structure of the CMP (GPO)₉ shows that the hydroxyproline residues are spaced by an intra- and inter-strand distance of 10 Å, a periodic distance which suggests the possibility of chromophore interaction (**Error! Reference source not found.**).⁵⁶ Additionally, the hydroxyl group provides a functional handle on which chromophores could potentially be covalently attached. The optimal distance for excimer and exciplex formation requires the chromophores be held apart at a distance of approximately 3.4

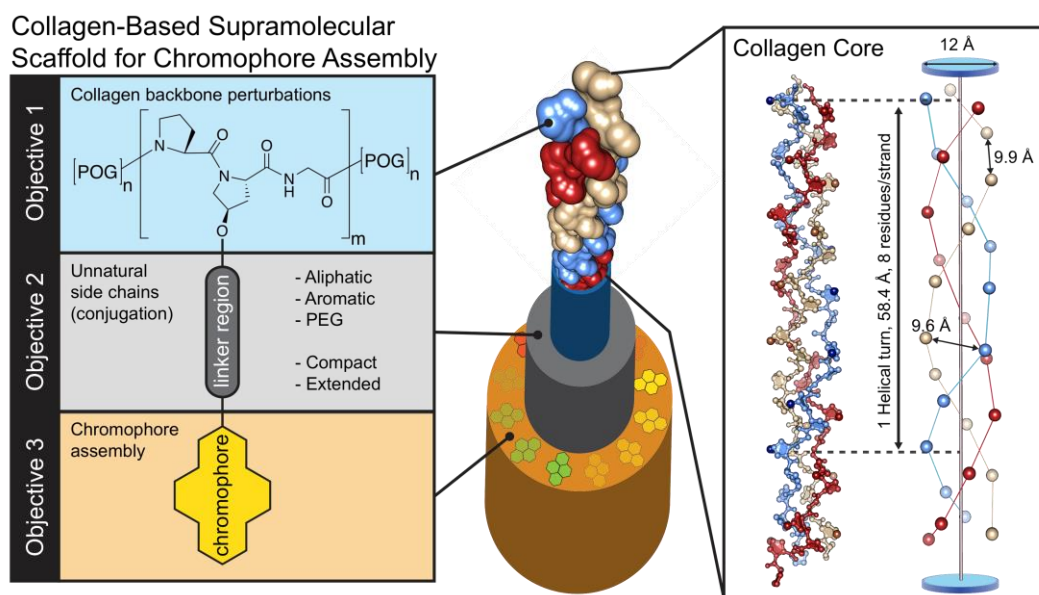


Figure 4.1 Proposed modification to collagen structure.

The hydroxyproline residue provides a functional handle on which linkers can be attached. Additionally, the crystal structure of collagen (shown here) shows the distance between chromophores will be approximately 10 Å.

Å,⁴⁶ thereby the use of a flexible linker for the attachment of chromophores was thought to be required. The linker was envisioned to be flexible enough to permit chromophore interaction, but still be rigid enough so as to minimize loss of emission through non-radiative decay. As such, the incorporation of a 2-carbon or 3-carbon linker terminated by a Boc-protected amine was affixed to the collagen backbone stemming from the hydroxyl group of hydroxyproline residues in the collagen (**Error! Reference source not found.**).

Precise positioning of chromophores on the collagen back-bone was expected to be obtained through the combination of solid phase peptide synthesis (SPPS) and the selective reactivity of an amine terminated linker with N-hydroxysuccinimide functionalized dyes. The viability of collagen to function as a scaffold for chromophore arrangement was probed by observing the effect of pyrene emission in the single stranded and triple-helical state of collagen. Pyrene is an extremely useful molecule in examining proximity effects due to its capability of forming excimers, which can be observed by its characteristic emission between 425-550 nm.⁵⁷

4.2 Results and Discussion

The two linker-substituted hydroxyproline amino acids (**Error! Reference source not found.**) were synthesized according to a modified procedure developed by Chmielewski and coworkers, and were incorporated into CMPs.⁵⁸ The impact of unnatural amino acid incorporation on triple helix self-assembly was monitored by circular dichroism (CD) spectroscopy experiments. All CMPs displayed a corresponding maximum ellipticity at 225 nm and a minimum ellipticity at 190 nm, indicating a propensity for triple helix formation. Additionally, all unsubstituted CMPs **1, 3, 5, 7, 9, and 11**

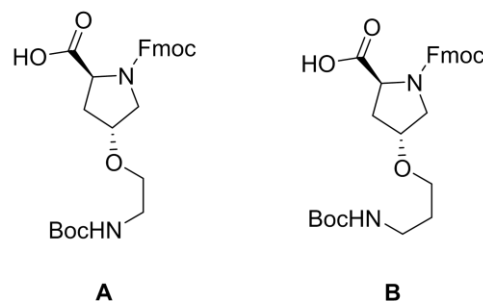


Figure 4.2. Structures of the two unnatural amino acids incorporated into CMPs

underwent a cooperative unfolding transition in thermal CD denaturation experiments (**Error! Reference source not found.**). Incorporation of multiple linker-substituted hydroxyprolines leads to successive destabilization of the collagen triple helix, a result of charge repulsion between protonated amines within the assembled structure.⁵⁹ With the addition of a single pyrene substitution, the thermal transition drops by 9°C for peptide **2** and was nonperturbing for peptide **4**. Adding one more pyrene to the CMP increases the thermal stability by 30°C for peptide **6** in comparison to **2** and by 18.5°C for peptide **8** in comparison to **4**. This increase in stability can be attributed to the hydrophobic π - π interactions between pyrene residues in water. Analysis of the CD spectrum of these pyrene substituted CMPs indicates all modified peptides continue to have a propensity for triple helix formation. By increasing the pyrene loading to three consecutive dyes, the thermal stability actually decreases in both peptides **10** and **12**, dropping to 57°C and 61°C, respectively. Loading the CMP with five pyrene dyes leads to insolubility of the CMP. These results indicate that while the addition of hydrophobic dyes may increase the thermal stability of the triple helix, overloading the CMP with dyes may introduce competitive assembly which may be detrimental to collagen triple helix formation.

Table 4.1 Thermal denaturation temperatures for unsubstituted and pyrene-substituted CMPs

CMP	X =		A		B			
	<u>Unsub.</u>		<u>Py-sub.</u>		<u>Unsub.</u>		<u>Py-sub.</u>	
	Entry	T_m (°C)	Entry	T_m (°C)	Entry	T_m (°C)	Entry	T_m (°C)
Ac-(POG) ₄ (PXG)(POG) ₄ -NH ₂	1	59.1	2	51.2	3	51.7	4	52.0
Ac-(POG) ₄ (PXG) ₂ (POG) ₃ -NH ₂	5	51.3	6	81.3	7	52.9	8	70.5
Ac-(POG) ₃ (PXG) ₃ (POG) ₃ -NH ₂	9	51.1	10	57.2	11	51.0	12	61.3

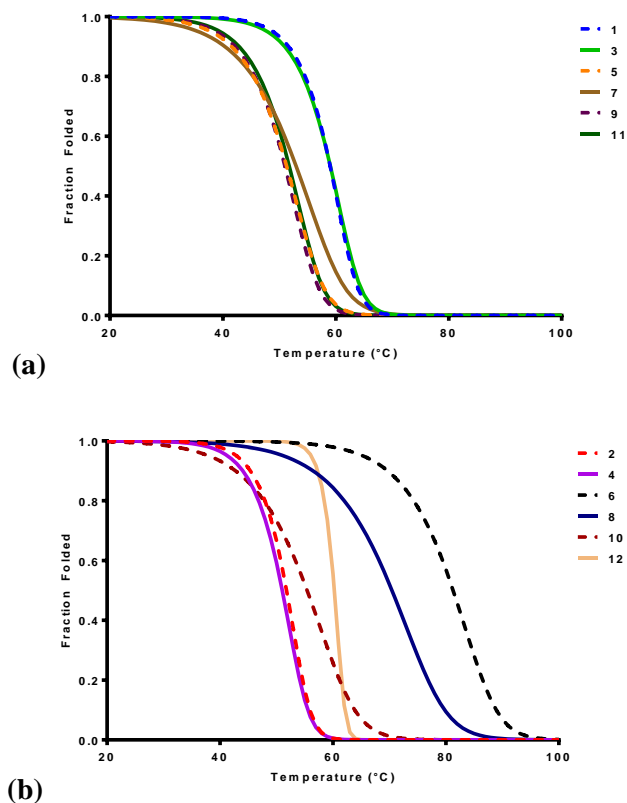


Figure 4.3. Fraction folded thermal denaturation plots for various chromophore substituted CMPs. (a) Plots of the unsubstituted collagen model peptides, and (b) plots of the pyrene substituted collagen model peptides. Dashed lines refer to plots of the 2C linker, solid lines refer to plots of the 3C linker.

Analysis of the fluorescence spectra of the pyrene substituted CMPs gives insight into how the chromophores interact. Both peptides **2** and **4** show a small degree of excimer formation at 494 nm at 20°C, with excimer formation greater in **4**. Monitoring the emission intensity of the pyrene system during thermal denaturation showed the disappearance of excimer emission at a thermal transition that correlated with CD thermal melts, suggesting the interaction of the pyrene molecules is a result of collagen triple-helix formation. Peptides **6** and **8** showed a dramatic increase in excimer emission at 20°C (**Error! Reference source not found.**) which decreased significantly upon denaturation of the triple helix at 80°C.

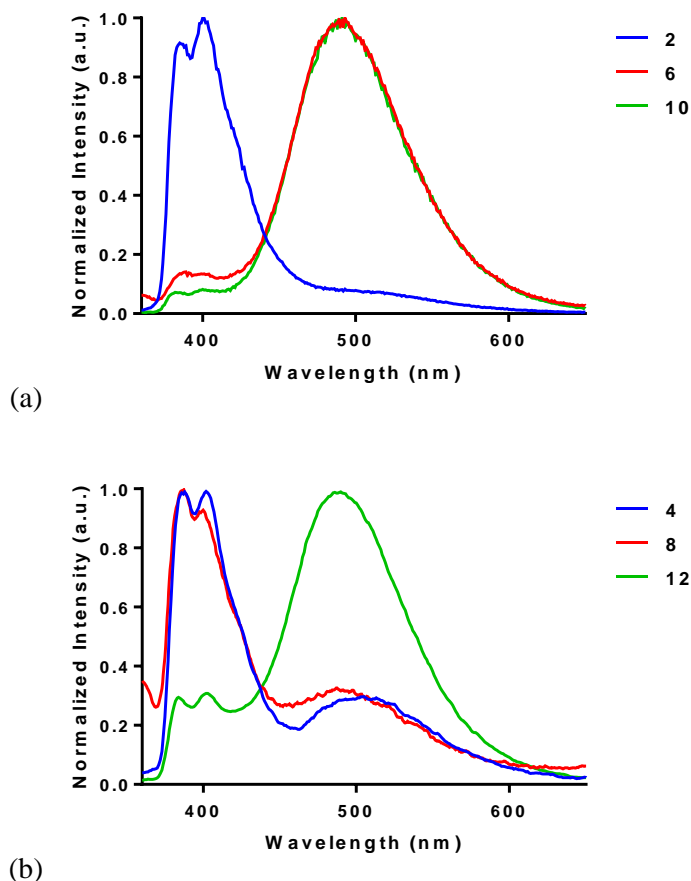


Figure 4.4. Emission spectra at 20°C for CMPs containing the (a) 2C linker and (b) 3C linker

An examination of the influence of dye placement was also undertaken. Synthesis of CMP **13** and **14** examined placing the pyrene residues in a skip-spaced orientation. Interestingly enough, these resulted in peptides which were insoluble, suggesting that this orientation encourages interdigitation of the collagen strands. Additionally, pyrene dyes were placed in the middle, N-terminus, and C-terminus of a collagen model peptide to assess how well the dyes were tolerated on the edges of peptide. Interestingly, the thermal stability of the CMP was dramatically enhanced by the incorporation of simply 2 dyes, however, no triple helix was observed with peptide **22** shows, indicating that loading the N-terminus with pyrene dyes appears to be detrimental with the 2-carbon linker. In general, greater stability is seen when the dyes are loaded on the terminus in comparison to dyes loaded in the middle of the CMP. This may be a result of

the perturbing nature of the hydrophobic dye. By tethering the strands together with hydrophobic interactions, the preference over these interactions may impede the natural hydrogen bonding network of collagen, thereby leading to the thermal denaturation observed.

Molecular dynamics simulations were conducted to investigate the interaction of the pyrene dyes on the collagen backbone. The dynamics calculations were run utilizing the program GROMACS using the force field parameters in the AMBER99SB package. The point charges of the unnatural amino acid **A'** and **B'** were calculated according to the parameters in the aforementioned force field package.⁶⁰

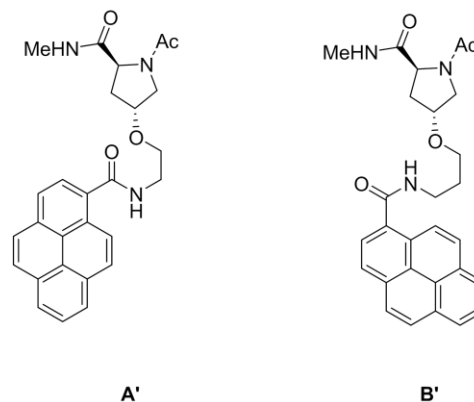


Figure 4.5. Structures used to calculate point charges in the MD simulation

Summarized, ground state solvent-free DFT calculations were performed to obtain the lowest energy conformations of the dye and linker, after which the electrostatic potential was calculated using Gaussian. These values were used as input parameters to perform an RESP charge fit using the AMBER package to obtain the point charges on the unnatural amino acid. Bond, angle, and dihedral force constants were obtained from the GAFF (General Amber Force Field) from the AMBER package.

Initial 50 ns simulations were run on models containing three dyes on a single strand. These calculations indicated all three pyrene dyes had the capability of intra-strand stacking (**Error! Reference source not found.**). Inter-strand interactions were assessed by running a series of nine simulations with a collagen with two pyrenes on one strand and one pyrene on an adjacent strand (**Error! Reference source not found.**). The results indicate very favorable intra-strand interactions with the less flexible 2C-linker, and suggest plausible inter-strand and intra-strand pyrene interactions with the 3C-linker.

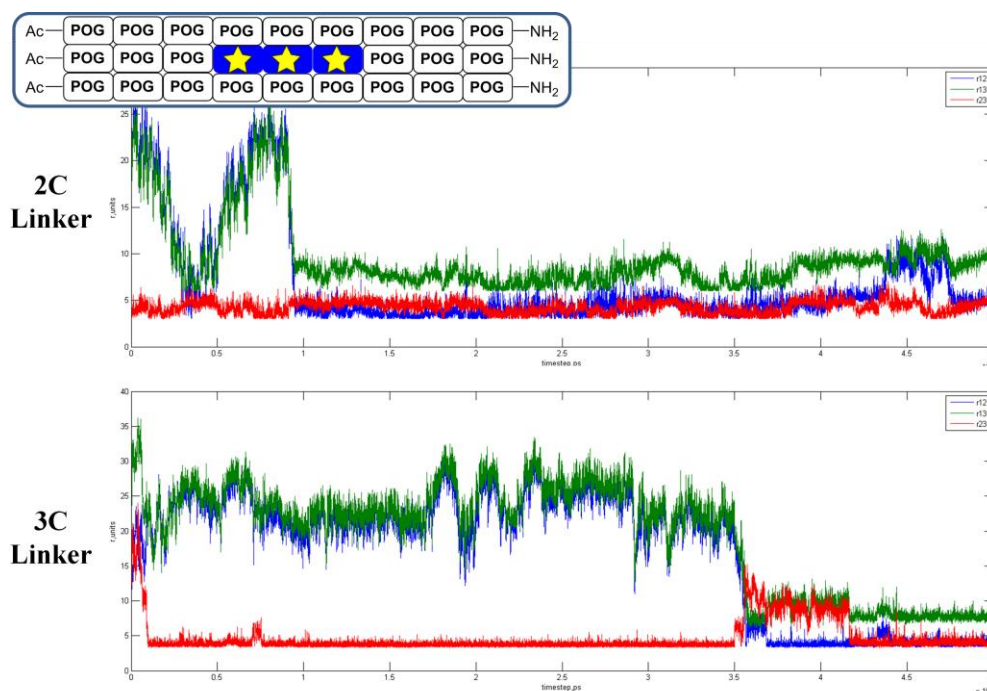


Figure 4.6. 50 ns MD simulation performed with the 2C linker and 3C linker

Distance between pyrene chromophores was monitored over the course of a 50 ns simulation. The 2C linker shows that all 3 pyrene dyes interact with each other within 10 ns. Due to the flexibility of the 3C linker, it takes much longer for the dyes to come into contact.

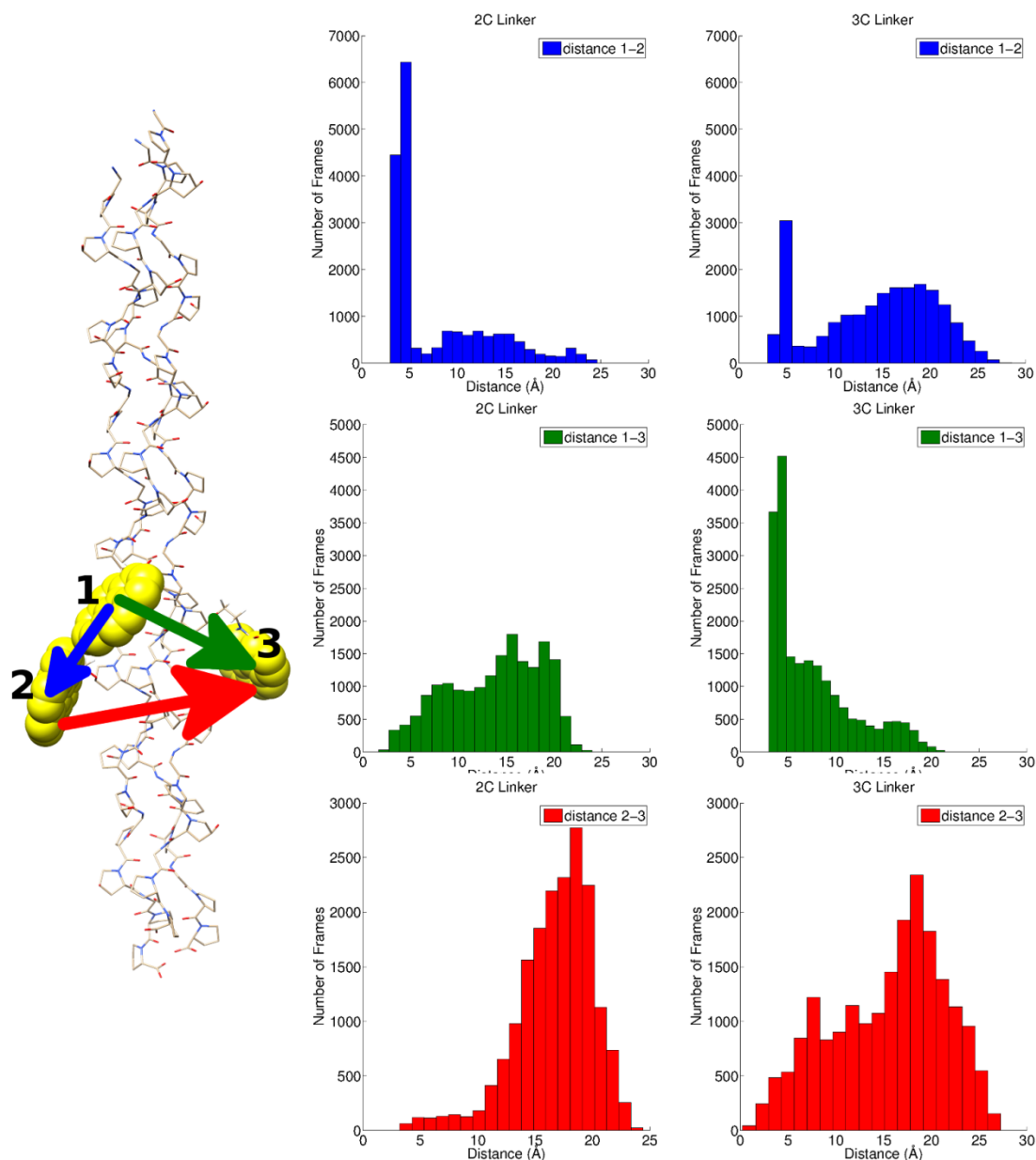


Figure 4.7. Histograms summarizing 9 simulations describing inter- and intra- strand interactions
 The dyes 1 and 2 refer to chromophores on the same strand (intrastrand interactions), whereas dye 3 is placed on an adjacent strand.

These results from these calculations were tested by synthesizing the collagen model peptides **24** and **26**. In these cases, peptides **24** and **26** are too short to allow triple helix formation, thereby allowing a method by which to observe the fluorescence properties of the dyes on a single strand. As suggested by the simulation, peptide **24** shows a significant degree of excimer emission in

comparison to peptide **26**, which suggests that intrastrand interactions are favored. Interestingly, peptide **26** shows almost no excimer formation when the peptides are on a single strand, indicating that self-assembly of the collagen triple helix has a significant effect in allowing the substituted chromophores to interact.

Table 4.2

CMP	X =		2C Linker		3C Linker			
			<u>Unsub.</u>	<u>Py-sub.</u>	<u>Unsub.</u>	<u>Py-sub.</u>		
	Entry	T_m (°C)	Entry	T_m (°C)	Entry	T_m (°C)	Entry	T_m (°C)
Ac-(POG) ₂ (PXG)(POG)-(PXG)(POG)(PXG)(POG) ₂ -NH ₂	-	-	-	-	-	-	13	No helix
Ac-(POG) ₃ (PXG)(POG)-(PXG)(POG) ₃ -NH ₂	-	-	-	-	-	-	14	No helix
Ac-(POG) ₇ (PXG) ₂ -NH ₂	15	52.9	16	73.4	17	52.2	18	75.5
Ac-(PXG) ₂ (POG) ₇ -NH ₂	19	51.9	20	No helix	21	47.4	22	76.6
Ac-(POG) ₂ (PXG) ₃ (POG) ₂ -NH ₂	23	24.9	24	No Helix	25	27.3	26	No Helix

Inter-strand and intra-strand pyrene interactions were further probed by titrating and incubating non-fluorescent (POG)₉ with **10** and **12**. Emission was monitored at both 500 and 400 nm in order to observe the change in excimer and monomer emission. As the equivalence of (POG)₉ increases, little change in the excimer and monomer emission intensities were observed with **10**. These results suggest that the high degree of excimer formation is likely a result of intra-strand interactions, and correlate well with the molecular dynamics, which suggest a 2C linker favors an intra-strand interaction. In the case of **12**, a general decrease in emission intensity can be observed, suggesting inter-strand interactions may be favorable. The incomplete disappearance of excimer emission can be attributed to the fact that intra-strand interactions are still possible, as suggested by the molecular dynamics simulations.

The incorporation of different dyes was also investigated on the collagen scaffold. To overcome the limitation of the insoluble pyrene dyes, the water soluble dye Cascade Blue was incorporated

on CMP **29**.⁶¹ The CD spectrum displayed a corresponding maximum at 225 nm and minimum at 200 nm, and also underwent thermal denaturation at 49°C, indicating the CMP was capable of forming a triple helix. No excimer formation, however, was observed. Additionally, the far red excimer dye **C** was synthesized and incorporated on CMP **30**.⁶² Thermal denaturation of the peptide indicated dye-incorporation increased the stability of the triple helix by 2.7°C. Additionally, assembly of the triple helix induced excimer emission of the dye as indicated by the emission at 632 nm.

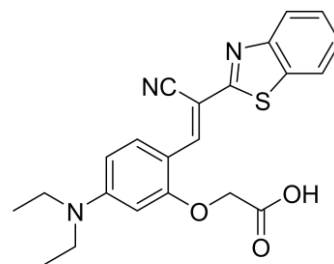


Figure 4.8 Far-red excimer dye **C**

Table 4.3 Thermal denaturation temperatures for non-pyrene dyes

CMP	Ac-(POG) ₄ (P-Dye-G)(POG) ₄ -NH ₂		3C Linker	
	Entry	<i>T_m</i> (°C)		
Unsubstituted	3	59.1		
Cascade Blue	29	49.6		
Dye C	30	61.7		

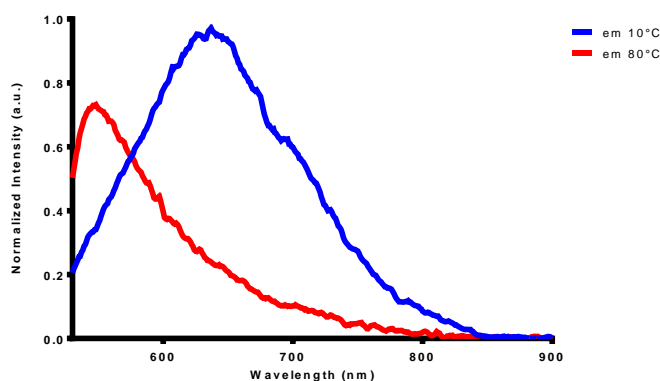


Figure 4.9 Emission spectra at 10°C and 80°C of CMP **30**

In the triple helical state, the collagen model peptide shows an emission maximum at 632 nm, which shifts to 544 nm when denatured.

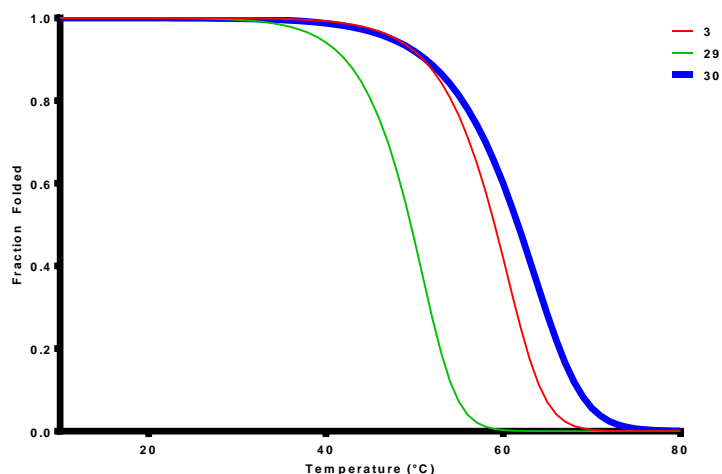


Figure 4.10 Fraction folded thermal denaturation plots for non-pyrene substituted CMPs

4.3 Conclusions

In summary, a new scaffold for the self-assembly of chromophores has been investigated. Chromophore interactions are possible as seen by extent of excimer emission observed. Excimer emission appears to be greatly enhanced as the collagen self-assembles into the triple helical state. The extent of the interaction is influenced by linker length, with intra-strand interactions appearing to be more favorable with the shorter 2C-linker according to molecular dynamics simulations and titrations with non-fluorescent (POG)₉. These results demonstrate the promise collagen holds as a scaffold to template the self-assembly of chromophores.

4.4 References

- (1) Wasielewski, M. R. *Acc. Chem. Res.* **2009**, 42 (12), 1910–1921.
- (2) Benveniste, A. L.; Creeger, Y.; Fisher, G. W.; Ballou, B.; Waggoner, A. S.; Armitage, B. A. *J. Am. Chem. Soc.* **2007**, 129 (7), 2025–2034.
- (3) Jana, B.; Ghosh, A.; Patra, A. *J. Phys. Chem. Lett.* **2017**, 4608–4620.
- (4) Frischmann, P. D.; Mahata, K.; Würthner, F. *Chem. Soc. Rev.* **2013**, 42 (4), 1847–1870.
- (5) Waggoner, A. S. *Curr. Opin. Chem. Biol.* **2006**, 10 (1), 62–66.
- (6) Gombert, A. *Photonics for Solar Energy Systems*; SPIE: Bas-Rhin, 2006.

- (7) García-Parajó, M. F.; Hernando, J.; Mosteiro, G. S.; Hoogenboom, J. P.; van Dijk, E. M. H. P.; van Hulst, N. F. *ChemPhysChem* **2005**, *6* (5), 819–827.
- (8) Scholes, G. D.; Rumbles, G. *Nat. Mater.* **2006**, *5* (9), 683–696.
- (9) Benveniste, A. L.; Creeger, Y.; Fisher, G. W.; Ballou, B.; Waggoner, A. S.; Armitage, B. a. *J. Am. Chem. Soc.* **2007**, *129* (7), 2025–2034.
- (10) Balakrishnan, K.; Datar, A.; Naddo, T.; Huang, J.; Oitker, R.; Yen, M.; Zhao, J.; Zang, L. *J. Am. Chem. Soc.* **2006**, *128* (22), 7390–7398.
- (11) Peng, H.-S.; Chiu, D. T. *Chem. Soc. Rev.* **2015**, *44* (14), 4699–4722.
- (12) Rybtchinski, B.; Sinks, L. E.; Wasielewski, M. R. *J. Am. Chem. Soc.* **2004**, *126* (39), 12268–12269.
- (13) Foster, S.; Finlayson, C. E.; Keivanidis, P. E.; Huang, Y.-S.; Hwang, I.; Friend, R. H.; Otten, M. B. J.; Lu, L.-P.; Schwartz, E.; Nolte, R. J. M.; Rowan, A. E. *Macromolecules* **2009**, *42* (6), 2023–2030.
- (14) Frischmann, P. D.; Mahata, K.; Würthner, F. *Chem. Soc. Rev.* **2013**, *42* (4), 1847–1870.
- (15) Leo, K.; Universita, T.; Riede, M.; Lu, B. *Compr. Semicond. Sci. Technol.* **2011**, *4*, 448–507.
- (16) Jurchescu, O. D.; Popinciuc, M.; van Wees, B. J.; Palstra, T. T. M. *Adv. Mater.* **2007**, *19* (5), 688–692.
- (17) Li, S.-L.; Xiao, T.; Lin, C.; Wang, L. *Chem. Soc. Rev.* **2012**, *41* (18), 5950–5968.
- (18) González-Rodríguez, D.; Schenning, A. P. H. J. *Chem. Mater.* **2011**, *23* (3), 310–325.
- (19) Elemans, J. A. A. W.; van Hameren, R.; Nolte, R. J. M.; Rowan, A. E. *Adv. Mater.* **2006**, *18* (10), 1251–1266.
- (20) Szent-Gyorgyi, C.; Schmidt, B. F.; Fitzpatrick, J. a J.; Bruchez, M. P. *J. Am. Chem. Soc.* **2010**, *132* (32), 11103–11109.
- (21) Hindin, E.; Forties, R. A.; Loewe, R. S.; Ambroise, A.; Kirmaier, C.; Bocian, D. F.;

- Lindsey, J. S.; Holten, D.; Knox, R. S. *J. Phys. Chem. B* **2004**, *108* (34), 12821–12832.
- (22) Malinovskii, V. L.; Wenger, D.; Häner, R. *Chem. Soc. Rev.* **2010**, *39* (2), 410–422.
- (23) Janssen, P. G. a; Vandenbergh, J.; van Dongen, J. L. J.; Meijer, E. W.; Schenning, A. P. H. *J. J. Am. Chem. Soc.* **2007**, *129* (19), 6078–6079.
- (24) Teo, Y. N.; Kool, E. T. *Chem. Rev.* **2012**, *112* (7), 4221–4245.
- (25) Teo, Y. N.; Kool, E. T. *Chem. Rev.* **2012**, *112* (7), 4221–4245.
- (26) Spillmann, C. M.; Medintz, I. L. *J. Photochem. Photobiol. C Photochem. Rev.* **2015**, *23*, 1–24.
- (27) Letsinger, R. L.; Wu, T. *J. Am. Chem. Soc.* **1995**, *117* (28), 7323–7328.
- (28) Letsinger, R. L.; Wu, T. *J. Am. Chem. Soc.* **1994**, *116* (2), 811–812.
- (29) Hariharan, M.; Zheng, Y.; Long, H.; Zeidan, T. A.; Schatz, G. C.; Vura-Weis, J.; Wasielewski, M. R.; Zuo, X.; Tiede, D. M.; Lewis, F. D. *J. Am. Chem. Soc.* **2009**, *131* (16), 5920–5929.
- (30) Lewis, F. D.; Zhang, Y.; Liu, X.; Xu, N.; Letsinger, R. L. *J. Phys. Chem. B* **1999**, *103* (13), 2570–2578.
- (31) Zheng, Y.; Long, H.; Schatz, G. C.; Lewis, F. D. *Chem. Commun.* **2005**, 4795–4797.
- (32) Letsinger, R. L.; Wu, T.; Yang, J.-S.; Lewis, F. D. *Photochem. Photobiol. Sci.* **2008**, *7* (7), 854.
- (33) Daublain, P.; Siegmund, K.; Hariharan, M.; Vura-Weis, J.; Wasielewski, M. R.; Lewis, F. D.; Shafirovich, V.; Wang, Q.; Raytchev, M.; Fiebig, T. *Photochem. Photobiol. Sci.* **2008**, *7* (12), 1501–1508.
- (34) Lewis, F. D.; Kalgutkar, R. S.; Wu, Y.; Liu, X.; Liu, J.; Hayes, R. T.; Miller, S. E.; Wasielewski, M. R. *J. Am. Chem. Soc.* **2000**, *122* (49), 12346–12351.
- (35) Lewis, F. D.; Zhang, L.; Kelley, R. F.; Mccamant, D.; Wasielewski, M. R. *Tetrahedron* **2007**, *63*, 3457–3464.

- (36) Lewis, F. D.; Zhang, L.; Zuo, X. *J. Am. Chem. Soc.* **2005**, *127* (28), 10002–10003.
- (37) Lewis, F. D.; Liu, X.; Miller, S. E.; Wasielewski, M. R. *J. Am. Chem. Soc.* **1999**, *121* (41), 9746–9747.
- (38) Langenegger, S. M.; Häner, R. *ChemBioChem* **2005**, *6* (12), 2149–2152.
- (39) Samain, F.; Malinovskii, V. L.; Langenegger, S. M.; Häner, R. *Bioorganic Med. Chem.* **2008**, *16* (1), 27–33.
- (40) Probst, M.; Langenegger, S. M.; Häner, R. *Chem. Commun.* **2014**, *50* (2), 159–161.
- (41) Varghese, R.; Wagenknecht, H. A. *Chem. - A Eur. J.* **2010**, *16* (30), 9040–9046.
- (42) Hwang, G. T.; Seo, Y. J.; Kim, B. H. *Tetrahedron Lett.* **2005**, *46* (9), 1475–1477.
- (43) Bouamaied, I.; Nguyen, T.; Rühl, T.; Stulz, E. *Org. Biomol. Chem.* **2008**, *6* (21), 3888–3891.
- (44) Fendt, L. A.; Bouamaied, I.; Thöni, S.; Amiot, N.; Stulz, E. *J. Am. Chem. Soc.* **2007**, *129* (49), 15319–15329.
- (45) Würthner, F.; Kaiser, T. E.; Saha-Möller, C. R. *Angew. Chemie - Int. Ed.* **2011**, *50* (15), 3376–3410.
- (46) Jenekhe, S. A.; Osaheni, J. A. *Science (80-.)*. **1994**, *265* (5173), 765–768.
- (47) Ren, R. X. F.; Chaudhuri, N. C.; Paris, P. L.; Rumney IV, S.; Kool, E. T. *J. Am. Chem. Soc.* **1996**, *118* (33), 7671–7678.
- (48) Gao, J.; Strässler, C.; Tahmassebi, D.; Kool, E. T. *J. Am. Chem. Soc.* **2002**, *124* (39), 11590–11591.
- (49) Shoulders, M. D.; Raines, R. T. *Annu. Rev. Biochem.* **2009**, *78*, 929–958.
- (50) Ricard-Blum, S. *Cold Spring Harb. Perspect. Biol.* **2011**, *3* (1), 1–19.
- (51) Zhang, Y.; Malamakal, R. M.; Chenoweth, D. M. *Angew. Chemie Int. Ed.* **2015**, *54* (37), 10826–10832.
- (52) Holmgren, S. K.; Bretscher, L. E.; Taylor, K. M.; Raines, R. T. *Chem. Biol.* **1999**, *6* (2),

63–70.

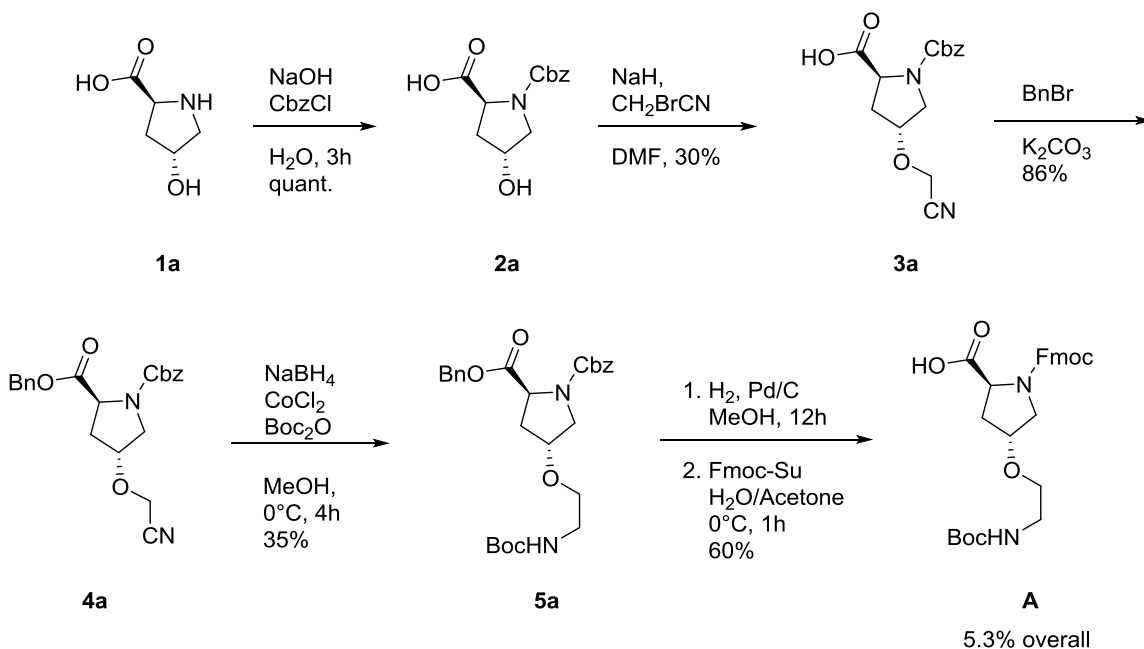
- (53) Erdmann, R. S.; Wennemers, H. *J. Am. Chem. Soc.* **2010**, *132* (40), 13957–13959.
- (54) Egli, J.; Siebler, C.; Maryasin, B.; Erdmann, R. S.; Bergande, C.; Ochsenfeld, C.; Wennemers, H. *Chem. - A Eur. J.* **2017**, *23* (33), 7938–7944.
- (55) Zhang, Y.; Malamakal, R. M.; Chenoweth, D. M. *J. Am. Chem. Soc.* **2015**, *137* (39), 12422–12425.
- (56) Bella, J.; Eaton, M.; Brodsky, B.; Berman, H. *Science* (80-.). **1994**, *266* (5182), 75–81.
- (57) Okuyama, K.; Miyama, K.; Mizuno, K.; Bächinger, H. P. *Biopolymers* **2012**, *97* (8), 607–616.
- (58) Fillon, Y. A.; Anderson, J. P.; Chmielewski, J. *J. Am. Chem. Soc.* **2005**, *127* (33), 11798–11803.
- (59) Gauba, V.; Hartgerink, J. D. *J. Am. Chem. Soc.* **2007**, *129* (48), 15034–15041.
- (60) Hornak, V.; Abel, R.; Okur, A.; Strockbine, B.; Roitberg, A.; Simmerling, C. *Proteins Struct. Funct. Bioinforma.* **2006**, *65* (3), 712–725.
- (61) Whitaker, J. E.; Haugland, R. P.; Moore, P. L.; Hewitt, P. C.; Reese, M.; Haugland, R. P. *Anal. Biochem.* **1991**, *198* (1), 119–130.
- (62) Han, G.; Kim, D.; Park, Y.; Bouffard, J.; Kim, Y. *Angew. Chemie Int. Ed.* **2015**, *127* (13), 3912–3916.

4.5 Supplemental Information

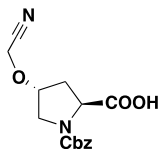
4.5.1 General Information

All commercial reagents and solvents were used as received. Fmoc-Pro-OH, Fmoc-Gly-OH, HATU and Rink Amide AM Resin (100-200 mesh) were purchased from Novabiochem. Fmoc-Hyp(tBu)-OH was purchased from Advanced Chemtech. Piperidine was purchased from American Bioanalytical. All remaining chemicals were purchased from Sigma Aldrich. Flash column chromatography was performed using Silicycle silica gel (55–65 Å pore diameter). Thin-layer chromatography was performed on Sorbent Technologies silica plates (250 µm thickness). High-resolution mass spectra were obtained at the University of Pennsylvania's Mass Spectrometry Service Center on a Micromass AutoSpec electrospray/chemical ionization spectrometer. Mass of long peptides were obtained via a Bruker Ultraflex III Matrix-assisted laser desorption/ionization (MALDI) mass spectrometer. Ultraviolet absorption spectrophotometry was performed on a JASCO V-650 spectrophotometer with a PAC-743R multichannel Peltier using quartz cells with a 1 cm cell path length. High performance liquid chromatography analysis was performed using a Jasco HPLC instrument equipped with a Phenomenex column (Luna 5u C18(2) 100A; 250 × 4.60 mm, 5 µm). Circular dichroism experiments were performed with a Jasco J-1500 CD Spectrometer with a 6-cell holder.

4.5.2 Experimental Procedures



Scheme 4.1 Synthesis of amino acid A



Compound (2a)

Z-Hyp-OH (5.40 g, 20.37 mmol, 1.0 eq) was dissolved in anhydrous THF (70 ml) and cooled to 0°C by ice-bath under Ar. To this solution NaH (60% dispersion in mineral oil, 1.71 g, 42.78 mmol, 2.1 eq) was added portionwise. After 60 minutes of stirring at 0°C, the, α -bromoacetonitrile (1.56 ml, 22.41 mmol, 1.0 eq) was then added to the reaction mixture over 10 minutes at -30°C. Stirring was kept for overnight with gradual warming to room temperature. Upon completion of the reaction, the solvent THF was removed under reduced pressure. Aqueous HCl solution (1 N) was carefully added to the residue with external cooling to adjust the pH of the mixture to about pH = 2. Extract the organic compound from this mixture by ethyl acetate (3

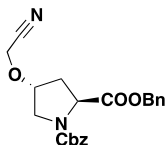
times). The organic layer was then dried with Na₂SO₄, and concentrated. Flash chromatography (40%-70% EtOAc in Hexanes) and the product was obtained as yellow oil (86%).

TLC: R_f = 0.25 (10% MeOH/DCM).

¹H NMR (500 MHz, CDCl₃) δ 7.39-7.23 (m, 5H), 5.22-5.10 (q, 1H), 5.02-4.97 (d, 0.5H), 4.88-4.84 (d, 0.5H), 4.85-4.78 (t, 0.5H), 4.76-4.72 (t, 0.5H), 4.20-4.14 (m, 0.5H), 4.10-4.06 (m, 0.5H), 3.90-3.80 (m, 0.5H), 3.73-3.40(m, 3H) 3.30-3.24 (m, 0.5H), 3.12-3.02 (m, 0.5H), 3.01-2.91 (m, 0.5H), 2.2-1.60 (m, 6H), 1.47 (s 4.5H), 1.43 (s, 4.5H).

¹³C NMR (125 MHz, CDCl₃) rotameric mixture: δ 176.09 (175.39), 157.52 (157.38), 154.71 (154.03), 136.69 (136.62), 128.50 (128.40), 128.36 (128.10), 127.78 (127.56), 82.55 (82.25), 67.06 (66.73), 56.02 (55.78), 47.55 (47.38), 46.80, 43.77 (43.42), 31.22 (30.19), 28.06 (27.98), 24.65 (24.57), 24.31 (23.56).

HRMS (ESI) calculated for C₂₁H₂₉N₃O₅ [M+Na]⁺ 426.2005, found 426.2007.



Compound (**3a**)

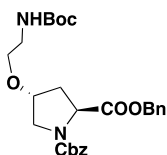
Compound **2a** (1.83 g, 6.0 mmol, 1.0 eq) was dissolved in 24 ml DMF at 0°C. Anhydrous K₂CO₃ (2.57 g, 15.0 mmol, 2.5 eq) and benzyl bromide (0.58 ml, 6.0 mmol, 1.0 eq) were sequentially slowly added. The mixture was allowed to react at this temperature for one and half hour and then at room temperature for another two hours. The reaction mixture was subjected to a gravity filtration to remove the insoluble salt and the filtrate was concentrated. Saturated LiI aqueous solution was added to the residue (caution, exothermic) and the mixture was extracted 3 times with ether. Combined organic layer was then dried with Na₂SO₄, and concentrated. Flash chromatography (25%-60% EtOAc in Hexanes) and the product was obtained as light-yellow oil (86%).

TLC: R_f = 0.44 (50% EtOAc/Hex).

^1H NMR (500 MHz, CDCl_3) δ 7.71 (bs, 1H), 7.39-7.11 (m, 10H), 5.20-4.97 (m, 4H), 4.81-4.76 (t, 1H), 4.68-4.62, 4.47-4.38 (t, 1H), 4.26-3.90 (m, 2H), 3.69-3.51, 3.5-3.43 (m, 2H), 3.18-3.12 (m, 1H), 3.03-2.92, 2.87-2.73 (m, 1H), 2.2-1.60 (m, 6H)

^{13}C NMR (125 MHz, CDCl_3) rotameric mixture: δ 175.56 (177.16), 169.82 (169.17), 160.92 (160.36), 155.18 (153.88), 136.44 (135.44), 128.75, 128.61, 128.56, 128.53, 127.47, 127.39, 128.23, 128.18, 127.96, 127.78, 67.17, (67.44), 66.77 (66.90), 57.04 (57.73), 47.05 (47.26), 46.77, 43.71 (43.85), 29.18 (29.96), 25.00 (25.23), 24.65, 23.56.

HRMS (ESI) calculated for $\text{C}_{12}\text{H}_{22}\text{N}_4$ $[\text{M}+\text{Na}]^+$ 517.2063, found 517.2063.



Compound (**5a**)

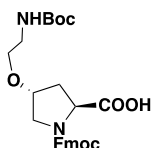
Compound **4a** (2.03 g, 5.15 mmol, 1.0 eq) was dissolved in 55 ml MeOH at 0°C. To this solution Boc_2O (1.69 g, 7.73 mmol, 1.5 eq) and $\text{CoCl}_2 \cdot 6\text{H}_2\text{O}$ (2.45 g, 10.30 mmol, 2.0 eq) were added. Sodium borohydride (1.95 g, 51.5 mmol, 10.0 eq) was portionwisely added to the reaction mixture over a period of 30 minutes at 0°C. Upon completion of the addition of NaBH_4 , the ice-bath was removed and the mixture was allowed to react for four hours. The reaction mixture was filtered through celite. Filtrate was concentrated, and water was added to the residue. Extract the mixture using EtOAc (3 times) and combined ethyl acetate layer was sequentially washed with 0.5 N HCl (aq) (1 \times), 5% KHCO_3 , (1 \times), and brine. The organic layer was then dried with Na_2SO_4 , and concentrated. Flash chromatography (25%-50% EtOAc in Hexanes) and the product was obtained as colorless oil (86%).

TLC: R_f = 0.25 (40% EtOAc/Hex).

¹H NMR (500 MHz, CDCl₃) δ 7.71 (bs, 1H), 7.39-7.11 (m, 10H), 5.20-4.97 (m, 4H), 4.81-4.76 (t, 1H), 4.68-4.62, 4.47-4.38 (t, 1H), 4.26-3.90 (m, 2H), 3.69-3.51, 3.5-3.43 (m, 2H), 3.18-3.12 (m, 1H), 3.03-2.92, 2.87-2.73 (m, 1H), 2.2-1.60 (m, 6H)

¹³C NMR (125 MHz, CDCl₃) rotameric mixture: δ 175.56 (177.16), 169.82 (169.17), 160.92 (160.36), 155.18 (153.88) 136.44 (135.44), 128.75, 128.61, 128.56, 128.53, 127.47, 127.39, 128.23, 128.18, 127.96, 127.78, 67.17, (67.44), 66.77 (66.90), 57.04 (57.73), 47.05 (47.26), 46.77, 43.71 (43.85), 29.18 (29.96), 25.00 (25.23), 24.65, 23.56.

HRMS (ESI) calculated for C₁₂H₂₂N₄ [M+Na]⁺ 517.2063, found 517.2063.



Compound (A)

Compound (**5a**) (855 mg, 1.72 mmol, 1.0 eq) was dissolved in MeOH (16 ml). To the reaction mixture 10% Pd/C (170 mg) was added and the mixture was allowed to stir at room temperature for 1 d. The reaction was filtered through Celite and the filtrate was concentrated under reduced pressure to obtain an oily residue. Nine ml saturated NaHCO₃ (aq) and 9 ml dioxane were subsequently added to the flask containing the residue, followed by addition of FmocOSu (637 mg, 1.89 mmol, 1.1 eq). The mixture was allowed to react overnight at room temperature. The reaction was quenched by dilution with di-ionized water and ethyl acetate. The aqueous layer was separated, washed one more time with ethyl acetate and acidified with 2N HCl (aq). The solution turned cloudy when the pH was adjusted to about 2. This mixture was extracted three times with ethyl acetate and the combined organic layer was washed with di-ionized water (1 ×), brine (1 ×), dried with Na₂SO₄, and concentrated under reduced pressure. Flash chromatography (45%-95% EtOAc in Hexanes) afforded the desired product as a foamy white solid. (60%).

TLC: R_f = 0.03 (100% EtOAc);

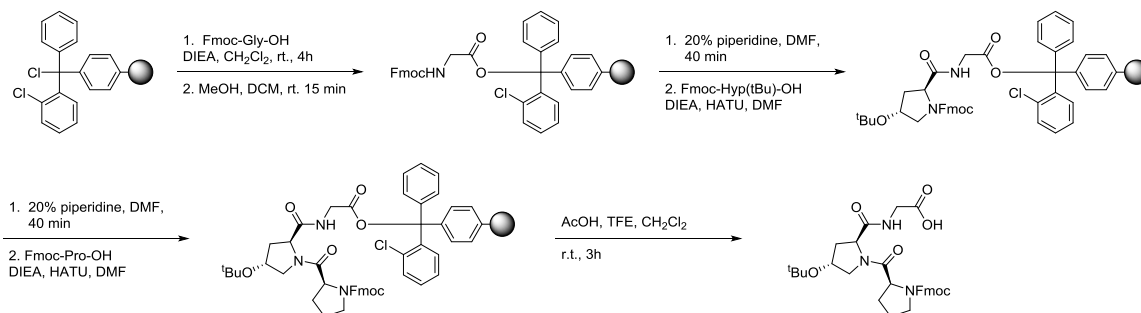
IR (thin film): ν 1725, 1674, 1526, 1450, 1403, 1266, 1183 cm^{-1} ;

^1H NMR (500 MHz, MeOD) δ 7.9 (s, 1H), 7.83-7.76 (d, J = 7.4 Hz, 2H), 7.69-7.57 (d, J = 7.4 Hz, 2H), 7.41-7.35 (t, J = 7.4 Hz, 2H), 7.33-7.27 (t, J = 7.4 Hz, 2H), 4.53-4.02 (m, 5H), 4.00-3.20 (m, 7H), 2.50-1.80 (m, 6H);

^{13}C NMR (125 MHz, MeOD) δ 175.5, 171.2, 163.1, 159.1, 145.3, 142.5, 128.8, 128.2, 126.3, 120.9, 79.4, 68.2, 61.2, 52.9, 50.0, 48.3, 45.0, 43.2, 30.4, 25.3;

HRMS (ESI) calculated for $\text{C}_{26}\text{H}_{28}\text{N}_4\text{O}_6$ $[\text{M}+\text{Na}]^+$ 515.1907, found 515.1909.

Synthesis of Fmoc-Pro-Hyp(tBu)-Gly-OH

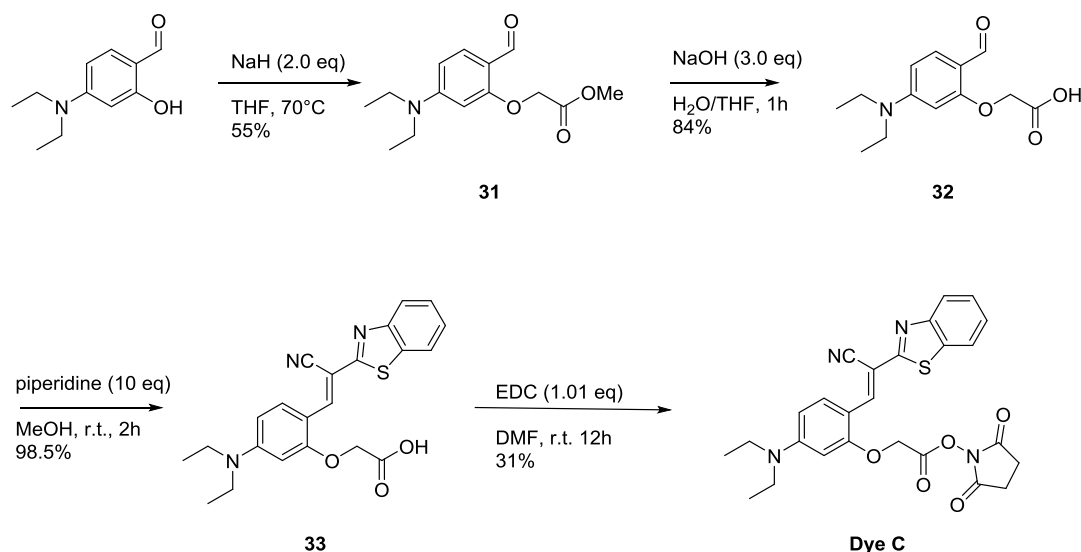


The synthesis of the tripeptide synthon FmocPOG-OH was carried out on 2-chlorotrityl chloride resin. To a solution of Fmoc-Gly-OH in dried CH_2Cl_2 , 2-chlorotrityl chloride resin and dried DIEA were added under nitrogen. The mixture was stirred for 10 minutes, and additional DIEA was added. The reaction was allowed to stir for 2h and was quenched with HPLC grade methanol to cap any remaining reactive trityl groups. After 15 min, the reaction was washed with CH_2Cl_2 and DMF. The Fmoc-protecting group was cleanly removed with 20% piperidine in DMF, and the resin was subsequently washed with DMF (6 x 20 mL). After deprotection, Fmoc-Hyp-OH, HATU, and DIEA in DMF were added to the glycine loaded 2-chlorotrityl chloride resin. After 4h, the resin was washed with DMF (6 x 20 mL). The Fmoc group was removed with 20% piperidine in DMF (20 mL, 15 min, 2x), and the resin was washed with DMF (6 x 20 mL). After deprotection, Fmoc-P-OH, HATU, and DIEA in DMF were added to the resin. After 5h, the resin was collected and rinsed with DMF (1x 20 mL), CH_2Cl_2 (5x 20 mL). The resin was treated

with 80% CH₂Cl₂, 10% AcOH, and 10% TFE at r.t. for 3h. The mixture was filtered and the filtrate was concentrated in vacuo. AcOH was removed by azeotroping benzene (3 x 30 mL). The resulting foamy solid residue was purified by silica gel column chromatography (5% MeOH, 95% CH₂Cl₂) to yield the desired compound as a foamy white solid.

Synthesis of trimeric building blocks:

The synthesis of the tripeptide synthon FmocPOG-OH was carried out on 2-chlorotrityl chloride resin. To a solution of Fmoc-Gly-OH in dried CH₂Cl₂, 2-chlorotrityl chloride resin and dried DIEA were added under nitrogen. The mixture was stirred for 10 minutes, an additional 5 mL of DIEA was added. The reaction was allowed to stir for 2h and was quenched with HPLC grade methanol to cap any remaining reactive trityl groups. After 15 min, the reaction was washed with CH₂Cl₂ and DMF. The Fmoc-protecting group was cleanly removed with 20% piperidine in DMF, and the resin was subsequently washed with DMF (6 x 20 mL). After deprotection, **A** or **B**, HATU, and DIEA in DMF were added to the glycine loaded 2-chlorotrityl chloride resin. After 4h, the resin was washed with DMF (6 x 20 mL). The Fmoc group was removed with 20% piperidine in DMF (20 mL, 15 min, 2x), and the resin was washed with DMF (6 x 20 mL). After deprotection, Fmoc-P-OH, HATU, and DIEA in DMF were added to the resin. After 5h, the resin was collected and rinsed with DMF (1x 20 mL), CH₂Cl₂ (5x 20 mL). The resin was treated with 80% CH₂Cl₂, 10% AcOH, and 10% TFE at r.t. for 3h. The mixture was filtered and the filtrate was concentrated in vacuo. AcOH was removed by azeotroping benzene (3 x 30 mL). The resulting foamy solid residue was purified by silica gel column chromatography (5% MeOH, 95% CH₂Cl₂) to yield the desired compound as a foamy white solid.



Scheme 4.2 Synthesis of far-red excimer dye C

Compound (**31**)

4-(diethylamino)salicylaldehyde (0.9662 g, 5.0 mmol) was added to a round bottom flask and dissolved in 83 mL anhydrous THF. Sodium hydride (60% dispersion in oil, 0.200 g, 5.0 mmol) was added slowly to the solution at room temperature, and the solution was allowed to stir for 15 min. Methyl bromoacetate was added slowly to the reaction vessel, changing the color of the solution from pale yellow to purple, and the solution was heated to reflux for 1.5 h. After cooling to 0°C, the reaction was slowly quenched with water and extracted with ethyl acetate. The organic layer was dried over MgSO_4 , filtered, and concentrated *in vacuo*. The residue was purified by automated column chromatography on silica gel using a gradient of 5% to 30% ethyl acetate/hexanes over 60 min to give **31** as a colorless oil (1.0499 g, 55%). ^1H NMR (500 MHz, CDCl_3): δ = 10.21 (s, 1H), 7.73 (d, 1H, J = 8.9 Hz), 6.33 (dd, 1H, J = 8.8 Hz, 2.0 Hz), 5.91 (d, 1H, J = 2.3 Hz), 4.72 (s, 2H), 3.81 (s, 3H), 3.40 (q, 4H, J = 7.1 Hz), 1.20 (t, 6H, 7.1 Hz)

Compound (**32**)

Product **31** (0.500 g, 1.884 mmol) was added to a round bottom flask and dissolved in THF (4.7 mL). A solution of 1.2 M NaOH (4.7 mL, 5.65 mmol, 3.0 eq) was added to the flask and stirred

at room temperature for 1h. The contents of the reaction were acidified to pH 2 with 10% HCl and extracted with EtOAc. The organic layer was dried over MgSO₄, filtered, and concentrated *in vacuo*. The product was found to be a green solid (0.396 g, 84%), and used without further purification. ¹H NMR (500 MHz, CDCl₃): δ = 9.74 (s, 1H), 7.53 (d, 1H, J = 8.8 Hz), 7.23 (m, 1H), 7.15 (m, 1H), 6.41 (dd, 1H, J = 8.8 Hz, 2.2 Hz), 6.09 (s, 1H), 4.72 (s, 2H), 3.42 (q, 4H, J = 7.1 Hz), 1.22 (m, 6H)

Compound (**33**)

Compound **32** (0.3955 g, 1.576 mmol) was dissolved in MeOH along with 2-benzothiazoloacetonitrile (0.2746 g, 1.576 mmol, 1.0 eq). Piperidine (1.9 mL, 18.908 mmol, 12 eq) was slowly added, and the mixture was allowed to stir at r.t. for 5h. After reaction, the pH was brought to 4 with 10% HCl and extracted with ethyl acetate. Several extractions are required, as the product is not very soluble. Dried over MgSO₄, filtered, and concentrated *in vacuo*. The red residue, product **33**, was used in the next step without further purification.

Compound (**Dye C**)

Compound **33** (0.100 g, 0.245 mmol) was dissolved in DMF (2.45 mL). EDC (0.038 g, 0.245 mmol, 1.0 eq) was added to the solution, and N-hydroxysuccinimide was quickly added afterward. The reaction was allowed to stir at room temperature for 12h. The reaction mixture was quenched with water, and the solution was extracted with ethyl acetate. The organic layer was washed with brine, dried over MgSO₄, filtered, and concentrated *in vacuo*. The residue was purified by automated column chromatography using a gradient of 10% to 100% EtOAc/hexanes over 70 min to yield a red solid (0.0386 g, 31%). ¹H NMR (360 MHz, CDCl₃): δ = 8.59 (s, 1H), 8.46 (d, 1H, J = 9.1 Hz), 8.04 (d, 1H, J = 8.1 Hz), 7.85 (d, 1H, J = 7.5 Hz), 7.56 (s, 1H), 7.47 (m, 1H), 7.35 (m, 1H), 6.49 (dd, 1H, J = 9.1 Hz, 2.2 Hz), 6.05 (d, 1H, J = 2.1 Hz), 5.12 (s, 2H), 3.48 (q, 4H, J = 7.2 Hz), 2.89 (s, 4H), 1.25 (t, 6H, J = 7.1 Hz)

4.5.3 General Protocols

Synthesis of collagen model peptides on solid support¹:

A 4 mL peptide synthesis flask was loaded with 32 mg (0.020 mmol) of PAL PEG Rink amide resin. The resin was washed with CH₂Cl₂ (4 x 2 mL) and DMF (4 x 2 mL). Piperidine (20% in DMF, 2 mL) was added to the reaction flask and the resin was stirred for 10 minutes. The piperidine solution was drained, and the resin was washed with DMF, CH₂Cl₂, MeOH, CH₂Cl₂, DMF (4 x 2 mL each). Fmoc-protected tripeptide synthons (3 eq, 0.06 mmol) in DMF (0.67 mL) were added to the reaction flask with HATU (3 eq, 0.06 mmol) and DIEA (6 eq, 0.12 mmol), and the flask was agitated for 2h. The resin was washed with DMF 6x. A solution of 2% DBU and 1% HOBt in DMF (3 x 1 mL) was added to the reaction flask and agitated for 1m each. The resin was washed with DMF 6x. This procedure was repeated until all amino acids were coupled to resin. The resin was washed with DMF 6x, and the Fmoc-protecting group was removed with a solution of 2% DBU and 1% HOBt in DMF (3 x 1mL, 1m each). The resin was washed with DMF 6x. A solution of 10% acetic anhydride and 6% N-methyl morpholine in DMF was added to the resin and agitated for 40m. The solution was washed with DMF once, and washed with CH₂Cl₂ 5x. A 3.6 mL solution of 2.5% TIPS and 2.5% H₂O was added to the resin and allowed to react for 35 min. The solution was carefully drained into a centrifuge tube of 11 mL of cold ether, after which a precipitate was clearly seen and centrifuged. The supernatant was decanted and disposed, and the precipitate was dissolved in a solution of 3 ml 18 MΩ H₂O and 1 mL HPLC grade acetonitrile. This solution was purified by reverse HPLC on a C18 reverse phased column with a gradient of 10-20% of solvent A (H₂O/0.1% TFA) to solvent B (acetonitrile) over 90 min with a flow rate of 4 mL/min (λ₂₁₄ and λ₂₅₄ detection). All peptides were characterized by MALDI-TOF mass spectrometry.

Protocol A – Resin Preparation followed by Fmoc-deprotection

The peptides used in this paper are synthesized by manual SPPS method with Rink Amide AM Resin (0.62 mmol/g) on a 0.02 mmol scale. Thirty-two mg Rink Amide resins were carefully weighed out and transferred to a 5 mL solid phase synthesis vessel. The resin was then swelled in 4 mL of DMF for 30 min. The solvent was drained, and the resin was washed with 3 mL of DMF (1 x). Piperidine in DMF (20% v/v) (3 mL) was added to the resin, followed by stirring at ambient temperature for 30 minutes. The solution was drained, and the resin was washed with DMF (6x).

Protocol B – Trimer building block coupling followed by Fmoc-deprotection

Fmoc-Xaa-Yaa-Gly-OH or Fmoc-Gly-Xaa-Yaa-OH (3 equiv) and HBTU (3 equiv) were dissolved in DMF (0.67 mL). DIEA (9 equiv) was subsequently added to the mixture, and the entire solution was transferred to the reaction vessel containing the resin. The mixture was stirred for 100 min, drained, and washed with DMF (6 mL, 6 x). One mL of Piperidine in DMF (v/v 20%) was added to the resin and followed by stirring at ambient temperature for 30 minutes. The solution was drained, and the resin was thoroughly washed with DMF (6x).

Protocol C– Acylation followed by Fmoc-deprotection

A solution of DIEA (0.11 mL, 30 equiv) and Ac₂O (0.06 mL, 30 equiv) in CH₂Cl₂ (3.4 mL) were added to the amino functionalized resin. This mixture was stirred for 1 h at room temperature. The solution was drained and thoroughly washed with CH₂Cl₂ (6 mL, 5 x).

Protocol D– Cleavage off the resin and collection of the crude product

The resin was suspended for 30 min in a 4 mL mixture of TFA/H₂O/TIPS (95:2.5:2.5) at room temperature. The filtrate was collected and dropwise added to cold Et₂O (~11 mL). The sample was cooled to 4 °C for approximately 1 h, during which a white solid precipitated. The resulted sample was centrifuged and the supernatant was decanted. The white solid was dissolved in 18 MΩ water and frozen to -80 °C before HPLC purification.

Protocol E– HPLC purification

MeCN (B) and water containing 1% TFA (A) were used as eluents. The flow rate used for semi-preparative HPLC was 4 mL/min and 1 mL/min for analytical HPLC. The crude sample was heated to 65 °C for 15 min before injecting to prevent preemptive triple helix formation.

Conjugation of chromophores to collagen:

A solution containing the NHS-ester of the desired chromophore (6 eq) in DMF is added to 5 mg of collagen along with DIEA (6 eq). The reaction is stirred at room temperature for 12h and monitored by MALDI-TOF mass spectrometry. The solution is purified by reverse HPLC on a C18 reverse phased column with a gradient of 1-30% solvent A (H₂O/0.1% TFA) to solvent B (acetonitrile) over 90 min with a flow rate of 4 mL/min (λ_{214} and λ_{254} detection) for hydrophilic dyes, and 30%-70% solvent A (H₂O/0.1% TFA) to solvent B (acetonitrile) over 90 min with a flow rate of 4 mL/min (λ_{214} and λ_{254} detection) for hydrophobic dyes. All peptides were characterized by MALDI-TOF mass spectrometry.

4.5.4 Peptide solution preparation

Peptides after HPLC purification were dried under vacuum. The dried samples were dissolved in PBS buffer (0.20 g KCl, 0.20 g KH₂PO₄, 8.0 g NaCl, 2.16 g Na₂HPO₄·7H₂O in 1.0 L H₂O) and the concentration of the stock solution was measured by a UV-Vis measurement applying $\epsilon = 6.0 \times 10^4 \text{ M}^{-1} \text{ cm}^{-1}$ as the extinction coefficient as previously reported.³ Solutions of peptides used in this study were then made into a 0.20 mM solution by diluting with the same buffer accordingly. Samples were incubated at 4 °C for at least 24 h before CD experiments.

4.5.5 CD Wavelength scan

Samples of 0.20 mM concentration in PBS buffer were used. CD spectra were recorded at a step of 1.0 nm from 260 nm to 190 nm at 10 °C with a 1.0 s equilibration time.

4.5.6 CD Thermal denaturation experiment

A sample of 0.20 mM concentration in PBS buffer was used. The wavelength that gave the highest absorption, 224 nm, was used as the wavelength monitored as a function of time in the thermal denaturation experiment. Averaging time was set to be 15 s with an equilibration time period of 2 min and the ellipticity of every 1 °C was recorded. The collected data from the experiments were fitted into a two-state model according to Engel et al.² to obtain the melting temperature (temperature at which 50% of the triple helix unfolds). The software Graphpad Prism 6 was used to develop the fit by the same procedure described by Erdmann & Wennemers.³

- (1) Lee, S.; Lee, J.; Chmielewski, J. *Angew. Chem. Int. Ed.* **2008**, 47(44), 8429-8432
- (2) Engel, J.; Chen, H. T.; Prockop, D. J.; Klump, H. *Biopolymers* **1977**, 16, 601.
- (3) Erdmann, R. S.; Wennemers, H. *Angew. Chem., Int. Ed.* **2011**, 50, 6835

4.5.7 Peptide Characterization, CD Spectra, and Fluorescence Spectra

CMP 1 Ac-(Pro-Hyp-Gly)₄-(Pro-A-Gly)-(Pro-Hyp-Gly)₄-NH₂

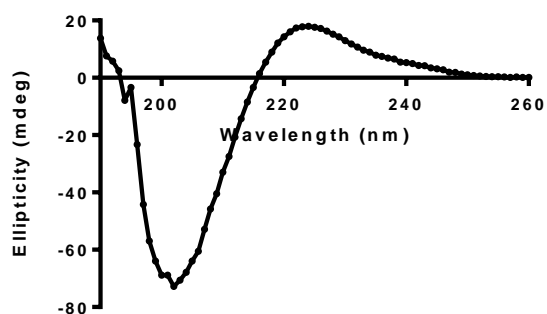


Figure 4.11 CD Spectra of CMP 1

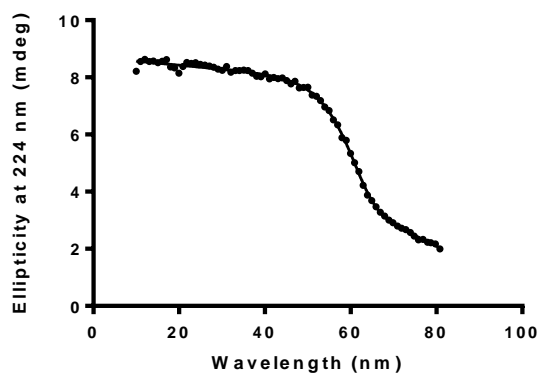


Figure 4.12 CD Thermal of CMP 1

MALDI MS: calculated [M+Na]⁺ 2529.18, found 2529.87

CMP 2 Ac-(Pro-Hyp-Gly)₄-(Pro-A(**py**)-Gly)-(Pro-Hyp-Gly)₄-NH₂

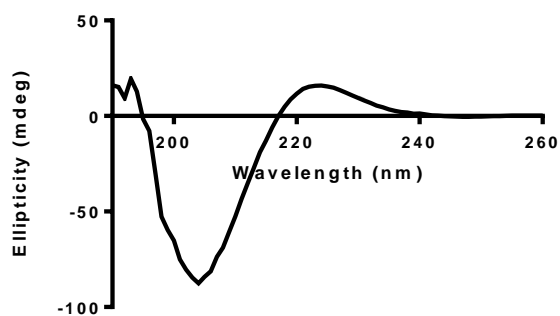


Figure 4.13 CD Spectra of CMP 2

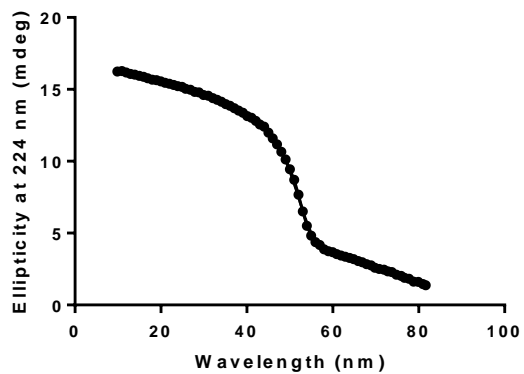


Figure 4.14 CD Thermal of CMP 2

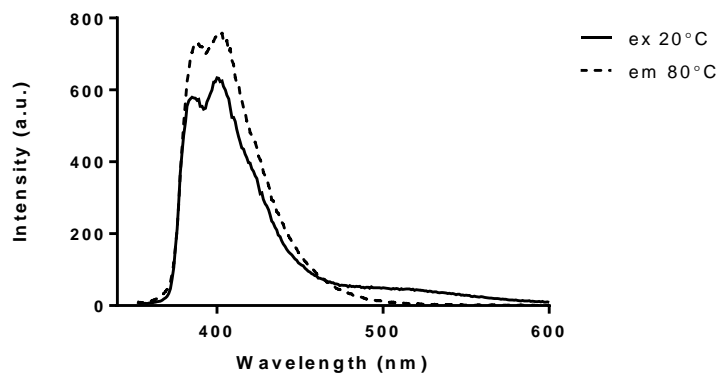


Figure 4.15 Emission spectra of CMP 2 ($\lambda_{\text{ex}} = 342 \text{ nm}$)

MALDI MS: calculated $[\text{M}+\text{Na}]^+$ 2756.23, found 2756.58

CMP 3 Ac-(Pro-Hyp-Gly)₄-(Pro-**B**-Gly)-(Pro-Hyp-Gly)₄-NH₂

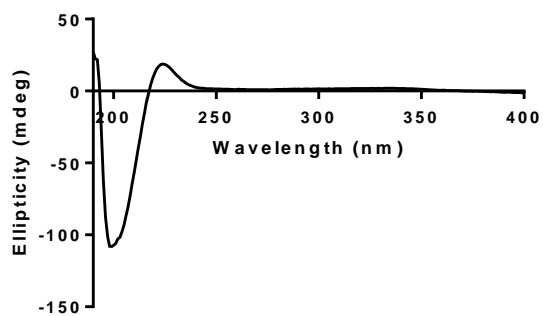


Figure 4.16 CD Spectra of CMP 3

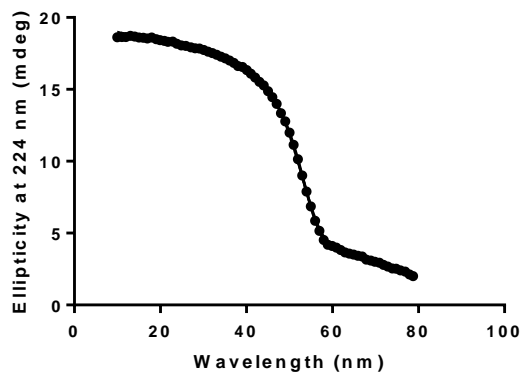


Figure 4.17 CD Thermal of CMP 3

MALDI MS: calculated $[M+Na]^+$ 2543.19, found 2542.86

CMP 4 Ac-(Pro-Hyp-Gly)₄-(Pro-**B(py)**-Gly)-(Pro-Hyp-Gly)₄-NH₂

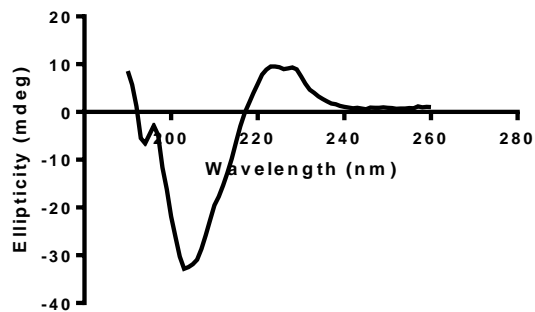


Figure 4.18 CD Spectrum of CMP 4

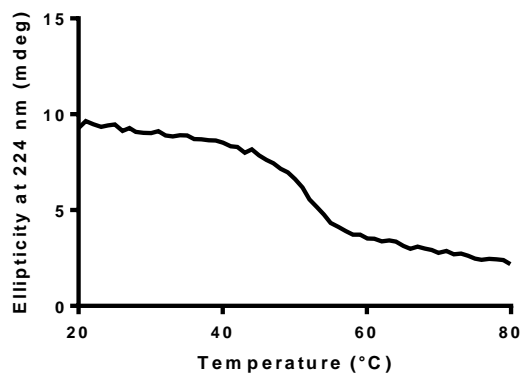


Figure 4.19 CD Thermal of CMP 4

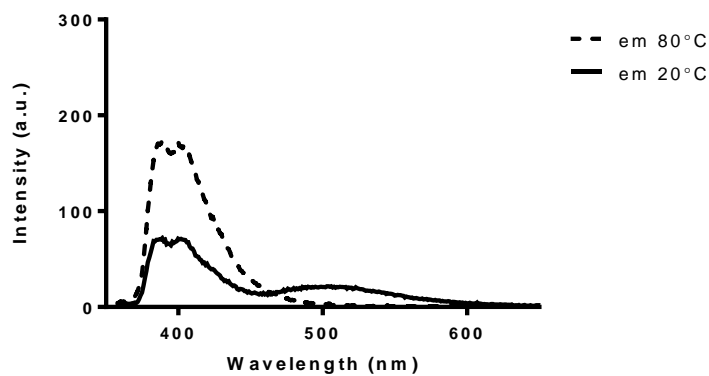


Figure 4.20 Emission Spectra of CMP 4 ($\lambda_{\text{ex}} = 342 \text{ nm}$)

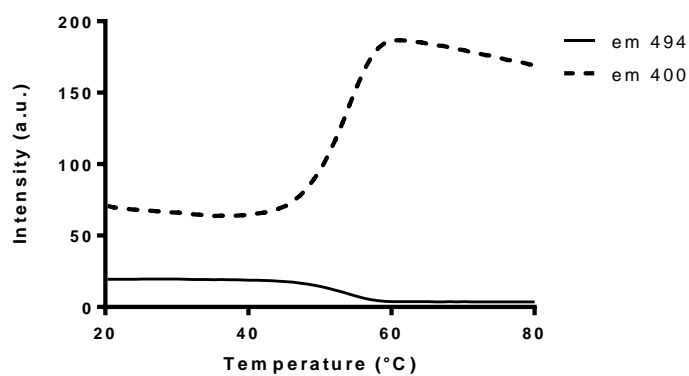


Figure 4.21 Fluorescence thermal of CMP 4 ($\lambda_{\text{ex}} = 342 \text{ nm}$)
MALDI MS: calculated $[\text{M}+\text{Na}]^+$ 2771.25, found 2771.89

CMP 5 Ac-(Pro-Hyp-Gly)₄-(Pro-A-Gly)₂-(Pro-Hyp-Gly)₃-NH₂

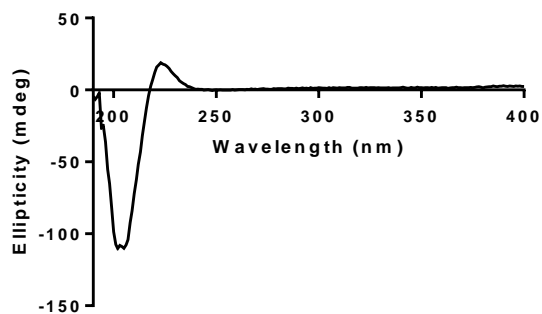


Figure 4.22 CD Spectra of CMP 5

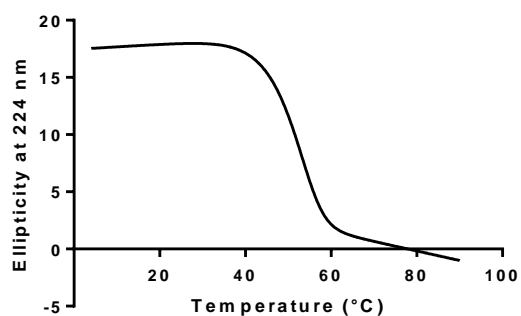


Figure 4.23 CD Thermal of CMP 5

MALDI MS: calculated $[M+Na]^+$ 2572.22, found 2571.17

CMP 6 Ac-(Pro-Hyp-Gly)₄-(Pro-A(py)-Gly)₂-(Pro-Hyp-Gly)₃-NH₂

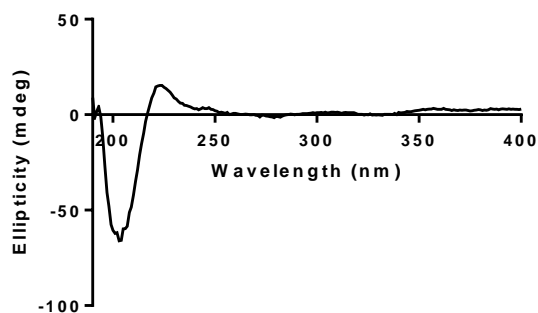


Figure 4.24 CD Spectra of CMP 6

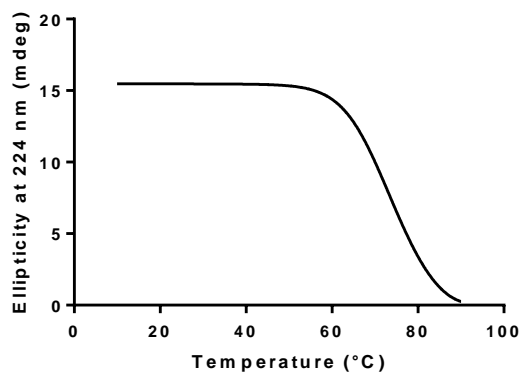


Figure 4.25 CD Thermal of CMP 6

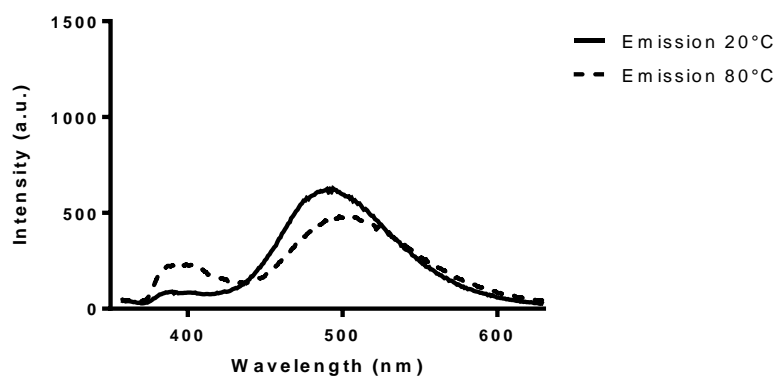


Figure 4.26 Emission Spectra for CMP 6 (ex = 342 nm)

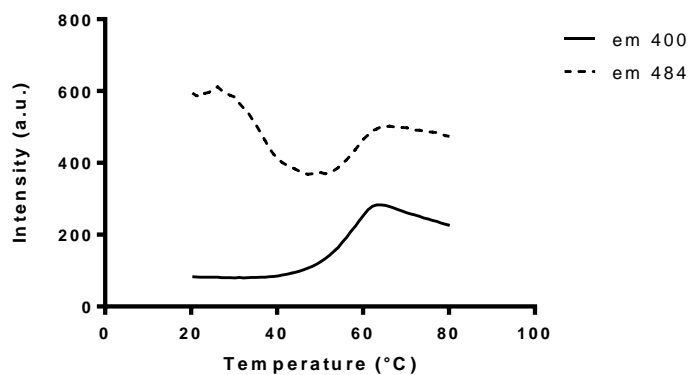


Figure 4.27 Fluorescence thermal of CMP 6

MALDI MS: calculated $[M+Na]^+$ 3028.33, found 3025.82

CMP 7 Ac-(Pro-Hyp-Gly)₄-(Pro-**B**-Gly)₂-(Pro-Hyp-Gly)₃-NH₂

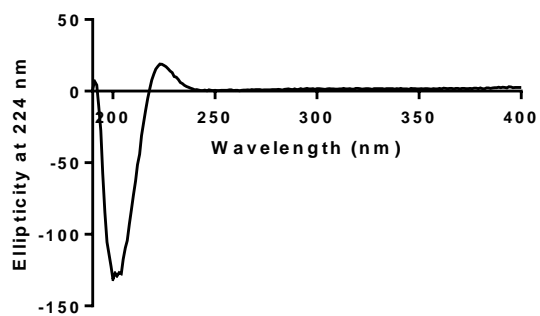


Figure 4.28 CD Spectra of CMP 7

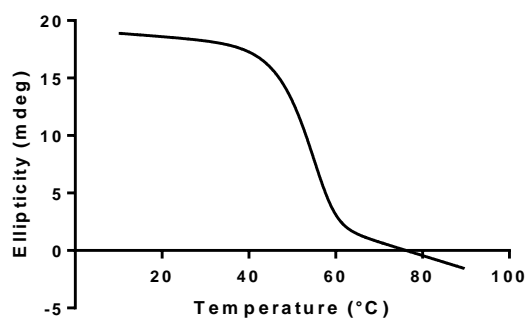


Figure 4.29 CD Thermal of CMP 7

MALDI MS: calculated $[M+Na]^+$ 2600.25, found 2600.03

CMP 8 Ac-(Pro-Hyp-Gly)₄-(Pro-**B(py)**-Gly)₂-(Pro-Hyp-Gly)₃-NH₂

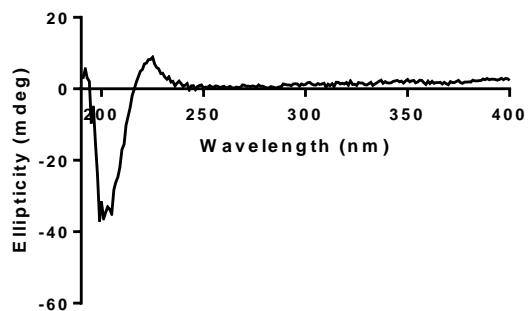


Figure 4.30 CD Spectra of CMP 8

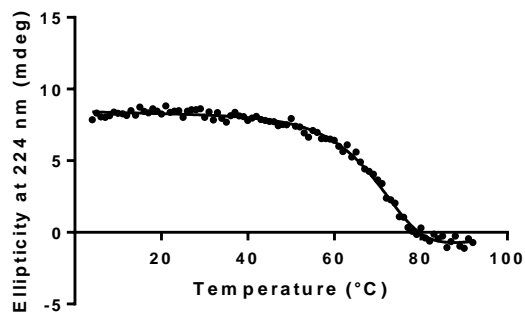


Figure 4.31 CD Thermal of CMP 8

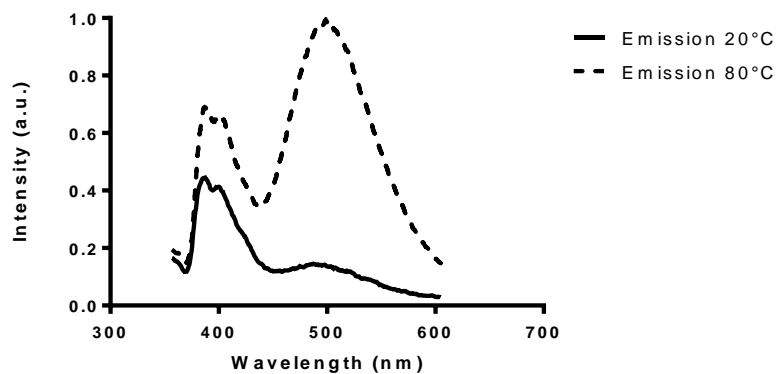


Figure 4.32 Emission Spectra of CMP 8

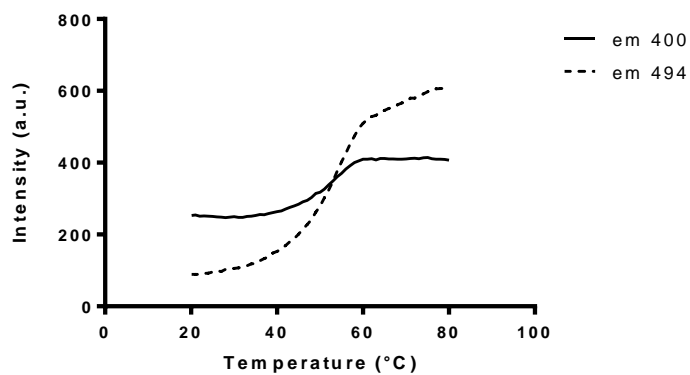


Figure 4.33 Fluorescence thermal of CMP 8

MALDI MS: calculated $[M+Na]^+$ 3056.37, found 3055.96

CMP **9** Ac-(Pro-Hyp-Gly)₃-(Pro-**A**-Gly)₃-(Pro-Hyp-Gly)₃-NH₂

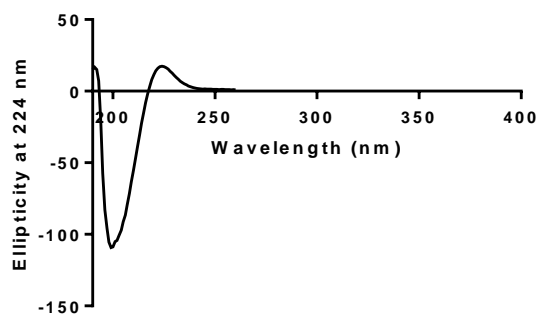


Figure 4.34 CD Spectra of CMP 9

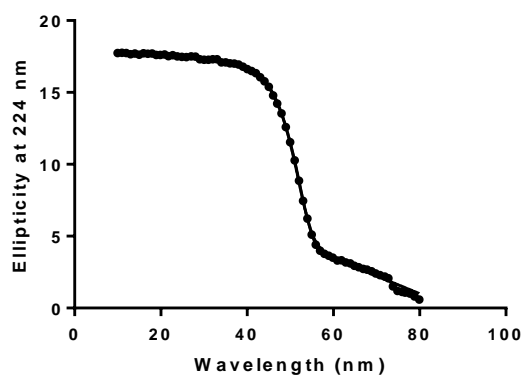


Figure 4.35 CD thermal of CMP 9

MALDI MS: calculated [M+Na]⁺ 2615.26, found 2615.03

CMP **10** Ac-(Pro-Hyp-Gly)₃-(Pro-**A(py)**-Gly)₃-(Pro-Hyp-Gly)₃-NH₂

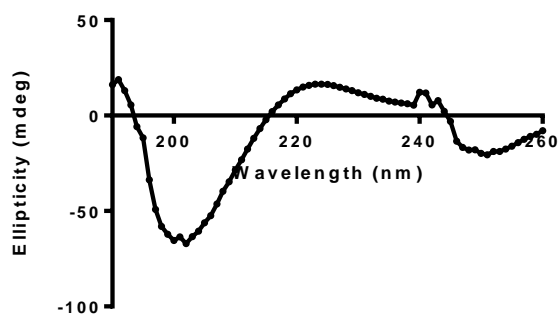


Figure 4.36 CD Spectra of CMP 10

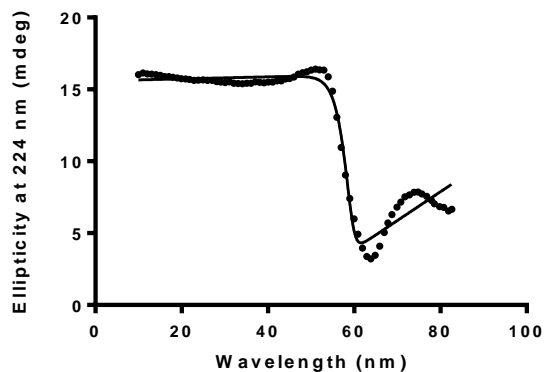


Figure 4.37 CD Thermal of CMP 10

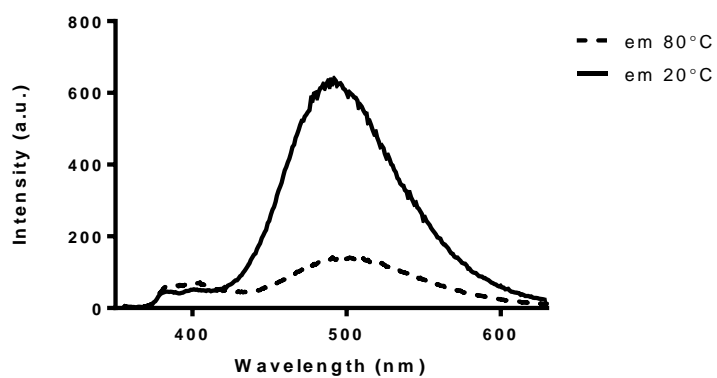


Figure 4.38 Emission spectra of CMP 10

MALDI MS: calculated $[M+Na]^+$ 3299.43, found 3298.37

CMP 11 Ac-(Pro-Hyp-Gly)₃-(Pro-**B**-Gly)₃-(Pro-Hyp-Gly)₃-NH₂

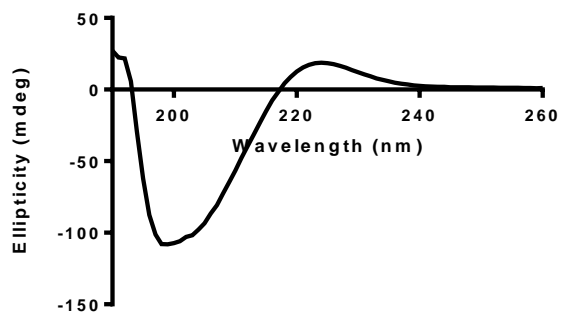


Figure 4.39 CD Spectra of CMP 11

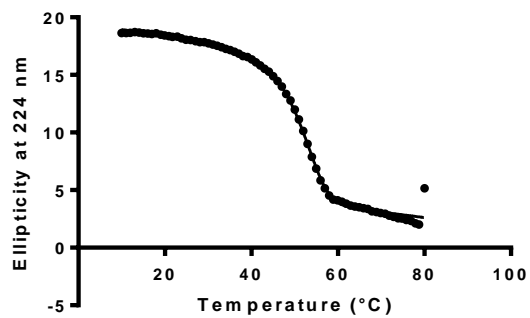


Figure 4.40 CD Thermal of CMP 11

MALDI MS: calculated $[M+Na]^+$ 2657.31, found 2656.69

CMP 12 Ac-(Pro-Hyp-Gly)₃-(Pro-**B(py)**-Gly)₃-(Pro-Hyp-Gly)₃-NH₂

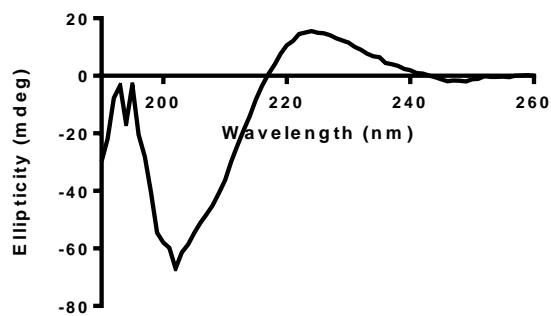


Figure 4.41 CD Spectra of CMP 12

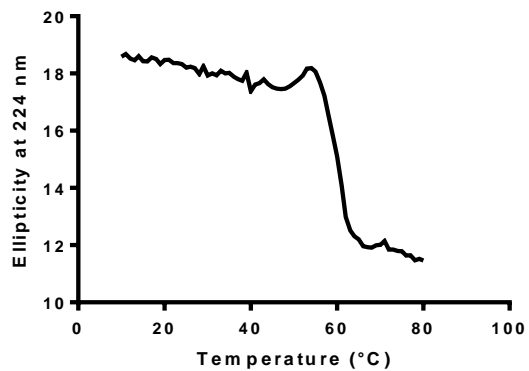


Figure 4.42 CD Thermal of CMP 12

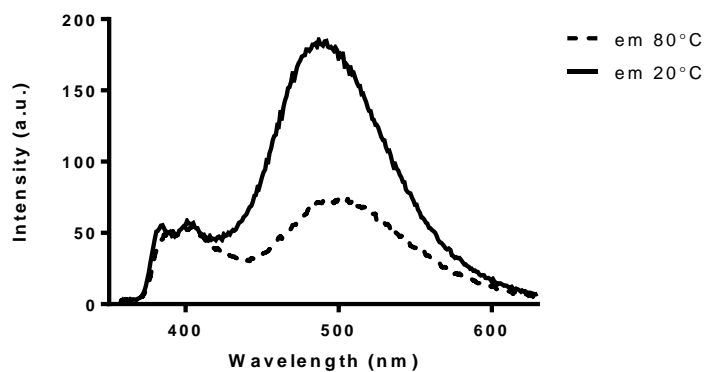


Figure 4.43 Emission spectra of CMP 12

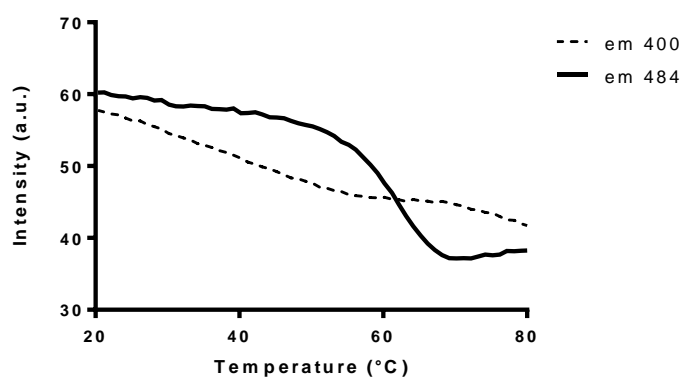


Figure 4.44 Fluorescence thermal of CMP 12

MALDI MS: calculated $[M+Na]^+$ 3341.48, found 3340.52

CMP 13 Ac-(Pro-Hyp-Gly)₂-(Pro-**B(py)**-Gly)-(Pro-Hyp-Gly)-(Pro-**B(py)**-Gly)-(Pro-Hyp-Gly)-
(Pro-**B(py)**-Gly)-(Pro-Hyp-Gly)₂-NH₂

MALDI MS: calculated $[M+Na]^+$ 3341.48, found 3341.13

CMP 14 Ac-(Pro-Hyp-Gly)₃-(Pro-**B(py)**-Gly)-(Pro-Hyp-Gly)-(Pro-**B(py)**-Gly)-(Pro-Hyp-Gly)₃-
NH₂

MALDI MS: calculated $[M+Na]^+$ 3056.37, found 3056.50

CMP **15** Ac-(Pro-Hyp-Gly)₇-(Pro-A-Gly)₂-NH₂

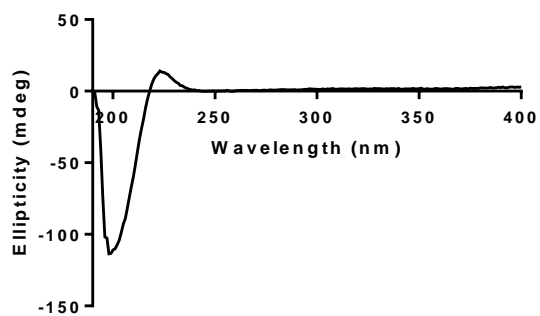


Figure 4.45 CD Spectra of CMP 15

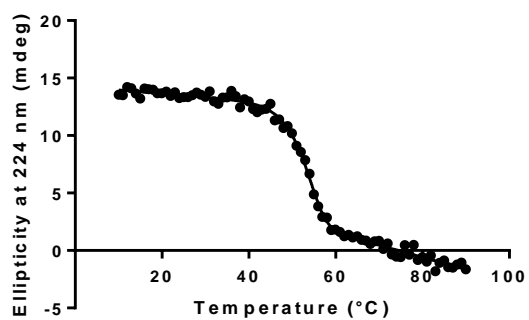


Figure 4.46 CD Thermal of CMP 15

MALDI MS: calculated [M+Na]⁺ 2572.22, found 2571.48

CMP **16** Ac-(Pro-Hyp-Gly)₇-(Pro-Apy-Gly)₂-NH₂

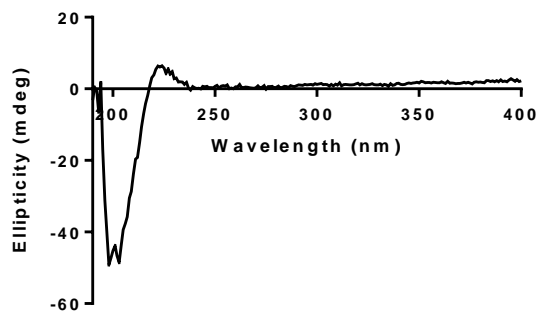


Figure 4.47 CD Spectra of CMP 16

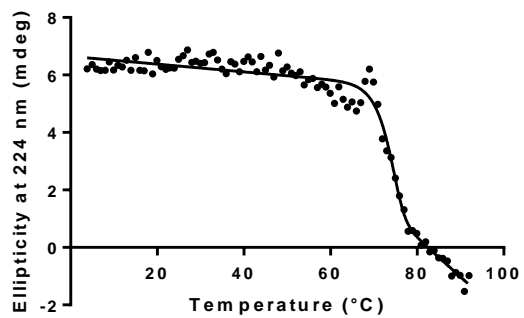


Figure 4.48 CD Thermal of CMP 16

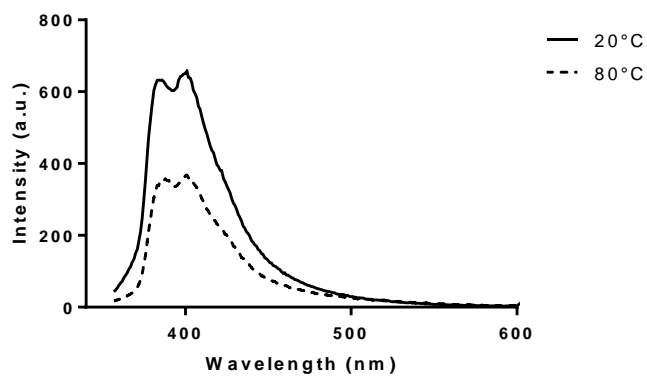


Figure 4.49 Emission Spectra of CMP 16

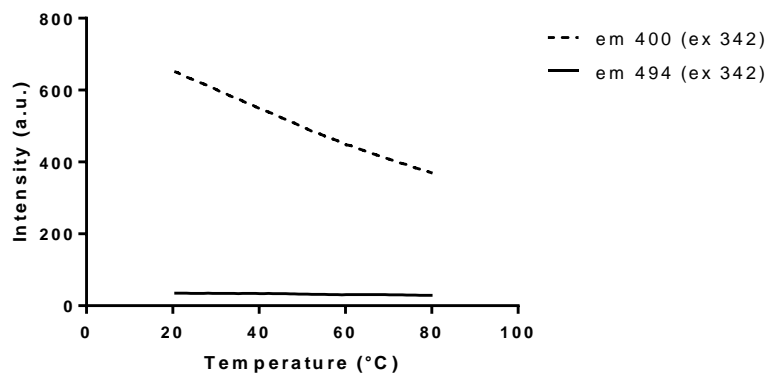


Figure 4.50 Fluorescence thermal of CMP 16

MALDI MS: calculated $[M+Na]^+$ 3028.33, found 3028.75

CMP 17 Ac-(Pro-Hyp-Gly)₇-(Pro-**B**-Gly)₂-NH₂

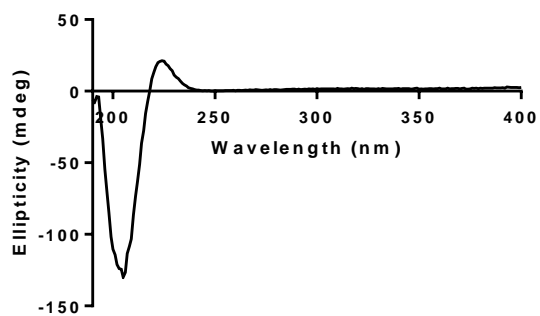


Figure 4.51 CD Spectra of CMP 17

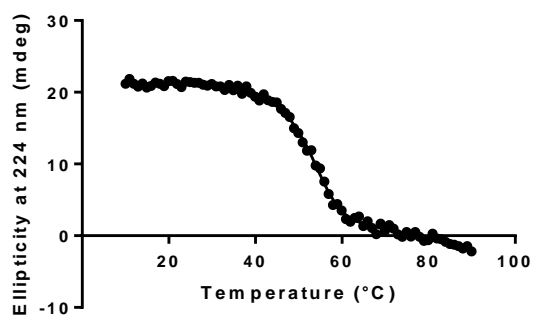


Figure 4.52 CD Thermal of CMP 17

MALDI MS: calculated $[M+Na]^+$ 2600.25, found 2598.61

CMP 18 Ac-(Pro-Hyp-Gly)₇-(Pro-**Bpy**-Gly)₂-NH₂

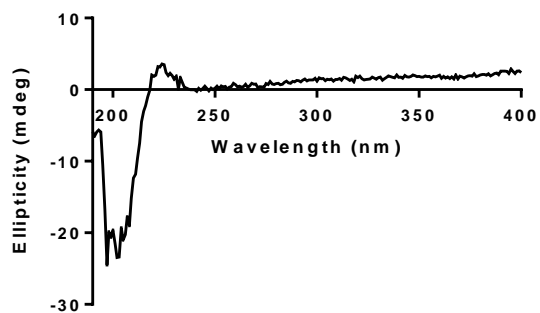


Figure 4.53 CD Spectra of CMP 18

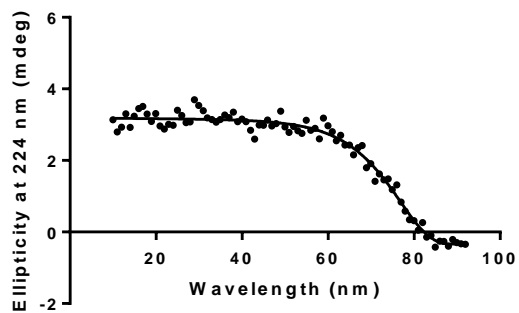


Figure 4.54 CD Thermal of CMP 18

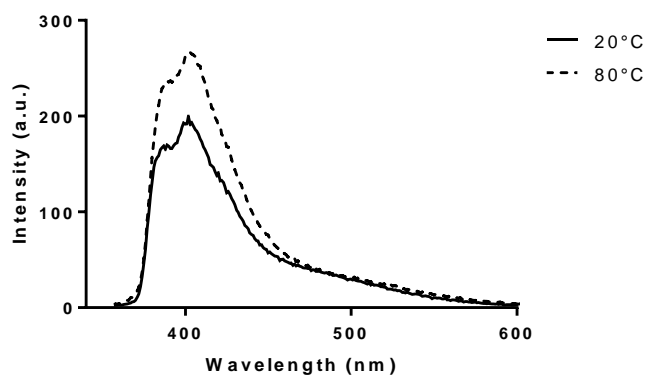


Figure 4.55 Emission Spectra of CMP 18

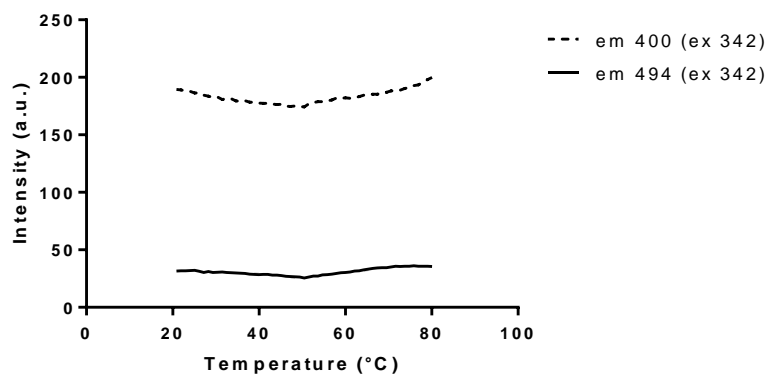


Figure 4.56 Fluorescence thermal of CMP 18

MALDI MS: calculated $[M+Na]^+$ 3056.37, found 3057.19

CMP **19** Ac-(Pro-A-Gly)₂-(Pro-Hyp-Gly)₇-NH₂

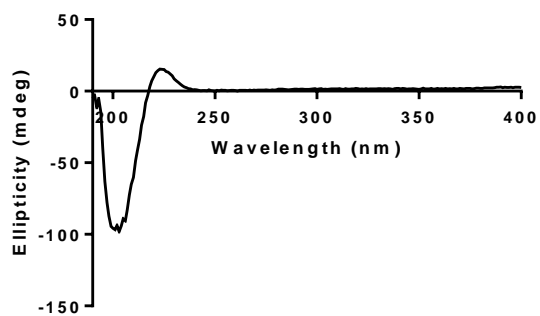


Figure 4.57 CD Spectra of CMP 19

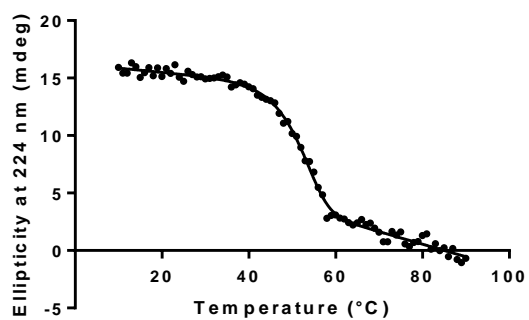


Figure 4.58 CD Thermal of CMP 19

MALDI MS: calculated [M+Na]⁺ 2572.22, found 2571.75

CMP **20** Ac-(Pro-Apy-Gly)₂-(Pro-Hyp-Gly)₇-NH₂

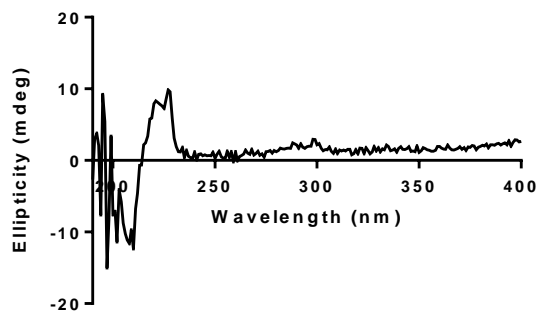


Figure 4.59 CD Spectra of CMP 20

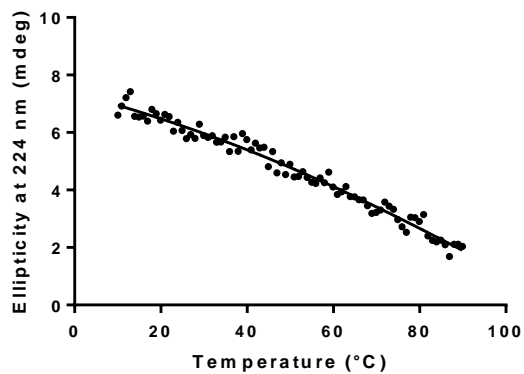


Figure 4.60 CD Thermal of CMP 20

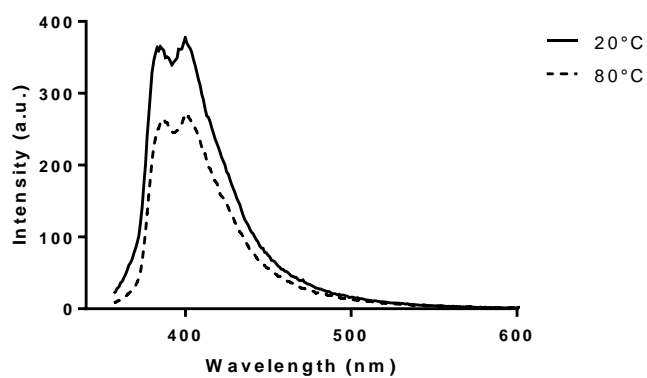


Figure 4.61 Emission spectra of CMP 20

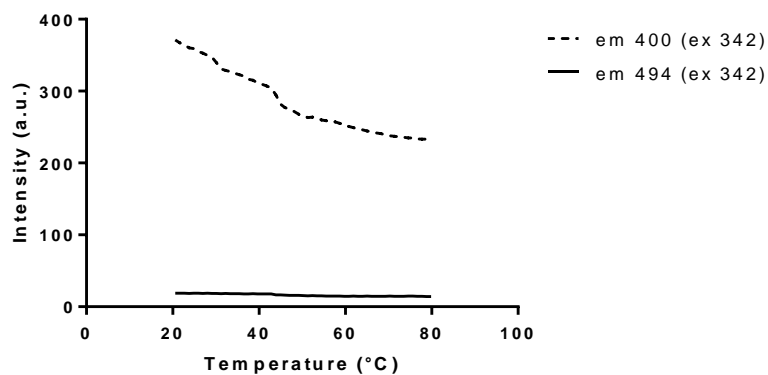


Figure 4.62 Fluorescence thermal of CMP 20

MALDI MS: calculated $[M+Na]^+$ 3028.33, found 3028.38

CMP 21 Ac-(Pro-**B**-Gly)₂-(Pro-Hyp-Gly)₇-NH₂

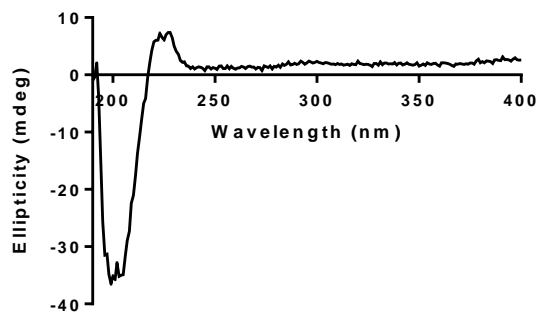


Figure 4.63 CD Spectra of CMP 21

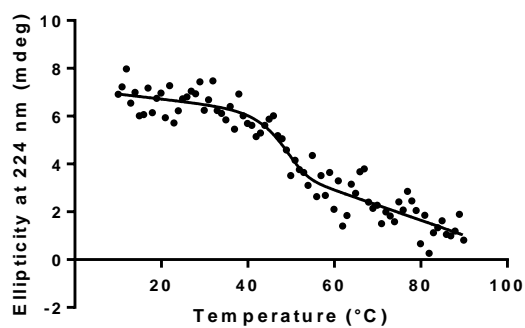


Figure 4.64 CD Thermal of CMP 21

MALDI MS: calculated [M+Na]⁺ 2572.22, found 2571.39

CMP 22 Ac-(Pro-**Bpy**-Gly)₂-(Pro-Hyp-Gly)₇-NH₂

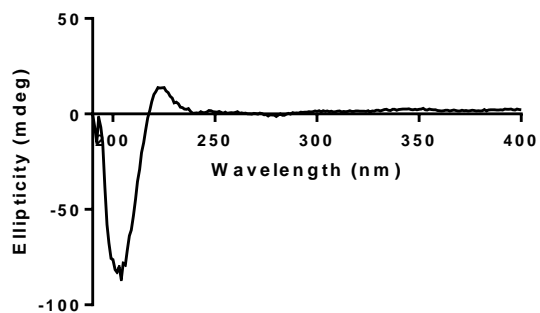


Figure 4.65 CD Spectra of CMP 22

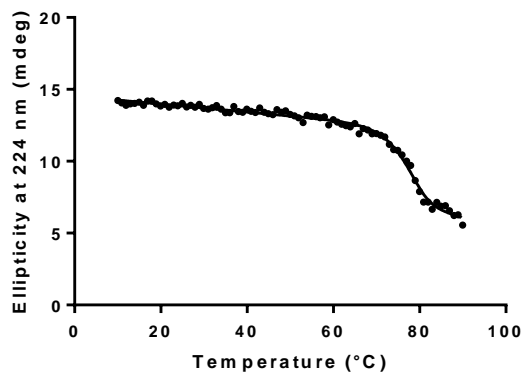


Figure 4.66 CD Thermal of CMP 22

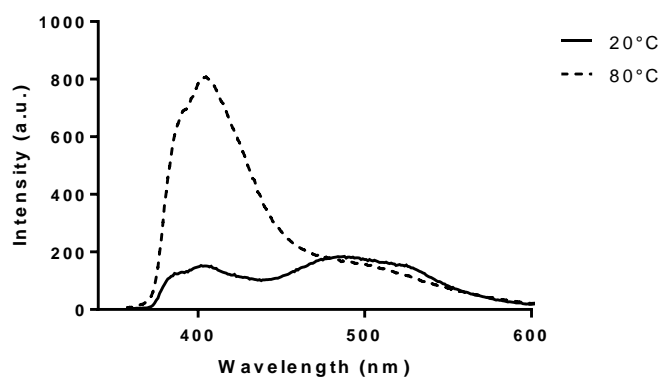


Figure 4.67 Emission spectra of CMP 22

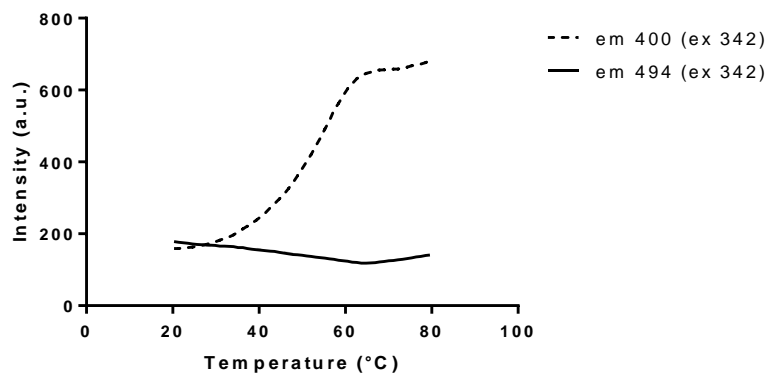


Figure 4.68 Fluorescence thermal of CMP 22

MALDI MS: calculated $[M+Na]^+$ 3028.33, found 3028.19

CMP **23** Ac-(Pro-Hyp-Gly)₂-(Pro-**A**-Gly)₃-(Pro-Hyp-Gly)₂-NH₂

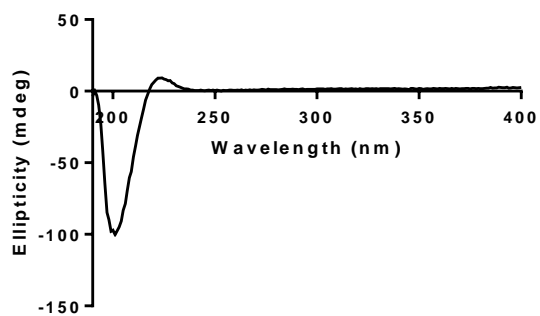


Figure 4.69 CD Spectra of CMP 23

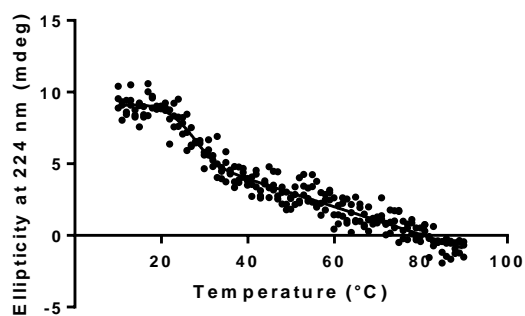


Figure 4.70 CD Thermal of CMP 23

MALDI MS: calculated $[M+Na]^+$ 2081.02, found 2080.80

CMP **24** Ac-(Pro-Hyp-Gly)₂-(Pro-**Apy**-Gly)₃-(Pro-Hyp-Gly)₂-NH₂

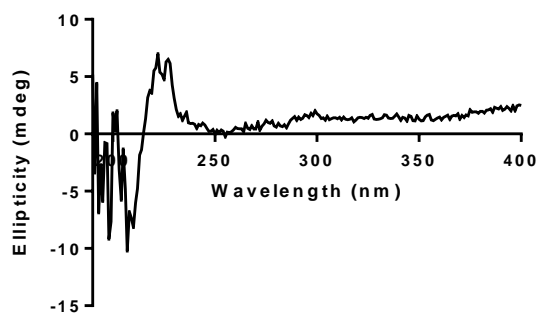


Figure 4.71 CD Spectra of CMP 24

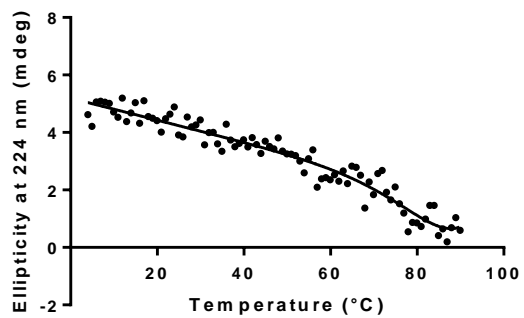


Figure 4.72 CD Thermal of CMP 24

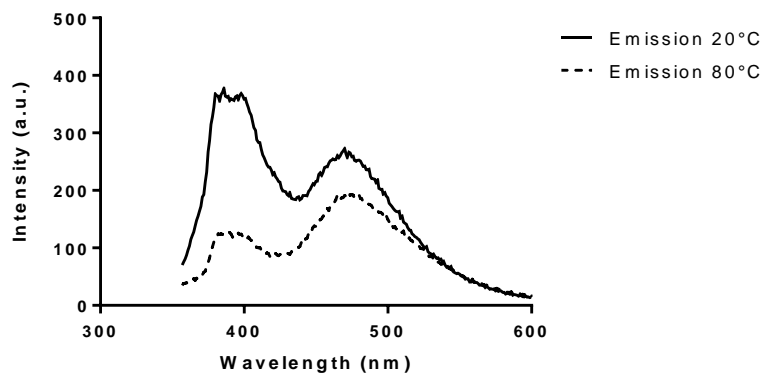


Figure 4.73 Emission spectra of CMP 24

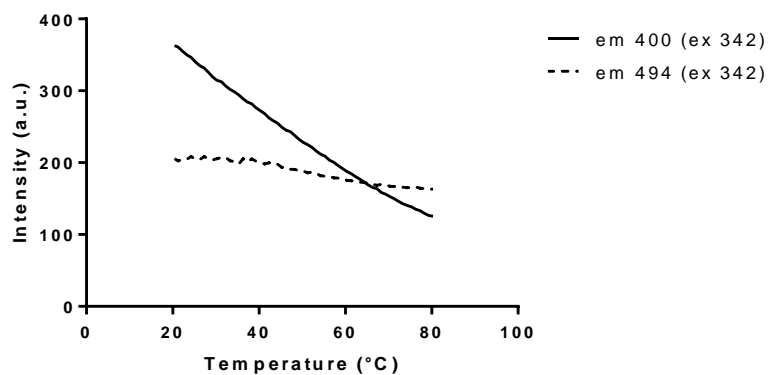


Figure 4.74 Fluorescence thermal of CMP 24

MALDI MS: calculated $[M+Na]^+$ 2765.19, found 2765.11

CMP **25** Ac-(Pro-Hyp-Gly)₂-(Pro-**B**-Gly)₃-(Pro-Hyp-Gly)₂-NH₂

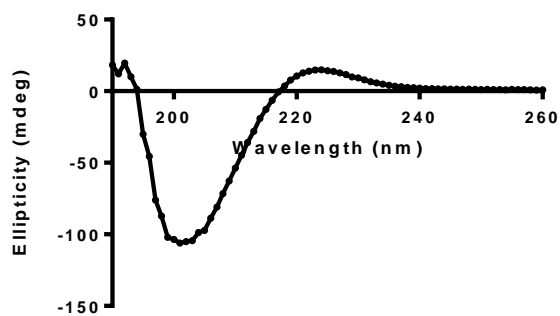


Figure 4.75 CD Spectra of CMP 25

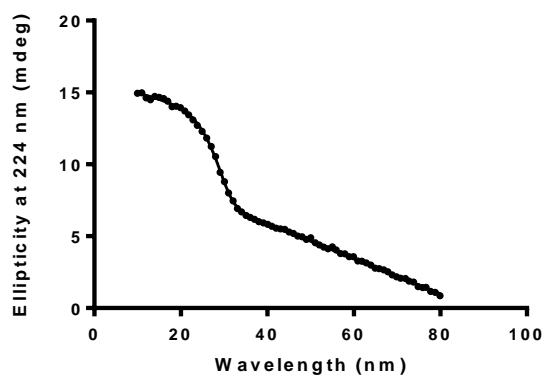


Figure 4.76 CD Thermal of CMP 25

MALDI MS: calculated [M+Na]⁺ 2123.06, found 2123.02

CMP **26** Ac-(Pro-Hyp-Gly)₂-(Pro-**Bpy**-Gly)₃-(Pro-Hyp-Gly)₂-NH₂

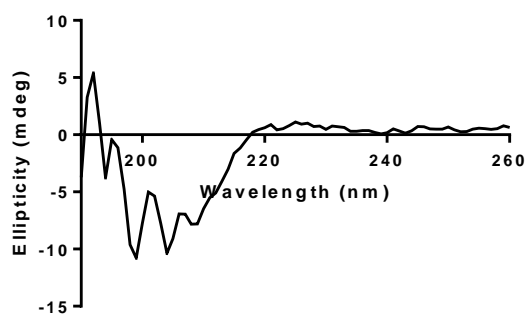


Figure 4.77 CD Spectra of CMP 26

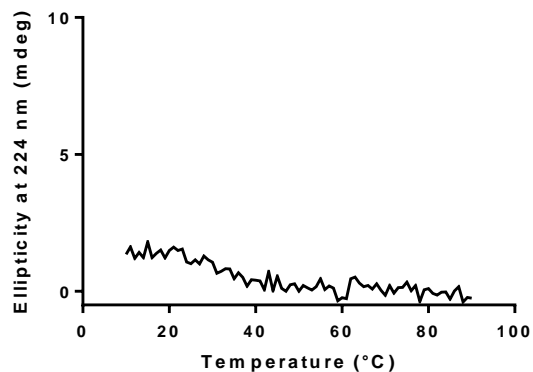


Figure 4.78 CD Thermal of CMP 26

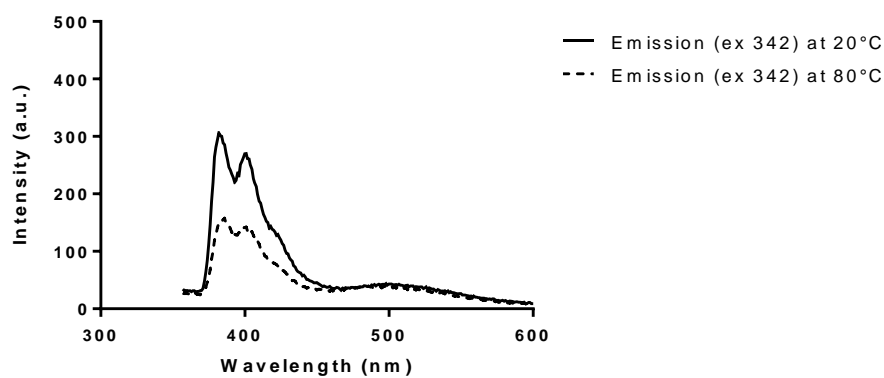


Figure 4.79 Emission spectra of CMP 26

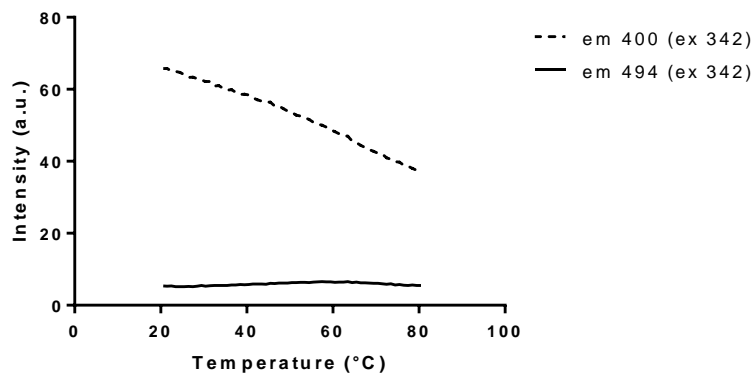


Figure 4.80 Fluorescence thermal of CMP 26

MALDI MS: calculated $[M+Na]^+$ 2807.24, found 2807.36

CMP 27 Ac-(Pro-Hyp-Gly)₂-(Pro-A-Gly)₅-(Pro-Hyp-Gly)₂-NH₂

MALDI MS: calculated $[M+Na]^+$ 2701.35, found 2700.58

CMP **28** Ac-(Pro-Hyp-Gly)₂-(Pro-**Apy**-Gly)₅-(Pro-Hyp-Gly)₂-NH₂

MALDI MS: calculated [M+Na]⁺ 3841.63, found 3840.98

CMP **29** Ac-(Pro-Hyp-Gly)₄-(Pro-**B(CB)**-Gly)-(Pro-Hyp-Gly)₄-NH₂

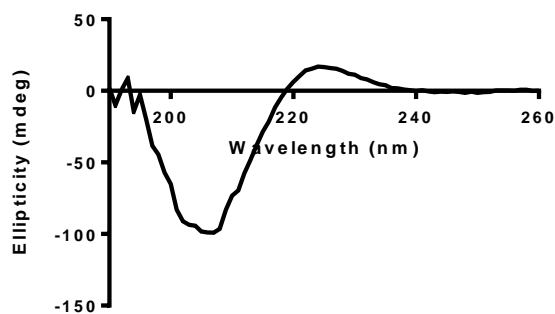


Figure 4.81 CD Spectra of CMP 29

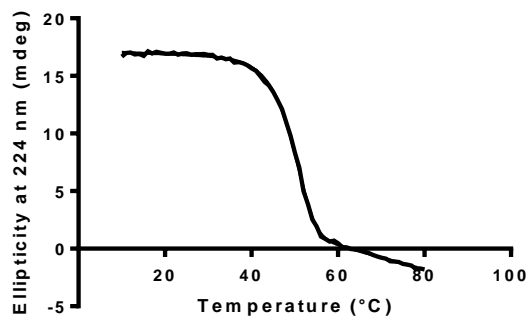


Figure 4.82 CD Thermal of CMP 29

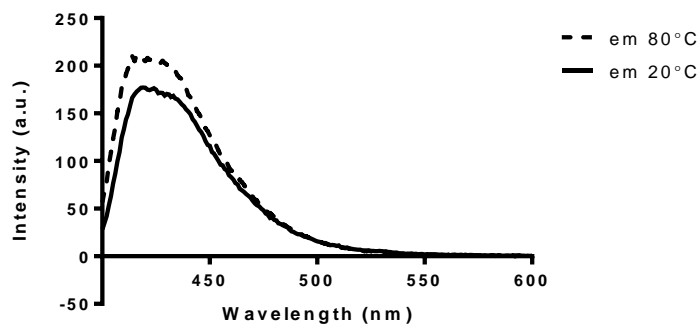


Figure 4.83 Emission spectra of CMP 29

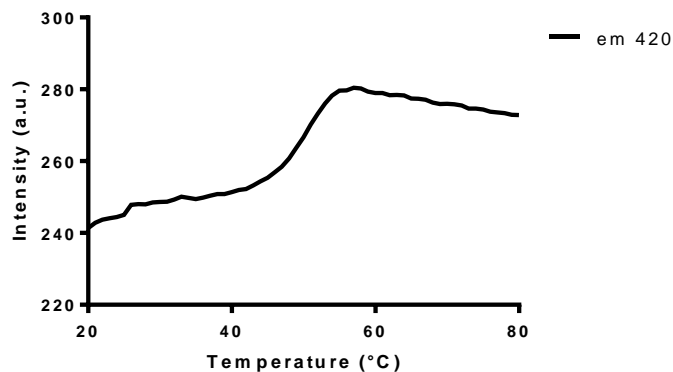


Figure 4.84 Fluorescence thermal of CMP 29

MALDI MS: calculated $[M+2Na]^+$ 3107.08, found 3107.76

CMP 30 Ac-(Pro-Hyp-Gly)₄-(Pro-**B(dyeC)**-Gly)-(Pro-Hyp-Gly)₄-NH₂

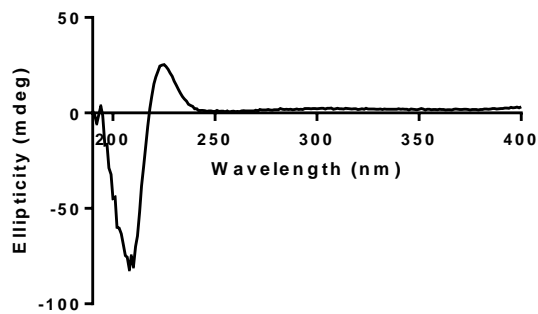


Figure 4.85 CD Spectra of CMP 30

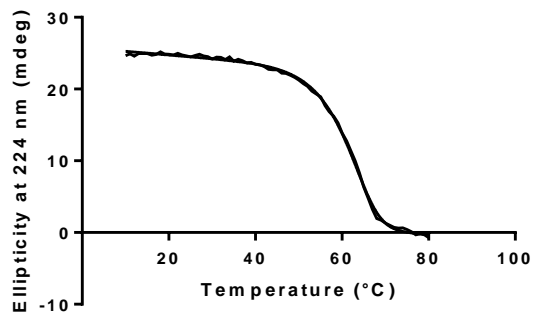


Figure 4.86 CD thermal of CMP 30

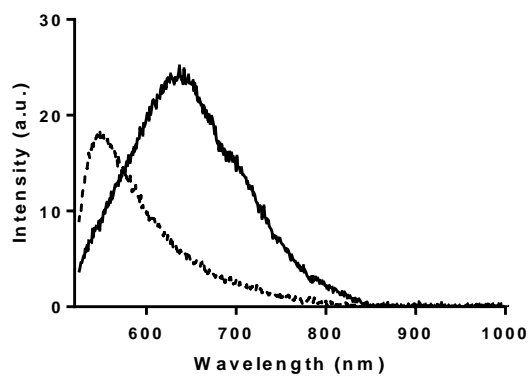


Figure 4.87 Emission spectra of CMP 30

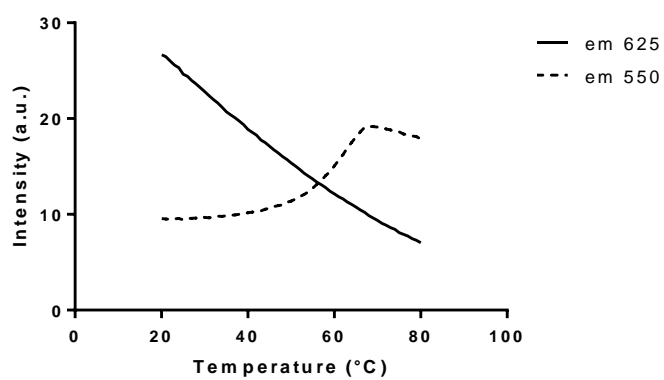
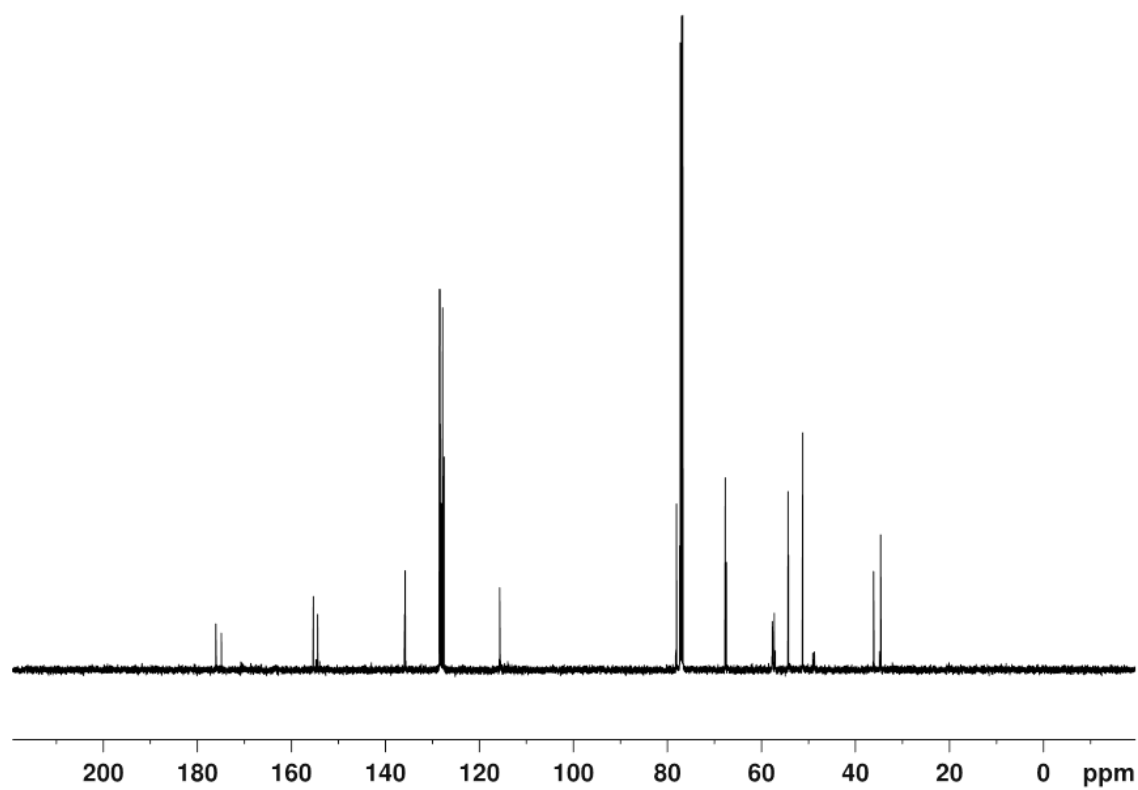
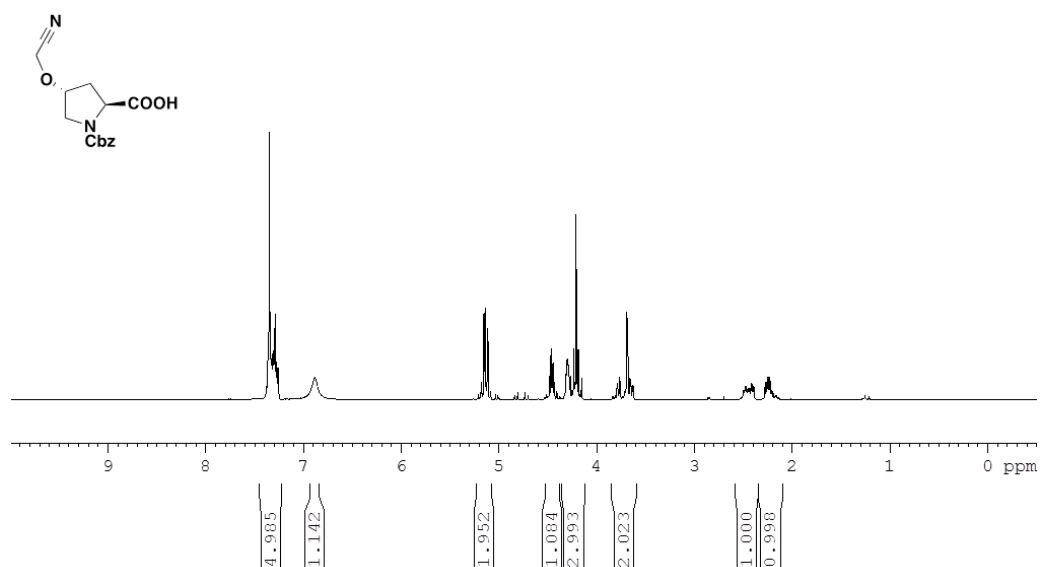
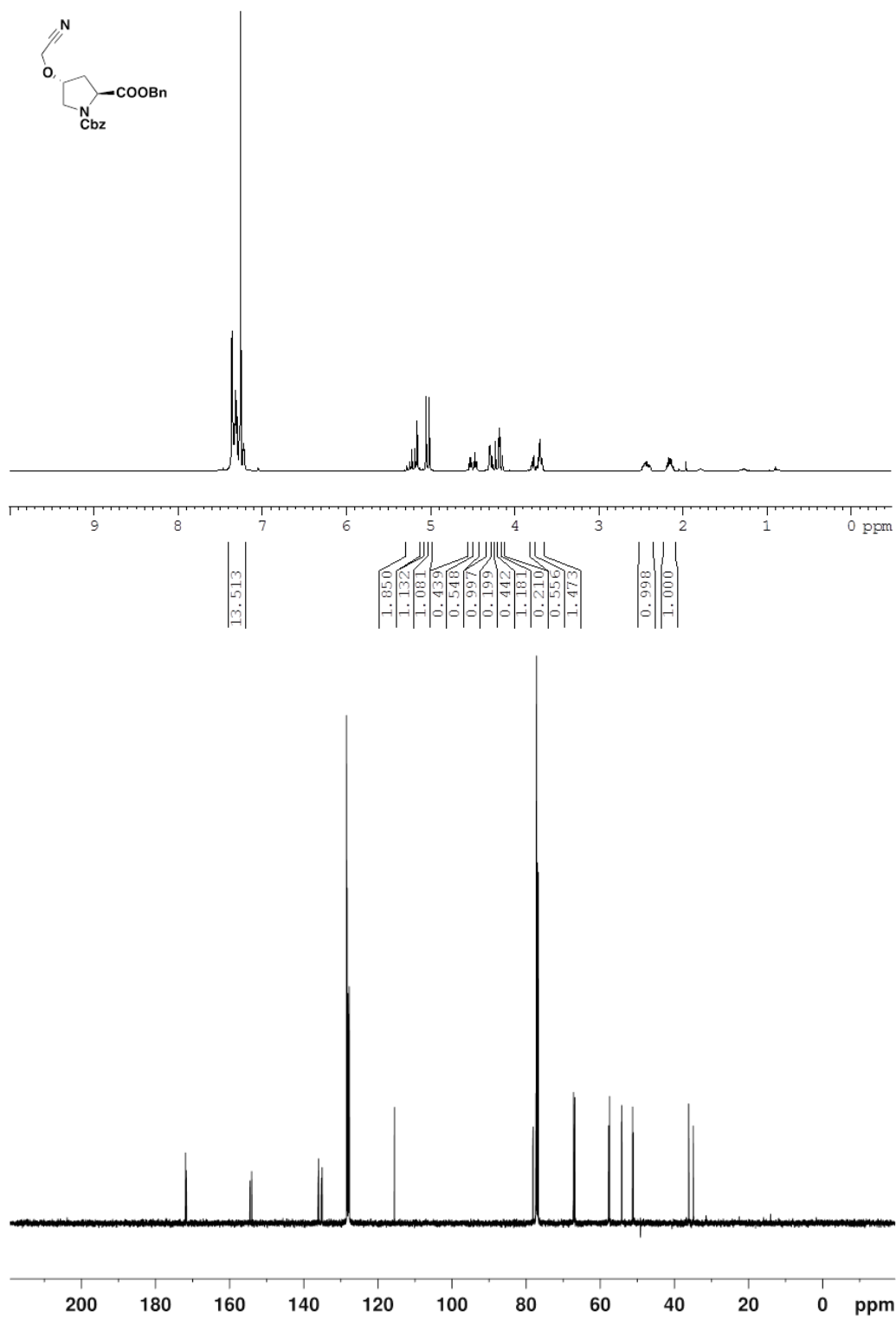
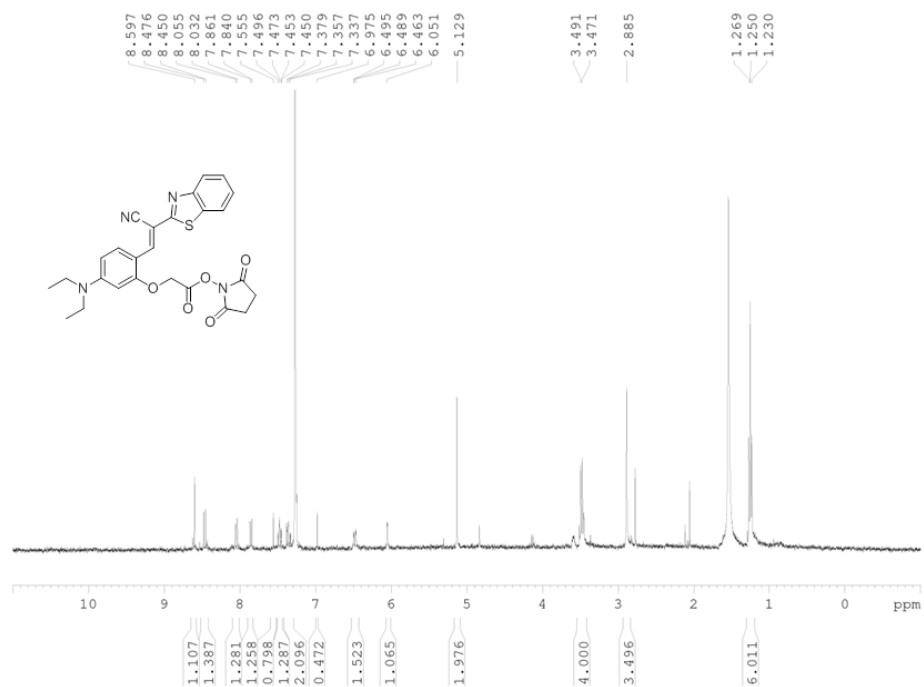
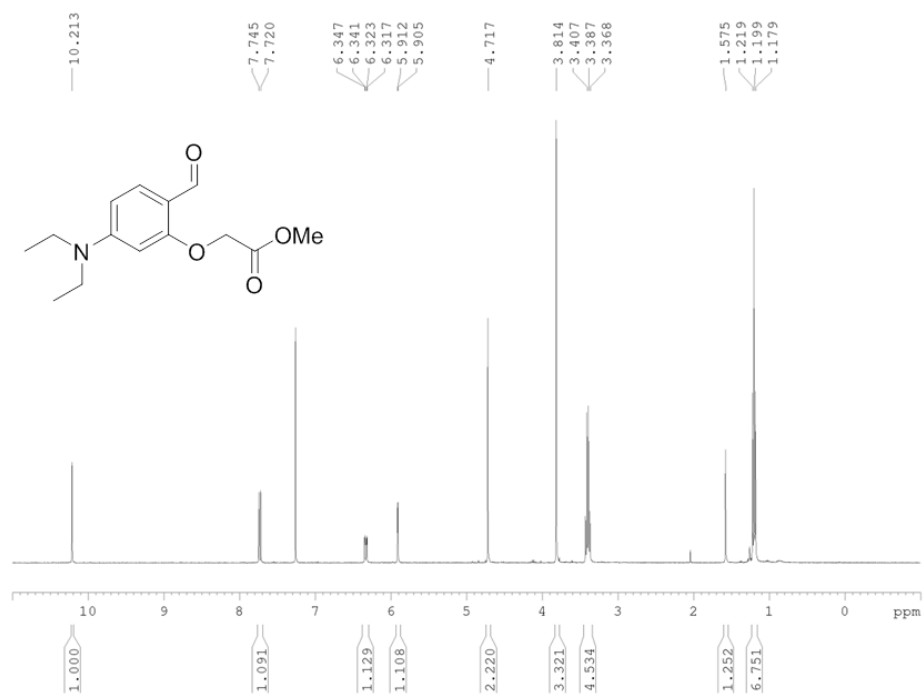


Figure 4.88 Fluorescence thermal of CMP 30

MALDI MS: calculated $[M+Na]^+$ 2932.31, found 2932.93

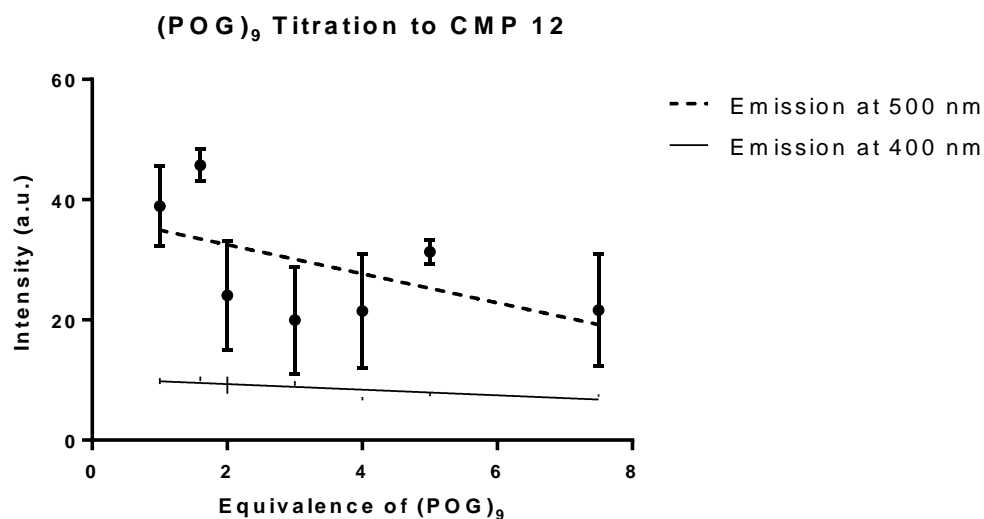
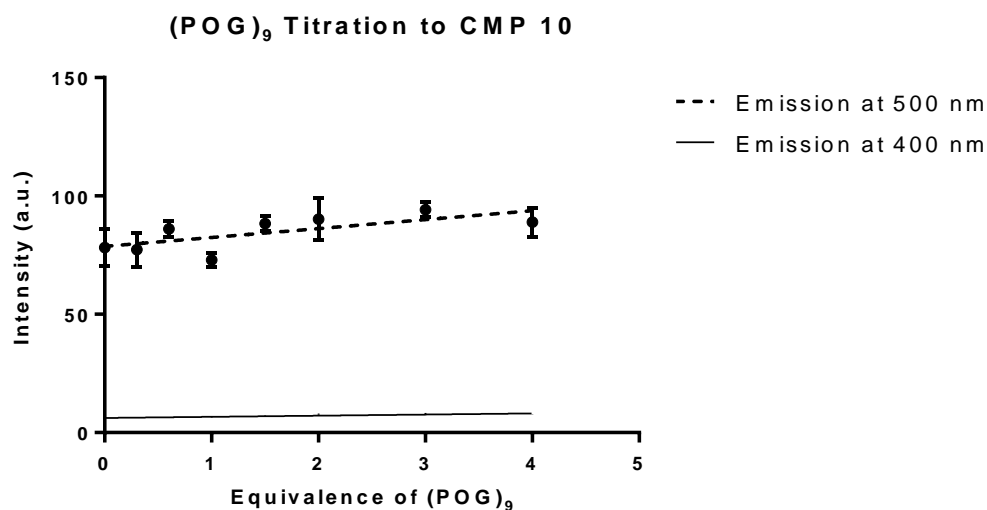






4.5.8 Titration Data

The titrations were performed by incubating CMPs with varying concentrations of (POG)₉. CMPs were heated in a heat block to 80°C and allowed to incubate at 0°C for 12h before fluorescence measurements. The final concentration of pyrene substituted CMPs were kept at 0.2 mM, and fluorescence reading were performed at a concentration of 1 uM for the pyrene substituted CMP.



CHAPTER 5: INVESTIGATION OF DELTA-AZAPROLINE INCORPORATION INTO COLLAGEN

5.1 Introduction

The use of unnatural amino acids for the stabilization of collagen has been of high interest to researchers over the last 30 years.¹⁻⁴ Several insights into the various factors which affect the structure and stability of the collagen triple helix have been discovered through the incorporation of mutant amino acids.^{2,5} Elegant work by Raines and coworkers found the substitution of fluoroproline for hydroxyproline in the Yaa position of collagen led to hyper-stabilization of the collagen triple helix, overturning the previous theory that an external hydrogen bonding matrix contributed to the stability incurred by hydroxyproline incorporation.² Future work with the incorporation of 4*S*- and 4*R*- methyl proline added insight to the role of preorganization on the assembly of collagen. Wennemers and coworkers built upon the current theory to create a pH sensitive collagen assembly through the incorporation of her amino proline derivatives.^{6,7} Further insight by Engelman and coworkers theorized that a weak stabilizing interaction occurred between the C α -H of the amino acid residues participate in weak hydrogen bonding interactions with adjacent carbonyls.⁸ This interaction was confirmed by later work from our lab through the replacement of the glycine residue with aza-glycine.⁹ Earlier work in our lab also showed the non-perturbing nature of incorporating the amino acid alpha-azaproline into the Xaa position of collagen, showing that incorporation of a stereodynamic amino acid was tolerated within the collagen structure.

The incorporation of aza-peptides into the collagen structure has also shown the capability of enhancing collagen stability through the addition of additional hydrogen bonds.^{9,10} As such, an investigation of other aza-peptides with the potential to stabilize the collagen triple helix was undertaken. Analysis of the crystal structure of collagen led us to believe that incorporation of a δ -azaproline residue, when inserted in the Xaa position of collagen, had the potential to participate in a hydrogen bond with carbonyl groups on adjacent strands.

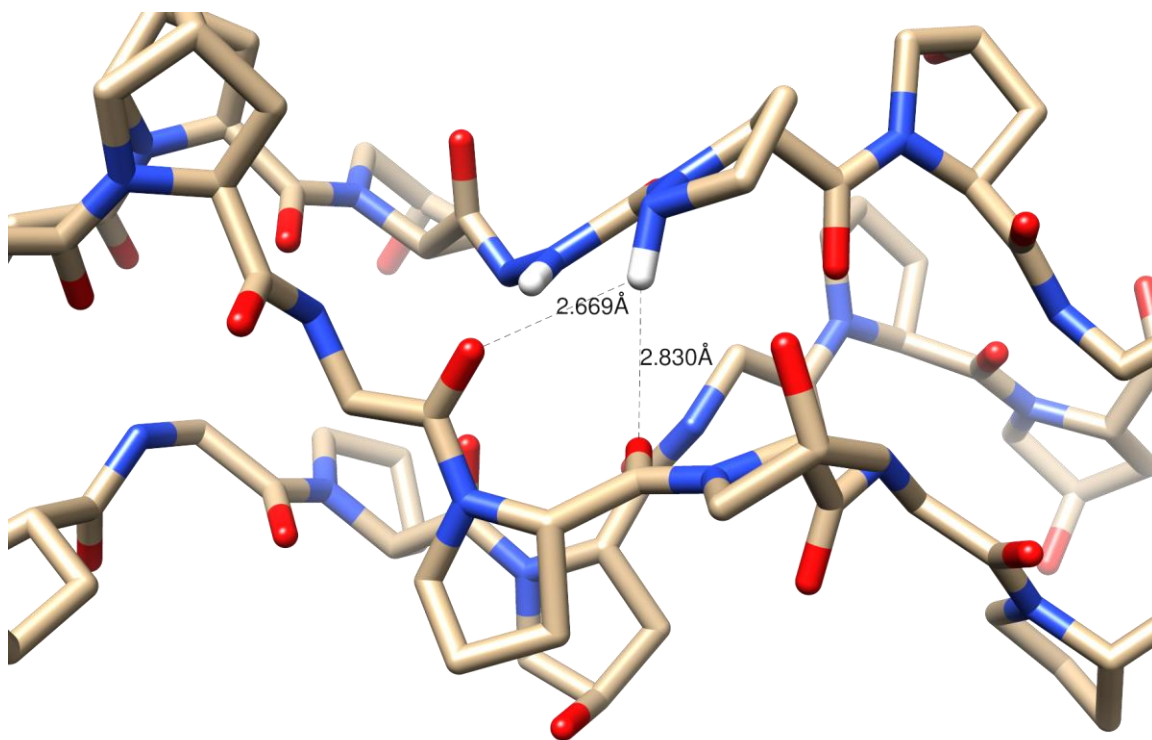
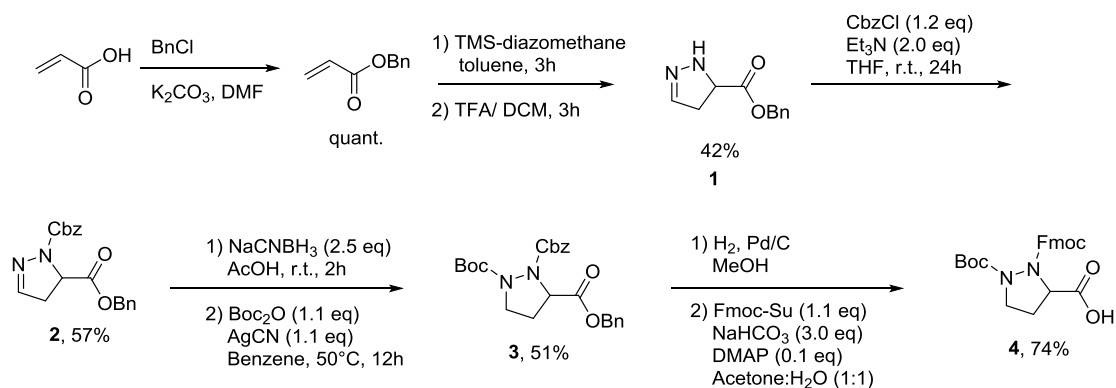


Figure 5.1 Proposed hydrogen bonding interaction from the incorporation of a delta-azaproline

5.2 Results and Discussion

The synthesis of the δ -azaproline residue was carried out in a racemic fashion beginning with cycloaddition of benzyl acrylate and TMS-diazomethane (**Error! Reference source not found.**). Deprotection of the trimethyl silyl group results in an isomerization to compound **1**, and the free amine is subsequently protected by a carboxybenzyl (Cbz) group resulting in compound **2**. Compound **2** can be reduced to the secondary amine using a mixture of sodium cyanoborohydride and acetic acid, and Boc protection of this amine can be carried out in the presence of silver cyanide and Boc anhydride. The silver cyanide is necessary to disrupt the internal hydrogen bond between the δ -N-H and the carbonyl of the Cbz group by forming a favorable complex with the carbonyl; this leaves the amine free to react with the Boc anhydride.¹¹ The finished product **4** is obtained by cleaving the benzyl protected acid and Cbz protected amine simultaneously through a



Scheme 5.1 Proposed synthesis of δ -azaproline

reduction with H_2 and Pd/C. The free amine is then selectively Fmoc protected in the presence of Fmoc-succinimide and DMAP, giving compound **4** in 50% yield. By coupling

4 to hydroxyproline using solid phase synthesis, the two diastereomers **Z1** and **Z2** can be separated and incorporated into separate collagen model peptides.

The CD spectrum of CMP **A1** and CMP **A2** showed a corresponding maximum at 224 nm and a minimum at 200 nm, initially suggesting both could undergo formation of a triple helix.

However, subjecting both peptides to a thermal denaturation showed CMP **A1** had a linear transition, whereas CMP **A2** displayed a cooperative unfolding. This data together implies that CMP **A2** contains the

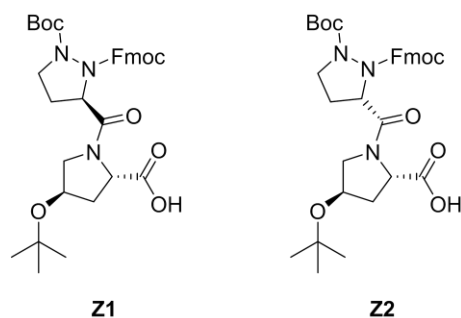


Figure 5.2 Final products for δ -azaproline incorporation

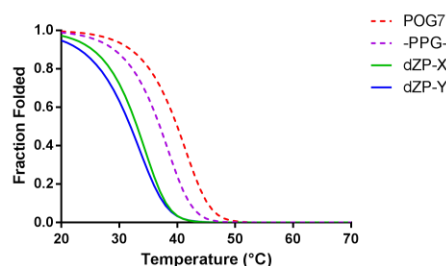


Figure 5.3 Fraction folded thermal denaturation plot

Table 5.1 Thermal denaturation temperatures for select CMPs

Entry	Ac-(POG) ₃ XYG(POG) ₃ -NH ₂	T_m (°C)
C1	-Pro-Hyp-	40.0
C2	-Pro-Pro-	37.0
A2	-dZP-Hyp-	34.5
A3	-Pro-dZP	31.9

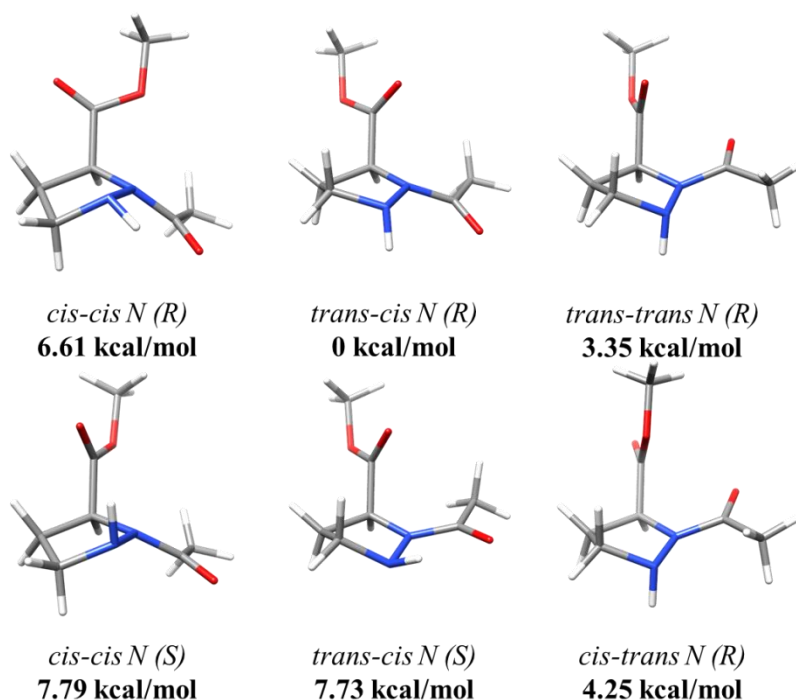


Figure 5.4 Summary of computational analysis of cis-trans conformations of δ -azaproline

diastereomer which is configurationally similar to L-proline.³ The thermal transition displayed by CMP **A2** showed that incorporation of the δ -azaproline actually resulted in a 6°C destabilization of the collagen triple helix. Additionally, the CMP **A2** was subjected to pH 2.6 and pH 10 and the thermal stability assessed. In both cases, no significant change in thermal stabilization was observed, suggesting the free δ -N was not easily protonated. An investigation of the influence of δ -azaproline in the Yaa position was also undertaken. In this case, the A3 was synthesized by solid phase synthesis and the two CMPs separated by HPLC. As similar to other collagen model peptides, the spectrum displayed a maximum at 224 nm and a minimum at 200 nm. Analysis of the thermal transition showed that the amino acid was allowed in the Yaa position, however a corresponding destabilization of approximately 8°C was observed.

In order to explain the cause of the destabilization, DFT calculations were performed on the δ -azaproline structure. A computational study was undertaken also to analyze the degree of ring-pucker of δ -azaproline, as an endo pucker is favored in the Xaa position of collagen.¹² The

calculations suggested that the doubly *trans* conformation of proline was the second lowest energy state, only succeeded by the *trans-cis* conformation. The preference for the *cis*-amide orientation for the acetyl group was explained by the propensity of the carbonyl to participate in a favorable hydrogen bonding interaction with the δ -nitrogen. The calculations also confirmed the adoption of the *endo* pucker in both the *trans-trans* conformation and the *trans-cis* conformation. Only when both amide bonds were in a *cis-cis* conformation did the amino acid favor an *exo* pucker. Interestingly, conformations where the δ -N adopted an S configuration were approximately 1 kcal/mol higher in energy than when the δ -N adopted an R configuration, suggesting that both conformations are likely in the structure (with the exception of the *trans-cis* conformation). Previous NMR studies also seemed to suggest that δ -azaproline has a propensity to form *cis*-amide bonds.¹¹ The assembly of collagen may therefore be affected by introducing an entropic barrier which hinders triple helix formation, thus contributing to an increased destabilization.

5.3 Conclusions and Future Outlook

While the incorporation of δ -azaproline has a destabilizing effect on the collagen triple helix, it still remains an unprecedented modification to collagen. Functionalization of the δ -C on proline has not been explored and constitutes an interesting site for modification, particularly in the Xaa position due to its close proximity with adjacent strand carbonyls. The results from this study show that the δ -azaproline amino acid is tolerated in both the Xaa and Yaa positions of collagen, suggesting that the amino acid is malleable in its preferred puckered conformation. Further investigations must be done examining the allowance of δ -azaproline along each position of the collagen chain. Different positions on the chain may have induce favorable hydrogen bonding interactions. Considering the success of aforementioned incorporation, other modifications involving functionalization of the δ -C may provide new avenues by which to stabilize the

collagen triple helix. For instance, addition of a δ -amino or δ -hydroxyl group may allow a hydrogen bonding donor to be in close proximity to the carbonyls on the backbone of collagen, which may contribute to an increased stability. These types of modifications also may provide a functional handle for the post-synthetic modification of collagen model peptides.

5.4 References

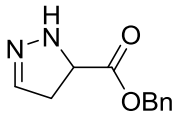
- (1) Shoulders, M. D.; Raines, R. T. *Annu. Rev. Biochem.* **2010**, 78, 929–958.
- (2) Holmgren, S. K.; Bretscher, L. E.; Taylor, K. M.; Raines, R. T. *Chem. Biol.* **1999**, 6 (2), 63–70.
- (3) Erdmann, R. S.; Wennemers, H. *J. Am. Chem. Soc.* **2010**, 132 (40), 13957–13959.
- (4) Gauba, V.; Hartgerink, J. D. *J. Am. Chem. Soc.* **2007**, 129 (48), 15034–15041.
- (5) Shoulders, M. D.; Hodges, J. A.; Raines, R. T. *J. Am. Chem. Soc.* **2006**, 128 (25), 8112–8113.
- (6) Egli, J.; Siebler, C.; Maryasin, B.; Erdmann, R. S.; Bergande, C.; Ochsenfeld, C.; Wennemers, H. *Chem. - A Eur. J.* **2017**, 23 (33), 7938–7944.
- (7) Siebler, C.; Erdmann, R. S.; Wennemers, H. *Angew. Chem. Int. Ed. Engl.* **2014**, 53 (39), 10340–10344.
- (8) Senes, A.; Ubarretxena-Belandia, I.; Engelman, D. M. *Proc. Natl. Acad. Sci.* **2001**, 98 (16), 9056–9061.
- (9) Zhang, Y.; Malamakal, R. M.; Chenoweth, D. M. *J. Am. Chem. Soc.* **2015**, 137 (39), 12422–12425.
- (10) Zhang, Y.; Malamakal, R. M.; Chenoweth, D. M. *Angew. Chemie Int. Ed.* **2015**, 54 (37), 10826–10832.
- (11) Duttagupta, I.; Misra, D.; Bhunya, S.; Paul, A.; Sinha, S. *J. Org. Chem.* **2015**, 80, 10585–10604.
- (12) Shoulders, M. D.; Raines, R. T. *Annu. Rev. Biochem.* **2009**, 78, 929–958.

Supporting Information

5.4.1 General Information

All commercial reagents and solvents were used as received. Fmoc-Pro-OH, Fmoc-Gly-OH, HATU and Rink Amide AM Resin (100-200 mesh) were purchased from Novabiochem. Fmoc-Hyp(tBu)-OH was purchased from Advanced Chemtech. Piperidine was purchased from American Bioanalytical. All remaining chemicals were purchased from Sigma Aldrich. Flash column chromatography was performed using Silicycle silica gel (55–65 Å pore diameter). Thin-layer chromatography was performed on Sorbent Technologies silica plates (250 µm thickness). High-resolution mass spectra were obtained at the University of Pennsylvania's Mass Spectrometry Service Center on a Micromass AutoSpec electrospray/chemical ionization spectrometer. Mass of long peptides were obtained via a Bruker Ultraflex III Matrix-assisted laser desorption/ionization (MALDI) mass spectrometer. Ultraviolet absorption spectrophotometry was performed on a JASCO V-650 spectrophotometer with a PAC-743R multichannel Peltier using quartz cells with a 1 cm cell path length. High performance liquid chromatography analysis was performed using a Jasco HPLC instrument equipped with a Phenomenex column (Luna 5u C18(2) 100A; 250 × 4.60 mm, 5 µm). Circular dichroism experiments were performed with a Jasco J-1500 CD Spectrometer with a 6-cell holder.

5.4.2 Experimental Procedures

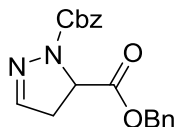


1

Compound (**1**)

Benzyl acrylate (5.0 mL, 32.7 mmol) was flashed through a silica plug using EtOAc to remove the stabilizer 4-aminophenol. The collected solvent was concentrated *in vacuo* and the oily residue was used without further purification. The residue was placed under argon and dissolved in anhydrous toluene (54 mL, 0.62 M). Trimethylsilyl diazomethane (25 mL, 50 mmol, 1.5 eq) was added slowly to the round bottom flask, and the solution was allowed to react for 3h. After consumption of benzyl acrylate was observed, the entire solvent was removed *in vacuo*, care being taken to place acetic acid in the trap to quench any Trimethylsilyl diazomethane. The residue was dissolved in CH₂Cl₂ and cooled to 0°C. Trifluoroacetic acid (7.7 mL, 3.0 eq) was slowly added to the reaction vessel with stirring, and the reaction was allowed to stir for 12h. The entire reaction solvent was removed *in vacuo* and the residue purified by column chromatography to yield a pale yellow oil (5.734 g, 86%).

¹H NMR (300 MHz, CDCl₃) δ: 7.35 (m, 5H), 6.80 (s, 1H), 6.03 (bs, 1H), 5.18 (m, 2H), 4.26 (dd, 1H, J = 11.0 Hz, 5.1 Hz), 3.03 (m, 2H)



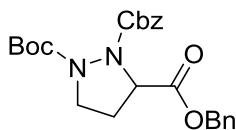
2

Compound (2)

Compound **1** (5.734 g, 28.152 mmol) was dissolved in CH_2Cl_2 (54 mL) and cooled to 0°C .

Triethylamine (9.1 mL, 65.4 mmol) was added to the reaction vessel, and benzyl chloroformate (6.9 mL, 49.050 mmol) was slowly added. After stirring for 1h, the reaction was quenched with H_2O , and the reaction was extracted with ethyl acetate 3x. The organic layer was collected and dried over Mg_2SO_4 , filtered, and concentrated *in vacuo*. The residue was purified by automated column chromatography using a gradient from 30% to 80% EtOAc/hexanes over 60 minutes to afford a pale yellow oil (7.64 g, 80%).

^1H NMR (360 MHz, CDCl_3) δ : 7.33 (m, 10H), 6.84 (s, 1H), 5.18 (m, 4H), 4.78 (dd, 1H, $J = 6.1$ Hz, 6.0 Hz), 3.25 (m, 1H), 2.95 (m, 1H), 1.68 (s, 1H)



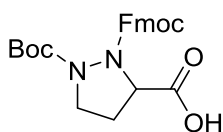
3

Compound (3)

Compound **2** (7.650 g, 22.663 mmol) was mixed in acetic acid (75.4 mL) and sodium cyanoborohydride (3.56 g, 56.582 mmol) was slowly added to the reaction. After stirring at r.t. for 1h, H_2O was added to the reaction mixture and quenched with solid K_2CO_3 until basic. The solution was extracted with ethyl acetate and dried over MgSO_4 , filtered, and concentrated *in vacuo*. The residue was taken up in benzene (113 mL). AgCN (4.030 g, 30.10 mmol) was added to the solution and allowed to stir for 10 minutes. Boc_2O (9.879 g, 45.266 mmol) was subsequently added, and the reaction mixture was heated to 50°C for 12h. The AgCN was

carefully filtered and properly disposed of in a separate waste container, and the solution was extracted with ethyl acetate and water. The organic layer was collected and dried over MgSO_4 , filtered, and concentrated *in vacuo*. The residue was purified by automated column chromatography using a gradient of 30% to 80% EtOAc/hexanes to yield compound **3** as a pale viscous oil (4.842 g, 49%)

^1H NMR (360 MHz, CDCl_3) δ : 7.33 (m, 10H), 5.18 (m, 4H), 4.81 (s, 1H), 4.09 (m, 1H), 3.19 (m, 1H), 2.36 (m, 1H), 2.25 (m, 1H), 1.37 (s, 9H)



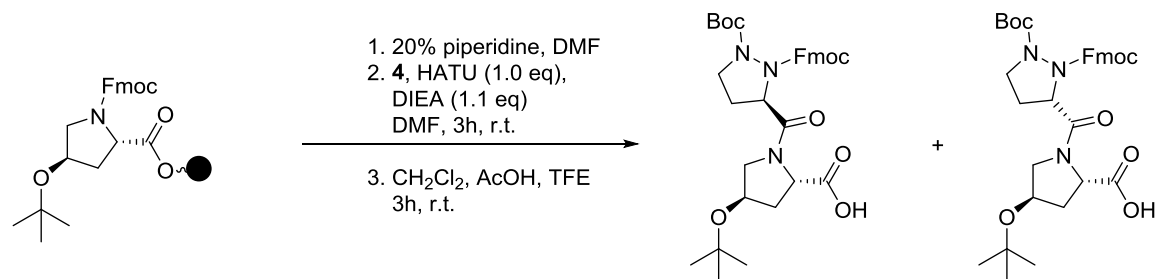
4

Compound (**4**)

Compound **3** (4.842 g, 11.004 mmol) was taken up in MeOH (100 mL) and purged with argon. 10% Pd/C (0.9685 g, 20% by wt.) was carefully added to the solution and stirred. One balloon of H_2 was used to flush out the argon from the reaction vessel, and a second balloon of H_2 was placed over the reaction. After reacting for 1h, the reaction was carefully filtered over Celite without allowing the filter-aid to go dry and washed with methanol. The filtrate was concentrated and was taken up in a 1:1 mixture of H_2O :acetone. NaHCO_3 (2.773 g, 33.012 mmol) was added to the solution along with DMAP (0.148 g, 1.210 mmol), and the reaction was cooled to 0°C . Fmoc-O-succinimide (4.083 g, 12.104 mmol) was added to the mixture, and the reaction was allowed to stir for 12h. The reaction was then brought to pH 4 and extracted with ethyl acetate. The organic layer was dried over MgSO_4 , filtered, and concentrated *in vacuo*, and the residue was purified by automated column chromatography using a gradient of 50% -100% EtOAc/hexanes to yield a pale viscous oil which crystallized into a crispy white solid after azeotroping with CH_2Cl_2 (2.692 g, 56%).

^1H NMR (500 MHz, CDCl_3) δ : 7.76 (d, 2H, $J = 7.5$ Hz), 7.61 (m, 2H), 7.41 (m, 2H), 7.30 (m, 2H), 4.73 (m, 1H), 4.57 (m, 1H), 4.42 (m, 1H), 4.26 (t, 1H, $J = 7.1$ Hz), 4.10 (m, 1H), 3.16 (q, 1H, $J = 9.5$ Hz), 2.50 (m, 1H), 2.28 (m, 1H), 1.50 (s, 9H)

Synthesis of Dimer on Solid Phase Support:



Scheme 5.2. Proposed method to separate out the δ -azaproline enantiomers

Fmoc-Hyp(O^tBu)-OH was loaded on to 2-chlorotrityl chloride resin by adding the resin to a solution of dried CH_2Cl_2 containing Fmoc-Hyp(O^tBu)-OH and DIEA. After 10 minutes, an additional 5 mL of DIEA was added. The reaction was allowed to stir for 2h, and was quenched with HPLC methanol to cap any unreacted trityl groups on resin. After 15 min, the resin was washed with CH_2Cl_2 and DMF. The Fmoc-protecting group was cleanly removed with 20% piperidine in DMF, and the resin was subsequently washed with DMF (6 x 10 mL). After deprotection, **4** was coupled to the unprotected Hyp residue using HATU and DIEA in DMF. After 2h, the resin was washed with DMF (6 x 10 mL). The dipeptide was cleaved by treatment with 80% CH_2Cl_2 , 10% AcOH, and 10% TFE at r.t. for 2h. The mixture was filtered and concentrated *in vacuo*. The resulting solid was purified by column chromatography (1% AcOH, 3% iPrOH, 96% CH_2Cl_2). Residual AcOH was removed by azeotroping benzene.

Z1: ^1H NMR (500 MHz, CDCl_3) δ : 7.76 (d, 2H, $J = 7.3$ Hz), 7.62 (t, 2H, $J = 7.3$ Hz), 7.40 (t, 2H, 7.5 Hz), 7.31 (m, 2H), 4.93 (m, 1H), 4.64 (m, 1H), 4.29 (m, 1H), 4.07 (m, 2H), 3.96 (m, 1H), 3.49

(m, 1H), 3.26 (m, 2H), 2.59 (m, 2H), 2.00 (m, 2H), 1.47 (s, 9H), 1.19 (s, 9H). HRMS (ESI)

calculated for $C_{33}H_{41}N_3O_8$ $[M+H]^+$ 608.2894, observed $[M+H]^+$ 608.2961

Z2: 1H NMR (500 MHz, $CDCl_3$) δ : 7.77 (d, 2H, $J = 7.6$ Hz), 7.61 (t, 2H, $J = 7.4$ Hz), 7.39 (t, 2H, $J = 6.9$ Hz), 7.30 (m, 2H), 4.87 (m, 1H), 4.66 (m, 1H), 4.58 (d, 1H, $J = 6.6$ Hz), 4.32 (m, 2H), 4.23 (m, 1H), 4.06 (m, 1H), 3.67 (m, 1H), 3.22 (m, 2H), 2.53 (m, 2H), 1.98 (m, 3H), 1.48 (s, 9H), 1.18 (s, 9H) HRMS (ESI) calculated for $C_{33}H_{41}N_3O_8$ $[M+H]^+$ 608.2894, observed $[M+H]^+$ 608.2970

5.4.3 General Protocols

A 4 mL peptide synthesis flask was loaded with 32 mg (0.020 mmol) of PAL PEG Rink amide resin. The resin was washed with CH_2Cl_2 (4 x 2 mL) and DMF (4 x 2 mL). Piperidine (20% in DMF, 2 mL) was added to the reaction flask and the resin was stirred for 10 minutes. The piperidine solution was drained, and the resin was washed with DMF, CH_2Cl_2 , MeOH, CH_2Cl_2 , DMF (4 x 2 mL each). Fmoc-protected tripeptide synthons (3 eq, 0.06 mmol) in DMF (0.67 mL) were added to the reaction flask with HATU (3 eq, 0.06 mmol) and DIEA (6 eq, 0.12 mmol), and the flask was agitated for 2h. The resin was washed with DMF 6x. A solution of 2% DBU and 1% HOBt in DMF (3 x 1 mL) was added to the reaction flask and agitated for 1m each. The resin was washed with DMF 6x. This procedure was repeated until all amino acids were coupled to resin. The resin was washed with DMF 6x, and the Fmoc-protecting group was removed with a solution of 2% DBU and 1% HOBt in DMF (3 x 1mL, 1m each). The resin was washed with DMF 6x. A solution of 10% acetic anhydride and 6% N-methyl morpholine in DMF was added to the resin and agitated for 40m. The solution was washed with DMF once, and washed with CH_2Cl_2 5x. A 3.6 mL solution of 2.5% TIPS and 2.5% H_2O was added to the resin and allowed to react for 35 min. The solution was carefully drained into a centrifuge tube of 11 mL of cold ether, after which a precipitate was clearly seen and centrifuged. The supernatant was decanted

and disposed, and the precipitate was dissolved in a solution of 3 ml 18 MΩ H₂O and 1 mL HPLC grade acetonitrile. This solution was purified by reverse HPLC on a C18 reverse phased column with a gradient of 10-20% of solvent A (H₂O/0.1% TFA) to solvent B (acetonitrile) over 90 min with a flow rate of 4 mL/min (λ₂₁₄ and λ₂₅₄ detection). All peptides were characterized by MALDI-TOF mass spectrometry.

Protocol A – Resin Preparation followed by Fmoc-deprotection

The peptides used in this paper are synthesized by manual SPPS method with Rink Amide AM Resin (0.62 mmol/g) on a 0.02 mmol scale. Thirty-two mg Rink Amide resins were carefully weighed out and transferred to a 5 mL solid phase synthesis vessel. The resin was then swelled in 4 mL of DMF for 30 min. The solvent was drained, and the resin was washed with 3 mL of DMF (1 x). Piperidine in DMF (20% v/v) (3 mL) was added to the resin, followed by stirring at ambient temperature for 30 minutes. The solution was drained, and the resin was washed with DMF (6x).

Protocol B – Trimer building block coupling followed by Fmoc-deprotection

Fmoc-Xaa-Yaa-Gly-OH or Fmoc-Gly-Xaa-Yaa-OH (3 equiv) and HBTU (3 equiv) were dissolved in DMF (0.67 mL). DIEA (9 equiv) was subsequently added to the mixture, and the entire solution was transferred to the reaction vessel containing the resin. The mixture was stirred for 100 min, drained, and washed with DMF (6 mL, 6 x). One mL of Piperidine in DMF (v/v 20%) was added to the resin and followed by stirring at ambient temperature for 30 minutes. The solution was drained, and the resin was thoroughly washed with DMF (6x).

Protocol C– Acylation followed by Fmoc-deprotection

A solution of DIEA (0.11 mL, 30 equiv) and Ac₂O (0.06 mL, 30 equiv) in CH₂Cl₂ (3.4 mL) were added to the amino functionalized resin. This mixture was stirred for 1 h at room temperature. The solution was drained and thoroughly washed with CH₂Cl₂ (6 mL, 5 x).

Protocol D– Cleavage off the resin and collection of the crude product

The resin was suspended for 30 min in a 4 mL mixture of TFA/H₂O/TIPS (95:2.5:2.5) at room temperature. The filtrate was collected and dropwise added to cold Et₂O (~11 mL). The sample was cooled to 4 °C for approximately 1 h, during which a white solid precipitated. The resulted sample was centrifuged and the supernatant was decanted. The white solid was dissolved in 18 MΩ water and frozen to -80 °C before HPLC purification.

Protocol E– HPLC purification

MeCN (B) and water containing 1% TFA (A) were used as eluents. The flow rate used for semi-preparative HPLC was 4 mL/min and 1 mL/min for analytical HPLC. The crude sample was heated to 65 °C for 15 min before injecting to prevent preemptive triple helix formation.

Synthesis of trimeric building blocks:

The synthesis of the tripeptide synthon FmocPOG-OH was carried out on 2-chlorotrityl chloride resin. To a solution of Fmoc-Gly-OH in dried CH₂Cl₂, 2-chlorotrityl chloride resin and dried DIEA were added under nitrogen. The mixture was stirred for 10 minutes, and additional DIEA was added. The reaction was allowed to stir for 2h and was quenched with HPLC grade methanol to cap any remaining reactive trityl groups. After 15 min, the reaction was washed with CH₂Cl₂ and DMF. The Fmoc-protecting group was cleanly removed with 20% piperidine in DMF, and the resin was subsequently washed with DMF (6 x 20 mL). After deprotection, **A** or **B**, HATU, and DIEA in DMF were added to the glycine loaded 2-chlorotrityl chloride resin. After 4h, the resin was washed with DMF (6 x 20 mL). The Fmoc group was removed with 20% piperidine in DMF (20 mL, 15 min, 2x), and the resin was washed with DMF (6 x 20 mL). After deprotection, Fmoc-P-OH, HATU, and DIEA in DMF were added to the resin. After 5h, the resin was collected and rinsed with DMF (1x 20 mL), CH₂Cl₂ (5x 20 mL). The resin was treated with 80% CH₂Cl₂, 10% AcOH, and 10% TFE at r.t. for 3h. The mixture was filtered and the filtrate was concentrated in vacuo. AcOH was removed by azeotroping benzene (3 x 30 mL). The resulting foamy solid residue was purified by silica gel column chromatography (5% MeOH, 95% CH₂Cl₂) to yield the desired compound as a foamy white solid.

5.4.4 Peptide solution preparation

Peptides after HPLC purification were dried under vacuum. The dried samples were dissolved in PBS buffer (0.20 g KCl, 0.20 g KH₂PO₄, 8.0 g NaCl, 2.16 g Na₂HPO₄·7H₂O in 1.0 L H₂O) and the concentration of the stock solution was measured by a UV-Vis measurement applying $\epsilon = 6.0 \times 10^4 \text{ M}^{-1} \text{ cm}^{-1}$ as the extinction coefficient as previously reported.³ Solutions of peptides used in this study were then made into a 0.20 mM solution by diluting with the same buffer accordingly. Samples were incubated at 4 °C for at least 24 h before CD experiments.

5.4.5 CD Wavelength scan

Samples of 0.20 mM concentration in PBS buffer were used. CD spectra were recorded at a step of 1.0 nm from 260 nm to 190 nm at 10 °C with a 1.0 s equilibration time.

5.4.6 CD Thermal denaturation experiment

A sample of 0.20 mM concentration in PBS buffer was used. The wavelength that gave the highest absorption, 224 nm, was used as the wavelength monitored as a function of time in the thermal denaturation experiment. Averaging time was set to be 15 s with an equilibration time period of 2 min and the ellipticity of every 1 °C was recorded. The collected data from the experiments were fitted into a two-state model according to Engel et al.² to obtain the melting temperature (temperature at which 50% of the triple helix unfolds). The software Graphpad Prism 6 was used to develop the fit by the same procedure described by Erdmann & Wennemers.³

(1) Lee, S.; Lee, J.; Chmielewski, J. *Angew. Chem. Int. Ed.* **2008**, 47(44), 8429-8432

(2) Engel, J.; Chen, H. T.; Prockop, D. J.; Klump, H. *Biopolymers* **1977**, 16, 601.

(3) Erdmann, R. S.; Wennemers, H. *Angew. Chem., Int. Ed.* **2011**, 50, 6835

5.4.7 Peptide Characterization and CD Spectra

CMP A1: Ac-(POG)₃(Z1-G)(POG)₃-NH₂

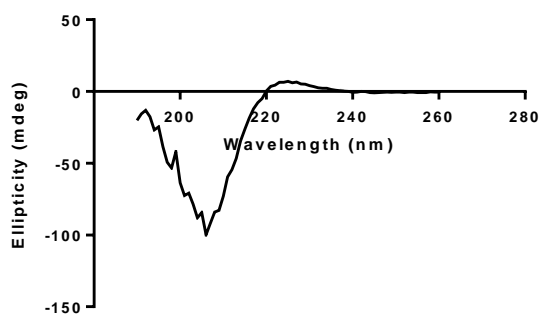


Figure 5.5 CD Spectra of A1 in pH 2.6

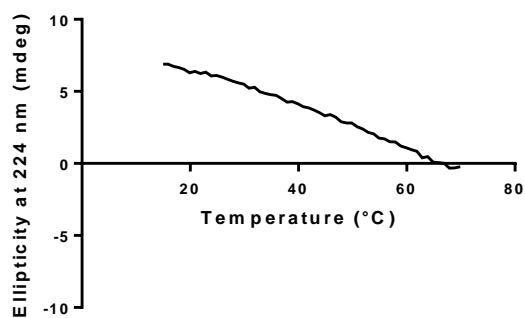
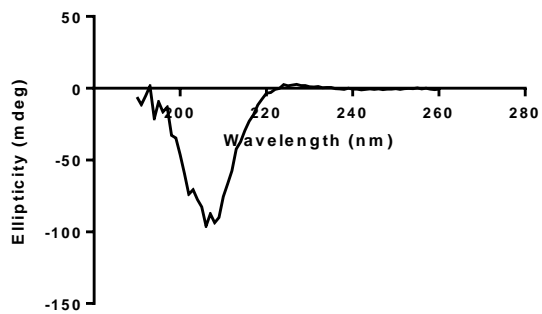


Figure 5.6 CD Thermal of A1 in pH 2.6



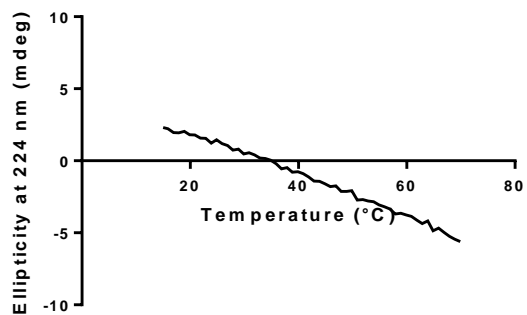


Figure 5.7 CD thermal of A1 at pH 7.4

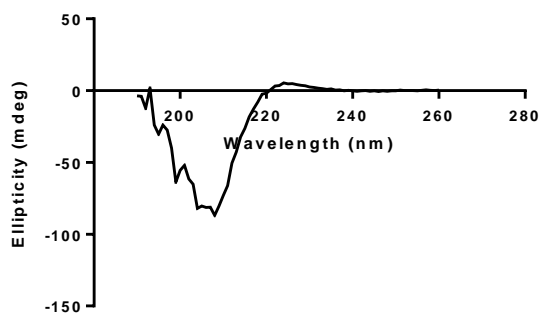


Figure 5.8 CD Spectra of A1 at pH 10.6

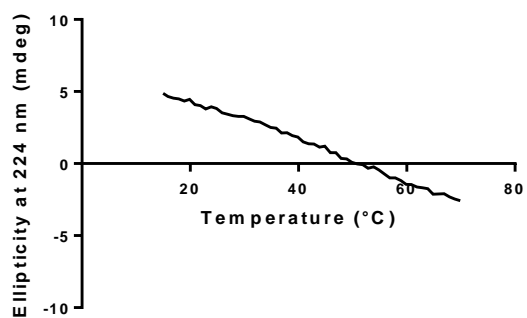


Figure 5.9 CD thermal of A1 at pH 10.6

MALDI MS: calculated $[M+Na]^+$ 1952.89, found 1954.49

CMP A2: Ac-(POG)₃(Z2-G)(POG)₃-NH₂

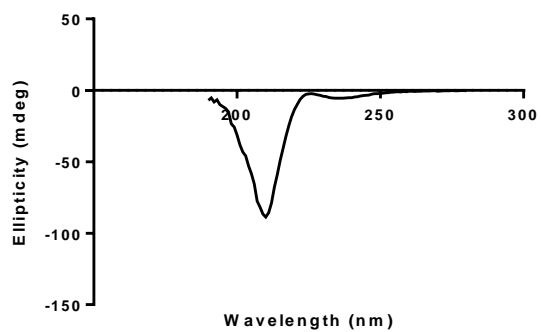


Figure 5.10 CD Spectra of CMP A2 at pH 2.6

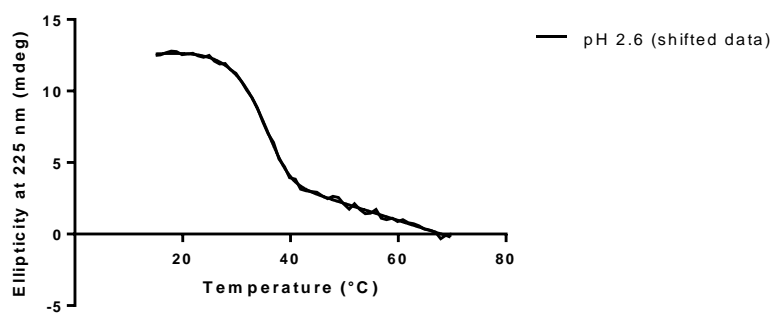


Figure 5.11 CD thermal of CMP A2 at pH 2.6

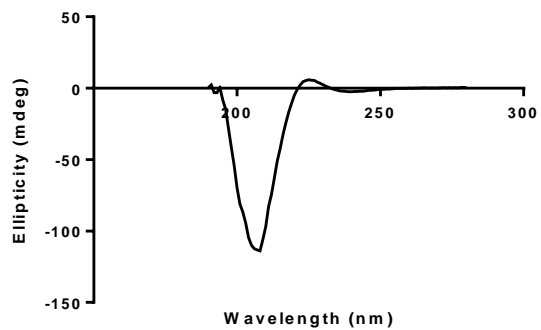


Figure 5.12 CD Spectra of A2 at pH 7.4

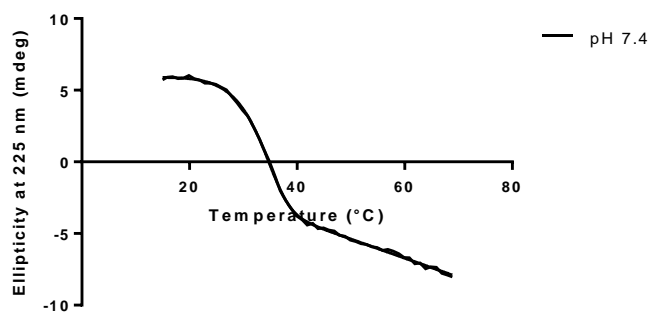


Figure 5.13 CD thermal of A2 at pH 7.4

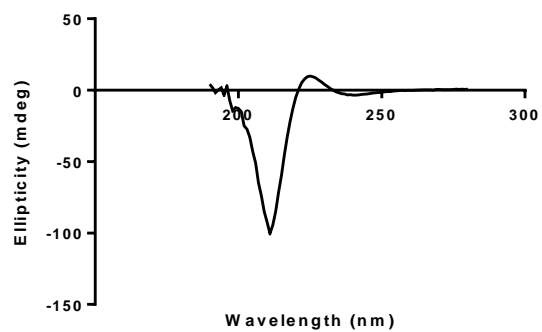


Figure 5.14 CD Spectra of A2 at pH 10.9

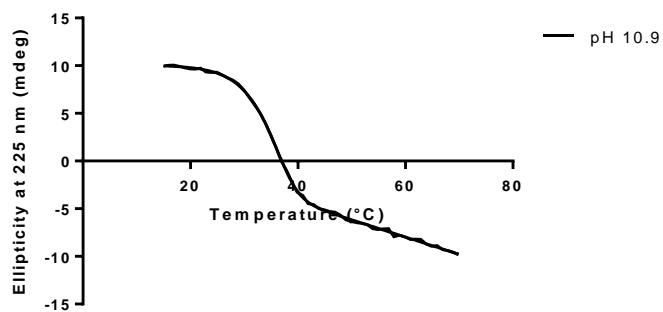


Figure 5.15 CD thermal of A2 pH 10.9

MALDI MS: calculated $[M+Na]^+$ 1952.89, found 1953.97

CMP A3: Ac-(POG)₃(P-4 -G)(POG)₃-NH₂

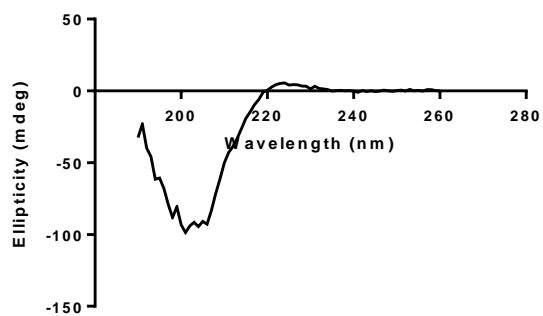


Figure 5.16 CD Spectra of A3

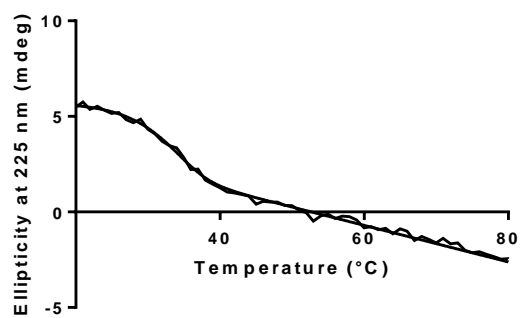
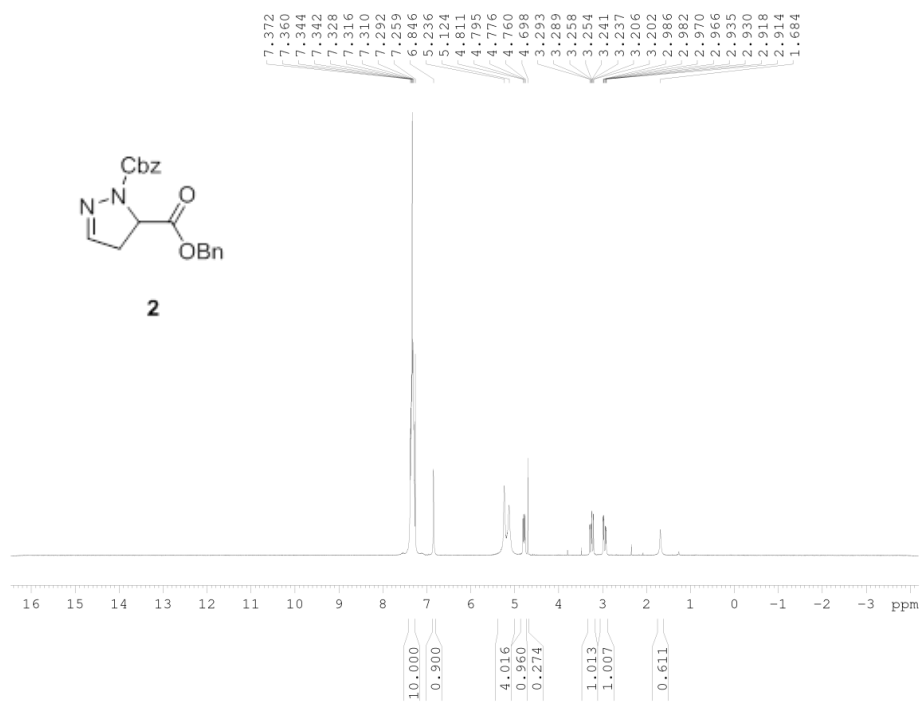
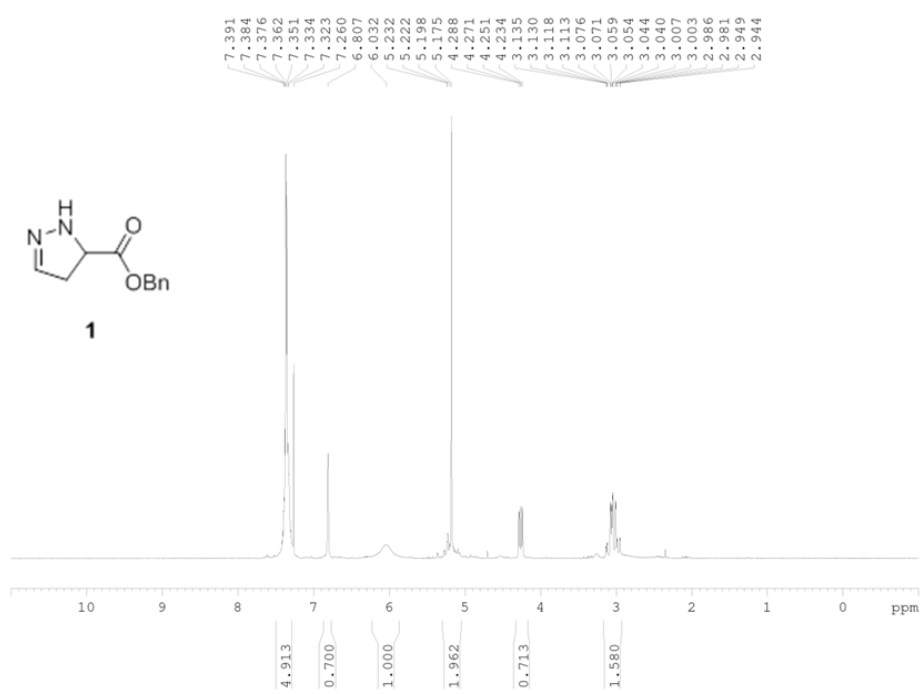
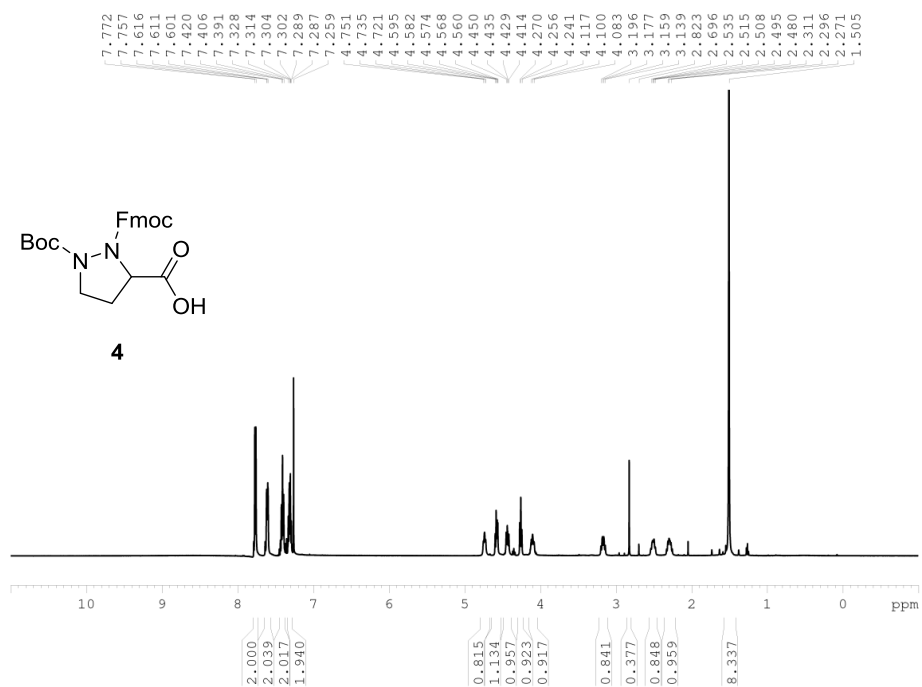
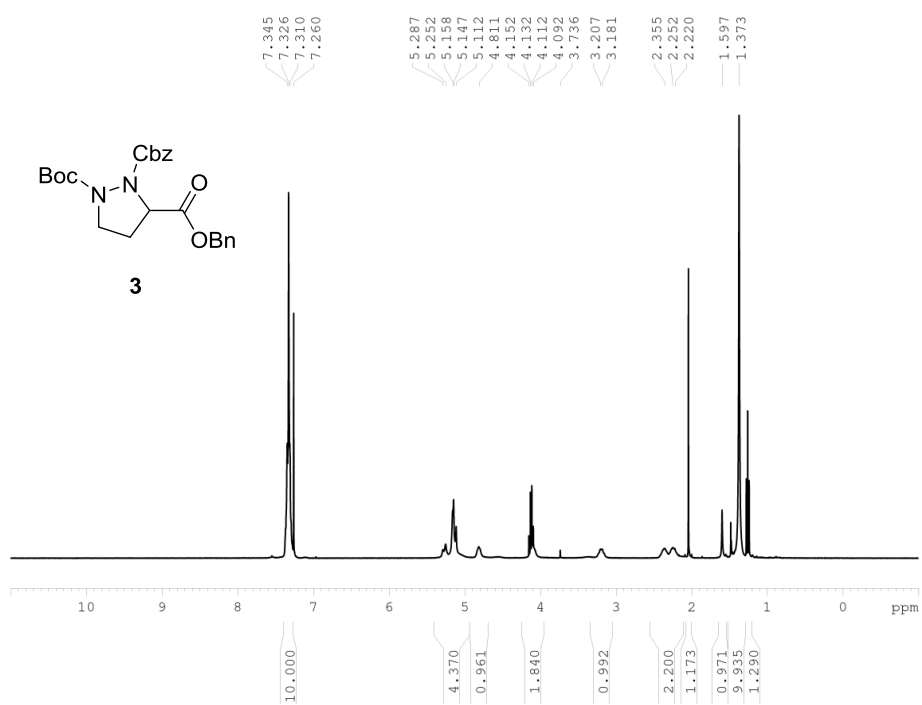


Figure 5.17 CD Thermal of A3

MALDI MS: calculated [M+Na]⁺ 1936.89, found 1936.75





5.4.8 Computational Coordinates

All calculations were performed using Gaussian 09. All local minima were optimized in the gas phase using DFT-B3LYP method with the 6-311+G(2d,p) basis set;

dAZP_b3lyp_6311G2dp_5-18cis_16-20cis_N_R-H

H	-3.1824	-2.2484	-0.8841
C	-3.1645	-1.1915	-0.633
H	-3.8848	-0.9672	0.1532
H	-3.3894	-0.5839	-1.5086
O	-1.825	-0.926	-0.1755
C	-1.5824	0.345	0.1818
O	-2.4102	1.2176	0.1656
C	-0.1365	0.5147	0.6719
H	-0.0828	0.0266	1.6456
C	0.2838	2.0072	0.7459
H	0.5078	2.3118	1.7674
H	-0.532	2.6255	0.3777
C	1.5203	2.0829	-0.1646
H	1.5749	3.0174	-0.7226
H	2.4417	1.9616	0.4199
N	1.2996	0.9593	-1.0952
H	2.1731	0.5989	-1.4789
N	0.8346	-0.0868	-0.2311
C	1.6548	-1.1594	-0.0006
O	2.6907	-1.2965	-0.6368
C	1.1814	-2.1816	1.013
H	0.1061	-2.3476	0.9578
H	1.7109	-3.1112	0.8168
H	1.4318	-1.8556	2.0269

dAZP_b3lyp_6311G2dp_5-18cis_16-20cis_N_S-H

C	3.4581	0.7727	-0.3094
H	3.9686	1.5986	0.1783
H	4.0461	-0.1415	-0.2397
H	3.271	0.9988	-1.3584
O	2.2109	0.6179	0.3972
C	1.4255	-0.3849	-0.0368
O	1.7195	-1.127	-0.9404
C	0.097	-0.4285	0.7106
H	0.1596	0.1891	1.6023
C	-0.3438	-1.881	1.0147
H	-0.497	-2.033	2.0832
H	0.4154	-2.5811	0.6696
C	-1.6515	-2.0405	0.202
H	-1.7505	-3.0218	-0.2616
H	-2.5251	-1.8676	0.834
N	-1.6159	-1.0023	-0.8326
H	-1.0212	-1.3102	-1.5994
N	-0.9494	0.0777	-0.2064
C	-1.571	1.3174	-0.1414
O	-2.589	1.5646	-0.7457
C	-0.8659	2.363	0.7099
H	0.2143	2.3733	0.5636
H	-1.2854	3.3302	0.4446
H	-1.0602	2.1838	1.7714

dAZP_b3lyp_6311G2dp_5-18cis_16-20trans_N_R-H

C	2.5934	-0.8847	1.3203
H	2.4196	-1.0882	2.3738
H	2.7525	-1.8119	0.7711
H	3.4581	-0.235	1.1889
O	1.3993	-0.237	0.8483
C	1.4179	0.1069	-0.4535
O	2.3804	0.0087	-1.166

C	0.109	0.7562	-0.8987
H	0.1287	0.7284	-1.9877
C	-0.0222	2.2003	-0.3568
H	-0.4835	2.8369	-1.1149
H	0.9427	2.6344	-0.096
C	-0.9635	2.0263	0.8451
H	-0.4121	1.6805	1.7201
H	-1.5148	2.9298	1.106
N	-1.902	0.9708	0.4336
H	-2.5931	1.3901	-0.1888
N	-1.0966	0.1048	-0.3675
C	-1.2083	-1.2594	-0.3136
O	-0.3948	-1.9583	-0.8955
C	-2.3853	-1.8183	0.4521
H	-3.3257	-1.5652	-0.0431
H	-2.2777	-2.8998	0.487
H	-2.4291	-1.4001	1.4579

dAZP_b3lyp_6311G2dp_5-18cis_16-20trans_N_S-H

C	2.5931	-0.8847	1.3205
H	2.4192	-1.0881	2.3741
H	2.7521	-1.8121	0.7715
H	3.4579	-0.2351	1.189
O	1.3992	-0.2367	0.8483
C	1.4179	0.1067	-0.4536
O	2.3803	0.0079	-1.1662
C	0.1091	0.7563	-0.8988
H	0.1289	0.7287	-1.9878
C	-0.0219	2.2004	-0.3567
H	-0.4832	2.8372	-1.1147
H	0.9429	2.6343	-0.0958
C	-0.9632	2.0262	0.8453
H	-0.4119	1.6803	1.7204
H	-1.5143	2.9297	1.1063

N	-1.9018	0.9709	0.4337
H	-2.593	1.3903	-0.1884
N	-1.0967	0.105	-0.3678
C	-1.2083	-1.2593	-0.3137
O	-0.3951	-1.9583	-0.8959
C	-2.3854	-1.8181	0.4523
H	-3.3258	-1.5653	-0.043
H	-2.2775	-2.8995	0.4874
H	-2.4291	-1.3997	1.4579

dAZP_b3lyp_6311G2dp_5-18trans_16-20cis_N_R-H

C	-3.6635	-0.621	-0.1259
H	-4.4701	-0.4703	0.5864
H	-3.8432	-0.0532	-1.0382
H	-3.5629	-1.6761	-0.3778
O	-2.4727	-0.1488	0.5318
C	-1.338	-0.253	-0.1894
O	-1.2836	-0.7056	-1.2999
C	-0.1548	0.2752	0.6293
H	-0.1661	-0.2571	1.5824
C	-0.2341	1.8004	0.8558
H	0.253	2.0509	1.8003
H	-1.2605	2.1612	0.8901
C	0.5817	2.3281	-0.3311
H	-0.0369	2.3695	-1.2317
H	1.0061	3.3176	-0.1641
N	1.6583	1.3573	-0.5391
H	2.4642	1.5667	0.05
N	1.1172	0.1111	-0.0639
C	1.9776	-0.9487	0.034
O	3.1543	-0.8355	-0.2605
C	1.3771	-2.2526	0.5268
H	0.4617	-2.5029	-0.0111
H	2.1182	-3.0326	0.3707
H	1.1476	-2.2038	1.5954

dAZP_b3lyp_6311G2dp_5-18trans_16-20cis_N_S-H

C	3.5571	-0.4864	0.2488
H	4.4027	-0.4416	-0.432
H	3.7082	0.1801	1.0973
H	3.4092	-1.5017	0.6146
O	2.4167	-0.0635	-0.5233
C	1.2481	-0.0374	0.1436
O	1.1174	-0.3588	1.295
C	0.1434	0.5079	-0.7603
H	0.3796	0.2446	-1.7922
C	0.0493	2.0481	-0.5877
H	-0.2931	2.4935	-1.522
H	1.0051	2.4943	-0.3168
C	-1.0272	2.1855	0.4884
H	-0.6059	1.9824	1.4807
H	-1.4943	3.1705	0.4894
N	-1.9993	1.1794	0.0531
H	-2.5731	0.8062	0.8085
N	-1.1848	0.0643	-0.3721
C	-1.6297	-1.1886	-0.08
O	-2.6881	-1.3506	0.513
C	-0.7837	-2.3561	-0.544
H	-0.2038	-2.7311	0.3016
H	-1.4589	-3.1463	-0.8688
H	-0.0995	-2.1115	-1.3574

dAZP_b3lyp_6311G2dp_5-18trans_16-20trans_N_R-H

C	3.4998	-0.5152	0.1946
H	4.3105	-0.6271	-0.5204
H	3.7609	0.2082	0.9666
H	3.264	-1.4706	0.6618
O	2.3717	-0.0535	-0.5689
C	1.259	0.174	0.1435
O	1.1875	0.0914	1.343

C	0.1207	0.6578	-0.7543
H	0.4007	0.4921	-1.7938
C	-0.2131	2.1375	-0.4549
H	-0.5498	2.633	-1.3685
H	0.6442	2.6858	-0.0655
C	-1.3688	2.016	0.5518
H	-0.9843	1.8022	1.5491
H	-2.0121	2.8952	0.5926
N	-2.1406	0.8535	0.0866
H	-2.7055	1.1491	-0.7097
N	-1.1391	-0.0262	-0.4257
C	-1.1649	-1.3774	-0.1961
O	-0.2003	-2.0601	-0.5008
C	-2.4335	-1.9467	0.3939
H	-3.274	-1.8209	-0.2923
H	-2.2709	-3.0061	0.5771
H	-2.6929	-1.4306	1.3185

dAZP_b3lyp_6311G2dp_5-18trans_16-20trans_N_S-H

C	3.4998	-0.5152	0.1946
H	4.3105	-0.6271	-0.5204
H	3.7609	0.2082	0.9666
H	3.264	-1.4706	0.6618
O	2.3717	-0.0535	-0.5689
C	1.259	0.174	0.1435
O	1.1875	0.0914	1.343
C	0.1207	0.6578	-0.7543
H	0.4007	0.4921	-1.7938
C	-0.2131	2.1375	-0.4549
H	-0.5498	2.633	-1.3685
H	0.6442	2.6858	-0.0655
C	-1.3688	2.016	0.5518
H	-0.9843	1.8022	1.5491
H	-2.0121	2.8952	0.5926
N	-2.1406	0.8535	0.0866
H	-2.7055	1.1491	-0.7097

N	-1.1391	-0.0262	-0.4257
C	-1.1649	-1.3774	-0.1961
O	-0.2003	-2.0601	-0.5008
C	-2.4335	-1.9467	0.3939
H	-3.274	-1.8209	-0.2923
H	-2.2709	-3.0061	0.5771
H	-2.6929	-1.4306	1.3185

CHAPTER 6: CHEMICAL MODIFICATIONS TO CARBON BLACK

6.1 Introduction

Carbon black is a highly hydrophobic and aromatic carbonaceous compound which readily forms aggregates and agglomerates in solution. It is one of the oldest manufactured products, being synthesized from the pyrolysis of carbonaceous materials.¹ Its use can be traced back to the ancient Chinese and Egyptians. Although similar in structure to activated carbon, its true form actually has a smaller surface-area-to-volume ratio. In the last hundred years, carbon black has seen significant use in the automotive industry due to the discovery of the reinforcing effect it had when added to natural rubber.¹ In recent years, it has found reuse as the main component in industrial black paint. Improving jetness, a property describing the degree of how black a surface appears, for the generation of visually appealing black surfaces is currently highly desired in the commercial automotive industry. However, carbon black, being an extremely hydrophobic compound, has a tendency to form large aggregates and agglomerates in solution. Jetness, on the other hand, is typically increased by reducing the sizes of aggregates of pigment particles. Therefore in order to improve the jetness of pigments containing carbon black, it becomes necessary to develop methods to prevent or hinder the aggregation of the carbon black particles.

Several strategies have been employed to accomplish this aim. The most common approach to overcome aggregation is through the use of polymers. Typically, polymers are grafted on to the surface of carbon black. Bulky substituents on the polymer chain attached to carbon black hinder the π - π stacking of the particles, which in turn lead to greater dispersive properties. Additionally, polymers have been utilized to encase carbon black particles. These polymers are termed dispersants. Zhang and coworkers were able to create a pH responsive polymer substituted with aryl amino groups and sulfonates capable of encasing carbon black particles to improve their dispersive properties.² At higher pH values, the carbon black particles were found to have particle sizes less than 100 nm. A similar approach was taken by Wang and coworkers, who encapsulated particles of carbon black with polyvinyl alcohol and polyacrylamide to generate

nanoparticles sized between 73-75 nm.³ Custom block copolymers were constructed by Antonietti and coworkers to encapsulate particles as low as 90 nm.⁴ Polymer chains have also been grown on the surface of carbon black for the purpose of dispersing particles. A variety of methods have been utilized, such as ATRP,^{5,6} polyether synthesis,⁷ and thiol chain transfer polymerization.⁸

Functionalization of carbon black with small molecules has been met with some success. Schukat and coworkers were able to show carbon black was capable of undergoing Diels-Alder reactions with maleic acid derivatives.⁹ Through these reactions, he was able to show the carbon black derivatives were able to form dispersions in water when the maleic acid derivatives were functionalized with water solubilizing groups such as carboxylates and sulfates. Other groups have opted to synthesize small water solubilizing chains to covalently attach to the periphery of the carbon black particles, as in the case of Wu and coworkers.¹⁰ With their particular chain, Wu was able to obtain a particle size of approximately 232 nm after grafting. Use of small molecules to construct dendrimers on the surface of carbon black has also been a strategy that resulted in improved dispersion of carbon black.¹¹⁻¹³ Building upon the work of Tsubokawa and coworkers, we envisioned improved dispersion of carbon black could be obtained through building small dendrimers with amines terminated by water solubilizing groups.

6.2 Results and Discussion

The base carbon black used as a starting material was pre-oxidized, resulting in the functionalization of carboxylic acids, lactones, phenols, anhydrides, and esters on the periphery of the material. The material was found to be insoluble in typical organic solvents, including acetonitrile, chloroform, hexane, toluene, p-xylene, tetrahydrofuran, acetone, DMSO, and methanol, although dispersion appeared to be aided in alcoholic solvents. Additionally, the material could not be analyzed by NMR due to its solubility, and also was not capable of being ionized by MALDI. In order to differentiate between favorable and unfavorable functionality, a

technique was developed to monitor the change in percent transmittance over time through a UV-cuvette as a suspension of carbon black particles settled (Supporting Figure 6.3). Results of this assay suggested promising functionality included polyamines, acid groups, and

Initial modification of carbon black was accomplished through functionalization of the carboxylic acids on the surface to amide bonds. The number of carboxylic acids was estimated using a Boehm titration and was discovered to be approximately 0.5 mmol/g of carbon black. Functionalization of the surface of carbon black was envisioned to be accomplished through activation of the carboxylic acids on the surface with thionyl chloride followed by the addition of different amines. A small library of compounds with different functionalities was synthesized, which was then characterized by the developed screening assay. Results from this initial screening assay suggested that functionality containing multiple amines, carboxylic acids, and sulfonic acids aided dispersion.

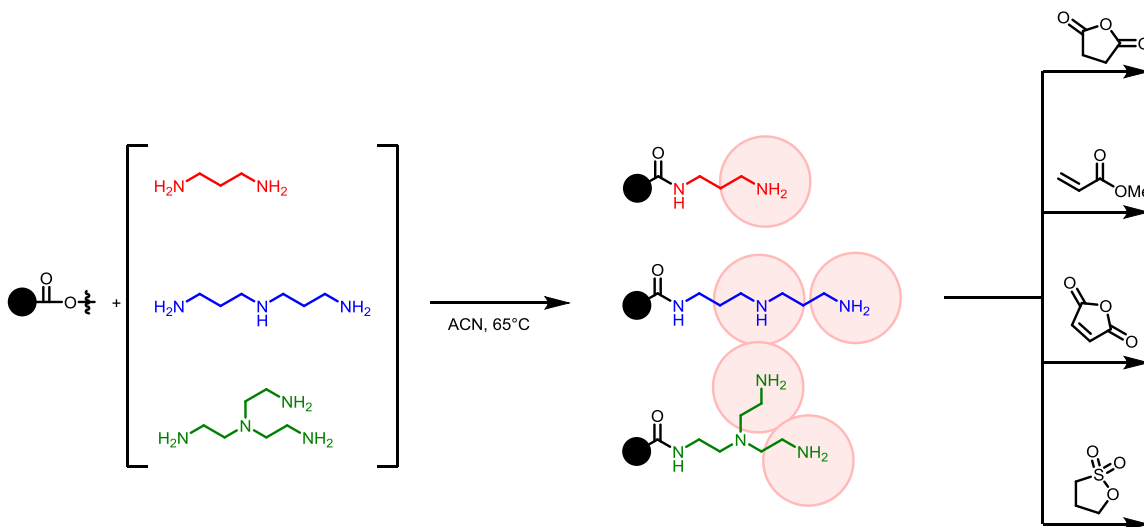
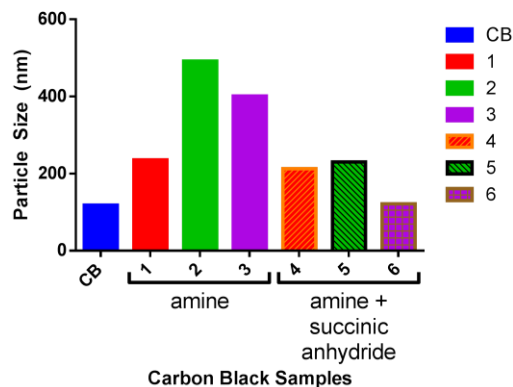


Figure 6.1. Proposed amine functionalization strategy for carbon black

In order to improve the dispersion of the carbon black, two strategies were employed. Firstly, the carbon surface was functionalized with various polyamines. These in turn would be reacted with solubilizing functionalities including succinic anhydride or cyclic sultone, after which their influence on particle size was observed (**Error! Reference source not found.**). Three amines were investigated, and included 1,3-diaminopropane (A1), bis-(3-aminopropyl)amine (A2), and (tris-aminoethyl)amine (A3) to specifically look at monoamine-, diamine-, and branched-diamine effects on dispersion, respectively. While



Entry	Order of Functionalization (refer to table of acronyms)	Particle Size (nm)
1	CB	118.1
2	CB-A1	235.8
3	CB-A2	491.6
4	CB-A3	401.1
5	CB-A1-C	212.6
6	CB-A2-C	230.1
7	CB-A3-C	121.6

Figure 6.2 Effect of functionalization with amine and succinic anhydride

straight amine functionalization always resulted in a larger particle size, reaction with succinic anhydride always led to a size reduction of the carbon black particle (**Error! Reference source not found.**). Reaction with cyclic sultone reduced particle size, however never to the degree of succinic anhydride. All carbon black derivatives synthesized in this manner displayed improved dispersion at higher pH values. Amine functionalized carbon black derivatives did show some improvement in dispersion at lower pH values, however a significant change was not observed in particle size. Promising functionalities included substitution with A3 followed by reaction with succinic anhydride, as well as reaction with methyl acrylate followed by reaction with A2 (Supporting Table 6.2).

Inspired by Tsubokawa and coworkers, a series of short-chain dendrimers built upon the carbon black periphery were synthesized. This was accomplished by three different methods. The first

method involved functionalizing the carbon black with free amines by activating with thionyl chloride and quenching with amine. The amines would be reacted with succinic anhydride, and dendrimer chains would be built with successive reactions of activation by thionyl chloride, quenching with amine, followed by a second reaction with succinic anhydride. This method was

Table 6.1 Summary of top 10 promising functionalizations

Entry	Order of Functionalization (refer to table of acronyms)	Particle Size (nm)
30	CB-A1-MAC-A1-MAC-OH	104.5
27	CB-A1-MAC-OH	119.2
7	CB-A3-C	121.6
29	CB-A1-MAC-A1-MAC	129.3
26	CB-A1-MAC	140.7
28	CB-A1-MAC-A1	154.6
32	CB-A2-MAC-A2	170.0
33	CB-A2-MAC-A2-MAC	192.7
5	CB-A1-C	212.6
6	CB-A2-C	230.1

attempted using bis(3-aminopropyl)amine, but unfortunately resulted in quickly precipitating carbon black by the 3rd generation. This suggested that cross-linking could occur between carbon black particles if the dendrimers became too long.

The second method involved dendrimer construction through successive reactions between methyl acrylate and amines. The carbon black particles were expected to undergo a Diels-Alder reaction with methyl acrylate, similar how carbon black has been reacted with maleic anhydride.¹⁴ The methyl esters which result from this reaction were expected to react with free amines used to build the dendrimer. As before, the dendrimer was constructed with bis(3-aminopropyl)amine as the linking amine, however these reactions were unsuccessful in reducing particle size past the 2nd generation. Similar reactions were performed with maleic anhydride, however no appreciable size reduction was seen with these dendrimers. Hydrolysis of the methyl ester terminated dendrimers did appear to be successful in reducing particle size, though not to the extent of unfunctionalized carbon black

The last method for dendrimer construction combined the approach of the two previous methods. Rather than starting the dendrimer synthesis with a Diels-Alder reaction, amine

functionality was placed on the periphery of the carbon black particles through activation with thionyl chloride followed by quenching with the amine of interest. These free amines were reacted with methyl acrylate in order to begin the dendrimer synthesis. Success in dendrimer functionalization was monitored by changes in the thermogravimetric analysis (TGA) plot of each carbon black sample, which suggested the dendrimer was not being completely functionalized by the 3rd generation. This was exemplified particularly well with dendrimer extension with bis(3-aminopropyl)amine. As was the case of the second method dendrimers, hydrolysis of the methyl ester terminated dendrimers was successful in reducing particle size, though again not to the extent of unfunctionalized carbon black.

6.3 Conclusions and Future Outlook

Functionalization of oxidized carbon black was found to be best accomplished through modification of the carboxylic acid groups on the surface. While functionalization of the carbon black periphery is ideally modified without the use of harsh activating agents, very limited success of covalent modification was observed through Diels-Alder mechanisms according to the TGA measurements. The results of the dendrimer synthesis indicate care must be taken in selecting amines to use as a linker, as cross linking can occur at longer lengths. Promising methodology which resulted in modestly smaller carbon black particle sizes included hydrolyzing methyl acrylate functionalized carbon black. Insight into various methods by which to functionalize the carbon black periphery was also obtained. Because dendrimer construction is limited to 3 generations, better success may be obtained by initially constructing polymers of varying lengths in solution prior to grafting on to the carbon black surface. Specifically, grafting a methyl acrylate polymer on the surface followed by subsequent hydrolysis may significantly improve the carbon black dispersion. Additionally, use of radical polymerization techniques such as ATRP or RAFT may be more successful at attaching longer solubilizing chains on the carbon black periphery, potentially reducing the size of the carbon black aggregates.

6.4 References

- (1) Donnet, J.-B.; Bansal, R. C.; Wang, M.-J. *Carbon Black: Science and Technology*, 2nd ed.; Marcel Dekker, Inc.: New York, 1993.
- (2) Yang, J.; Tang, B.; Qiu, W.; Zhang, S. *Carbon N. Y.* **2012**, *50* (15), 5621–5624.
- (3) Li, H. Y.; Chen, H. Z.; Xu, W. J.; Yuan, F.; Wang, J. R.; Wang, M. *Colloids Surfaces A Physicochem. Eng. Asp.* **2005**, *254* (1–3), 173–178.
- (4) Tiarks, F.; Landfester, K.; Antonietti, M. *Macromol. Chem. Phys.* **2001**, *202* (1), 51–60.
- (5) He, H.; Zhong, M.; Konkolewicz, D.; Yacatto, K.; Rappold, T.; Sugar, G.; David, N. E.; Matyjaszewski, K. *J. Mater. Chem. A* **2013**, *1* (23), 6810.
- (6) Liu, T.; Casado-Portilla, R.; Belmont, J.; Matyjaszewski, K. *J. Polym. Sci. Part A Polym. Chem.* **2005**, *43* (20), 4695–4709.
- (7) Guo, C.; Zhou, L.; Lv, J. *Polym. Polym. Compos.* **2013**, *21* (7), 449–456.
- (8) Fu, S.; Zhang, L.; Tian, A.; Xu, Y.; Du, C.; Xu, C. *Ind. Eng. Chem. Res.* **2014**, *53* (24), 10007–10014.
- (9) Bergemann, K.; Fanghänel, E.; Knackfuß, B.; Lüthge, T.; Schukat, G. *Carbon N. Y.* **2004**, *42* (11), 2338–2340.
- (10) Huang, J. F.; Shen, F.; Li, X. H.; Zhou, X. Q.; Li, B. Y.; Xu, R. L.; Wu, C. F. *J. Colloid Interface Sci.* **2008**, *328* (1), 92–97.
- (11) Tsubokawa, N.; Satoh, T.; Murota, M.; Sato, S.; Shimizu, H. *Polym. Adv. Technol.* **2001**, *602* (December 2000), 596–602.
- (12) Ichioka, H.; Satoh, T.; Hayashi, S.; Fujiki, K.; Tsubokawa, N. *React. Funct. Polym.* **1998**, *37*, 75–82.
- (13) Taniguchi, Y.; Ogawa, M.; Gang, W.; Saitoh, H.; Fujiki, K.; Yamauchi, T.; Tsubokawa, N. *Mater. Chem. Phys.* **2008**, *108* (2–3), 397–402.
- (14) Zhou, X.; Li, Q.; Wu, C. *Appl. Organomet. Chem.* **2008**, *22*, 78–81.

Supporting Information

6.4.1 General Information

The carbon black samples were obtained from Axalta and were used without further purification. Carbon black samples were sonicated on a QSonica Q700 probe sonicator using a ½” probe tip prior to reaction. IR spectra were obtained by preparing 10 mg of sample in 100 mg of KBr and taken by ATR. TGA measurements were performed on a TA Instruments Q600 SDT. DLS measurements were obtained on a Zetasizer Nano after sonication. The sedimentation assay was performed on a JASCO V-650 spectrophotometer.

6.4.2 Sedimentation Assay

Carbon black samples (10 mg) were suspended in H₂O or Ethanol (10 mL). The solution was added to a 1 mL polystyrene cuvette and placed in the UV-Vis. The percent transmittance at 470 nm was measured over the course of 8h, sampling every 30s. The data was plotted percent transmittance over time, and the slope of the linear increase in percent transmittance was plotted on a separate graph against the X-intercept.

6.4.3 Functionalization of Carbon Black

Method 1A: Functionalization with Amines

Carbon black (5g) was added to a reaction vessel and suspended in acetonitrile (35 mL). The sample was sonicated at 40A with 1s pulse on and 1s pulse off for 1 minute. To this solution, thionyl chloride (5 mL) was added and allowed to react at 65°C for 2h. The reaction transferred to a round bottom flask and solvent and reactants were removed *in vacuo*. The resulting residue was transferred to a reaction vessel and suspended in acetonitrile (35 mL). The sample was sonicated at 40A with 1s pulse on and 1s pulse off for 1 minute. The amine of interest (1.0 mL)

was added to this mixture and heated to 65°C for 12h. The reaction was purified by successive centrifugation and decantation with acetonitrile until amine was no longer observed by TLC.

Method 1B: Functionalization of Amine Terminated Carbon Black

Amine-functionalized carbon black (1g) was added to a reaction vessel and suspended in acetonitrile (10 mL). Succinic anhydride (200 mg) or 1,3-propane sultone (200 mg) were added to the reaction vessel sonicated at 40A with 1s pulse on and 1s pulse off for 1 minute. The reaction was then heated to 80°C and allowed to react for 12h. After reacting, the reaction was cooled and centrifuged and decanted three times using acetonitrile (45 mL x 3), sonicating between centrifugation to break up the centrifugation pellet.

Method 2: Diels Alder reaction with Carbon Black

Carbon black (5g) was added to a reaction vessel and suspended in acetonitrile (20 mL). Methyl acrylate (1.0 mL) or maleic anhydride (400 mg) were added to the reaction vessel and sonicated at 40A with 1s pulse on and 1s pulse off for 15 min. The reaction was then heated to 80°C for 12h. Reactions were purified by successive centrifugation, decantation and washing with acetonitrile (80 mL x 3).

Method 3A: Dendrimer Construction with Activating Agents

Amine-functionalized carbon black prepared by Method 1A were reacted with succinic anhydride as in Method 1B. After reaction, the carbon black samples were functionalized with a new set of amines using the Method 1A protocol, followed by functionalization with succinic anhydride using Method 1B.

Method 3B: Dendrimer Construction with Methyl Acrylate or Maleic Anhydride Functionalized Carbon Black

Methyl acrylate functionalized carbon black (1 g) was added to a reaction vessel and suspended in acetonitrile (10 mL). The reaction was sonicated at 40A with 1s pulse on and 1s pulse off for 1 min. The amine of interest (1 mL) was added to the reaction mixture and heated to 65°C for 12h. The reaction was cooled and purified by successive centrifugation, decantation and washing with acetonitrile until amine was no longer seen by TLC (45 mL x 3). The carbon black was re-suspended in acetonitrile and sonicated at 40A with 1s pulse and 1s pulse off for 1 min. A second round of methyl acrylate (1 mL) or maleic anhydride (200 mg) was added to the reaction mixture to extend the dendrimer.

Method 3C: Dendrimer Construction with Amine-functionalized Carbon Black and Methyl Acrylate

Amine-functionalized carbon black (1g) was prepared according to Method 1A and suspended in acetonitrile (10 mL). The reaction was sonicated at 40A with 1s pulse on and 1s pulse off for 1 min. Methyl acrylate (1 mL) was added to the reaction mixture and heated to 65°C for 12h. After reacting, the carbon black was purified by successive centrifugation, decantation and washing with acetonitrile (45 mL x 3). Dendrimer synthesis was then proceeded via Method 3B.

6.4.4 Sedimentation Assay Results

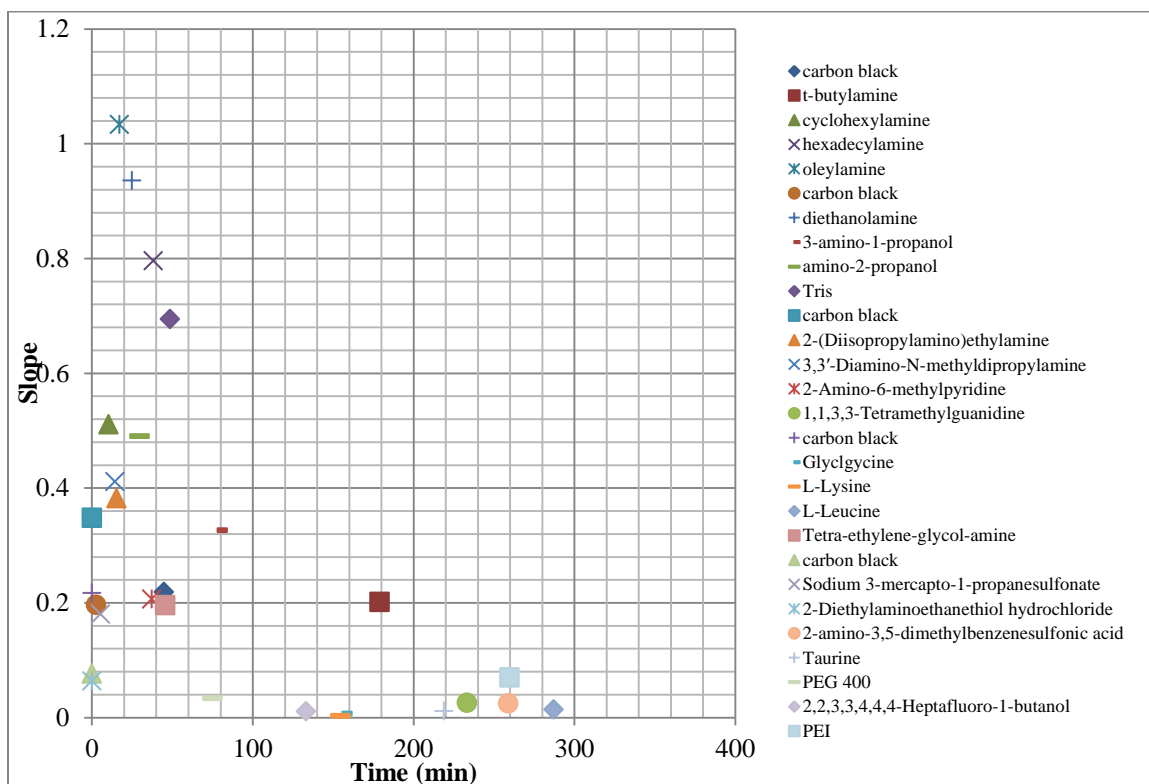


Figure 6.3 Results of the Sedimentation Assay

The functionalization of the lower right hand corner of the graph represent beneficial functionality, the functionalization in the lower left hand corner represents neutral functionality, and the functionalization in the upper left hand corner represents detrimental functionality.

6.4.5 Table of Acronyms

CB	Carbon black	-A1	Reacted with 1,3-diaminopropane
-A2	Reacted with bis-(3-aminopropyl)-amine	-A3	Reacted with tris(3-aminoethyl)amine
-MAC	Reacted with methyl acrylate	-MAN	Reacted with maleic anhydride
-C	Reacted with succinic anhydride	-S	Reacted with 1,3-propane sultone
-OH	Hydrolyzed		

6.4.6 DLS Measurements of Carbon Black Products

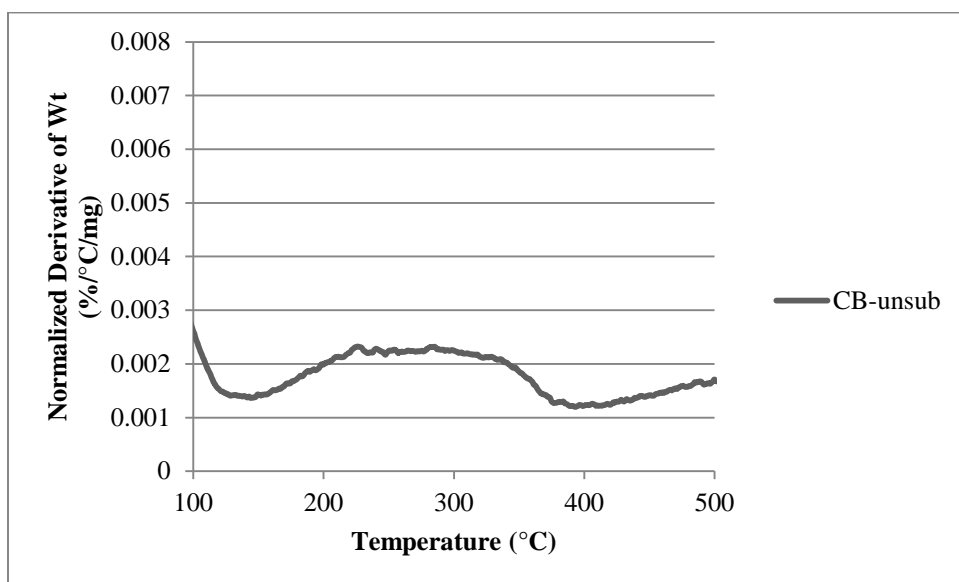
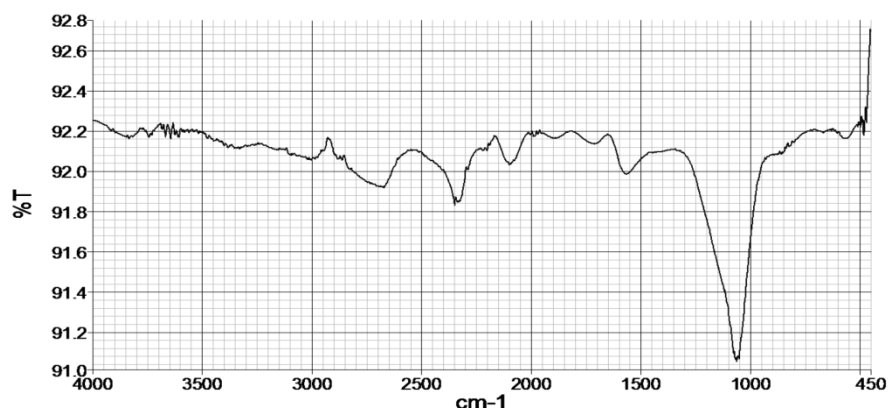
Table 6.2 Summary of Particle Sizes for Functionalized Carbon Black

Entry	Order of Functionalization (refer to table of acronyms)	Particle Size (nm)
1	CB	118.1
2	CB-A1	235.8

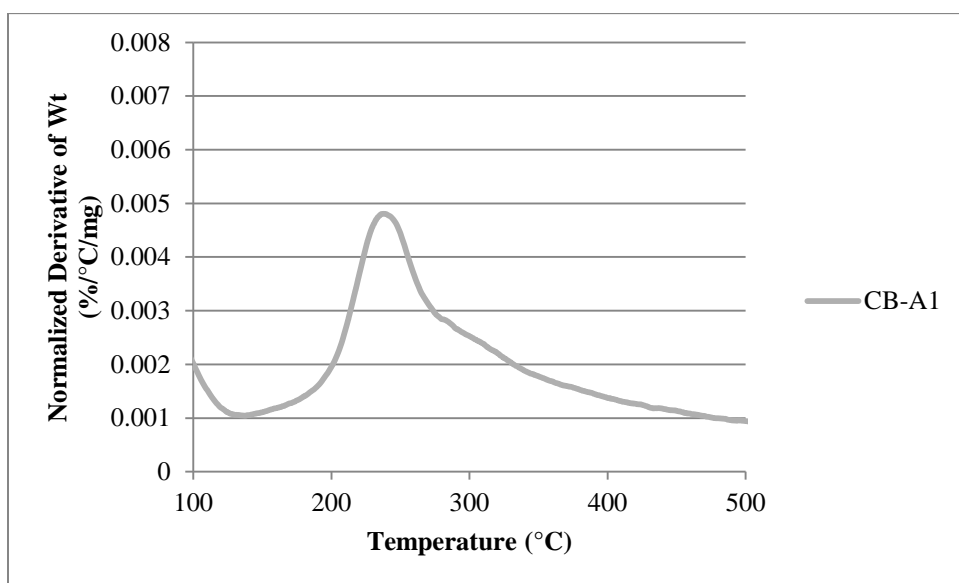
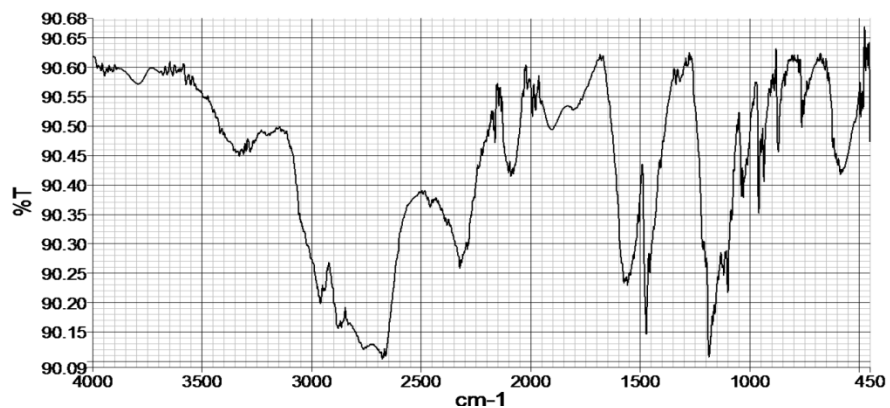
3	CB-A2	491.6
4	CB-A3	401.1
5	CB-A1-C	212.6
6	CB-A2-C	230.1
7	CB-A3-C	121.6
8	CB-A1-S	306.3
9	CB-A2-S	244.9
10	CB-A3-S	291.8
11	CB-MAN	150.6
12	CB-MAN-OH	119.6
13	CB-MAN-A2	202.2
14	CB-MAN-A2-MAN	321.0
15	CB-MAN-A2-MAN-A2	1723
16	CB-MAC	148.1
17	CB-MAC-A2	121.2
18	CB-MAC-A2-MAC	197.1
19	CB-MAC-A2-MAC-A2	209.8
20	CB-MAC-A1	117.1
21	CB-MAC-A1-C	110.6
22	CB-MAC-A2-C	163.8
23	CB-MAC-A3	122.6
24	CB-MAC-A3-C	222.7
25	CB-A1-MAC	140.7
26	CB-A1-MAC-OH	119.2
27	CB-A1-MAC-A1	154.6
28	CB-A1-MAC-A1-MAC	129.3
29	CB-A1-MAC-A1-MAC-OH	104.5
30	CB-A2-MAC	279.9
31	CB-A2-MAC-A2	170.0
32	CB-A2-MAC-A2-MAC	192.7

6.4.7 Characterization of Functionalized Carbon Black

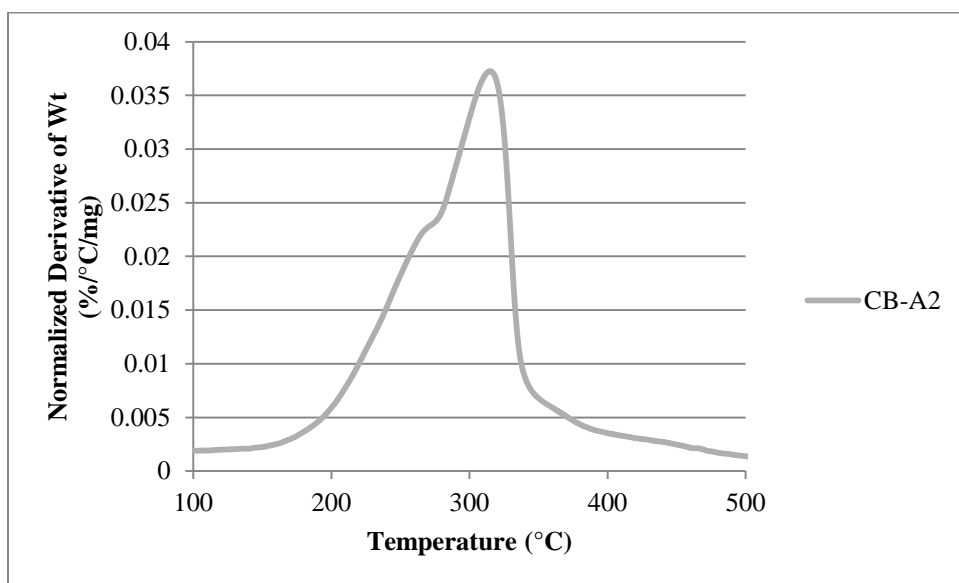
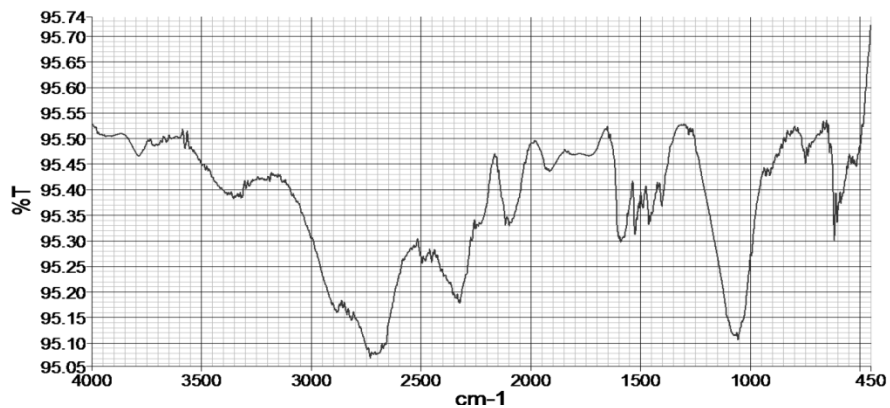
CB (1)



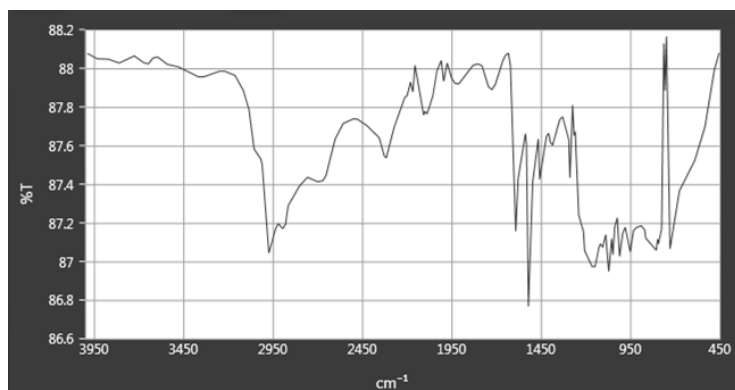
CB-A1 (2)

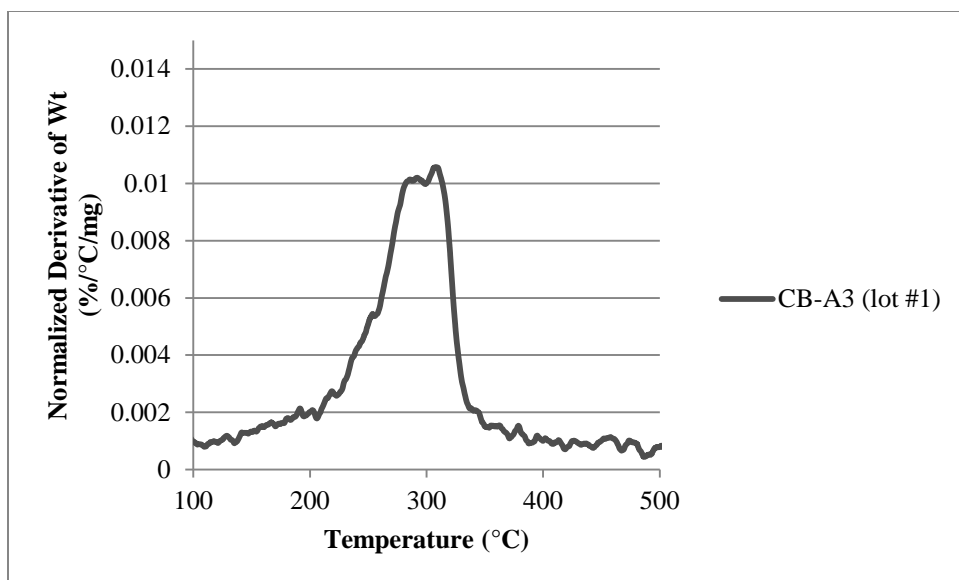


CB-A2 (3)

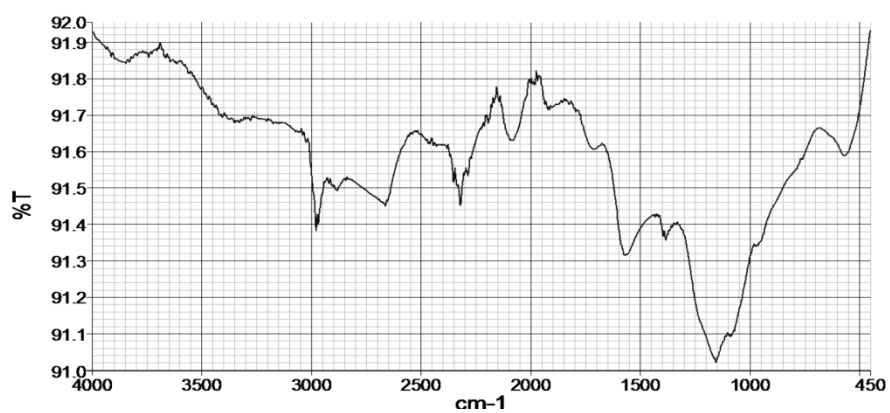


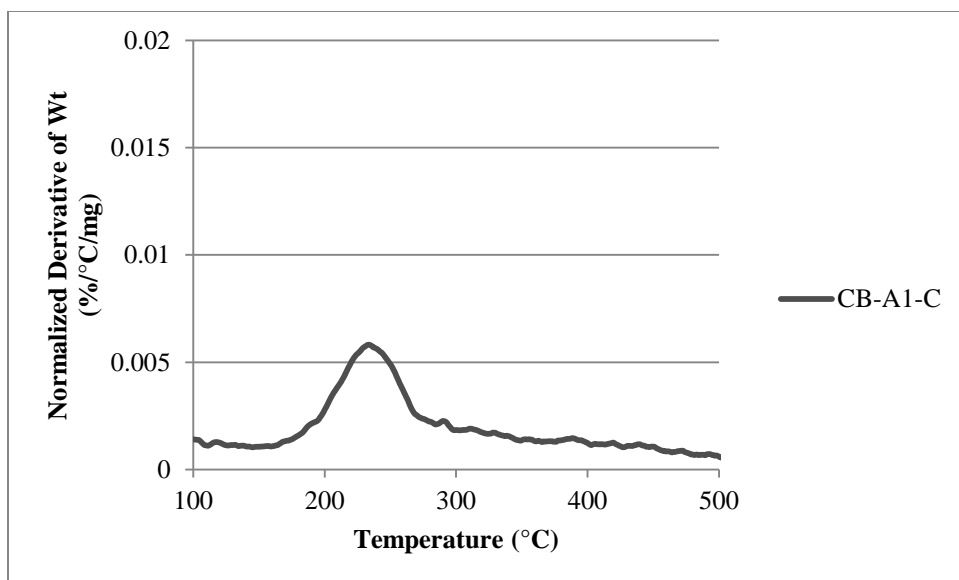
CB-A3 (4)



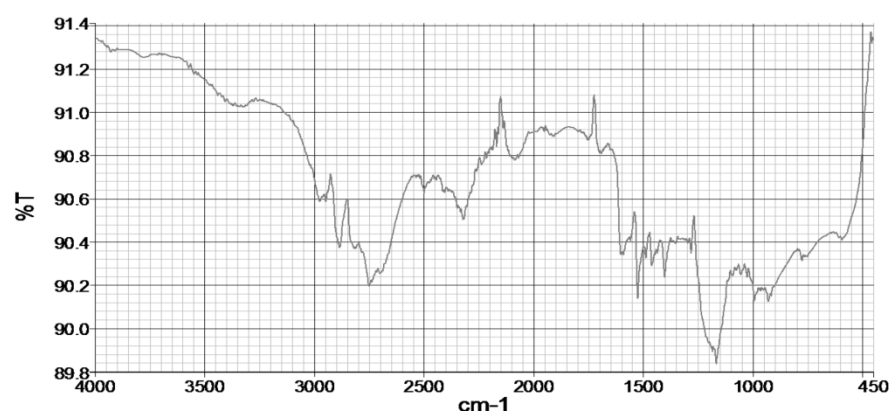


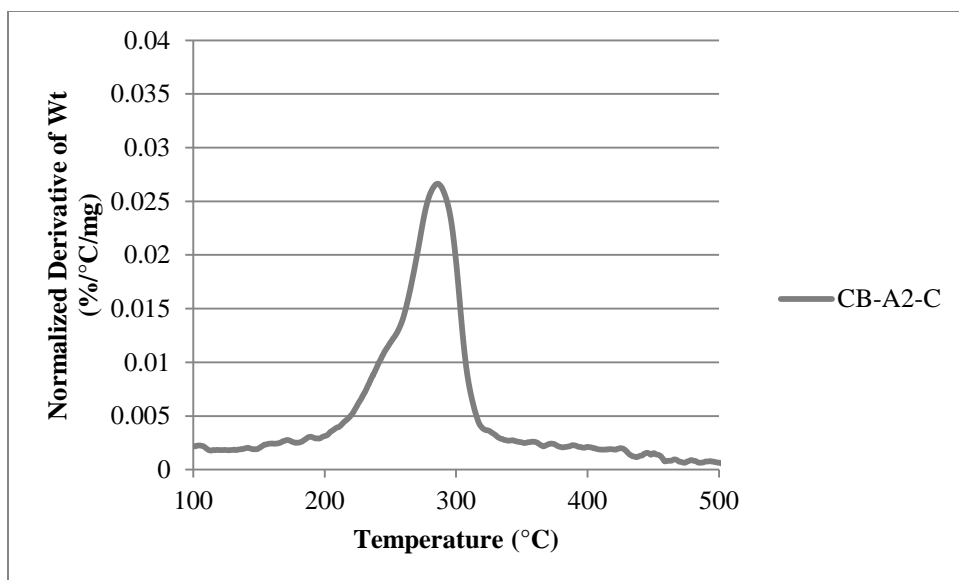
CB-A1-C (5)



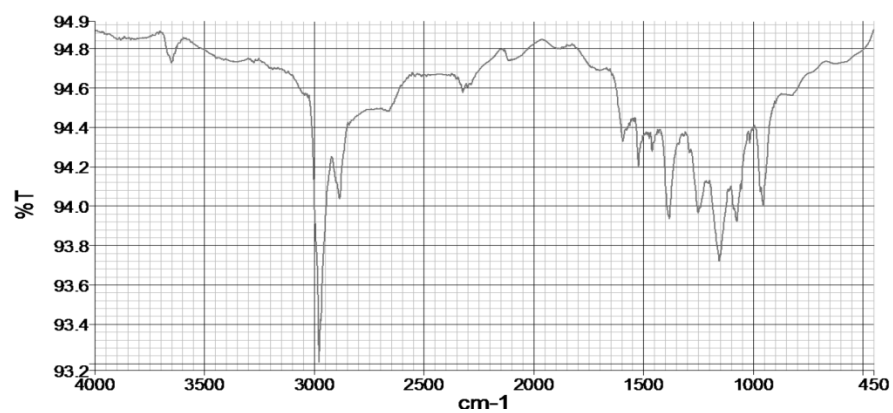


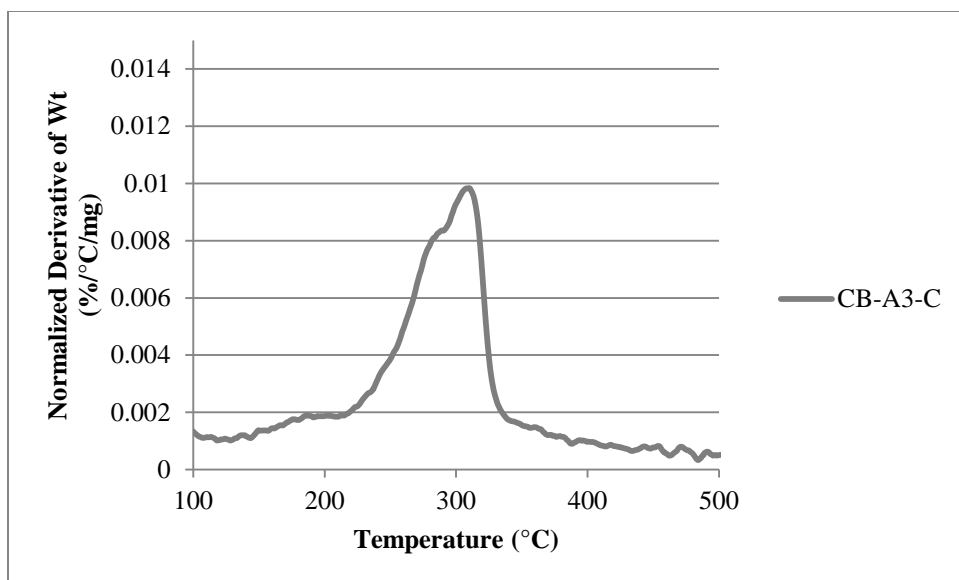
CB-A2-C (6)



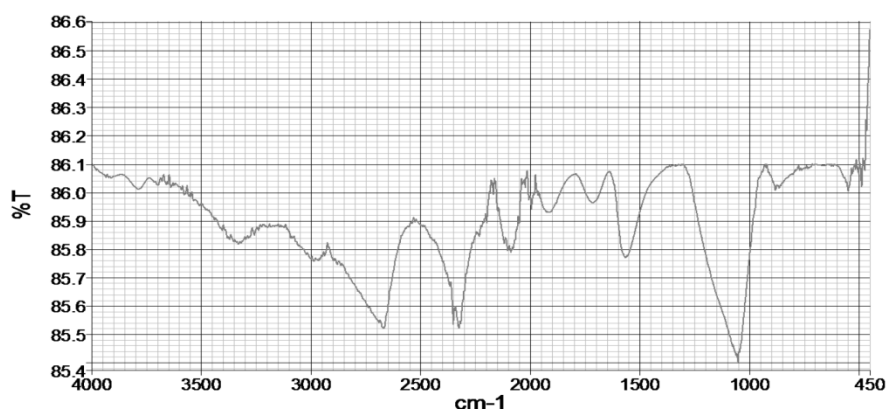


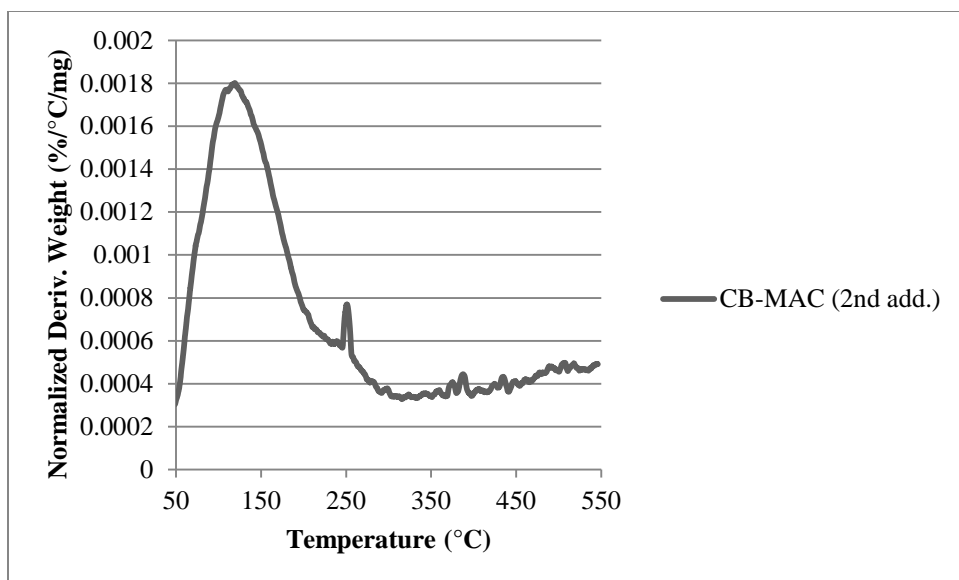
CB-A3-C (7)



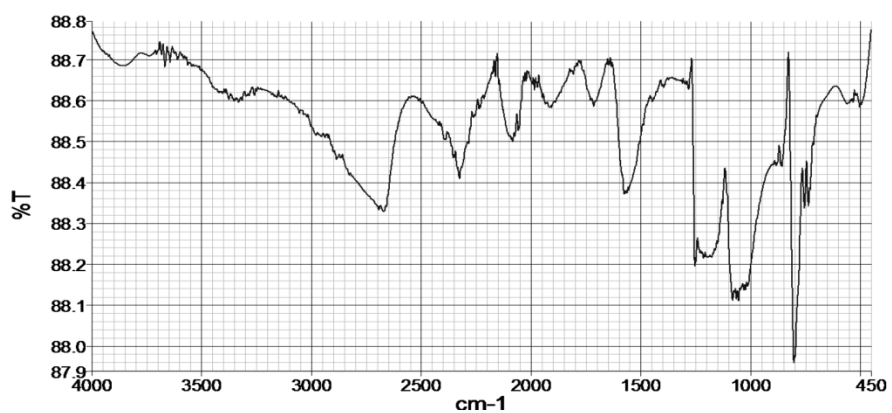


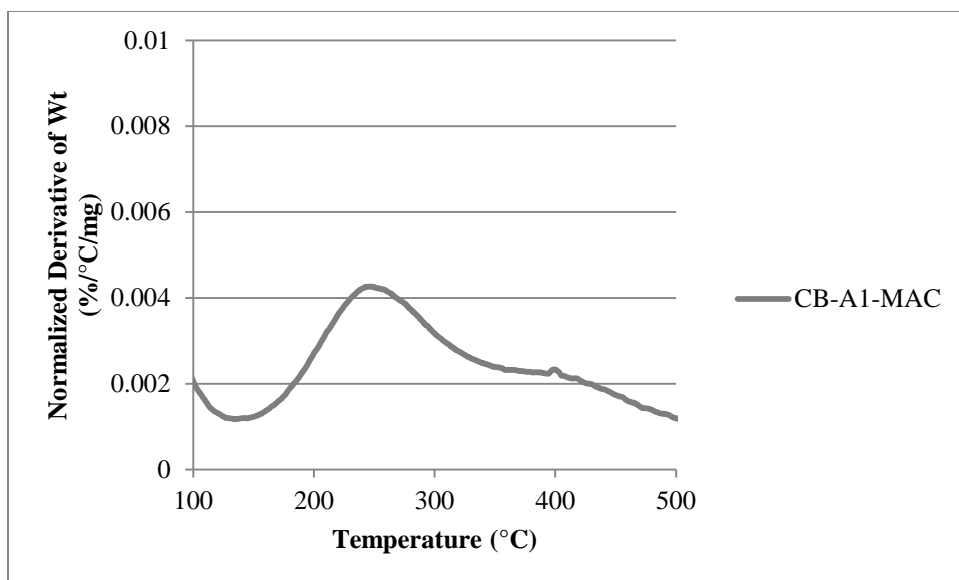
CB-MAC (16)



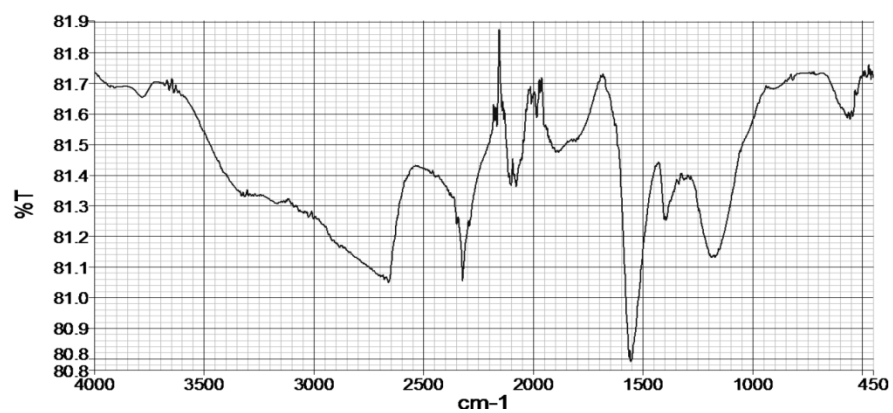


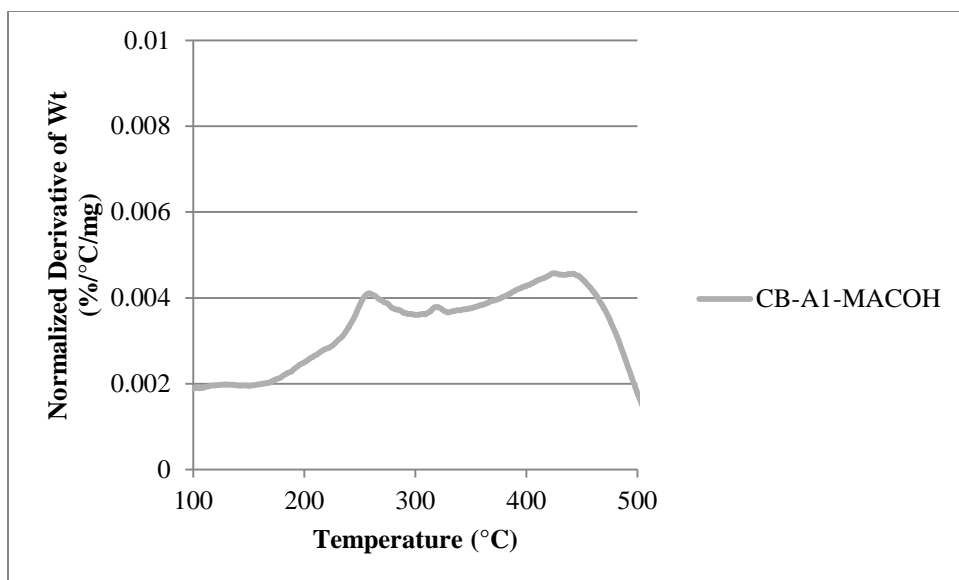
CB-A1-MAC (26)



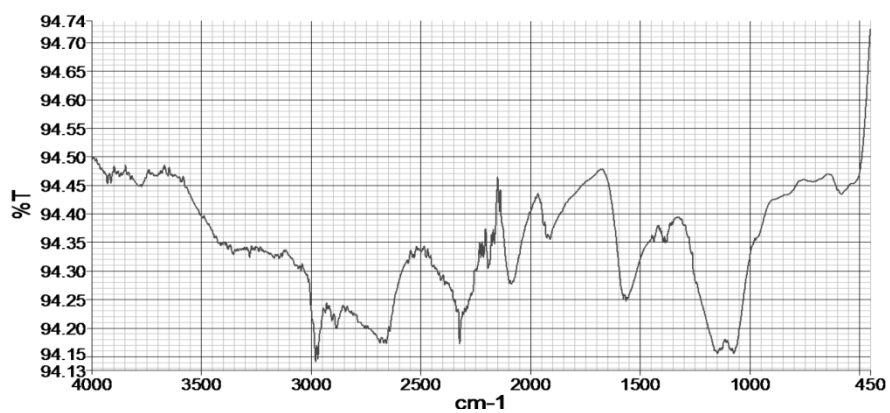


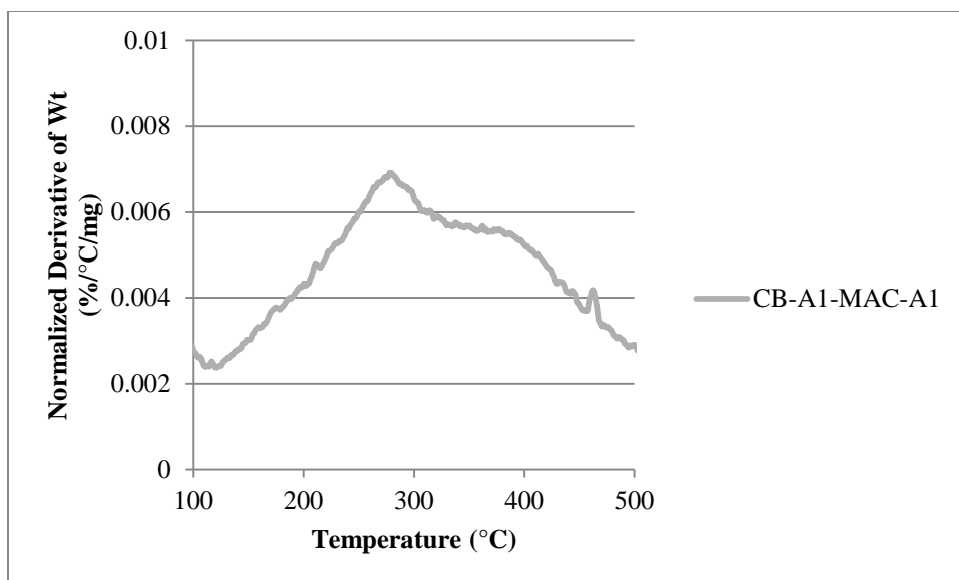
CB-A1-MAC-OH (27)



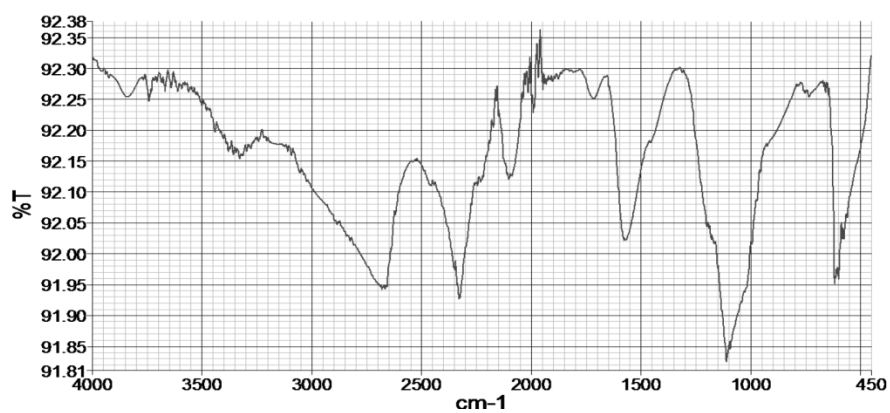


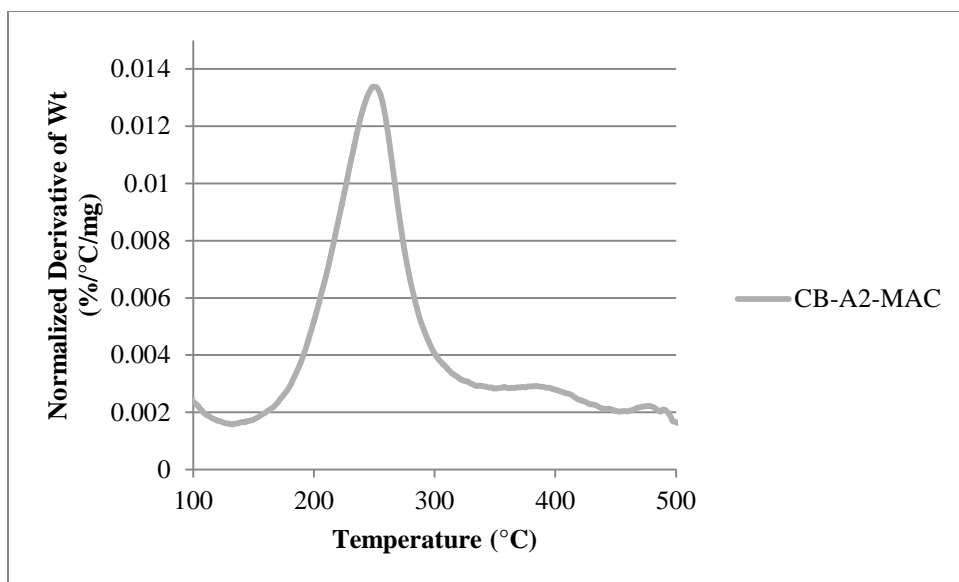
CB-A1-MAC-A1 (28)



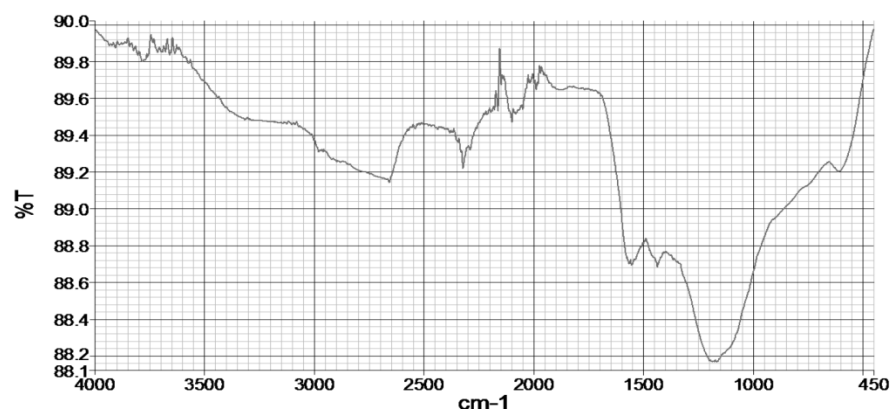


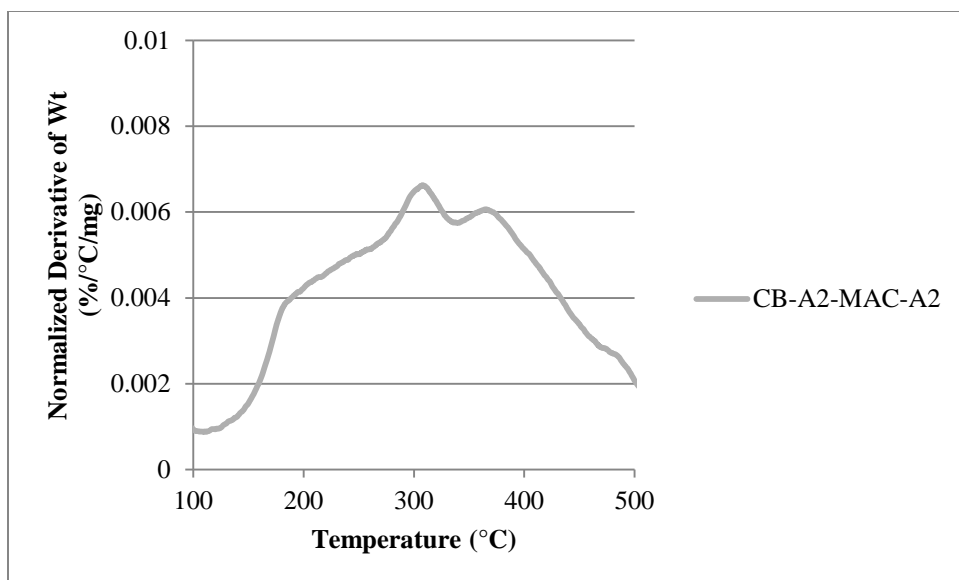
CB-A2-MAC (31)



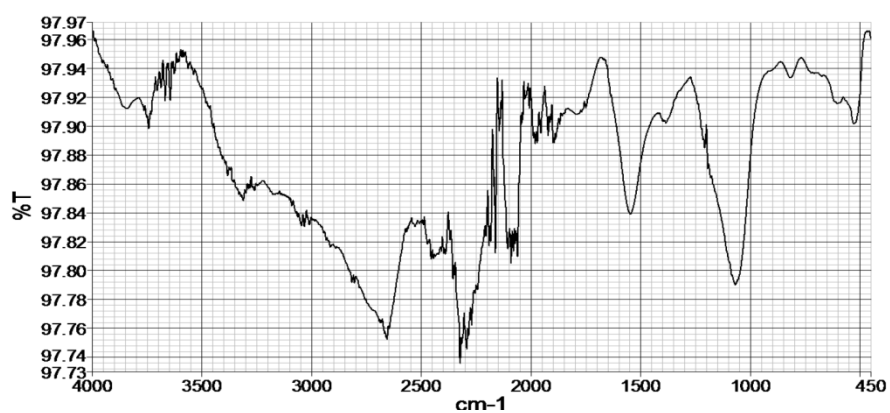


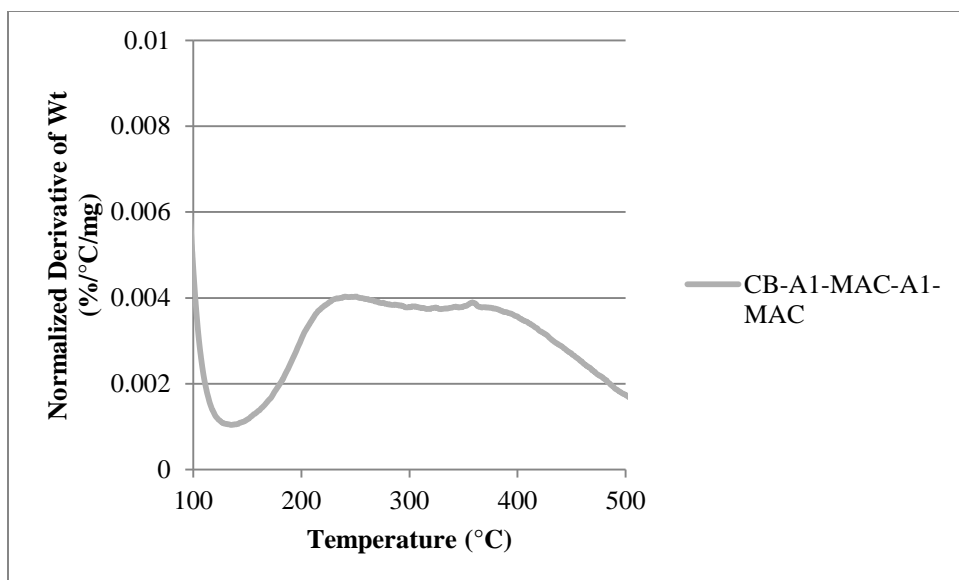
CB-A2-MAC-A2 (32)





CB-A2-MAC-A2-MAC (**33**)





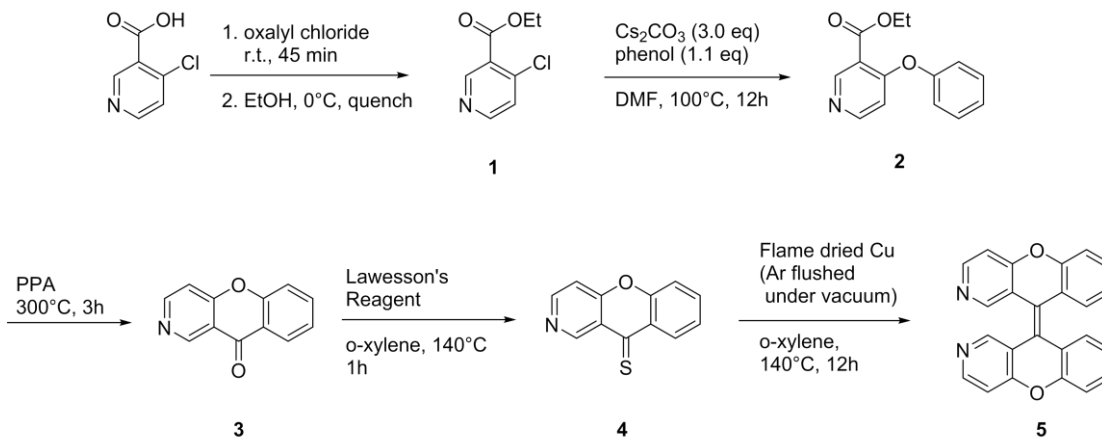
CHAPTER 7: INSIGHTS INTO 2N-XYLOPYRIDINE DERIVATIVES

7.1 Introduction

The development of novel fluorescent dyes has been of interest to researchers over the course of many years. Small, nonperturbing imaging agents with useful photophysical properties such as high extinction coefficients, high quantum yields, and high photostability have applicability from use as sensors to observation of protein structure and function. Of the many kinds of dyes being developed, photoactivatable dyes are a particular class of fluorophore that continues to be a powerful tool for studying biological systems. These probes have the unique ability to change their fluorescence properties simply by inducing a chemical change in the fluorophore through a photochemical process. As such, many different probes have been developed via a number of different processes, including photoisomerization^{1,2}, photo-uncaging³⁻⁵, photodecomposition of azides⁶, and photoclick reactions⁷⁻⁹. Recent work in our lab has discovered a new scaffold capable of acting as a photo-switchable probe which can significantly red-shift its emission through a simple 6π electrocyclization and oxidation.¹⁰ Derivatization of various isomers of this scaffold has led to the discovery of highly selective mitochondrial imaging agents¹¹, lysosome specific probes¹², and DNA-binders¹⁰. Here, we describe the synthesis and properties of the 2N isomer of the xylopyridine scaffold.

7.2 Results and Discussion

The synthesis of **3** was envisioned via the route in **Error! Reference source not found.**. This method differs slightly from the original synthesis of the first isomer, 3N-xylopyridine, where chlorination of 4-cyanopyridine was performed. Here, we start with 4-chloronicotinic acid. The chlorine on this molecule is extremely labile to S_NAr due to the fact the system is a pyridine ring and the position substituted *ortho*- to the chlorine is a carbonyl. Such is the reactivity of this site that dimerization of **1** is observed at room temperature in a standing vial of the compound. As such, the synthesis to **3** was undertaken all in one step without isolation of each component. Initial activation and ethyl protection of 4-chloronicotinic acid was found to be efficiently



Scheme 7.1 Synthesis of 2N-xylopyridine (5)

performed with oxalyl chloride and quenching with ethanol. This compound was reacted with phenol in a very efficient S_NAr to generate product **2**. Friedel-Crafts acylation to achieve aza-xanthone **3** was performed in neat polyphosphoric acid. Thione formation was accomplished simply by reacting **3** with Lawesson's reagent, which was subsequently dimerized with a Cu mediated coupling to generate **5**.

Interestingly, compound **5** does not share the very large Stokes shift or a very red-shifted emission exhibited by its isomers. However, it was shown to undergo photocyclization very rapidly. Simply using a UV lamp irradiating **5** on a TLC plate at 365 nm is enough to induce the cyclization, with the photochemical process taking mere seconds. Utilization of the Rayonette photoreactor was instrumental in providing an efficient means by which to scale up the photocyclized product, with the photocyclization of 10 mg of **5** completing within 30 min. A unique attribute of this isomer was its almost negligible shift in emission spectra upon photocyclization. Although the dye does not have a dramatic photoswitching ability, the dye was visibly seen to get brighter upon photocyclization. This effect was observed to be more pronounced in different solvents. Specifically, while **5** was dimly fluorescent in ethanol, the photocyclized products **6** and **7** were shown to overcome this solvent effect as seen by their

dramatic increase in fluorescence intensity (Supporting Figure 7.5, Supporting Figure 7.6). All dyes **5-7** were found to be quenched in water.

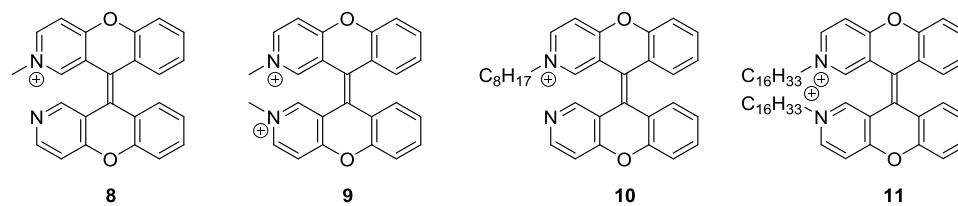


Figure 7.1 Structures of methylated and alkylated derivatives

Contrary to the photocyclized products, the methylated and alkylated products **8-11** (Figure 7.1) did show a corresponding red-shift in their emission, moving the emission

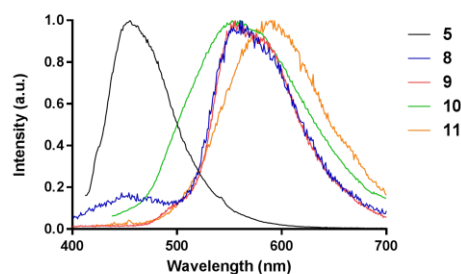


Figure 7.2 Emission spectra of compound **5**, **8**, **9**, **10**, and **11**

λ_{max} from 453 nm to approximately 553 nm (**Error! Reference source not found.**). Another interesting effect was observed when subjecting the Z isomer **6** to solutions of varying pH. While compound **6** is largely insoluble in water, in the presence of 1% DMSO, it is capable of interacting with ions in water. As such, a dramatic increase in fluorescence intensity was observed

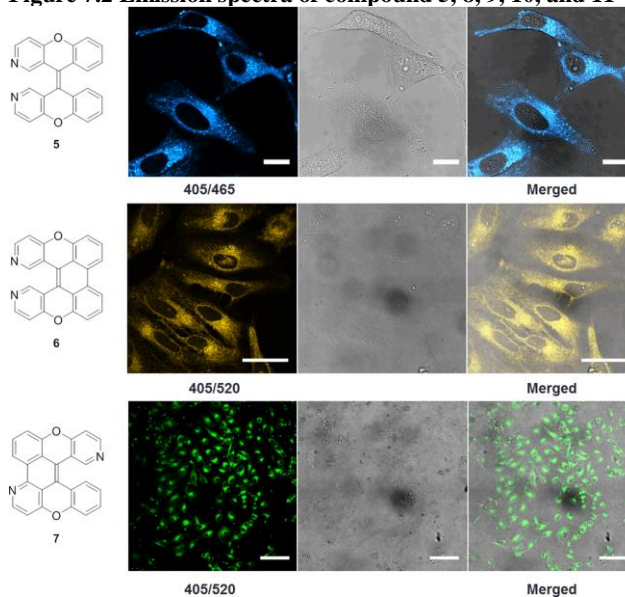


Figure 7.3 Cell imaging studies for compounds **5**, **6**, and **7**

as the pH was dropped to below 0, as well as a red-shifting of the emission to 571 nm (Supporting Figure 7.12). The fluorescence intensity and emission of compound **6** also seemed to be affected

by the presence of different ions. An ion screen was conducted with the compounds, and it was discovered that while most ions paired with this dye result in either non-perturbing or quenching interactions, there is a shift in emission which is observed when Zn^{2+} binds to the dye (Supporting Figure 7.11). This shift of 20 nm is unique to this system, and provides an interesting example of how this scaffold could be developed further for selective binding to this ion. These derivatives were incubated in HeLa cells to observe if any selective organelle binding was observed (**Error! Reference source not found.**), much like its isomeric mitochondrial and lysosomal stains. While the derivatives proved to be cell permeable, they only displayed nonselective binding.

7.3 Conclusion and Future Outlook

The 2N-xylopyridine scaffold holds a great deal of promise as a novel addition to the dixanthylidine based photoactivatable dyes. The proximity of the pyridine rings allows for potential ion binding, as was investigated earlier. This 2,2' arrangement also allows the dye to be used as a ligand for large metals, which allows for a potentially unique application with luminescent probes. In particular, ligating compound **5** to transition metals such as Ru and Ir may provide an avenue by which to obtain doubly or even triply photoactivatable luminescent probes. Additionally, functionalizing the benzene ring of **5** with electron donating or withdrawing groups or expanding the ring conjugation to naphthyl or phenanthryl groups may succeed in generating interesting multispectrum imaging agents. Continued exploration of this scaffold is required.

7.4 References

- (1) Gagey, N.; Neveu, P.; Benbrahim, C.; Goetz, B.; Aujard, I.; Baudin, J.-B.; Jullien, L. *J. Am. Chem. Soc.* **2007**, *129* (32), 9986–9998.
- (2) Cho, S.-Y.; Song, Y.-K.; Kim, J.-G.; Oh, S.-Y.; Chung, C.-M. *Tetrahedron Lett.* **2009**, *50* (33), 4769–4772.
- (3) Kobayashi, T.; Komatsu, T.; Kamiya, M.; Campos, C.; González-Gaitán, M.; Terai, T.; Hanaoka, K.; Nagano, T.; Urano, Y. *J. Am. Chem. Soc.* **2012**, *134* (27), 11153–11160.

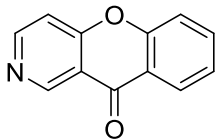
- (4) Faal, T.; Wong, P. T.; Tang, S.; Coulter, A.; Chen, Y.; Tu, C. H.; Baker, J. R.; Choi, S. K.; Inlay, M. A. *Mol. BioSyst.* **2015**, *11* (3), 783–790.
- (5) Ballister, E. R.; Aonbangkhen, C.; Mayo, A. M.; Lampson, M. A.; Chenoweth, D. M. *Nat. Commun.* **2014**, *5*, 5475.
- (6) Lord, S. J.; Conley, N. R.; Lee, H. D.; Samuel, R.; Liu, N.; Twieg, R. J.; Moerner, W. E. *J. Am. Chem. Soc.* **2008**, *130* (29), 9204–9205.
- (7) An, P.; Yu, Z.; Lin, Q. *Org. Lett.* **2013**, *15* (21), 5496–5499.
- (8) Yu, Z.; Ho, L. Y.; Lin, Q. *J. Am. Chem. Soc.* **2011**, *133* (31), 11912–11915.
- (9) Lim, R. K. V.; Lin, Q. *Acc. Chem. Res.* **2011**, *44* (9), 828–839.
- (10) Rarig, R.-A. F.; Tran, N. M.; Chenoweth, D. M. *J. Am. Chem. Soc.* **2013**, *135* (24), 9213–9219.
- (11) Tran, M. N.; Chenoweth, D. M. *Angew. Chemie Int. Ed.* **2015**, *54* (22), 6442–6446.
- (12) Tran, M. N.; Rarig, R.-A. F.; Chenoweth, D. M. *Chem. Sci.* **2015**, *6* (8), 4508–4512.

7.5 Supporting Information

7.5.1 General Information

All reagents were purchased either from Sigma Aldrich or Acros Organics and used without any further purification. Anhydrous solvents were purchased from Fisher Scientific and passed through an alumina column of a solvent purification system. Column chromatography was performed using 230-400 mesh silica gel from Silicycle. Reversed phase column chromatography was carried out using a CombiFlash Rf System with a RediSep Rf Gold C18 column from Teledyne ISCO. High performance liquid chromatography (HPLC) was performed using a Phenomenex column (Luna 5u C18(2) 100A; 250 x 4.60 mm, 5 micron) on a Jasco HPLC system. ^1H -NMR and ^{13}C -NMR data were collected on a Bruker DMX 500 (500 MHz). High resolution mass spectrometry was performed by Dr. Rakesh Kohli or Dr. Charles Ross III at the Mass Spectrometry Facility of the Department of Chemistry, University of Pennsylvania using a Waters LCT Premier XE Mass Spectrometer (model KE 332). UV-Vis absorption spectra were recorded in a semi-micro 1-cm-pathlength quartz cuvette purchased from Starna Cells on a Jasco V-650 spectrophotometer. Fluorescence emission spectra were obtained using a micro square 1-cm-pathlength quartz fluorimeter cuvette from Starna Cells on a Horiba Jobin-Yvon FluoroLog.

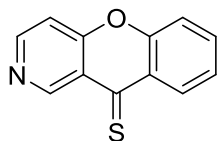
7.5.2 Experimental Procedures



3

A mixture of 4-chloronicotinic acid (15.730 g, 0.100 mol) and oxalyl chloride (21 mL) was prepared in CH_2Cl_2 (270 mL). DMF (3.5 mL) was added to the reaction slowly, and the reaction was allowed to stir at r.t. for 6h. The reaction was cooled to 0°C and EtOH (100 mL) was added slowly to the reaction. All solvents were removed *in vacuo*, and the remaining residue was suspended in EtOAc and filtered. The solid was collected, weighed (9.897 g), added to a round bottom flask. Phenol (5.508, 58.528 mmol) was added to the flask along with cesium carbonate (9.967 g, 30.6 mmol) and the mixture was suspended in DMF (213 mL). The reaction was heated to 100°C and allowed to react for 2h. After the reaction, the reaction was filtered and the filtrate was concentrated. The residue was taken up in polyphosphoric acid (50 g) and reacted at 180°C . After the reaction, the reaction was quenched with NaOH, and extracted with EtOAc. During the extraction, a pale brown solid was collected by filtration, which was pure **3** by NMR. The remaining organic layer was extracted with EtOAc, dried over MgSO_4 and concentrated *in vacuo*. The product was pure at this stage and did not require further purification (6.585 g, 63%).

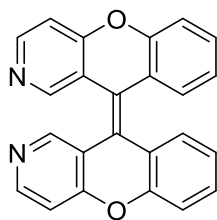
^1H NMR (500 MHz, CDCl_3) δ : 9.53 (s, 1H), 8.81 (d, 1H, $J = 5.9$ Hz), 8.36 (dd, 1H, $J = 7.9$ Hz, 1.6 Hz), 7.79 (m, 1H), 7.53 (d, 1H, $J = 3.1$ Hz), 7.45 (dt, 1H, $J = 7.0$ Hz, 1.6 Hz), 7.39 (d, 1H, $J = 5.9$ Hz)



4

Compound **3** (1.000 g, 5.076 mmol) was taken up in o-toluene (100 mL) and Lawesson's reagent (1.232 g, 3.046 mmol) was added to the reaction vessel. The reaction was heated to 140°C and allowed to react for 1h. The reaction was cooled, and the reaction contents were run through a silica column with 80% EtOAc/ hexanes as an eluent. The product was isolated as a green solid (1.0069 g, 93%)

¹H NMR (500 MHz, CDCl₃) δ: 9.80 (bs, 1H), 8.81 (bs, 1H), 8.67 (dd, 1H, J = 8.2 Hz, 1.6 Hz), 7.79 (m, 1H), 7.48 (d, 1H, J = 8.4 Hz), 7.41 (m, 1H)

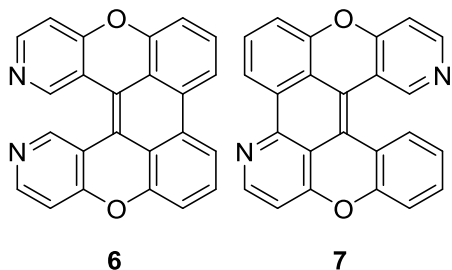


5

Compound **5**

Copper powder (9.193 g, 144.77 mmol) was placed in a round bottom flask and placed under vacuum and flame dried after repeating a cycle of placing under vacuum and back purging with argon three times. Compound **4** (0.9069 g, 4.258 mmol) was added to this vial, along with anhydrous o-xylene. The entire mixture was heated to 145°C for 3h. After the reaction, the mixture was placed on silica and eluted with 100% EtOAc. The pure product was collected as a light brown solid (0.413 g, 53%)

¹H NMR (500 MHz, CD₂Cl₂) δ: 8.38 (m, 4H), 7.33 (t, 4H, 9.6 Hz), 7.21 (m, 4H), 6.99 (m, 2H)

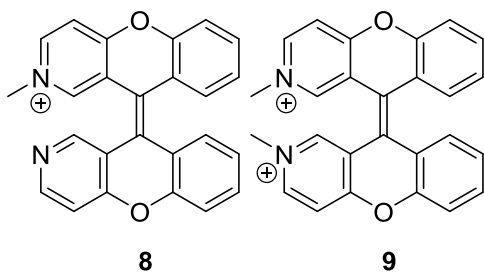


Compound **6** and **7**

Compound **5** (50 mg, 0.1377 mmol) was dissolved in THF (14 mL) in a vial and a catalytic amount of iodine was added to the reaction. Propylene oxide (0.5 mL, 7.29 mmol) was added to the reaction, and the vial was suspended in a Rayonette photoreactor and irradiated with 365 nm light for 30 min. The contents of the reaction were added directly to silica and purified using 30% EtOAc/ CH₂Cl₂ to afford two yellow powders. Yield **6** (25 mg, 50%) Yield **7** (20 mg, 40%)

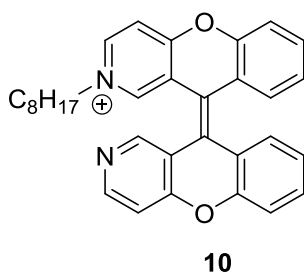
Compound **6**: ¹H NMR (500 MHz, CD₂Cl₂) δ: 8.83 (bs, 2H), 8.05 (d, 2H, J = 7.8 Hz), 7.36 (m, 2H), 7.25 (d, 2H, J = 7.5 Hz), 7.2 (m, 2H), 7.01 (t, 2H, J = 8.1 Hz)

Compound **7**: ¹H NMR (500 MHz, CD₂Cl₂) δ : 9.17 (s, 1H), 8.71 (d, 1H, J = 5.2 Hz), 8.64 (dd, 1H, J = 7.1 Hz, 1.1 Hz), 8.37 (d, 1H, J = 5.5 Hz), 8.06 (d, 1H, J = 8.1 Hz, 1.5 Hz), 7.58 (t, 1H, J = 7.9 Hz), 7.38 (m, 1H), 7.27 (m, 1H), 7.10 (d, 1H, J = 5.2 Hz), 7.08 (d, 1H, J = 5.6 Hz), 7.04 (m, 1H)



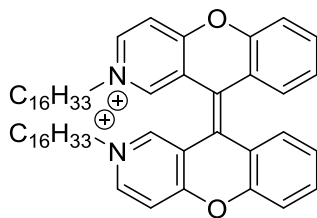
Compound 8 and 9

Compound **5** (2 mg, 0.005 mmol) was suspended in toluene and heated to 80°C with dimethyl sulfate (1.1 mL 0.5% solution in toluene). After reacting for 12h, the product was extracted into H₂O and purified by HPLC. The dimethylated product was isolated from the HPLC.



Compound 10

Compound **5** (2 mg) was reacted with 1-iodooctane (30 µL) and heated in toluene (1.1 mL) at 100°C for 12h. The product was extracted with H₂O, and the organic layer was purified by HPLC.



Compound 11

Compound **5** (2 mg) was heated in CHCl_3 (1.1 mL) with 1-iodohexadecane (19.4 mg) at 60°C for 12h. Product was extracted with H_2O . Solution was centrifuged, and supernatant was purified by HPLC.

7.5.3 Fluorescence Properties

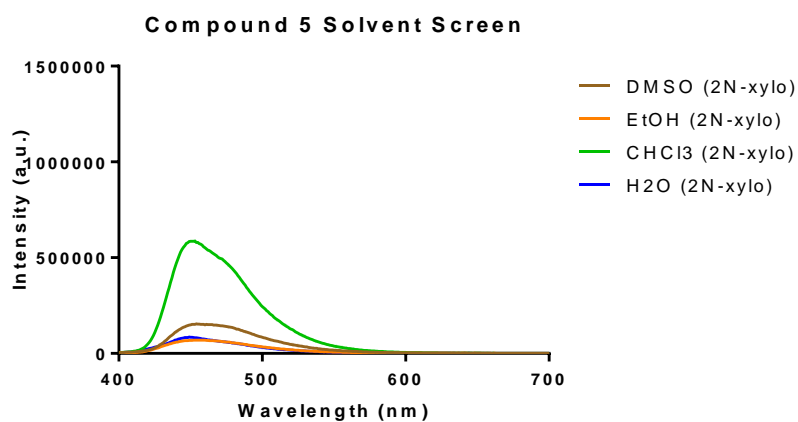


Figure 7.4 Emission spectra of compound in various solvents ($\lambda_{\text{ex}} = 397 \text{ nm}$)

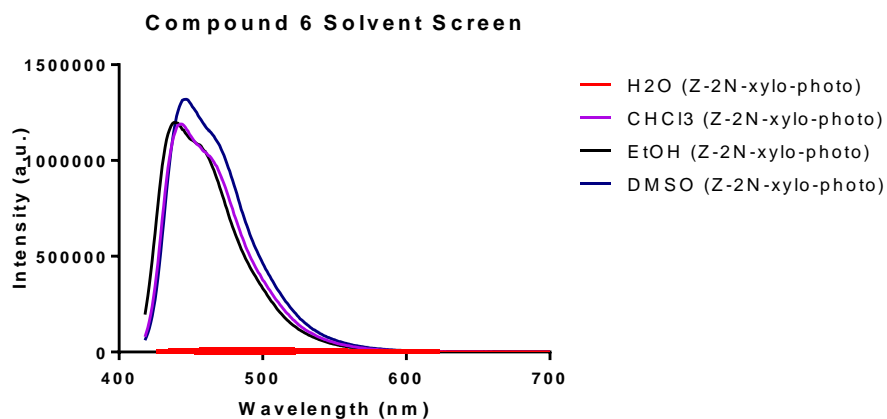


Figure 7.5. Emission spectra of compound 6 in various solvents ($\lambda_{\text{ex}} = 397 \text{ nm}$)

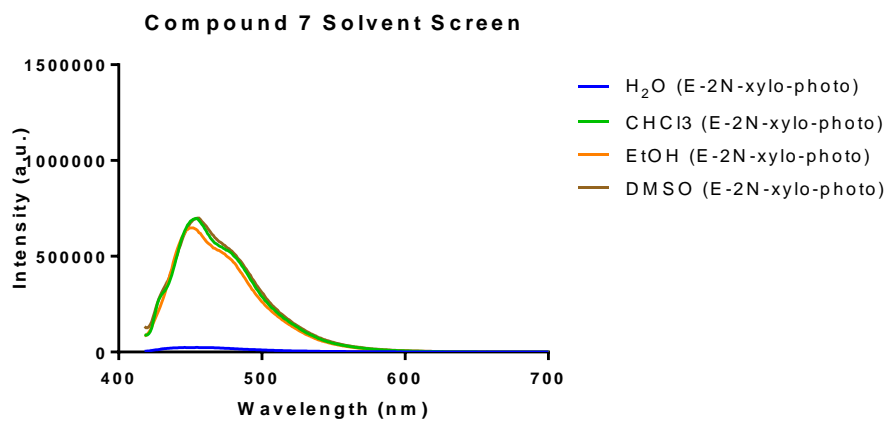


Figure 7.6 Emission spectra of compound 7 in various solvents ($\lambda_{\text{ex}} = 397 \text{ nm}$)

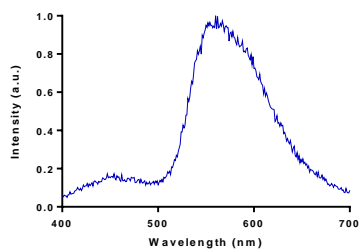


Figure 7.7 Emission spectra of 8 in H₂O ($\lambda_{\text{ex}} = 466 \text{ nm}$)

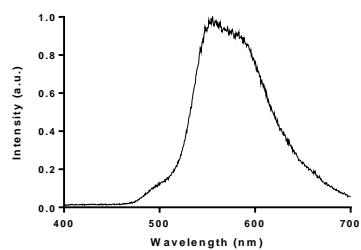


Figure 7.8 Emission spectra of 9 in H₂O ($\lambda_{\text{ex}} = 480$ nm)

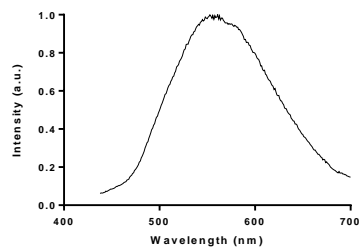


Figure 7.9 Emission spectra of 10 in H₂O ($\lambda_{\text{ex}} = 423$ nm)

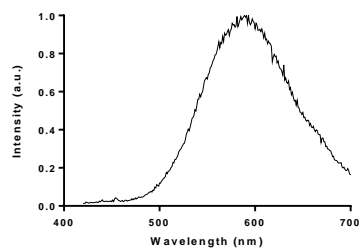


Figure 7.10 Emission spectra of 11 in H₂O ($\lambda_{\text{ex}} = 362$ nm)

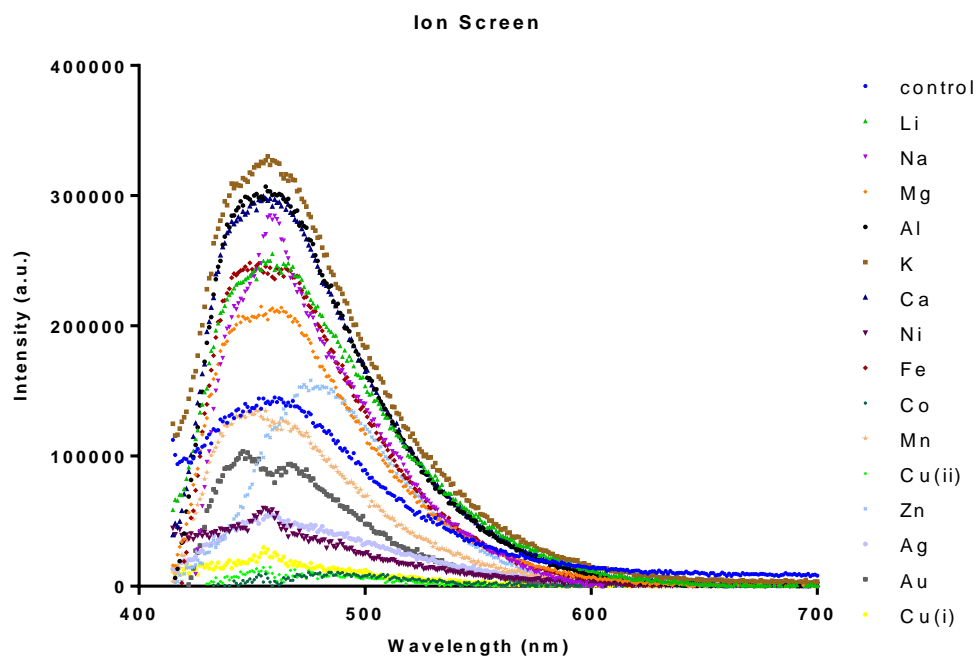


Figure 7.11 Emission spectra of 6 recorded in the presence of different ions ($\lambda_{\text{ex}} = 397 \text{ nm}$)

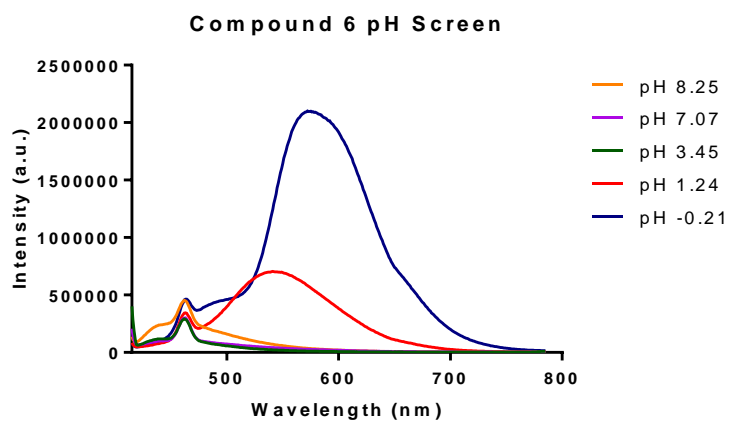


Figure 7.12. Compound 6 pH screen ($\lambda_{\text{ex}} = 397 \text{ nm}$)

7.5.4 NMR Spectra

